STI/E-TR-25066
31 May 1983

TRACKING AND DATA ACQUISITION SYSTEM (TDAS) FOR THE 1990'S

VOLUME VI

TDAS NAVIGATION SYSTEM ARCHITECTURE

DRAFT FINAL REPORT

Prepared by:

Bryant D. Elrod
Alan Jacobsen
Ronald A. Cook
Ram-Nandan P. Singh

Prepared Under:

Contract NAS5-26546

Prepared for:

NASA Goddard Space Flight Center
Greenbelt, Maryland 20771

STANFORD TELECOMMUNICATIONS INC.

6888 Elm St. • Suite 3A • McLean, VA 22101 • (703) 893-3220

TECHNICAL REPORT STANDARD TITLE PAGE

1. Report No.	2. Government Accession No.	3. Recipient's Catalog No.

4. Title and Subtitle	5. Report Date
Study of a Tracking and Data Acquisition System (TDAS) for the 1990's Volume VI: TDAS Navigation System Architecture	31 May 1983 6. Performing Organization Code
7. Author(s) B.D. Elrod, A. Jacobsen, R.A. Cook, R.N.P. Singh	8. Performing Organization Report No. STI/E-TR-25066
9. Performing Organization Name and Address Stanford Telecommunications, Inc. 6888 Elm Street McLean, Virginia 22101	10. Work Unit No. 11. Contract or Grant No. NAS5-26546
12. Sponsoring Agency Name and Address National Aeronautics and Space Administration Goddard Space Flight Center Greenbelt Road Greenbelt, Maryland 20771 J.J. Schwartz Code 831	13. Type of Report and Period Covered Draft Final Report 14. Sponsoring Agency Code
15. Supplementary Notes	

16. Abstract

This report is the DRAFT FINAL REPORT for Task 15, "Study of Alternative User Tracking Techniques with TDAS", and the navigation part of Task 5, "TDAS System Architecture.

The report examines TDAS-based one-way range and doppler methods for providing user orbit and time determination, specifically:

- Forward Link Beacon Tracking - with on-board processing of independent navigation signals broadcast continuously by TDAS spacecraft,
- Forward Link Scheduled Tracking - with on-board processing of navigation data received during scheduled TDAS forward link service intervals,
- Return Link Scheduled Tracking - with ground-based processing of user generated navigation data during scheduled TDAS return link service intervals.

The study includes a system level definition and requirements assessment for for each alternative, an evaluation of potential navigation performance and comparison with TDAS mission model requirements. TDAS satellite tracking is also addressed for two alternatives: BRTS and VLBI tracking.

17. Key Words (Selected by Author(s))	18. Distribution Statement
Satellite Navigation, Orbit Determination Time Transfer Tracking VLBI	

19. Security Classif. (of this report)	20. Security Classif. (of this page)	21. No. of Pages	22. Price*
Unclassified	Unclassified		

*For sale by the Clearinghouse for Federal Scientific and Technical Information, Springfield, Virginia 22151.

ACKNOWLEDGEMENT

The authors are grateful to John Coffman, Charlie Newman, and Jerry Teles of GSFC for their advice and many valuable suggestions during the course of the study. Appreciation is also due to Danny Mistretta of GSFC for his help with the SEA and RDGTDS programs and to Dick Campion of Bendix for helping us with ORAN.

PREFACE

This report documents the technical results obtained from navigation system definition studies performed under Tasks 5 and 15 of Contract NAS5-26546, "Tracking Data Acquisition System (TDAS) Study". Task 5 (TDAS System Architecture) and Task 15 (Alternative User Navigation Techniques with TDAS) were part of a two year pre-Phase A concept definition study for TDAS as the proposed successor to TDRSS, currently under development.

SCOPE OF WORK

The TDAS study covers a fifteen year planning period, (1995-2005). Potential missions to be flown in this time frame include free flyers, support vehicles and a space station/platform. Much of the TDAS requirement will be to support low earth orbit (LEO) missions in terms of communications, navigation and TT&C. Additional requirements could stem from user mission activities in higher (e.g., synchronous) orbits, and in support of inter-orbital transfers of materials and men for maintenance and repair in space, or for retrieval of platforms and experiments.

This report is Volume VI of nine volumes constituting the final report for the TDAS pre-Phase A study. Volume titles, largely self-explanatory, are given below:

- Volume I Executive Summary
- Volume II TDAS User Community Characteristics
- Volume III TDAS Communications Mission Model
- Volume IV TDAS Space Segment Architecture
- Volume V TDAS Ground Segment Architecture and Operations Concept
- Volume VI TDAS Navigation System Architecture
- Volume VII TDAS Space Technology Assessment
- Volume VIII TDAS Frequency Planning
- Volume IX TDAS Cost Summaries

OVERVIEW OF VOLUME VI

The navigation architecture aspect of this study involves examination of TDAS-based tracking alternatives for providing user orbit and time determination (OD/TD). Two-way range and doppler tracking as implemented in TDRSS is also an alternative for ground-based navigation support with TDAS. However, the primary focus here will be on one-way range and doppler tracking methods, specifically:

- Forward Link Beacon Tracking (FLBT) - with on-board processing of independent navigation signal transmissions broadcast continuously by TDAS spacecraft,

- Forward Link Scheduled Tracking (FLST) - with on-board processing of navigation data received during scheduled TDAS forward link service intervals, and

- Return Link Scheduled Tracking (RLST) - with ground-based processing of user-generated navigation data during scheduled TDAS return link service intervals.

This study addresses system configurations and requirements to support each method and assesses the potential navigation performance as a function of user orbit, TDAS constellation options and other parameters. Results are then compared with accuracy requirements in the TDAS mission model. Impacts of the above alternatives on both TDAS and users are evaluated and key issues/tradeoffs are identified. The study also considers TDAS satellite tracking for two options (BRTS and VLBI)* to identify system configuration impacts of the TDAS constellation options and compare potential tracking accuracy performance.

---

* BRTS - Bilateration Ranging Transponder System
VLBI - Very Long Baseline Interferometry.

MAJOR FINDINGS

Results of the study are summarized in Section 6. The major conclusions are:

- TDAS Beacon Tracking (FLBT) will satisfy all users in the TDAS mission model with position accuracy requirements down to 10 m.

- Scheduled tracking alternatives (FLST, RLST) can also meet the accuracy requirements except at low altitudes where performance is sensitive to:

  - Drag Uncertainty
  - Frequency of Tracking and/or
  - Frequency of Navigation Data Uploads (RLST/only)

- A two or three satellite TDAS constellation impacts performance as follows:

  - Selecting two satellites leads to tradeoff between coverage and accuracy. Increased satellite spacing improves coverage, but a point is reached where performance in high inclination orbits begins to degrade (130° spacing appears better than 162°).

  - Selecting three satellites provides full coverage and up to a 2:1 advantage in navigation accuracy over two satellites.

- Projected TDAS tracking accuracy requirements (25 m-position and 2.5 mm/sec-velocity) can be met with VLBI tracking but not with a minimal* BRTS configuration.

* 2 Bilateration Ranging Transponder System (BRTS) sites per TDAS spacecraft.

TABLE OF CONTENTS

TABLE OF CONTENTS (Cont.)

LIST OF FIGURES

LIST OF FIGURES (Cont.)

LIST OF FIGURES (Cont.)

LIST OF TABLES

SECTION 1

INTRODUCTION*

1.1 BACKGROUND

By the 1990's, NASA missions will require extending TDRSS capabilities for user tracking and orbit determination in terms of greater speed, accuracy and throughput efficiency. Requirements are also expected to increase for on-board, real-time navigation data (orbit, time and attitude) to support mission operations, e.g., data annotation, antenna pointing, rendezvous etc.

A review of technology trends has identified various techniques (existing or under investigation) which could potentially support future orbit and/or time determination needs using ground-based or quasi-autonomous methods. These can be broadly categorized according to the measurement technology employed:

- RF Signal Detection (range, range-rate, range-difference)
- LASER Reflection (range)
- Optical (angle)

A summary description of the various techniques is included in Volume II of the TDAS Study Report [1].

With TDRSS, RF methods are the basis for providing user tracking services. The focus in this volume will be on extensions to these techniques to support TDAS user navigation and TDAS satellite tracking.

The primary technique for TDRS and user orbit determination (OD) via TDRSS utilizes ground-derived two-way range and/or doppler data and requires a

---

* A glossary of acronyms is provided in Appendix F.

coherent forward and return link during scheduled tracking intervals (see [2] and Figure 1-1a). This technique can also support user time determination (TD), since clock calibration parameters (bias, drift) may be estimated simultaneously in the OD process.* An alternate tracking technique is also offered, which employs one-way doppler data measured at the ground from user transmissions during scheduled MA return link service (see [2] and Figure 1-1b). User clock calibration cannot be performed with this method (only oscillator calibration). An advantage, however, is that return links are more plentiful and easier to schedule than a coherent two-way link (20 vs 2).

The improved coverage and faster, centralized data collection available with TDRSS should substantially increase the throughput efficiency, of ground-based OD/TD with these techniques. However, achieving the capacity for multi-user support with rapid turnaround or near real-time requirements will depend on computational enhancements at the TDRSS/OSCF. A current goal with hardware upgrades in process and proposed software developments is to achieve, by the late 1980s, a 10 minute turnaround between the end of a tracking pass and an updated orbit computation. [4]

An on-board OD/TD capability would provide timely navigation data and also relieve TDRSS ground requirements for routine mission support. A one-way technique has been developed in which a TDRSS user would extract doppler data during scheduled MA forward link service for on-board OD only (see [5,6] and Figure 1-1c). Ground tests are planned for 1984 to demonstrate the approach and associated user equipment enhancements: doppler extractor, stable oscillator and navigation computer (hardware/software). [7] Further developments will depend on test results and user initiatives.

---

* Clock calibration is also possible with separate two-way measurements once the orbit is determined. [3]

FIGURE 1-1: TDRSS OPTIONS FOR USER NAVIGATION

A) TWO-WAY RANGE & DOPPLER TRACKING (GROUND-BASED OD/TD VIA NCC/OSCF)

B) RETURN LINK DOPPLER TRACKING (GROUND-BASED OD VIA NCC/OSCF)

C) FORWARD LINK DOPPLER TRACKING (TENTATIVE) (ON-BOARD OD)

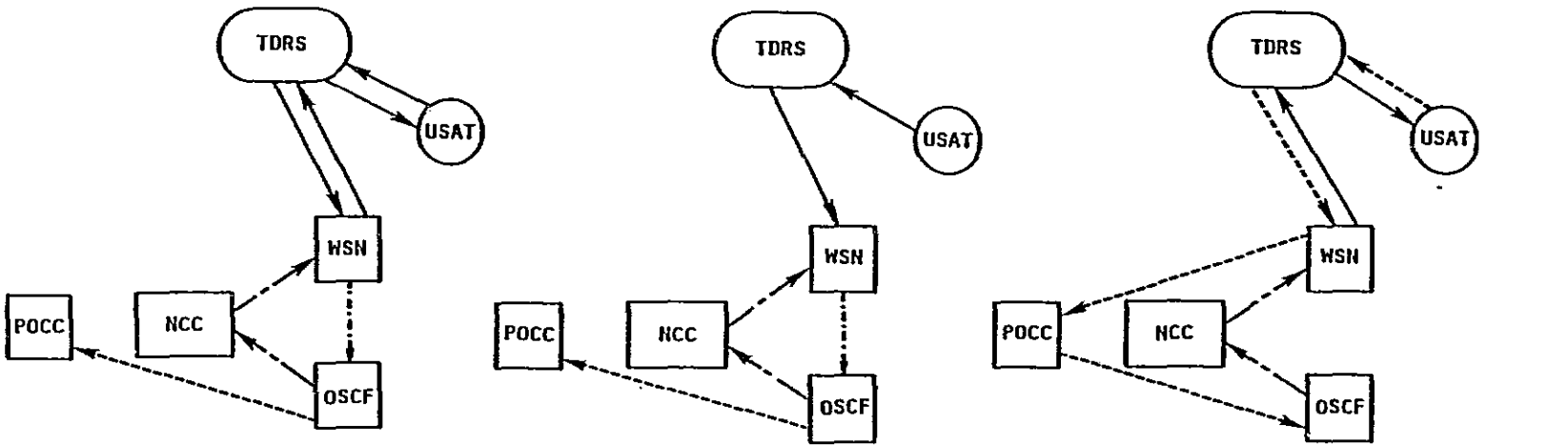

LEGEND:

- TRACKING SIGNALS: ————————
- TRACKING DATA: (RANGE/DOPPLER) -·-·-·-·-·-
- COMPUTED ORBIT AND/OR TIME DATA ----------
- ACQUISITION DATA — — — — —

STANFORD TELECOMMUNICATIONS INC.

With respect to future navigation performance, inquiries were made, as part of the TDAS study [1b]*, to determine potential user position and time accuracy requirements. Aside from Topex-type missions*, the most stringent position accuracy requirement is in the 10 m (1σ) range. This pertains to advanced resource observation type missions and a proposed space station. The most stringent time accuracy requirement (relative to UTC) is 1 μsec (1σ), which applies to several classes of missions.

1.2 TDAS NAVIGATION ARCHITECTURE GOALS

In accordance with the preceding discussion, the goals of the navigation architecture study are as follows:

- Reduce ground requirements for routine two-way tracking support
- Support user on-board orbit and time determination
- Provide users timely access to ground-derived navigation data, and,
- Meet navigation accuracy requirements ($\geq$ 10 m) of TDAS mission model.

1.3 TASK ASSIGNMENT

The TDRSS two-way tracking technique is a candidate for ground-based support of user navigation in the TDAS era. This study will examine alternative one-way tracking techniques that also support user orbit and time determination with TDAS. The specific alternatives to be studied are:

* Appendix A provides a summary of the TDAS mission model and navigation requirements.

- Forward Link Beacon Tracking (FLBT) - based on low power signals continuously broadcast by TDAS satellites to permit range and doppler measurements for on-board use.

- Forward Link Scheduled Tracking (FLST) - based on ground originated signals during scheduled contact periods which permit range and doppler measurements for on-board use.

- Return Link Scheduled Tracking (RLST) - based on user generated signals during scheduled contact periods for ground-based range and doppler measurements.

The study shall include a system level definition and requirements assessment for each configuration. An accuracy analysis based on applicable error models shall be performed for comparison of navigation performance among alternatives and against requirements in the TDAS mission model. Impacts on both TDAS and users and key tradeoffs will be identified and compared.

1.4 OVERVIEW OF METHODOLOGY

The methodology followed in pursuing this task is summarized in Figure 1-2. The first step was to define the tracking configuration in terms of functions and system elements needed to support each alternative. The second step was to consider signal processing aspects beginning with a definition of the tracking signal in each case, then a link performance analysis to identify EIRP and/or G/T requirements and finally estimation of the measurement accuracy for range and doppler (range-rate) data types.

The third step was to address TDAS satellite tracking to identify possible system configuration impacts of TDAS constellation alternatives and to determine representative estimates of potential ephemeris accuracy. The analysis focused on two options:

FIGURE 1-2: USER ONE-WAY NAVIGATION ALTERNATIVES STUDY

OVERVIEW

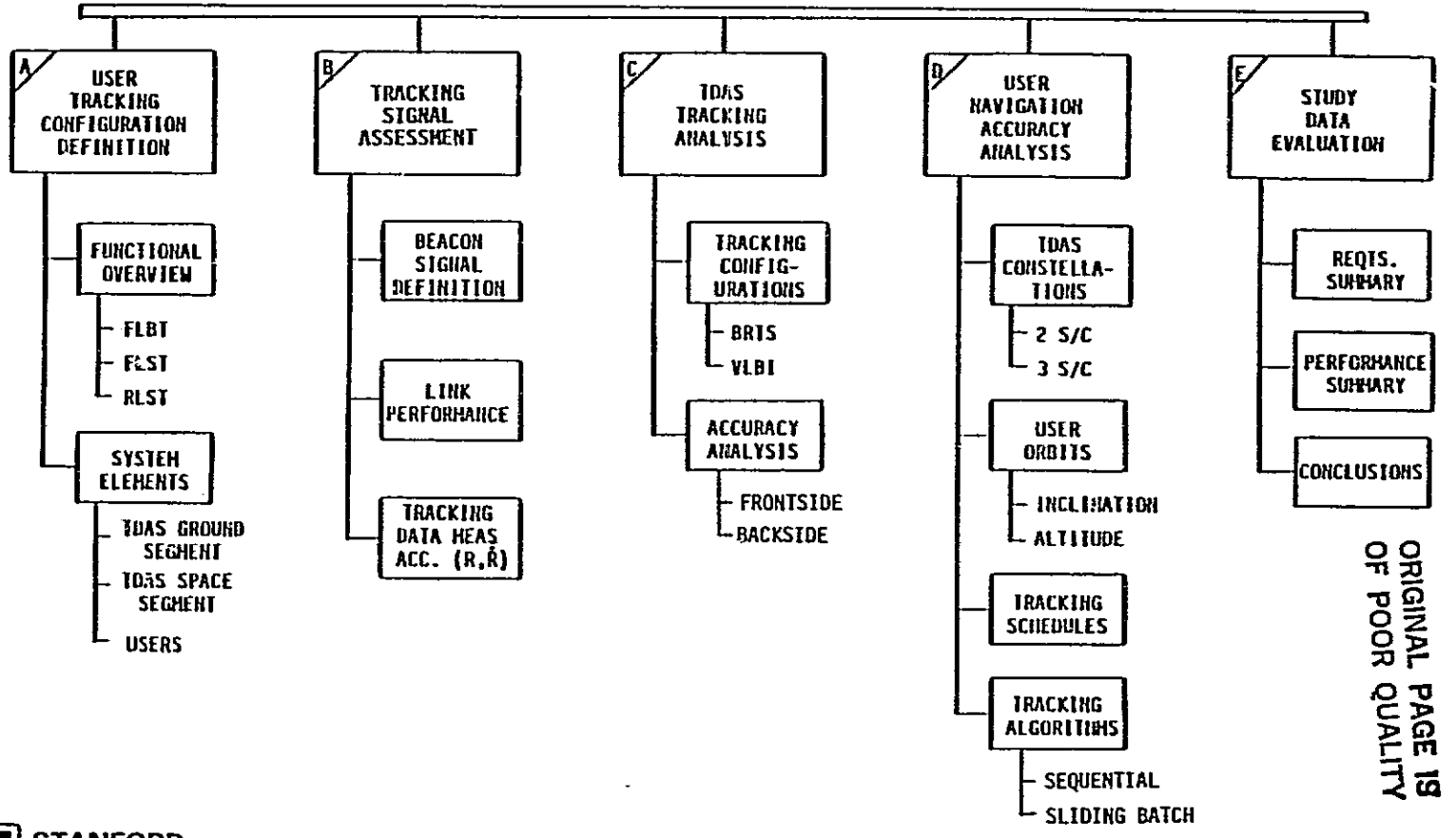

STANFORD TELECOMMUNICATIONS INC.

- BRTS Tracking - the primary technique for TDRS tracking [8], and

- VLBI Tracking - proposed as a BRTS enhancement or eventual replacement. [9]

The fourth step was to evaluate potential user navigation performance in terms of OD/TD accuracy for the three tracking alternatives. Cases for evaluation were defined to assess both two and three satellite TDAS constellations, several classes of user orbits, different tracking schedules and two algorithms for tracking data processing (sequential and sliding batch).

The last step was to summarize the study data, compare navigation performance results with requirements defined in the TDAS mission modal and then integrate the key findings in terms of a proposed system architecture to support user navigation functions.

1.5 OVERVIEW OF THE REPORT

Results of the efforts outlined above are presented in succeeding sections and in serveral appendices which contain much of the supporting detail. Section 2 describes the functions and system elements defining the configuration for each tracking alternative. Section 3 and Appendix B cover the signal processing analysis aspects. Section 4 and Appendix C consider the TDAS satellite tracking analysis. Section 5 and Appendices D and E present results of the navigation performance evaluation. Section 6 contains the summary data and study conclusions.

SECTION 2

USER TRACKING CONFIGURATION DEFINITION*

The proposed TDAS architecture design [1a,d] extends TDRSS data relay capabilities with enhanced SMA services for multiple access users and more SA channels (KSA + WSA + LSA) for single access users. This section defines the system configurations for supporting one-way user tracking (FLBT, FLST or RLST) assuming (for description purposes) that it is provided at S-Band.

In practice, however, the scheduled tracking alternatives (FLST or RLST) could also be accomodated via the SA services, as necessary. On the other hand, beacon tracking (FLBT) must be a generally available broadcast service and thus is not compatible with the SA services. While FLBT operation in a totally independent band is a possible option, frequency spectrum and user/system equipment considerations tend to favor S-Band reuse.

The following two subsections present the system functions and major elements needed for supporting each alternative. A concluding subsection compares tracking signals and data handling interface requirements for the user, space and ground segments.

2.1 FORWARD LINK TRACKING (FLBT/FLST)

An overview of the major functions involved with the two forward link tracking alternatives is shown in Figure 2-1. Tracking signals are uplinked from the ground at K_u-band, relayed by one or more TDAS satellites and received at S-band by the user for on-board processing. The fundamental differences between beacon and scheduled tracking relate primarily to the signal availability and format (discussed in Section 3).

* A glossary of acronyms is given in Appendix F.

FIGURE 2-1: FORWARD LINK BEACON & SCHEDULED TRACKING (FLBT & FLST) (FUNCTIONAL OVERVIEW)

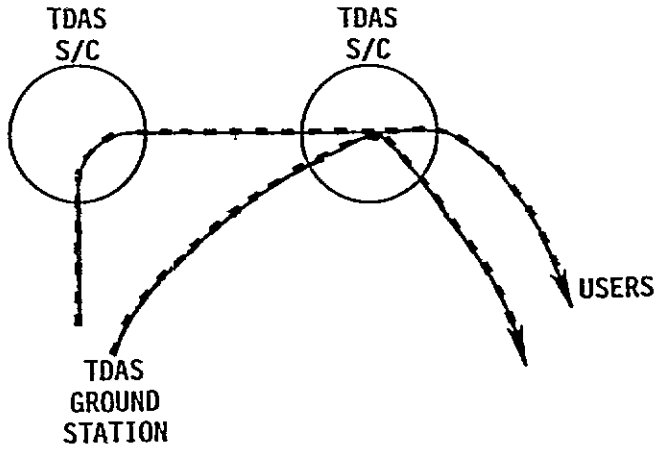

ELEMENTS	MAJOR FUNCTIONS	
	FORWARD LINK BEACON TRACKING (FLBT)	FORWARD LINK SCHEDULED TRACKING (FLST)
TDAS GROUND SEGMENT	TRACKING SIGNAL & ANCILLARY DATA* GENERATION AND UPLINK CONTINUOUS TRANSMISSION	TRANSMISSIONS DURING SCHEDULED SERVICE ONLY
TDAS SATELLITES	BENT PIPE RELAY FOR SMA USERS ONLY (VIA BROADBEAM ANTENNA-SINGLE SMA ELEMENT)	BENT PIPE RELAY FOR ALL SERVICES (SMA, KSA, WSA, LSA)
USERS	• RANGE/DOPPLER DATA MEASUREMENT • ON-BOARD ORBIT/TIME DETERMINATION	

* TDAS S/C ORBITS, RANGE/DOPPLER CORRECTION DATA, ETC.

The beacon signal is assumed to be generated by a TDAS ground terminal for broadcast by each TDAS satellite using a single element of the 60 element SMA antenna array. Users would receive continuous tracking signals while within a beacon antenna's ±13° field of view. The corresponding upper limit on user altitude for 100% coverage exceeds 3100 km for all TDAS constellations considered.*

In the scheduled mode, signals for tracking are available only during an allocated contact period as part of normal SMA service. Since each TDAS can support two SMA forward channels [1d], up to four simultaneous users theoretically could be supported with a two satellite TDAS constellation depending on channel scheduling policy.

A block diagram of essential elements in the forward link tracking configuration is shown in Figure 2-2. For FLBT support, a separate (beacon) signal generator is employed at the TDAS ground station and a dedicated K_u-to-S Band repeater is needed in each TDAS satellite [1d]. For either FLBT or FLST, the user requires a stable frequency standard, range and doppler extractors, a decoder for (ancillary) navigation data and a computing facility for on-board OD/TD processing. Also, the required ancillary data (time reference information, TDAS ephemerides, link calibrations, etc.) is generated by the ground segment and incorporated in the tracking signal.

2.2 RETURN LINK TRACKING (RLST)

An overview of the major functions involved with this alternative is shown in Figure 2-3. During scheduled return link intervals, user S-band transmissions for tracking are relayed to the ground (at K_u-band) by the assigned TDAS satellite. Range and range-rate (doppler) data are measured at the ground and ancillary data (timing**, position estimate, etc.) is decoded. The tracking data is processed to determine the user's orbit and clock parameters (e.g., bias, drift).

---

* Lower altitude coverage is governed by the zone of exclusion size for a given constellation (See [1d] for details).

** This includes the user's current time and a sync word for range ambiguity resolution at the ground.

FIGURE 2-2: TDAS FORWARD LINK CONFIGURATION

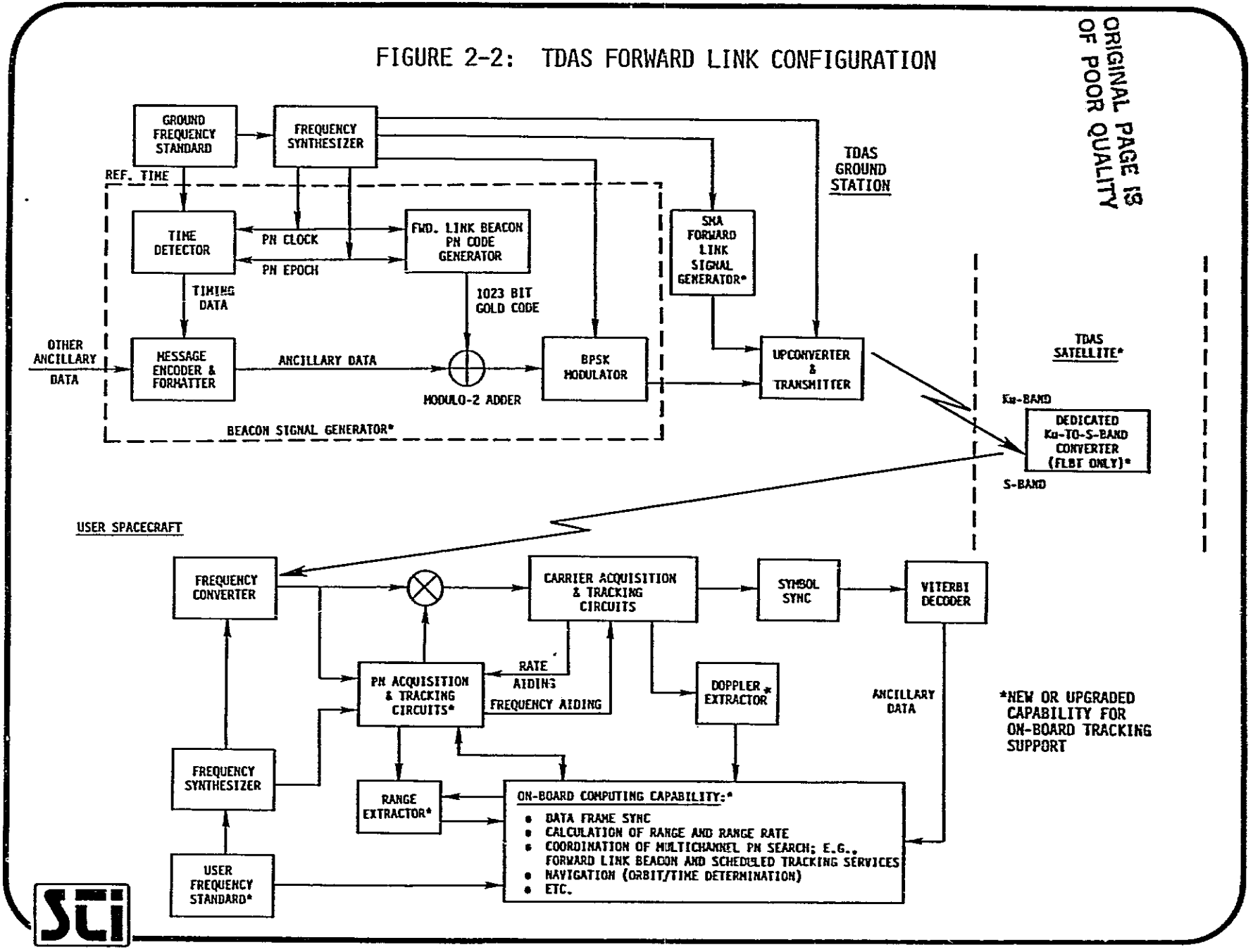

FIGURE 2-3: RETURN LINK SCHEDULED TRACKING (RLST) - FUNCTIONAL OVERVIEW

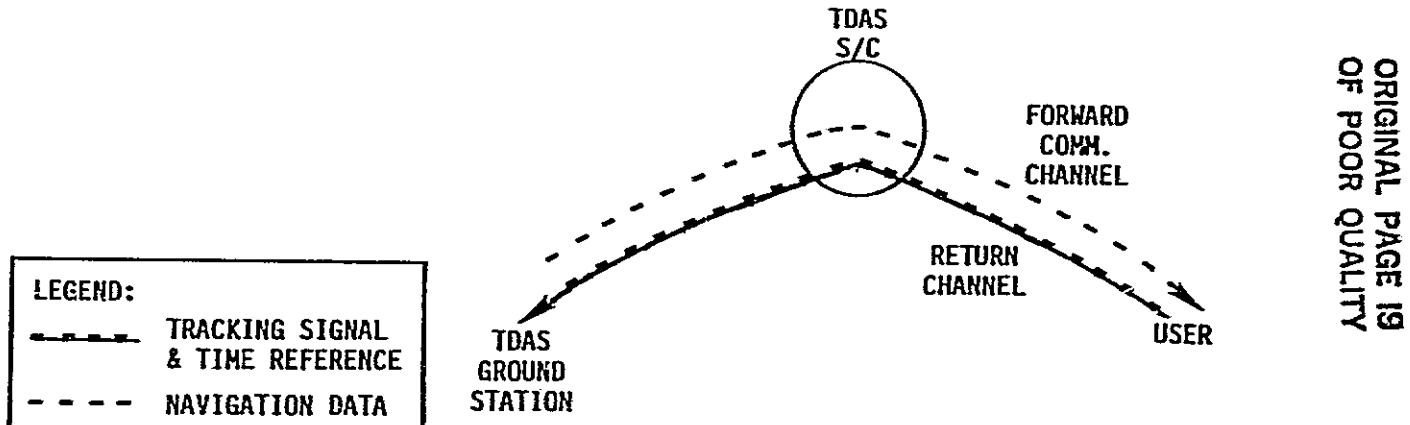

ELEMENTS	MAJOR FUNCTIONS
USERS	• TRACKING SIGNAL GENERATION AND TRANSMISSION DURING SCHEDULED RETURN LINK SERVICE • RECEIVE AND PROCESS GROUND-DERIVED DATA FOR ORBIT/CLOCK STATE PREDICTION UNTIL NEXT UPLOAD VIA SCHEDULED FORWARD LINK COMM. SERVICE
TDAS GROUND SEGMENT	• RANGE/DOPPLER DATA MEASUREMENT • USER ORBIT DETERMINATION AND CLOCK (OSC.) CALIBRATION • ORBIT PREDICTION DATA GENERATION AND TRANSMISSION TO USER AT SCHEDULED INTERVALS
TDAS SATELLITES	BENT PIPE RELAY FOR ALL SERVICES (SHA, KSA, WSA, LSA)

To support users with on-board navigation data requirements, the ground also generates orbit and time prediction data for subsequent upload to the user during a scheduled forward link service interval. Such prediction data could comprise algorithm coefficients for Keplerian arc and/or polynominal curve fitting models [10,11] and the applicable time intervals. A user receives the ground-derived navigation data and computes orbit and time prediction between uploads. The interval between uploads is an important factor considered in the navigation performance evaluation (see Section 5).

A block diagram of the essential elements in the return link tracking configuration is shown in Figure 2-4. For the ground segment, the same types of equipment used for two-way tracking support and user orbit verification could also be used for RLST functions. A ground computing capability would also be necessary for user OD/TD and prediction data generation with adequate turnaround. The user requires a stable frequency standard, means for ancillary data generation and formatting, and a computing facility for navigation data interpretation and propagation between uploads. There would be no impact on the TDAS satellite configuration with this option.

2.3 TRACKING SIGNAL AND DATA HANDLING INTERFACES

The multiple beam antenna and switch enhancements for TDAS spacecraft provide the capability for simultaneous, direct transmissions between the space segment and several ground stations [1d,e]. This provides possibilities for direct control of user spacecraft by the mission control centers (MCC) instead of interfacing through the Network Control Center (NCC) and White Sands (WSN) terminal as in TDRSS (see Figure 1-1).

Figure 2-5 illustrates options for tracking signal and navigation data flow with each of the one-way alternatives. Since the beacon signal for FLBT is a general resource, it is assumed to originate at WSN, the assumed control point for TDAS spacecraft [1e]. Navigation data computed on-board can be received by a TDAS ground terminal at the NCC directly and by MCCs

FIGURE 2-4: RETURN LINK SCHEDULED TRACKING SYSTEM CONFIGURATION

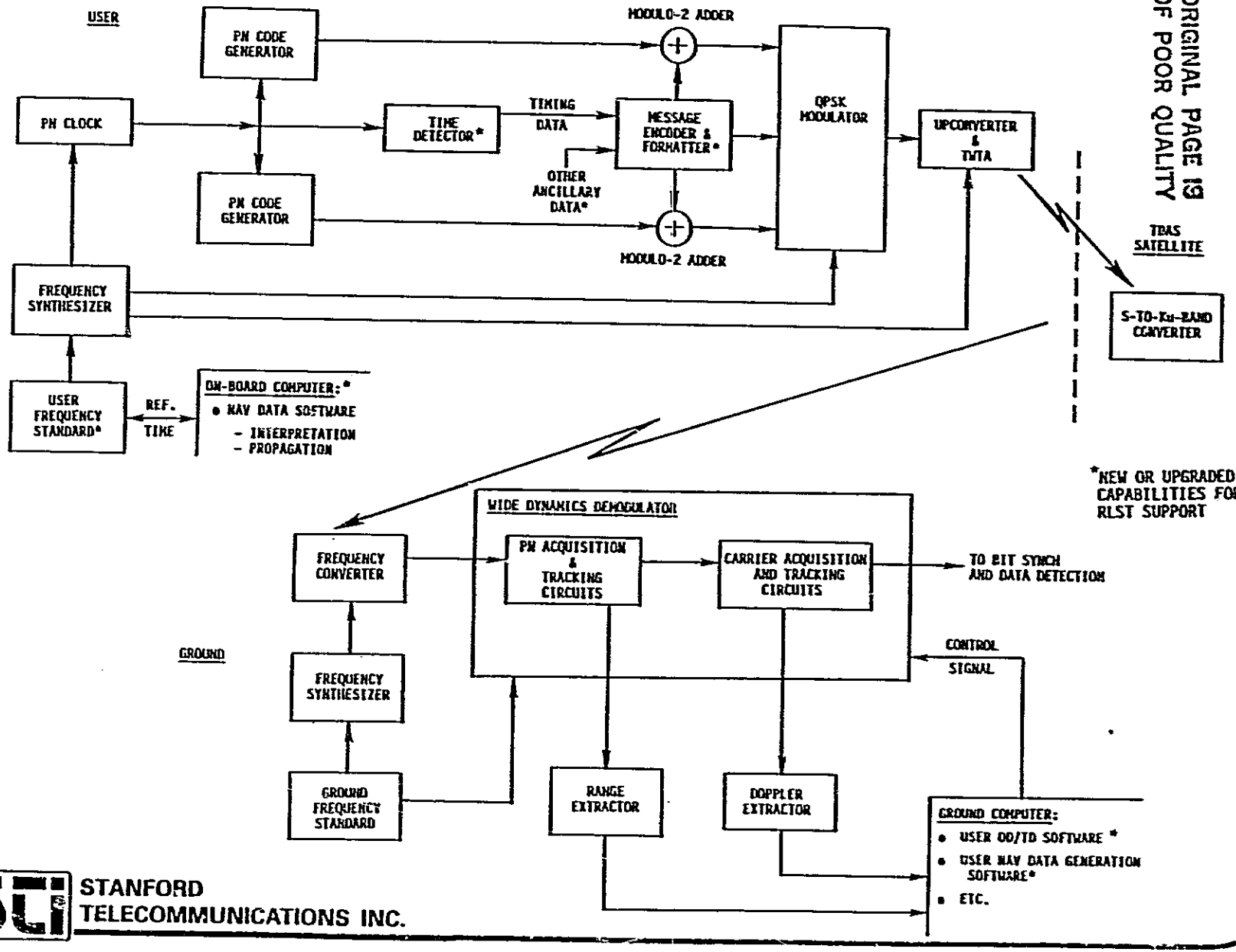

STANFORD TELECOMMUNICATIONS INC.

FIGURE 2-5: TRACKING SIGNAL AND DATA HANDLING INTERFACES (ONE-WAY TRACKING ALTERNATIVES)

A) FORWARD LINK BEACON TRACKING (FLBT)
(ON-BOARD OD/TD)

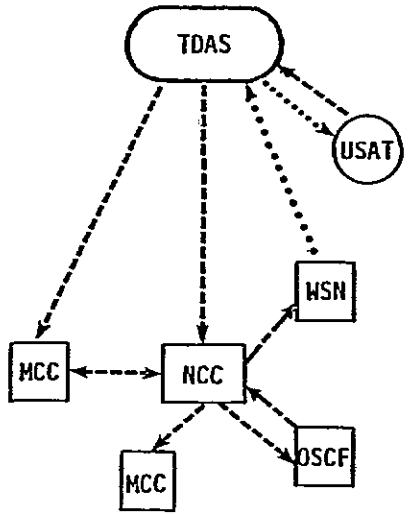

B) FORWARD LINK SCHEDULED TRACKING (FLST)
(ON-BOARD OD/TD)

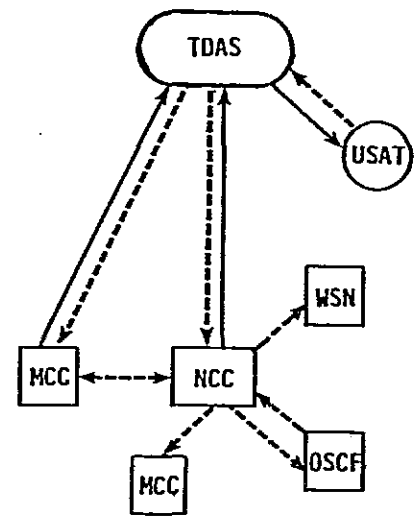

C) RETURN LINK SCHEDULED TRACKING (RLST)
(GROUND-BASED OD/TD VIA NCC/OSCF OR MCC)

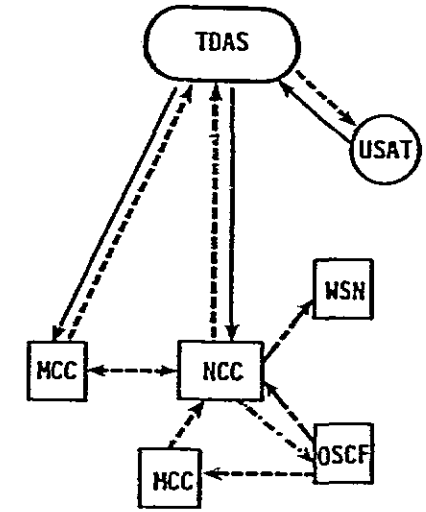

LEGEND:

- TRACKING SIGNALS:
  - SCHEDULED
  - BEACON
- TRACKING DATA: (RANGE/DOPPLER)
- COMPUTED ORBIT AND/OR TIME DATA
- ACQUISITION DATA

STANFORD TELECOMMUNICATIONS INC.

with direct space/ground access. Additional interfacility transfer of data can occur to support MCCs without direct space/ground access or for general coordination and/or verification functions. The latter includes WSN which has control of TDAS spacecraft facilities (e.g., SA antenna/telescope pointing).

With FLST (see Figure 2-5b) the user tracking signal is imbedded in the normal uplink data communication traffic so it can emanate from either the NCC or a cognizant MCC. Navigation data computed on-board can be distributed in the same manner discussed above for FLBT.

With RLST (see Figure 2-5c) the user tracking signal is imbedded in the normal downlink data communication traffic, so it can be received by either the NCC or cognizant MCC. Ground processing for user OD/TD can occur at the Orbit Support Computer Facility (OSCF) or at the MCC with subsequent interfacility data transfer as noted above. Since the two-way tracking with ground-based processing is also a TDAS alternative, Figure 2-6 is included for comparison with the RLST data flow.

FIGURE 2-6: TDAS TRACKING SIGNAL AND DATA HANDLING INTERFACES (TWO-WAY TRACKING ALTERNATIVES)

A) GROUND-BASED PROCESSING VIA NCC/OSCF

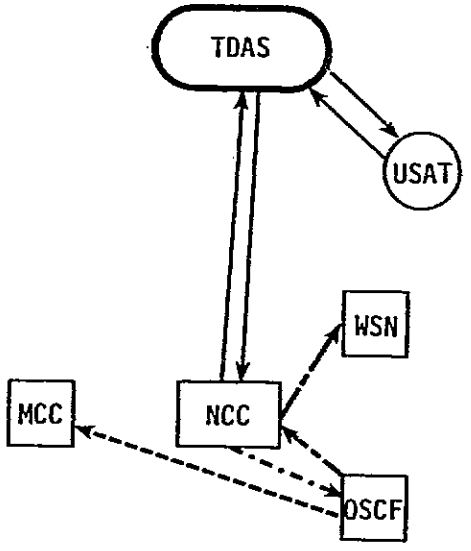

B) GROUND-BASED PROCESSING VIA MCC

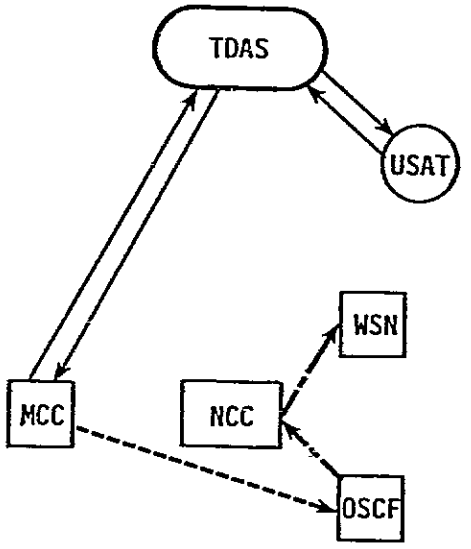

LEGEND:

- TRACKING SIGNALS: ————
- TRACKING DATA: (RANGE/DOPPLER) -·-·-·-
- COMPUTED ORBIT AND/OR TIME DATA - - - - -
- ACQUISITION DATA - - - - -

ORIGINAL PAGE IS OF POOR QUALITY

STANFORD TELECOMMUNICATIONS INC.

SECTION 3

TRACKING SIGNAL CHARACTERISTICS

The one-way alternatives for user navigation are distinguished by tracking signal generation, transmission, and/or processing aspects. This section presents: a tracking signal definition for each case (including a candidate beacon signal); results of link performance analyses to assess EIRP and G/T tradeoffs; and estimates of the measurement accuracy for range and range-rate (doppler) tracking data.

3.1 FORWARD LINK TRACKING (FLBT/FLST)

3.1.1 Tracking Signal Definition

On-board navigation by user spacecraft, as defined, requires that the received forward link signals provide the means to make range and range-rate measurements. Table 3-1 details the possible signal characteristics for two different modes: Forward Link Beacon Tracking (FLBT) and Forward Link Scheduled Tracking (FLST). Users may perform doppler only tracking of the signals to obtain range-rate values, but the signals are modulated by pseudonoise (PN) codes to also allow estimation of range delay. A chip rate of 3.0778 Mcps is assumed here in keeping with current TDRSS practice, although higher chip rates are perhaps possible. The employed PN codes are unique to each user in the case of FLST and unique to each TDAS satellite in the case of FLBT. The signals are also modulated by data, providing the user with, as a minimum, the TDAS ephemeris and the timing information necessary for clock synchronization purposes. It is assumed that, in addition to on-board navigation capabilities, user spacecraft will also possess Viterbi decoders to permit convolutional coding of the forward link data and a consequent 5 dB coding gain. Current technology has already placed such decoders on VLSI chips.

Forward Link Beacon Tracking: The ground-generated beacon signal is conceived to be transmitted to user spacecraft by a single element of the 60-element TDAS SMA antenna array. Due to the large beamwidth of a single

TABLE 3-1

FORWARD LINK TRACKING SIGNAL CHARACTERISTICS

SIGNAL CHARACTERISTICS	BEACON (FLBT)	SCHEDULED (FLST)
TYPE	• PN MODULATED BPSK DATA	• STAGGERED QUADRIPHASE PN (SQPN) (COMMAND & RANGE CHANNELS PER TDRSS)
CODE(S)	• UNIQUE 1023-CHIP GOLD CODE • 3.0778 x 10^6 CHIPS/SEC • 2.6 NS GRANULARITY (VIA INTERPOLATION TO 1/128 CHIP	• SHORT CODE (COMMAND CHANNEL/ 1023 CHIP GOLD CODE) • LONG CODE (RANGE CHANNEL/ 256 x 1023 CHIPS USED TO RESOLVE RANGE AMBIGUITY • 3.0778 x 10^6 CHIPS/SEC
DATA*	• INCLUDES ANCILLARY DATA (E.G., TDAS EPHEMERIS, TIME REFERENCE AND PN EPOCH) $\leq$ 1000 BITS/ FRAME • CONVOLUTIONALLY-CODED (RATE ½) • DATA RATE ~ 100 BPS • ASSEMBLED INTO 1000 BIT FRAMES (10 SECONDS) • SYNC WORD IN EACH FRAME RESOLVES AMBIGUITY	• INCLUDES ANCILLARY DATA (SIMILAR TO FLBT) • CONVOLUTIONALLY-CODED (RATE ½)
DOPPLER COMPENSATION	• NONE (NOT FEASIBLE FOR MULTIPLE USER SUPPORT, BUT COORDINATION WITH FLST ENABLES REDUCTION OF DOPPLER UNCERTAINTY FOR INITIAL BEACON ACQUISITION	• PROVIDED FOR SIGNAL ACQUISITION

* MODULO-2 ADDED ASYNCHRONOUSLY TO PN CODE

element, the beacon is available to all users within the TDAS field of view (±13°). In supporting more than one user simultaneously, however, adjustment of the transmit frequency to compensate for doppler shifting between TDAS and the user is not feasible. The consequent search in frequency required for a user to acquire the beacon signal may be significantly reduced by orbit predictions from prior tracking intervals. Coordination with other modes of tracking would provide a basis for such knowledge. Beacon signal acquisition is discussed further in Section 3.1.3.

The beacon signal is assumed to comprise PN modulated BPSK data transmitted at a data rate of approximately 100 bps. Such a low data rate is consistent with: the EIRP provided from a single TDAS SMA antenna element, low gain user antennas, and system noise temperatures. The data would be assembled into frames of roughly 1000 bits, each frame containing, for example:

- TDAS ephemeris parameters
  - Keplerian arc parameters
  - ephemeris reference time
  - age of data
- TDAS timing and link calibration parameters
  - PN code epoch
  - polynomial correction coefficients
  - age of data
- Frame overhead
  - frame synchronization word
  - error control field
- Miscellaneous data
  - almanac parameters for other TDAS satellites
  - health of all TDAS satellites.

The data is assumed to be synchronous with the PN code, allowing bit synchronization of the data to resolve range ambiguity, e.g., [12,13].

Forward Link Scheduled Tracking: This mode is discussed based on data for navigation derived from scheduled forward link SMA transmissions. The signal structure is assumed to be the same as in TDRSS. Separate, simultaneous command and range channel signals are transmitted using staggered quadriphase shift keying (SQPSK) as the modulation technique. The command channel contains all data and is asynchronously modulated by a short (1023-chip) PN code, thus permitting rapid acquisition; the range channel is acquired separately and is modulated by a long (256 x 1023-chip) PN code to allow the resolution of range ambiguity. Since data is contained only in the command channel, unbalanced SQPSK modulation is employed, maintaining the ratio of power in the command channel to that in the range channel at 10 dB. The command and range channel PN codes are time-synchronized so that acquisition of the command channel's short code assists in acquisition of the range channel's long code. Acquisition of both the carrier frequency and PN codes is further aided by doppler compensation so that the carrier frequency received by the user is within a predictable tolerance.

3.1.2 Link Performance

Assessment of the error contribution in range and range-rate measurements due to thermal noise depends on the received C/N_0, the ratio of signal power to noise spectral density. Table 3-2 shows the TDAS SMA forward link budget used in this study. The TDAS satellites act as relays from the ground to the user spacecraft, comprising a two-link communication system. Since the weaker of the two links constrains the overall communication performance, only the satellite-to-user link is considered here. Reasonable values are assumed for the polarization and miscellaneous system losses; the path loss is calculated assuming a satellite-to-user distance of approximately 41,000 km. The ratio C/N_0 for the forward link is thus parameterized by the user spacecraft's antenna gain and system noise temperature (G/T) and the EIRP emitted by the TDAS satellite.

TABLE 3-2

TDAS SMA FORWARD LINK BUDGET

TDAS EIRP	(DBW)	EIRP*
SPACE LOSS	(DB)	-191.6
POLARIZATION LOSS	(DB)	-0.6
USER G/T	(DB/°K)	G/T
BOLTZMANN'S CONSTANT K	(DBW/(HZ-°K))	-228.6
MISC. LOSSES	(DB)	-2.5
C/N_O	(DB-HZ)	EIRP + G/T + 33.9

*NOTES:

- TDRS SMA EIRP PER ELEMENT = 25.9 DB
- TDAS BEACON SIGNAL EIRP $\geq$ 25.9 DBW (1 ELEMENT)
- TDAS SMA FORWARD LINK EIRP > 35.9 DBW (10 ELEMENTS)
- FOR SCHEDULED FORWARD LINK, RATIO OF COMMAND CHANNEL RADIATED POWER TO RANGE CHANNEL RADIATED POWER IS 10 DB.

The maximum data rate that can be supported at a given bit error rate is also a function of the received C/N_0. If a desired 10^{-5} bit error rate, a 5 dB gain obtained from convolutional coding, and a 3 dB margin are assumed, Figure 3-1 shows the achievable data rates as a function of user G/T, parameterized by several representative TDAS power levels. For the beacon case, decoding 100 bps ancillary data implies a user G/T requirement > -32 dB/°K. This is not a very stringent requirement considering that a 0 dB antenna gain and a 1000° K receiver system noise temperature is easily attainable.

3.1.3 Beacon Signal Acquisition

The requirements for user acquisition of the beacon signal are affected by its frequency uncertainty due to doppler shifting. As an example, the Motorola 2nd generation TDRSS user transponder design [14] specifies a minimum C/N_0 of 33 dB-Hz for acquisition in 20 seconds with a probability of .9, assuming a frequency uncertainty of 1.5 kHz and a two channel search in time and frequency. Figure 3-2 shows the user G/T and TDAS EIRP required to surpass this threshold. With a single-element EIRP of 25.9 dBW for the beacon signal, the user G/T must be greater than approximately -27 dB/°K to meet the conditions of the Motorola design. The uncertainty in frequency and time for the beacon will lead to longer acquisition times, but this may be acceptable in the case of beacon acquisition.

To ameliorate the signal acquisition task, future user transponder designs might use more than two channels to effect the PN code acquisition. Figure 3-3 shows a 3-channel configuration. All three channels could be used in acquiring the beacon with a resultant decrease in acquisition time. When scheduled service begins, one channel may remain dedicated to tracking the beacon while the remaining two channels acquire the doppler compensated forward link scheduled service. Use of the three channels could be directed by the user's on-board computer in various handover scenarios, as suggested in Figure 3-4. Furthermore, the acquisition search in time and frequency could take advantage of past tracking data to optimally conduct the search.

FIGURE 3-1: TDAS SMA FORWARD LINK: ACHIEVABLE DATA RATE VS. USER G/T

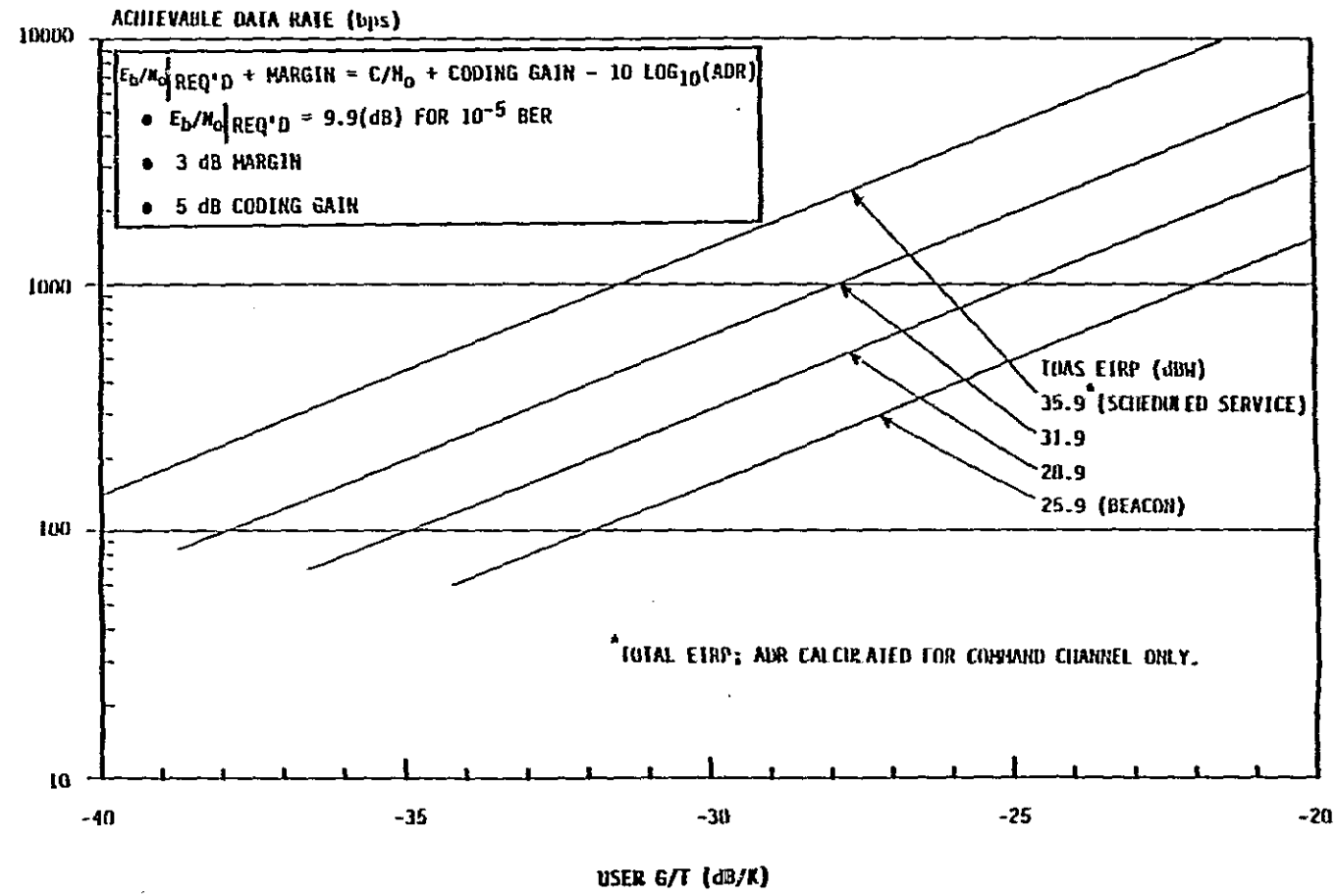

ORIGINAL PAGE IS
OF POOR QUALITY

STANFORD TELECOMMUNICATIONS INC.

FIGURE 3-2: TDAS SMA FORWARD LINK: PN CODE ACQUISITION THRESHOLD

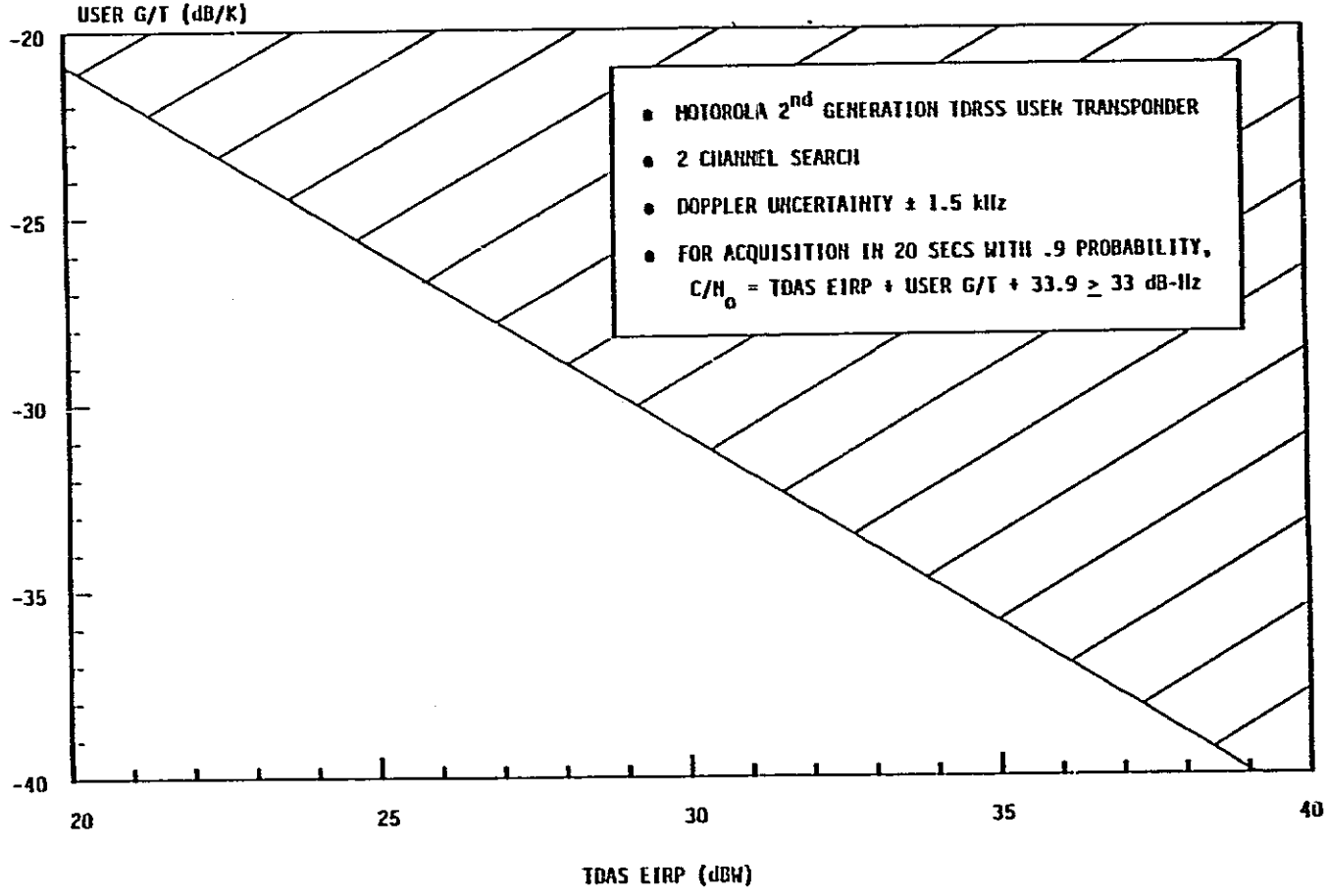

ORIGINAL PAGE IS
OF POOR QUALITY

STANFORD
TELECOMMUNICATIONS INC.

FIGURE 3-3: 3-CHANNEL SEQUENTIAL PN ACQUISITION

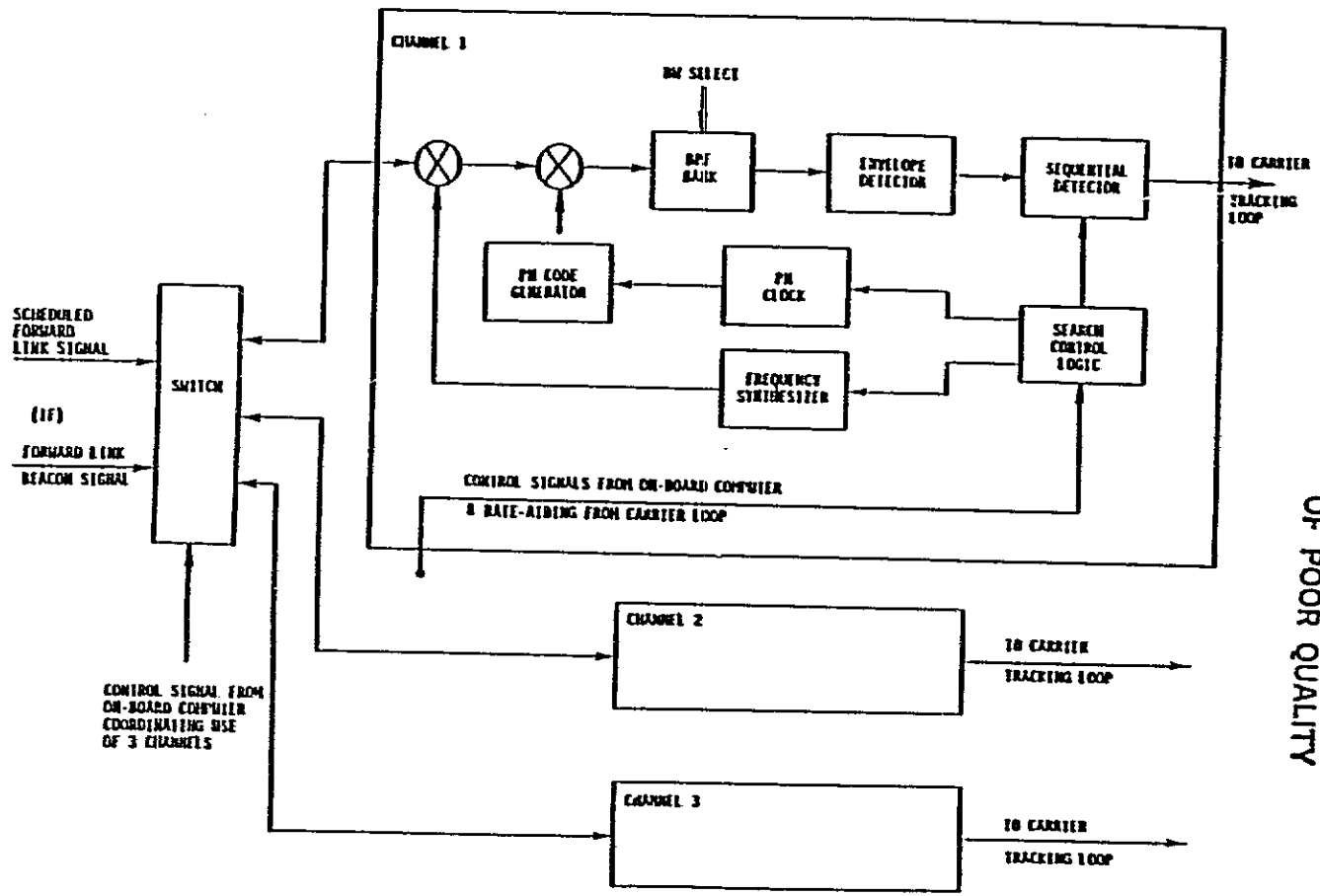

FIGURE 3-4: A SCENARIO FOR SCHEDULED SERVICE AND FLBT HANDOVER

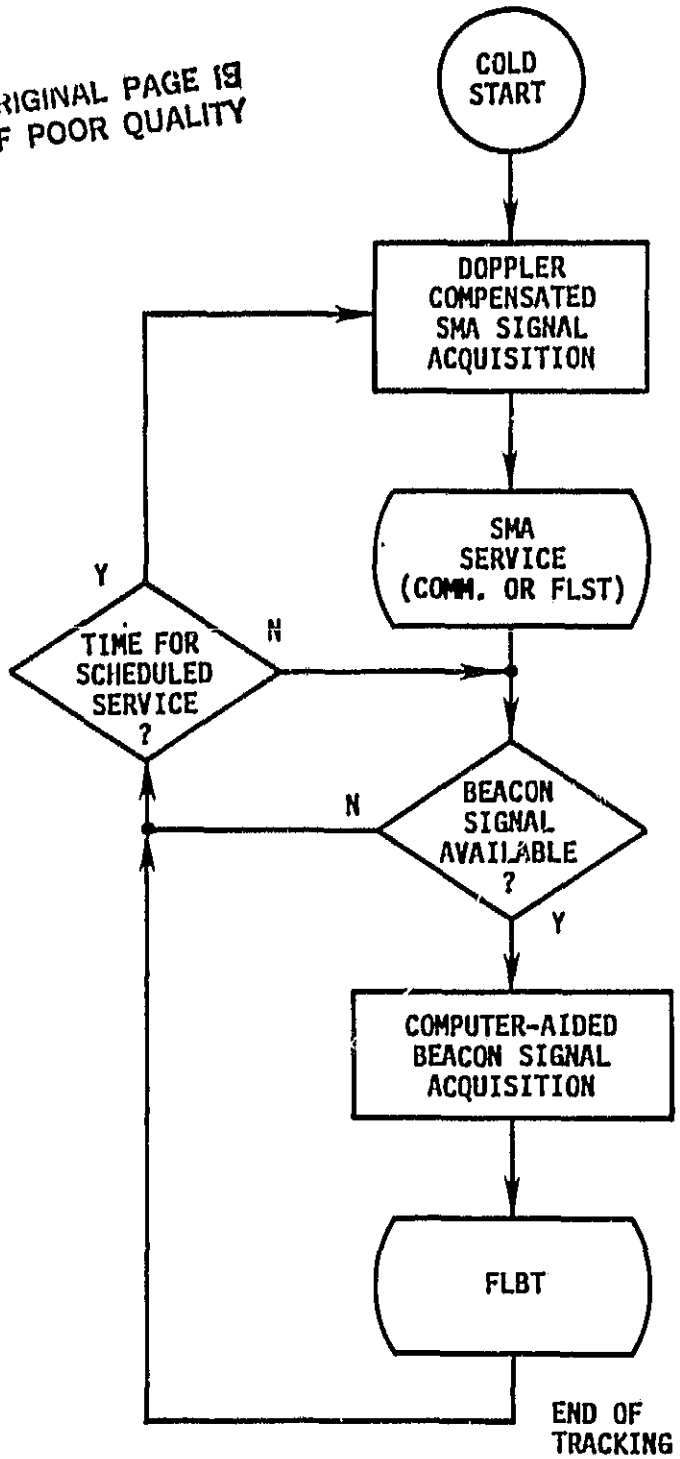

3.1.4 Tracking Data Measurement Accuracy

From the analyses of Appendix B, measurement errors for both FLBT and FLST modes were estimated and are shown in Table 3-3. The thermal noise calculations assume that the user G/T equals -27 dB/°K as a baseline value; code and carrier loop parameters are assumed to be in keeping with current design practice. It can be seen that the range error is dominated by systematic delay errors encountered in the ground-to-TDAS link. These are assumed to be roughly the same as specified for TDRSS, with a total systematic delay of 10 meters conjectured if a routine and thorough system calibration capability is implemented [15].

Range-rate error for FLBT is dominated by thermal noise, reflecting the relatively low power of the beacon signal. Increased beacon power and, of course, higher user G/T values would diminish the error. For FLST, phase noise introduced by the ground frequency standard and the voltage-controlled oscillators (VCO's) on-board the TDAS satellite are major components of the total range-rate error. The estimated phase noise contribution is derived from consideration of possible TDAS mixing frequency schemes, as detailed in Appendix B. The alternative of a K_a-band ground-to-TDAS link versus the K_u-band link used in TDRSS introduces additional phase noise into range-rate measurements due to the larger frequency multiplies involved, thus dominating the total range-rate error. Use of a crystal oscillator disciplined to the ground cesium frequency standard would, however, improve the ground contribution to phase noise. To estimate the impact, the analysis of Appendix B.3 was applied using the crystal oscillator phase noise spectral density for frequencies less than 1000 Hz and that of the cesium oscillator for frequencies greater than 1000 Hz as an approximation to the possible ground phase noise spectral density. This leads to a ground contribution of roughly .3 mm/s with a Ku-band pilot tone and roughly .6 mm/s with a K_a-band pilot tone. In comparison to the pessimistic values cited in Table 3-3 (1.8 and 2.0, respectively), the improvement is significant.

TABLE 3-3

SUMMARY OF FORWARD LINK TRACKING DATA MEASUREMENT ERRORS

ERROR CONTRIBUTOR		RMS RANGE ERROR (METERS) FLBT	RMS RANGE ERROR (METERS) FLST	RMS RANGE-RATE ERROR (MM/SEC) FLBT	RMS RANGE-RATE ERROR (MM/SEC) FLST	NOTES
THERMAL NOISE		4.9	1.0	5.5	1.8	• USER G/T = -27 dB/°K • PN TRACKING LOOP B_L = 1.0 Hz
TDAS SYSTEMATIC DELAY (ESTIMATED)	S/C	10.5	10.5	-	-	• ESTIMATES BASED ON TDRSS USER'S GUIDE (STDN 101.2 [2])
	GND	9.0	9.0			
		(10.0)*	(10.0)*			
PHASE NOISE (ESTIMATED)	USER	-	-	0.2	0.2	• 1-WAY DOPPLER TRACKING • K_U-BAND GROUND-TDAS LINK
	TDAS S/C			2.0 (4.4)**	2.0 (4.4)**	
	GND			1.8 (2.0)**	1.8 (2.0)**	
RSS	RANDOM	4.9	1.0	6.1 (7.3)**	3.2 (5.8)**	
	SYSTEMATIC	13.8	13.8	-	-	
		(10.0)*	(10.0)*			

* ESTIMATED TOTAL SYSTEMATIC DELAY WITH CALIBRATION [15].

** WITH K_a-BAND GROUND-TDAS LINK.

TABLE 3-4

RETURN LINK TRACKING SIGNAL CHARACTERISTICS

SIGNAL CHARACTERISTICS	SCHEDULED (RLST)
TYPE	STAGGERED QUADRIPHASE PN (SQPN) (PER TDRSS DG1-MODE 2/NONCOHERENT)
CODE	- 2047 CHIP GOLD CODES ON I AND Q CHANNELS (OFFSET $\geq$ 20,000 CHIPS) - 3.0778×10^6 CHIPS/SEC
DATA*	- INCLUDES USER PN CODE EPOCH, CURRENT TIME REFERENCE AND SYNCH WORD FOR AMBIGUITY RESOLUTION - CONVOLUTIONALLY-CODED (RATE 1/2)

*MODULO-2 ADDED ASYNCHRONOUSLY TO BOTH PN CODES

3.2 RETURN LINK TRACKING (RLST)

3.2.1 Tracking Signal Definition

As a one-way navigation option, RLST involves the ground tracking of non-coherent transmissions by user spacecraft using the S-band multiple access return service. The signal structure is assumed to be consistent with TDRSS DG1 Mode 2 [2] and is shown in Table 3-3. As with forward link tracking, an ultra-stable oscillator is required on-board the user spacecraft to provide an accurate time and frequency standard. The user-unique 2047-chip Gold codes on the I and Q channels are not long enough to resolve range ambiguity; the data must therefore be synchronously modulated by the PN codes to allow bit and frame synchronization at the ground receiver to eliminate the ambiguity. To support one-way navigation, the data must contain the user's PN code epoch and timing information.

3.2.2 Link Performance

In order to evaluate the measurement errors in Return Link Scheduled Tracking due to thermal noise, the link budget of Figure 3-5 was used to caluclate C/N_0. As in the calculations for forward link tracking, the stronger TDAS-to-ground link is neglected here. The budget assumes a G/T figure of -14.1 dB/°K per element of the 60-element TDAS SMA antenna array with the 60 elements providing a theoretical combiner gain of 17.7 dB. The received C/N_0 at the TDAS satellite (approximately equal to that received at the ground) is thus a function of the user EIRP. If a 10^{-5} bit error rate, a 5 dB convolutional coding gain and a 3 dB margin are assumed, Figure 3-5 shows the return link achievable data rate plotted against user EIRP. For example, a 1000 kbps user would require an EIRP $\approx$ 0 dBW.

3.2.3 Tracking Data Measurement Accuracy

Table 3-5 summarizes the RLST measurement errors estimated using the techniques of Appendix B. Salient performance characteristics of the Harris wide dynamics demodulator were used to model the ground receiver's response

FIGURE 3-5: TDAS SMA RETURN LINK: ACHIEVABLE DATA RATE VS. USER EIRP

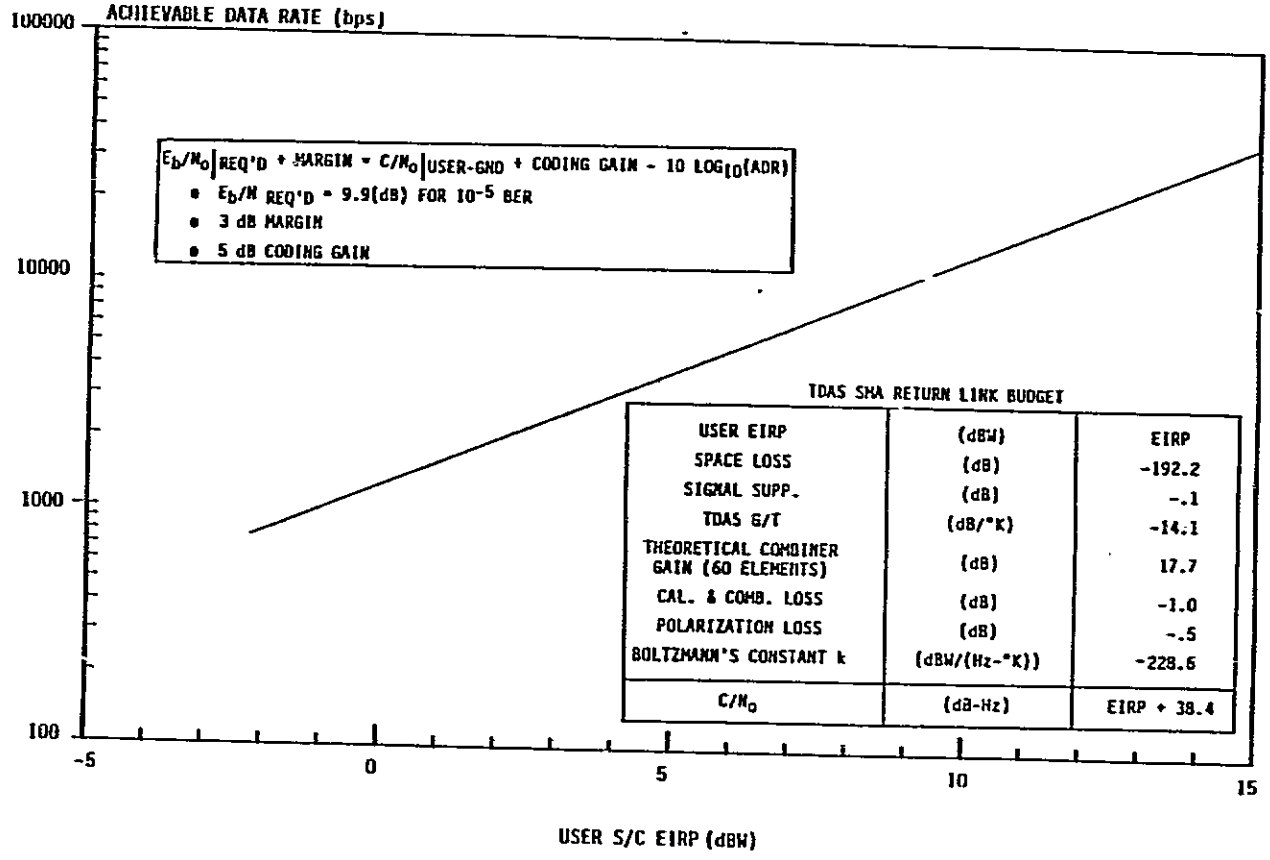

TABLE 3-5

SUMMARY OF RETURN LINK SCHEDULED TRACKING MEASUREMENT ERRORS

ERROR CONTRIBUTOR		RMS RANGE ERROR (METERS)	RMS RANGE-RATE ERROR (MM/SEC)	NOTES
THERMAL NOISE		2.5	3.5	• USER EIRP = 2 dBW • WIDE DYNAMICS DEMODULATOR
TDAS SYSTEMATIC DELAY (ESTIMATED)	S/C	10.5 (10.0)*		• ESTIMATES BASED ON TDRSS USER'S GUIDE (STDN 101.2 [2])
	GND	9.0	-	
PHASE NOISE (ESTIMATED)	USER		.2	• 1-WAY DOPPLER TRACKING • K_u-BAND GROUND-TDAS LINK
	TDAS S/C	-	2.8 (4.6)**	
	GND		5.7 (8.6)**	
RSS	RANDOM	2.5	7.3 (10.4)**	
	SYSTEMATIC	13.8 (10.0)*	-	

* ESTIMATED TOTAL SYSTEMATIC DELAY WITH CALIBRATION [15]

** WITH K_a-BAND TDAS S/C-GROUND LINK.

to thermal noise. As a baseline value, the user spacecraft is assumed to transmit an EIRP of 2 dBW, thus yielding a nominal C/N_0 of approximately 40.4 dBW at the demodulator. Systematic errors in range and range-rate measurements are estimated as for the forward link tracking modes. Again, TDAS systematic delays dominate the range error value.

Range-rate error is seen to depend most on phase noise introduced by the ground frequency standard. This result, however, pessimistically disregards the possible use in TDAS of a phase-locked crystal oscillator disciplined to the cesium frequency standard. If such a method were employed, the phase noise spectral density of the ground standard would be improved, reducing its phase noise contribution to range-rate errors. Calculations using the phase noise spectral density mentioned in Section 3.1.4 yield a ground contribution of .9 mm/s for a system using a K_u-band pilot tone and 1.5 mm/s with a K_a-band pilot tone. This compares to the quoted results of 5.7 mm/s and 8.6 mm/s, respectively. With this approximation, thermal noise becomes the dominate range-rate error source for RLST.

SECTION 4

TDAS TRACKING ANALYSIS

Accurate knowledge of TDAS satellite ephemerides is necessary for user navigation support and TDAS orbit maintenance functions. This section presents a preliminary analysis of TDAS satellite tracking to:

- Identify potential system configuration and operational impacts of TDAS constellation alternatives, and
- Estimate potential tracking accuracy based on BRTS and VLBI techniques.

An overview of the elements considered in pursuing this analysis is given in Figure 4-1.

4.1 TRACKING CONFIGURATIONS

Several constellation/network options identified in the TDAS study [1d,e], are illustrated in Figure 4-2. Satellite spacings as well as frontside/backside deployments were chosen to assess possible coverage improvements and data distribution alternatives for servicing multiple earth stations in CONUS. Distributed, direct access links to/from CONUS are achieved by satellite crosslinks and/or multi-beam antenna enhancements on the TDAS satellites.

In terms of TDAS tracking, however, the various constellation options can be reduced to two situations: frontside and backside satellites. The following subsections discuss BRTS and VLBI tracking configurations to support either case.

FIGURE 4-1: TDAS TRACKING ANALYSIS - OVERVIEW

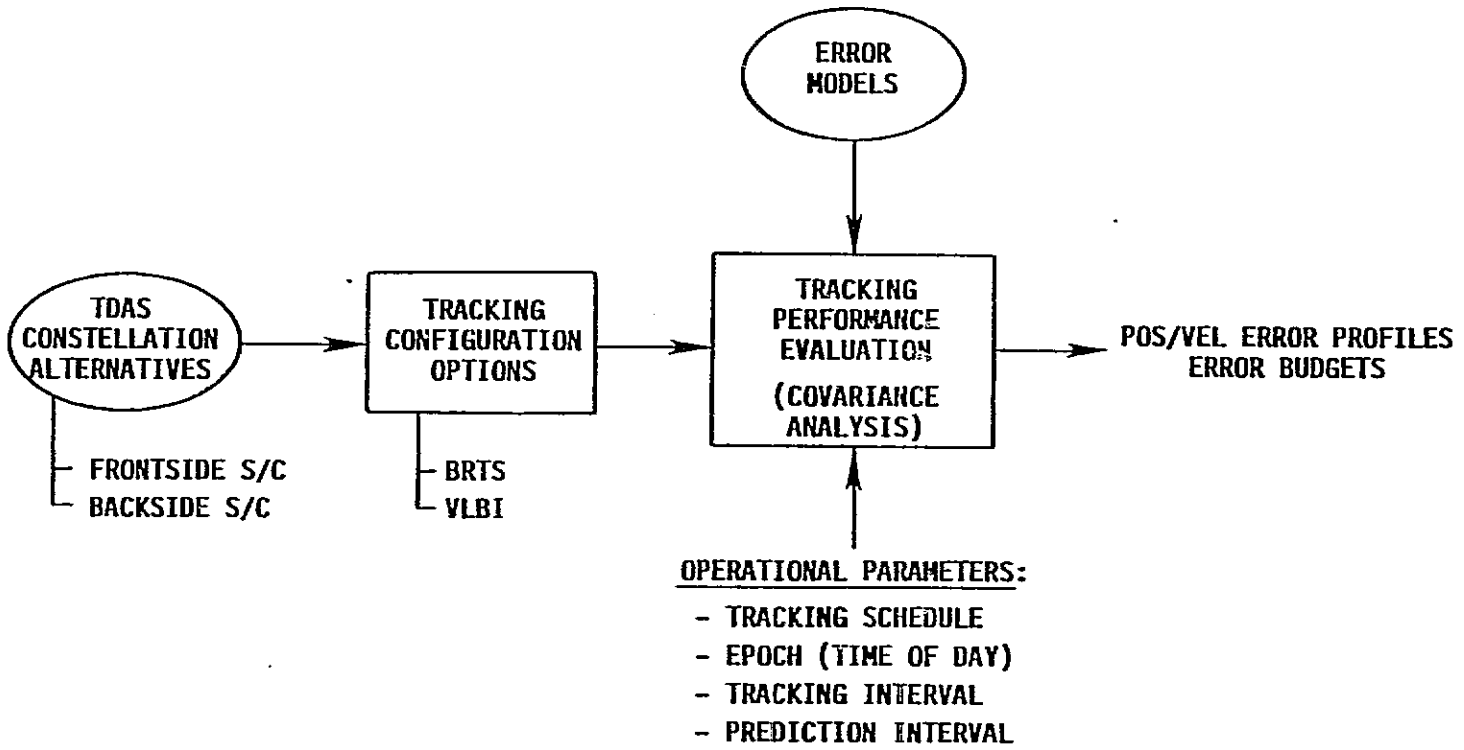

STANFORD TELECOMMUNICATIONS INC.

FIGURE 4-2: TDAS CONSTELLATION/NETWORK OPTIONS

OPTION 1: TWO FRONTSIDE

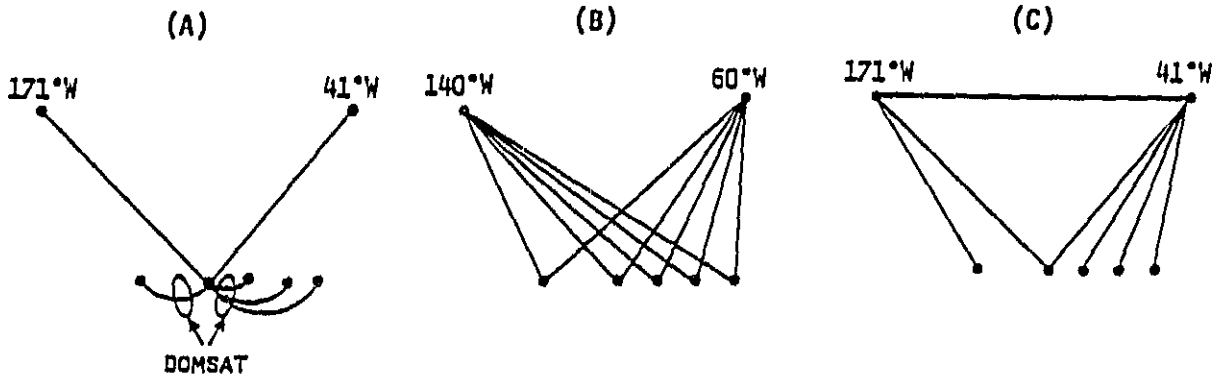

OPTION 2: ONE FRONTSIDE/ONE BACKSIDE

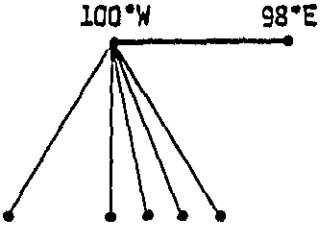

OPTION 3: TWO FRONTSIDE/ONE BACKSIDE

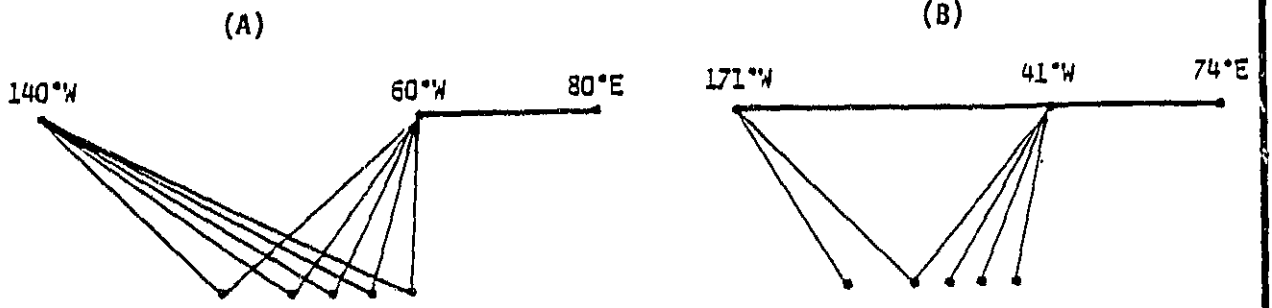

STANFORD TELECOMMUNICATIONS INC.

4.1.1 BRTS Tracking

Analogous to the TDRSS implementation, two-way range and range-rate tracking data ($R,\dot{R}$) are assumed to be acquired with Bilateration Ranging Transponders (BRT) operating at pairs of automated ground stations (one pair per TDAS). Tracking transmissions originate at White Sands (WSN) with replys from a co-located BRT and one at a geographically displaced site. A typical data rate would be 1-5 observations per minute for 5 minutes every hour, as expected for TDRSS. [8].

Figure 4-3 lists some geometrically compatible station pairs* that cover four of the TDAS locations considered. (see also Figure 4-4) Two satellites are at TDRS locations and a third (at 100°W) is in full view of CONUS. The fourth is a backside satellite (at 98°E) which requires a satellite-satellite crosslink in the BRTS configuration if WHS is the base location for originating transmissions. This impacts tracking accuracy, since measurements are also affected by uncertainties in the frontside satellite orbit.

The last two BRTS configurations suggested for backside TDAS tracking in Figure 4-3 employ <u>two</u> backside stations to offset the crosslink impact. In the first approach, one station is configured to emulate WHS for tracking data generation and measurement, but this would add a significant overseas hardware and maintenance requirements. In the second approach, each two-way measurement made between WHS and a backside station pair (S_2', S_2'') is differenced with a corresponding measurement (M_T) made between WHS and the backside TDAS. The effect is to cancel systematic uncertainties in the crosslink and frontside space/ground link. However, this also increases the noise error due to the additional measurement (M_T), although increasing the data rate sufficiently may permit additional data smoothing to offset this.

* Political issues regarding potential overseas sites were not considered.

FIGURE 4-3: BRTS CONFIGURATIONS FOR TDAS TRACKING

BRTS CONFIGURATIONS:

S = S -BAND
K = K_u-BAND
W = W -BAND

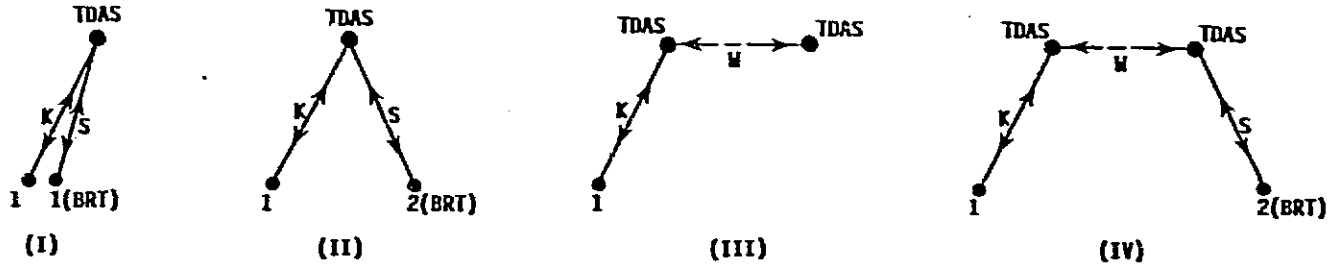

TDAS		TRACKING CONFIGURATION	STATION SITES STN 1	STN 2
FRONTSIDE	171°W	I,II	WHS	ALS*
	41°W			ACN*
	100°W			AGO, EIL or HAW
BACKSIDE	98°E	1/ III,IV	WHS	GWM, DGA or BUR
		2/ I,II	GWM	DGA or BUR
		3/ III,IV(2)	WHS	GWM & DGA or GWM & BUR

* EXISTING SITES FOR TDRSS.

FIGURE 4-4: POTENTIAL GROUND SITES TO SUPPORT TDAS SATELLITE TRACKING

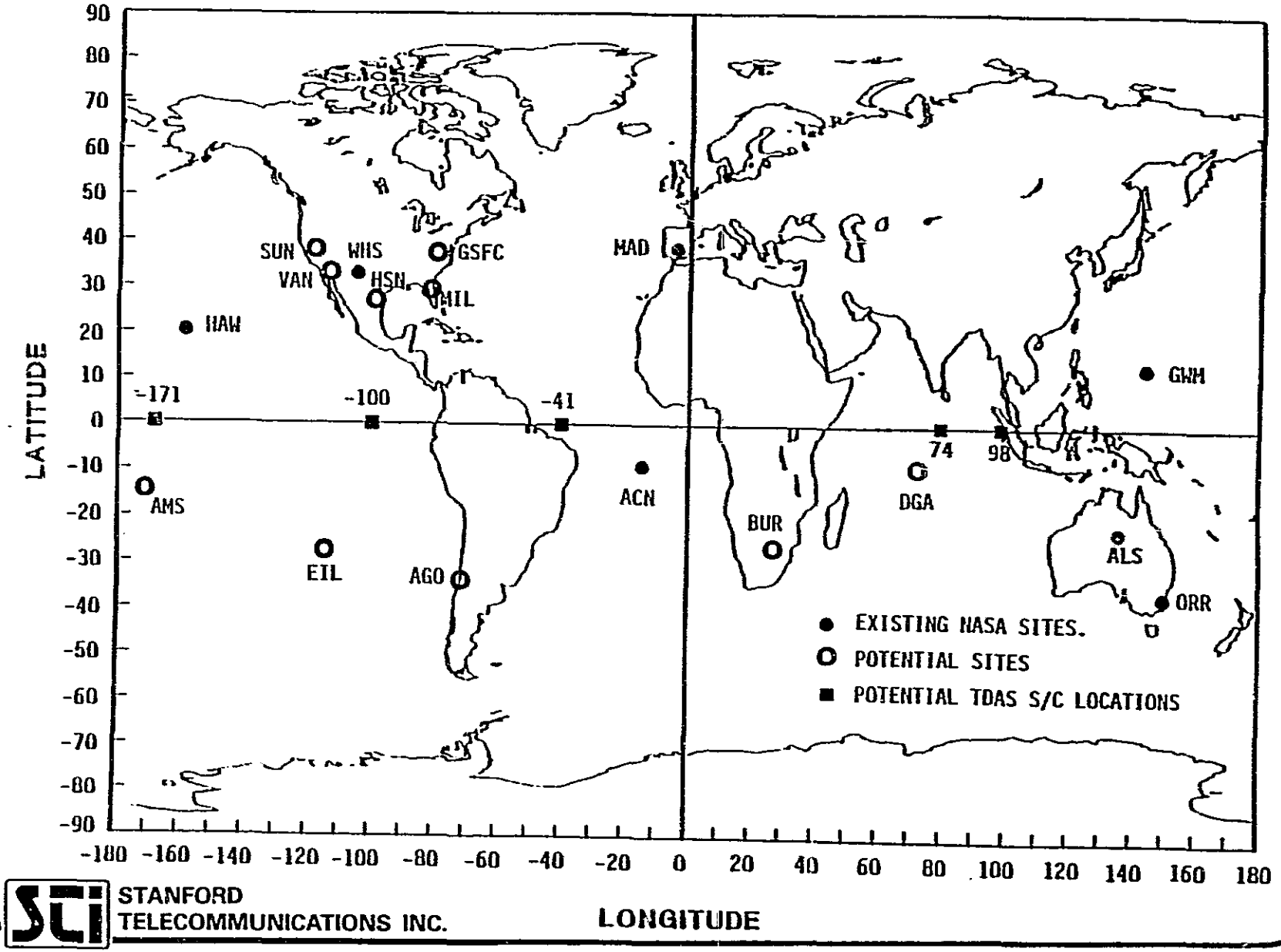

STANFORD TELECOMMUNICATIONS INC.

4.1.2 VLBI Tracking

The VLBI technique is under investigation as a possible BRTS enhancement [9] with potential for high accuracy TDRS tracking. The fundamental VLBI measurement data type is equivalent to the difference in range (ΔR) between a signal source and two receivers displaced along a known baseline. For a typical measurement, wideband RF signals are received at two sites, mixed down to baseband and recorded over a prescribed interval. Signal phase coherence and time synchronization are maintained at each site with an ultra-stable frequency standard. Subsequent crosscorrelation of the two signal streams determines the relative difference in time of arrival which equals (after converting to distance) the geometric range difference plus measurement errors (random and systematic). Investigators at GSFC using signals sampled from celestial radio sources by several VLBI stations report capabilities for ΔR measurement precision in the 0.3-3 cm range. [20]

For the TDAS application, tracking signals assumed to originate at WHS are relayed by the satellite constellation to automated VLBI ground stations. Received signals are time tagged and buffered and, on command, returned via TDAS to WHS for processing. A representative measurement data rate would be one processed pair of VLBI observations (ΔR) every hour per station set. Nominally, one set of three stations with adequate baseline geometry would be needed per TDAS satellite.

Figure 4-5 lists some geometrically-compatible 3 station sets that cover the 4 TDAS satellites considered (see also Figure 4-4). The station sets are grouped in terms of long and moderate baselines, the latter of interest in a CONUS-based VLBI network for frontside TDAS tracking. For the backside satellite, no significant impact on measurement accuracy due to the cross-link would be expected, since the equivalent time-of-arrival differencing in the signal processing tends to cancel common path uncertainties.

FIGURE 4-5: VLBI CONFIGURATIONS FOR TDAS TRACKING

VLBI CONFIGURATIONS:

S = S -BAND
K = K_u-BAND
W = W -BAND

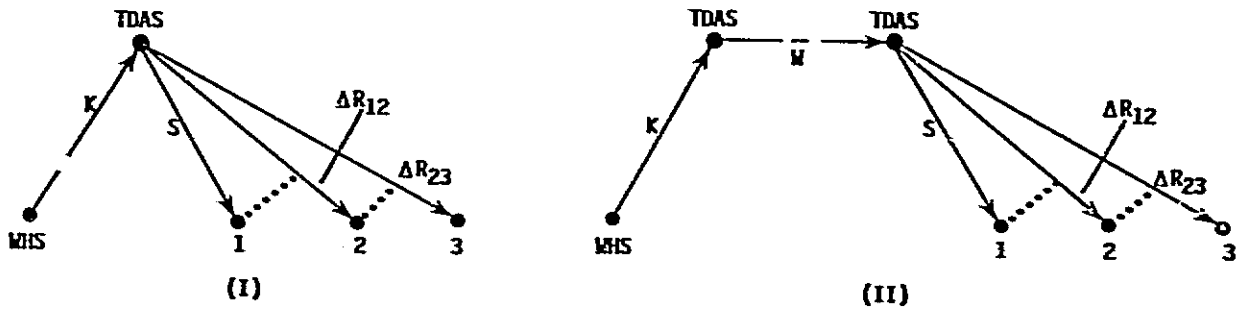

TDAS		TRACKING CONFIGURATION	STATION SITES (1, 2, 3) LONG BASELINE	STATION SITES (1, 2, 3) MODERATE BASELINE
FRONTSIDE	171°W	I	WHS, ALS, GWM or " , " , AGO	WHS, SUN, HAW or " , " , VAN
	41°W		WHS, ACN, MAD or " , " , AGO	GSFC, HSN, MIL
	100°W		WHS, HAW, AGO or " , " , EIL	GSFC, HSN, SUN
BACKSIDE	98°E	II	GWM, ALS, DGA or " , " , BUR	

ORIGINAL PAGE IS OF POOR QUALITY

Relative errors between stations (e.g., clock synchronization and baseline uncertainties) are a general concern, since they can have a significant impact on TDAS OD accuracy. A possible alternative to relieve stringent calibration requirements at each station is to periodically include VLBI differences, i.e., ΔVLBI measurements in the tracking process. For this, additional VLBI observations derived from a known celestial radio source are subtracted from TDAS VLBI observations made for the same station pair. The effect is to cancel station time synchronization errors and reduce effects of station survey errors on TDAS OD accuracy.

Of course, the ΔVLBI alternative would introduce additional equipment complexity at each station to also receive celestial source signals. Data handling requirements would also be increased. Equipment complexity and operational aspects are important issues especially for backside VLBI tracking since 3 remote stations per TDAS are involved compared to 1 (or perhaps 2) for BRTS.

4.2 TDAS TRACKING ACCURACY

Information about TDAS orbits is assumed to be provided for user OD/TD on a recurring basis. User navigation performance is then a function of TDAS orbit uncertainties in the interval between updates (i.e., prediction interval errors). To assess potential orbit prediction errors, an accuracy analysis was made of TDAS tracking with the BRTS and VLBI techniques. The following subsections discuss the error modelling approach and the major results. Additional details are given in Appendix C.

4.2.1 Error Modelling

In this study it was assumed that TDAS OD is performed for a prescribed epoch via batch processing of tracking observations taken over a given data arc (or tracking interval). The epoch solution propagated beyond the end of tracking (EOT) is the satellite orbit state in the prediction interval. Orbit prediction error covariances were evaluated using the ORAN program,

a linear covariance analysis tool [16, 17]. ORAN was configured to compute satellite orbit uncertainties versus time from epoch, given the following input data:

- Initial State Vector - All TDAS were assumed to be in 5°, circular, geosynchronous orbits with epoch location at the nominal longitude indicated in Figures 4-3 and 4-5.

- Tracking Station Locations - Stations pertaining to a given TDAS and tracking technique are identified in Figures 4-3, 4 and 5 with specific locations as tabulated in Appendix C.4.

- Tracking Schedule - BRTS observations were assumed to occur at 1/min for 5 mins/hr and VLBI observations at 1/min to 1/hr*.

- Tracking Error Model - Values are stated in Table 4-1. All local and dynamic errors were treated as systematic consider error sources in the analysis.

BRTS measurement errors are consistent with values used for TDRS OD analyses [18] assuming comparable equipment and link quality. Station errors were improved by 3:1 assuming better site survey capabilities in the TDAS time-frame.

VLBI measurement errors were considered at two levels: a baseline model consistent with values used in studies of a Deep Space Network (DSN) tracking application to TDRSS [19] and a reduced model which reflects achieved capabilities with VLBI stations observing celestial radio sources [20]. Station errors were taken to be the same as BRTS for the baseline model and an order of magnitude better for the reduced model.

* OD performance was evaluated as a function of VLBI data rate. (See Appendix C.3).

TABLE 4-1

TDAS TRACKING ERROR MODEL ASSUMPTIONS

ERROR SOURCE		1σ VALUES		
		BRTS	VLBI (BASELINE MODEL)	VLBI (REDUCED MODEL)
MEASUREMENT - BRTS ($R/\dot{R}$) - VLBI (ΔR)	NOISE	2 M/.13 CM/S	0.9 M	0.03 M
	BIAS	10 M/0 CM/S	3 M	0.1 M
LOCAL	STATIONS (X,Y,Z)	3 M	3 M	0.3 M
	TROPOSPHERIC REFRACTION	15%		
DYNAMIC	GM GRAV. POT.	10^{-7} 100% OF GEM5 - GEM1		
	SOLAR PRESSURE*	10%		

* TDAS AREA/WEIGHT = .042 M^2/KG (SAME AS TDRS).

STANFORD TELECOMMUNICATIONS INC.

The tropospheric and solar pressure errors reflect modelling inaccuracies and are standard values used in TDRS OD studies [18,19], although some improvement may be possible. The gravitational errors are conservative since further improvements are likely by the TDAS timeframe.

4.2.2 Error Analysis Results

TDRS studies indicate that the choice of tracking interval and reference epoch can significantly impact both definitive and predictive OD accuracy. A recent study [18] of TDRS tracking via BRTS evaluated orbit position/velocity uncertainties over a 24 hour prediction interval* as a function of each parameter. Results show that a judicious combination can be selected in which the maximum uncertainty in the prediction interval is at or near a minimum.

In the TDAS study it was decided to also consider the prediction interval as a selectable parameter. The basic rationale is that a sequence of shorter prediction intervals with better accuracy may be traded off against more frequent OD processing for user navigation data updating. In both BRTS and VLBI analyses efforts were made to identify multiple combinations (epoch/tracking interval/prediction interval) which, taken together, yield better accuracy over a 24 hour period than any one alone.

4.2.2.1 BRTS Tracking. TDAS position uncertainty was computed over a 24 hour prediction interval as a function of tracking interval and epoch for both frontside (100°W) and backside (98°E) cases. Figure (4-6) presents results plotted from the end of tracking (EOT) for several tracking intervals with a common epoch (satellite local noon) assumed in each case.**

* The 24 hour interval was considered since TDRS OD is planned to be performed only once per day.

** Epoch times are stated as Greenwich Mean Time. The tracking configurations are based on Figure 4-3: frontside tracking - Configurations I and II; backside tracking (Option 1) - Configurations III and IV (T100 means TDAS @ 100°W is the relay to/from the backside TDAS @ 98°E).

FIGURE 4-6: TDAS POSITION UNCERTAINTY IN PREDICTION INTERVAL VS. BRTS TRACKING INTERVAL

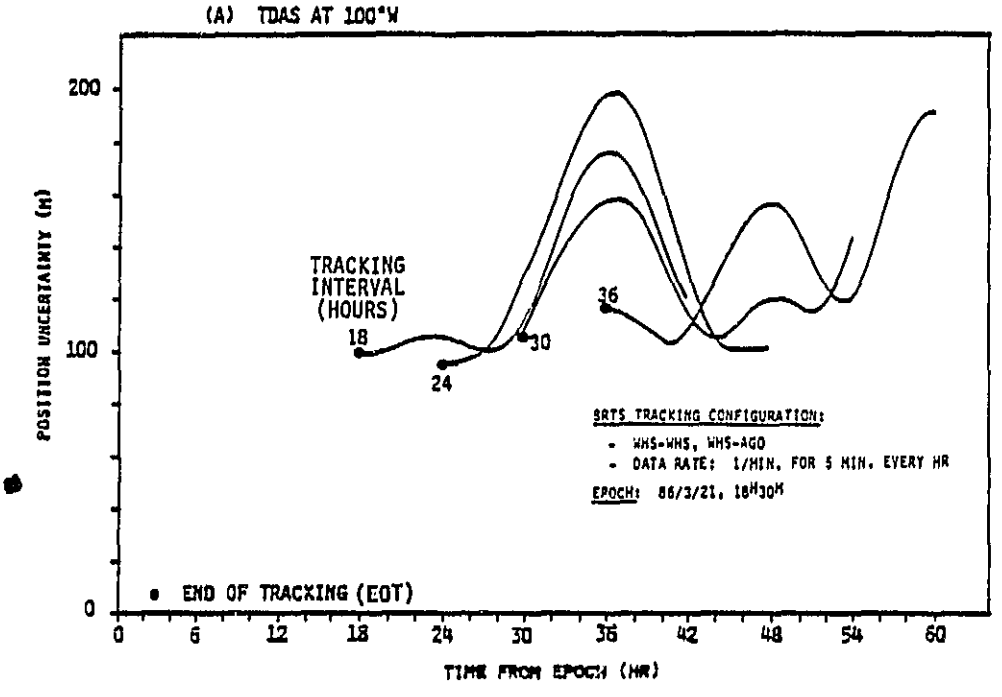

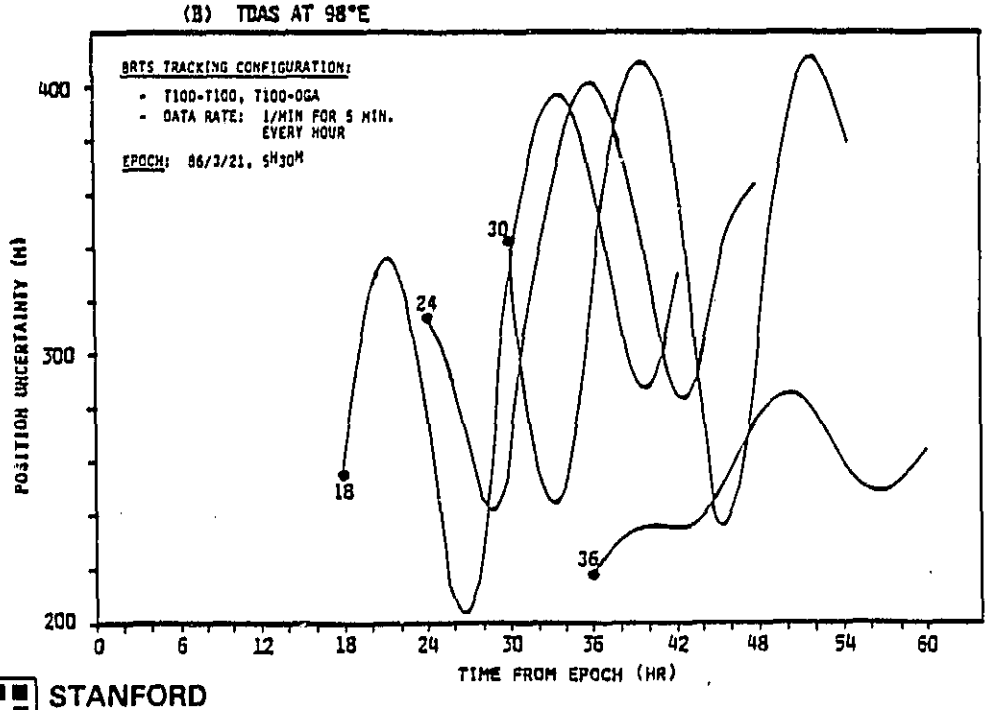

STANFORD TELECOMMUNICATIONS INC.

In the frontside results shown in Figure (4-6a), the peak uncertainty is due primarily to solar pressure modelling error, the leading error contributor. Consequently, the peak value turns out to be an oscillatory function of epoch with a 12 hour cycle over epoch time of day. As observed in Appendix C however, even the lowest peak values exceed, by at least 30%, the position uncertainty for the 18 hour tracking case in the 12 hour period after EOT (see Figure 4-6a). Also, because of the 12 hour cyclic property, approximately the same error profile occurs with epoch placed at local midnight. Thus, orbit predictions from two 18 hour tracking intervals with epochs at noon and midnight could be concatenated to produce a comparatively flat prediction error profile over 24 hours. Comparison of the maximum prediction uncertainties and primary contributors for continuous and concatenated cases is shown in Table 4-2.

For the backside case shown in Figure 4-6b, the results are also dominated by solar pressure effects. However, they also reflect the frontside TDAS orbit uncertainty which was assumed in this analysis to be constant (at the 100 m level) corresponding to the concatenated 12 hour prediction results discussed above. No significant benefit is apparent from using a similar approach in this case based on 36 hour tracking, since the peak uncertainty over 24 hours is nearly the same as over 12 hours. A comparison of the peak values and primary error contributors can be made from the data in Table 4-2. Corresponding peak TDAS velocity errors are in the 8 mm/sec and 19 mm/sec range for the frontside and backside tracking cases, respectively.

The preliminary observation here is that the orbit prediction uncertainty over 24 hours for the backside TDAS (with tracking configuration Option 1*) is apparently more than double that for the frontside TDAS. Certainly further analysis is warranted however, to evaluate possible improvements that alternative configurations and/or processing approaches may yield, e.g.,

* Tracking configuration options are defined in Figure 4-3.

TABLE 4-2

MAXIMUM TDAS POSITION ERROR IN 24 HOUR PREDICTION INTERVAL WITH BRTS TRACKING

TDAS	TRACKING INTERVAL (HOURS)	PREDICTION INTERVAL(S) (HOURS)	MAXIMUM POSITION ERROR (M)	PRIMARY ERROR CONTRIBUTORS* (M)
FRONTSIDE 100°W	18	24	175	150 (SP) 80 (B) 40 (S)
	18	12 + 12**	110	80 (B) 60 (SP) 45 (S)
BACKSIDE 98°E	36	24	290	230 (S') 175 (SP) 25 (B)
	36	12 + 12**	280	220 (S') 165 (SP) 25 (B)

* LEGEND: SP - SOLAR PRESSURE; B - BRT BIAS; S - STATION SURVEY;
S' - STATION SURVEY + T100 LOCATION (TDAS 100°W).

** CONCATENATED INTERVALS BASED ON TRACKING INTERVAL EPOCHS SPACED ~12 HOURS APART.

- Backside tracking configuration Options 2 or 3* which utilize another backside station.

- Joint data processing for frontside and backside TDAS OD that accounts for mutual error source correlations that an independent solution (assumed here) does not.

4.2.2.2 VLBI Tracking. TDAS position uncertainty was computed over a 24 hour prediction interval as a function of the VLBI tracking interval and TDAS location for two error models defined earlier in Table 4-1. One is a conservative (baseline) error model and the other is a more optimistic (reduced) error model.

Figure 4-7 presents results for the baseline model plotted from the end of tracking (EOT) with a common epoch (satellite local noon) assumed in each case. The results in Figure 4-7b indicate that VLBI tracking performance is relatively insensitive to TDAS location, frontside or backside.

As shown in Appendix C, solar pressure modelling error is a major contributor for the longer tracking intervals ($\geq$ 18 hours). Since this effect is also cyclic with epoch time of day, essentially the same error profiles result with epoch selected at local midnight. Thus, if the prediction interval segments for 18 and 36 hour tracking are concatenated appropriately, a significantly lower prediction uncertainty over 24 hours could be achieved than with any individual case alone.**

With the shorter tracking and prediction intervals ($\leq$ 12 hours), measurement and local error sources (noise, bias and station survey) are dominant elements. As illustrated in Figure 4-7a however, the prediction uncertainty increases significantly as the tracking interval decreases. While a slight improvement in prediction performance can be achieved by also estimating

* Tracking configuration options are defined in Figure 4-3.

**Results with VLBI bias estimation are given in Appendix C.3. These show that prediction segments for 18 and 12 hour tracking segments would give somewhat better accuracy that the 18 and 36 hour combination.

FIGURE 4-7: TDAS POSITION UNCERTAINTY IN PREDICTION INTERVAL VS. VLBI TRACKING INTERVAL AND TDAS LOCATION

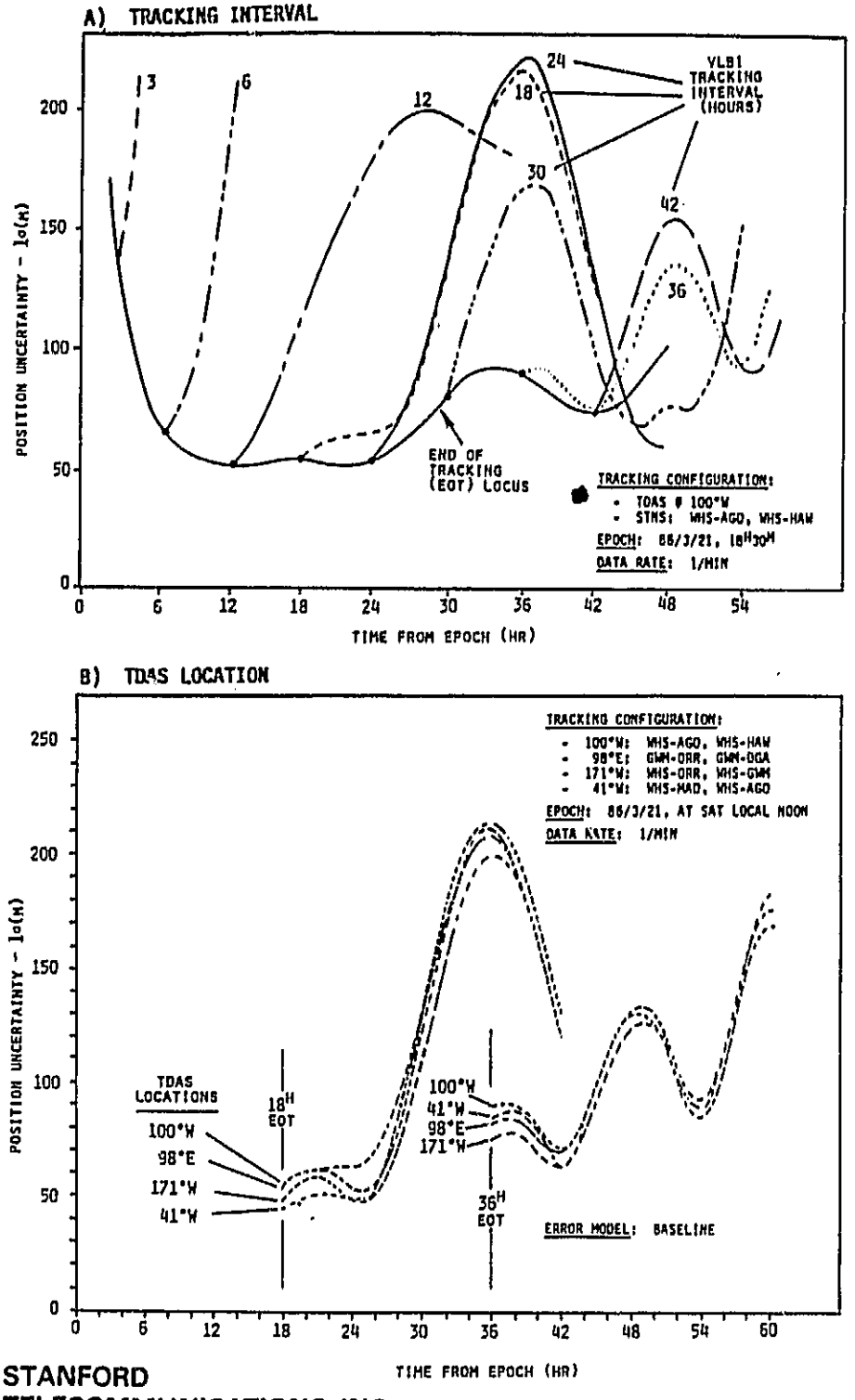

STANFORD TELECOMMUNICATIONS INC.

the VLBI measurement bias, no really significant benefit is apparent from using shorter tracking and prediction intervals, when VLBI measurement and local errors are at the levels assumed in the baseline model. However, if a VLBI implementation can be realized with these errors at the level assumed in the reduced model, a different situation emerges.

Figure 4-8 compares TDAS position uncertainties for short tracking and prediction intervals for both error models. In the latter case, the lowest position uncertainty over a given prediction interval occurs with 6 hour tracking. As observed in Appendix C, this is essentially the cross-over region between tropospheric and solar pressure effects with the latter becoming significant for longer tracking/prediction intervals. Thus, a sequence of short prediction intervals (e.g., 1 hour) could provide a position uncertainty in the range of 10 - 15m.

Figure 4-9 shows examples of TDAS position uncertainty from using multiple (concatenated) prediction segments over a 24 hour period. In the baseline case (Figure 4-9a)* the uncertainty ranges from 50 - 80m using 4 segments based on 18 and 36 hour tracking or 50 - 70m based on 18 and 12 hour tracking with VLBI measurement bias estimated. In the reduced case (Figure 4-9b)* the error ranges from 10 - 12m using 24 one hour segments based on 6 hour tracking intervals with epochs spaced one hour apart. A second curve based on 5% tropospheric error shows the improvement (to 5 - 8m over 24 hours) if better tropospheric error correction can be achieved. A comparison of the peak errors and primary error contributors in each case is given in Table 4-3. Maximum TDAS velocity errors corresponding to these position error results are at the 6 mm/sec and 1 mm/sec levels for the baseline and reduced error models, respectively.

* The assumed VLBI data rate of 1/hr (one ΔR pair/hr) is more representative that the 1/min rate assumed in Figures 4-7 and 4-8. Nevertheless, the computed results for these tracking intervals are identical with either rate. Tables C-1 and C-2 in Appendix C show the impact on prediction uncertainty for other tracking intervals.

FIGURE 4-8: TDAS POSITION UNCERTAINTY IN PREDICTION INTERVAL VS. VLBI TRACKING INTERVAL AND ERROR MODEL

ORIGINAL PAGE IS
OF POOR QUALITY

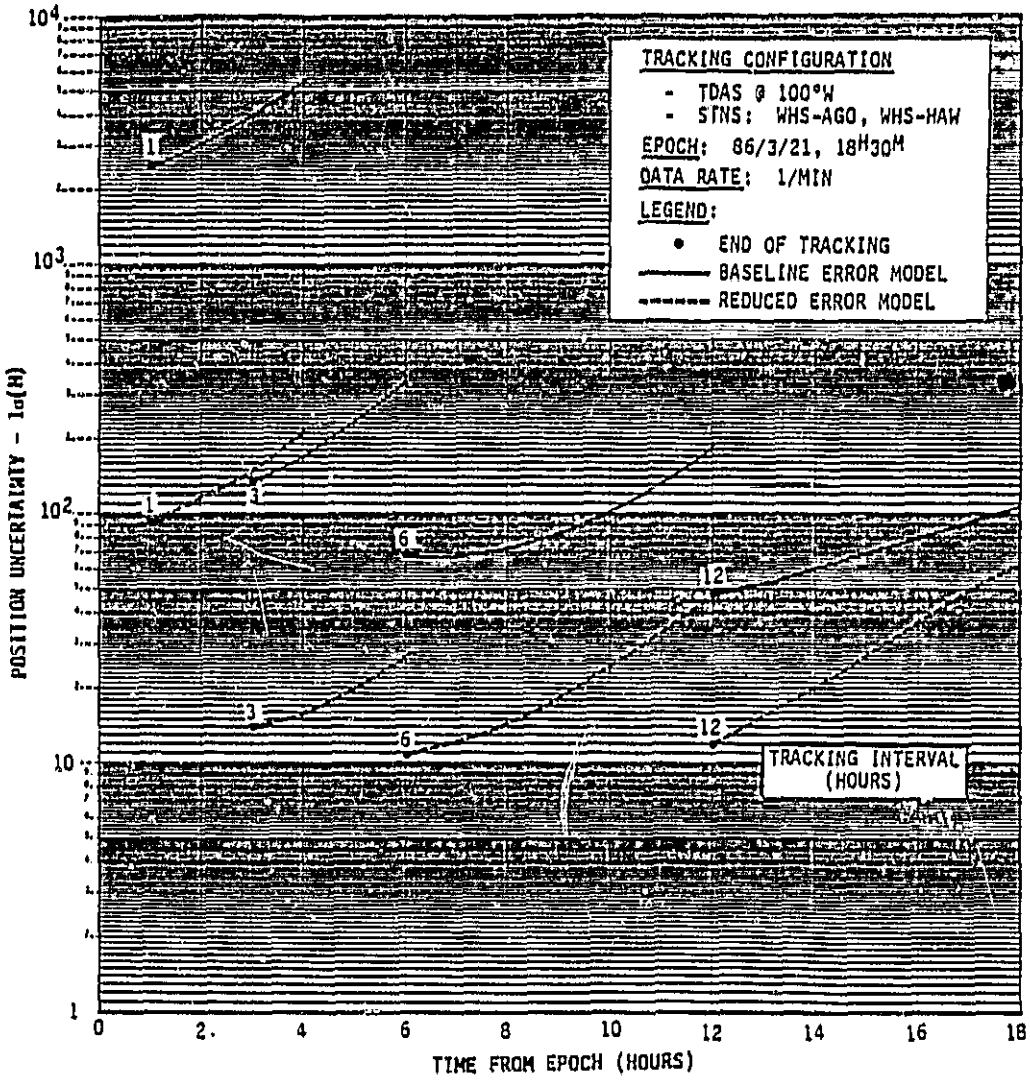

FIGURE 4-9: TDAS POSITION UNCERTAINTY IN 24 HOUR PREDICTION INTERVAL (BASED ON MULTIPLE VLBI TRACKING SEGMENTS)

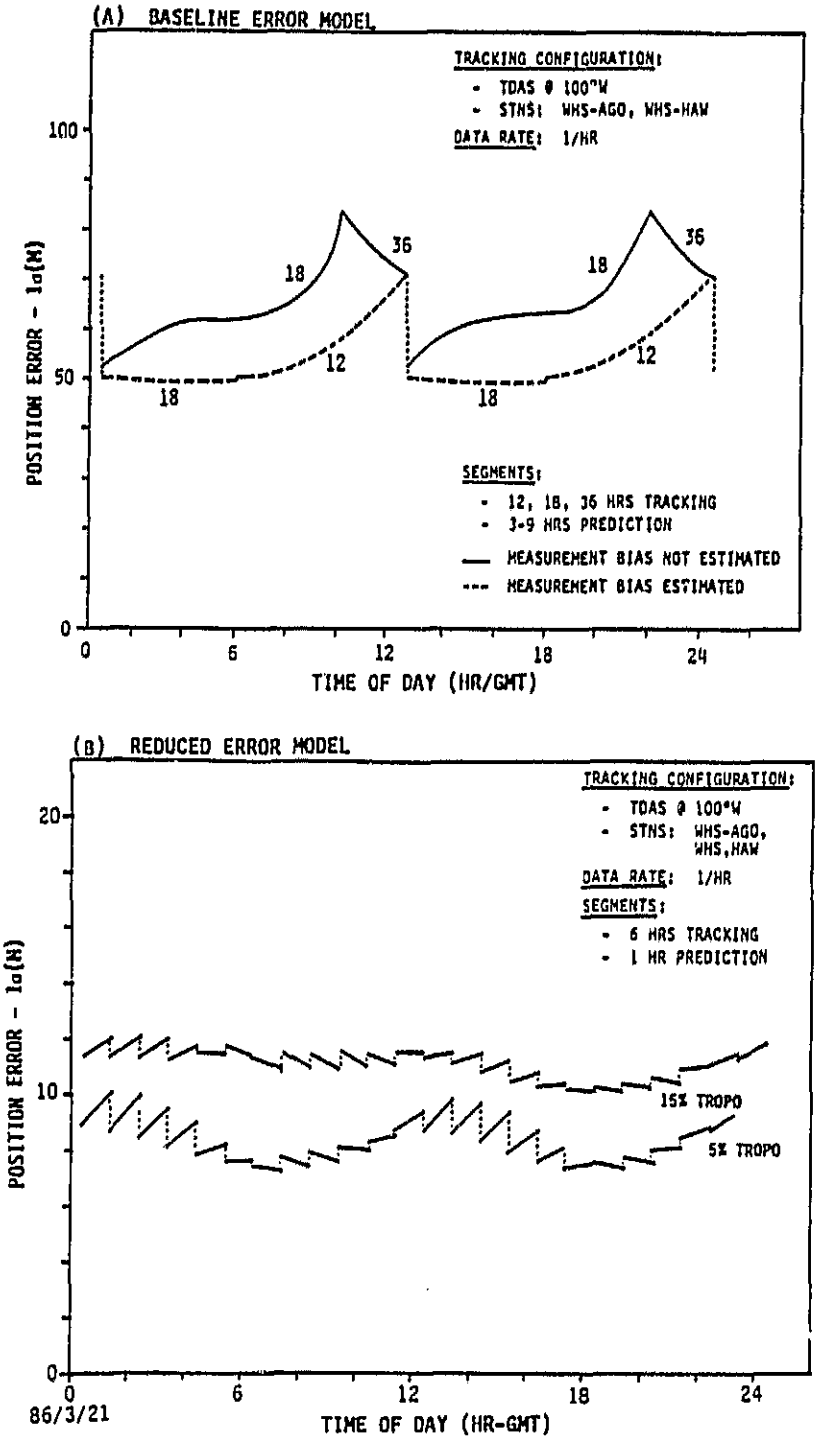

TABLE 4-3

MAXIMUM TDAS POSITION ERROR IN 24 HOUR PREDICTION INTERVAL WITH VLBI TRACKING

VLBI ERROR MODEL	TRACKING INTERVALS (HOURS)	PREDICTION INTERVAL		MAXIMUM POSITION ERROR* (M)	PRIMARY ERROR CONTRIBUTORS** (M)
		NO. SEGMENTS	LENGTH (HOURS)		
BASELINE	18/36	4	9/3	87	72 (SP) 45 (VB) 25 (S)
BASELINE (WITH BIAS ESTIMATED)	18/12	4	6/6	72	56 (SP) 45 (VN) 20 (S)
REDUCED	6	24	1	12	10 (TR) 6 (SP) 4 (S)
REDUCED (W. 5% TROPO)	6	24	1	8	6 (SP) 4 (S) 3 (TR)

* TDAS @ 100°W; STNS: WHS-AGO, WHS-HAW; DATA RATE = 1/HR

** LEGEND: SP - SOLAR PRESSURE
S - STATION SURVEY
VB - VLBI MEAS. BIAS
VN - VLBI MEAS. NOISE
TR - TROPOSHERE

ORIGINAL PAGE IS
OF POOR QUALITY

The foregoing results illustrate the significant improvement in TDAS OD accuracy that the VLBI technique could potentially provide. Moreover, this would apply to backside TDAS tracking as well, since crosslink range uncertainties are inherently cancelled out. It must be emphasized however, that achieving a 10m capability implies having measurement and station survey uncertainties at a level consistent with the reduced error model and using appropriate batch tracking/prediction interval combinations (or equivalent scheme) for OD processing. Thus, important areas for further study include:

- VLBI measurement precision (noise) with TDAS-based signals,
- Alternatives for VLBI tracking network calibration (time synchronization and baselines)
  - via ΔVLBI measurements (see discussion in Section 4.1.2) or
  - via terrestrial microwave links* and a geodetic survey receiver (e.g., GPS [21]),
- OD processing options
  - Algorithm (batch vs sequential)
  - Update rate vs prediction interval.

* This is applicable to CONUS-based tracking configurations (e.g., a connected element interferometer network) currently under study for TDRS [9]. Some preliminary results for TDAS are given in Appendix C.2.3.

SECTION 5

USER NAVIGATION PERFORMANCE EVALUATION

User navigation via TDAS is based on computing orbits and time from range and range-rate measurements and known TDAS orbits. This section presents an evaluation of potential navigation performance in terms of OD/TD accuracy for the three one-way tracking alternatives defined in Section 2.

5.1 OVERVIEW OF APPROACH

Figure 5-1 gives an overview of the elements considered in the analysis. Cases for evaluation were defined to assess several types of user orbits and the impact of TDAS constellation options, different tracking schedules and two algorithms for tracking data processing (sequential and sliding batch).

To evaluate user OD/TD accuracy two error analysis programs were employed:

- SEA Program [22] - for tracking based on sequential processing of measurement data, and
- RDGTDS [23] - for tracking based on batch processing of measurement data.

Given a tracking schedule and nominal TDAS and user orbits each program computes OD/TD error covariances and sensitivities versus time with respect to measurement noise and other applicable error sources. The following subsections discuss the tracking configurations and methodology, the error modelling approach and the major results. Further detailed results are contained in Appendices D and E.

FIGURE 5-1: NAVIGATION PERFORMANCE EVALUATION - OVERVIEW

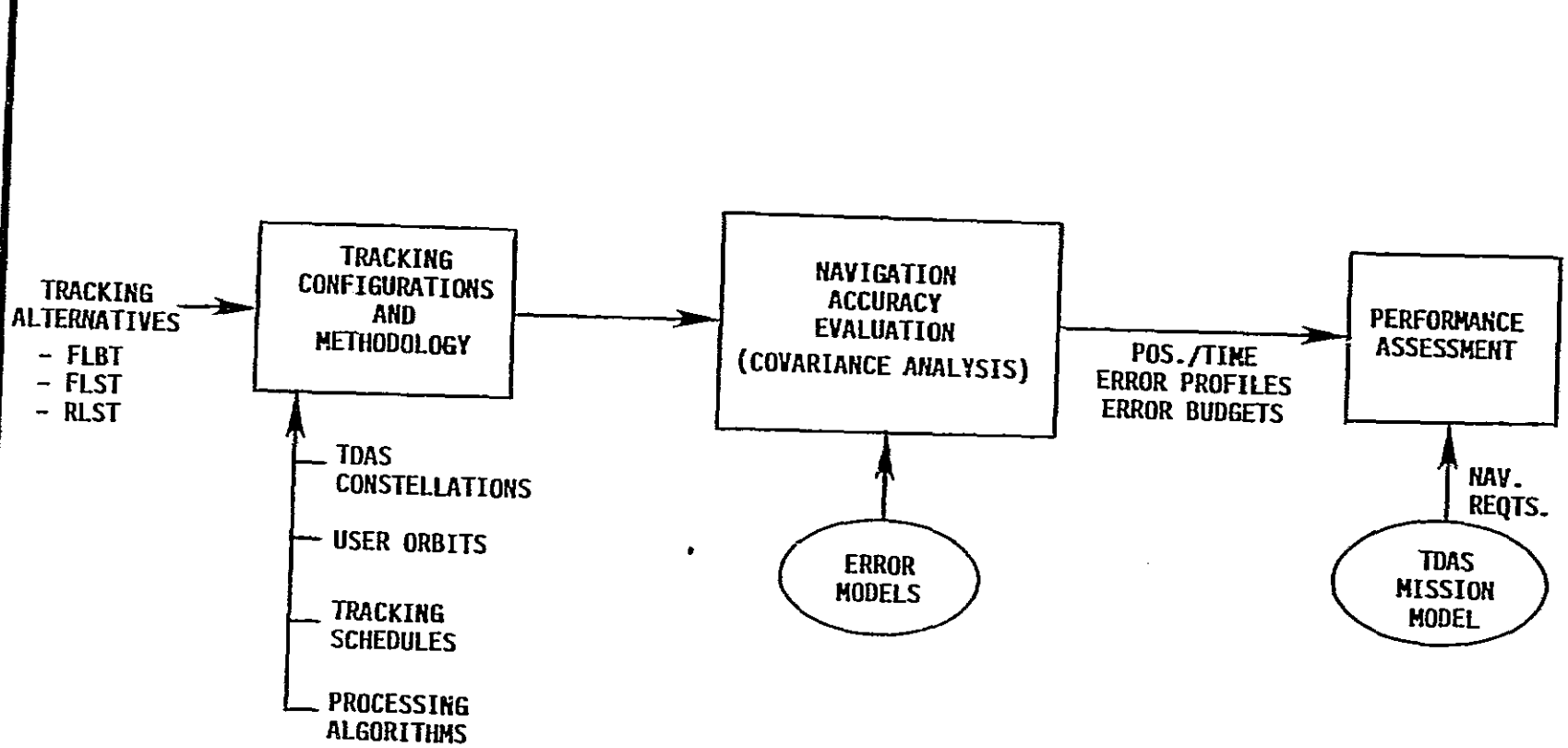

STANFORD TELECOMMUNICATIONS INC.

5.2 TRACKING CONFIGURATIONS AND METHODOLOGY

TDAS constellation and user orbit types considered in the performance evaluation are defined next. Then, tracking data scheduling and processing options assumed for the three tracking alternatives (FLBT, FLST and RLST) are discussed.

5.2.1 TDAS Constellations

The various constellation/network options considered in the TDAS study were discussed in Section 4. For purposes of this evaluation the three constellations shown in Figure 5-2 were selected. Option 1 is analogous to TDRSS with two satellites spaced 130° apart which provides 85-100% coverage at altitudes down to 200 km.* Option 2 also uses two satellites, but with the maximum allowable spacing, 162°**, which yields 98-100% coverage. Option 3 has three satellites, two deployed as in Option 1 and a third on the backside, which together provide 100% coverage.

5.2.2 User Orbits

Six orbits were selected to compare navigation performance for various orbit altitudes as shown in Figure 5-3. As is evident from Appendix A, (Table A-1), they are also indicative of the majority of potential user orbits in the TDAS mission model.

The low altitude (high drag) orbit types are of interest to determine whether more frequent tracking data, available with FLBT, is of significant benefit. The high and low inclination orbit types are of interest, since their coverage and geometrical properties can differ significantly. In the high inclination case, the % coverage is generally greater, but opportunities for (good) doppler tracking can be reduced. This occurs whenever the user orbit normal points sufficiently toward a TDAS, thereby

---

* A detailed discussion of coverage characteristics as a function of satellite spacing is given in [1d].

** This is to avoid earth occulation of the TDAS-TDAS crosslink.

FIGURE 5-2: TDAS CONSTELLATION OPTIONS CONSIDERED

OPTION 1: TWO FRONTSIDE S/C

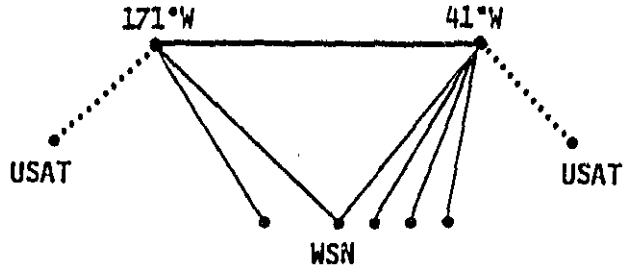

OPTION 2: ONE FRONTSIDE/ONE BACKSIDE S/C

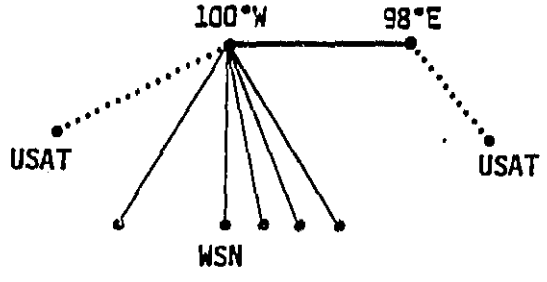

OPTION 3: TWO FRONTSIDE/ONE BACKSIDE S/C

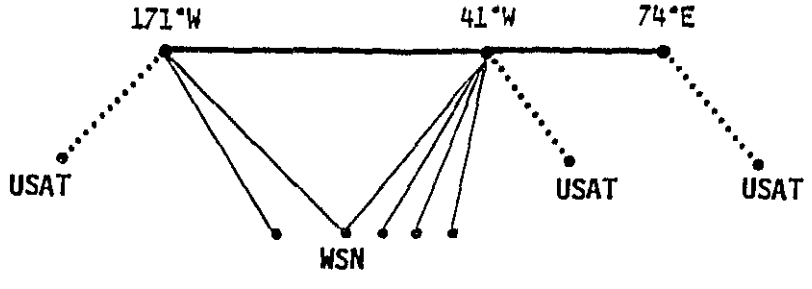

FIGURE 5-3: USER ORBITS CONSIDERED

ORIGINAL PAGE IS
OF POOR QUALITY

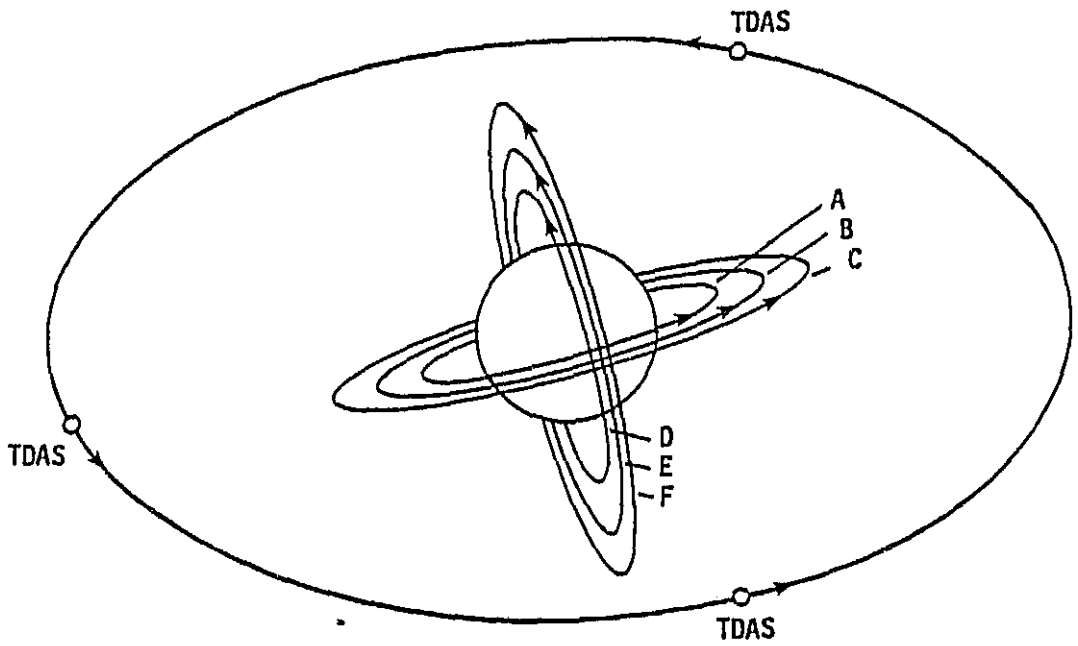

USER ORBITS

TYPE	INCLINATION	ALTITUDE
A	28°	200 KN
B	"	600
C	"	1000
D	97°	200
E	98°	600
F	"	1000

reducing the range change over a pass. In the limit, there is no range change (zero doppler), yet full visibility.

5.2.3 Tracking Data Processing and Scheduling Methodology

One-way range and range-rate ($R,\dot{R}$) are the fundamental data types employed for user OD/TD with each tracking alternative. System configurations and technical considerations for deriving these data were covered in Sections 2 and 3. This discussion pertains to measurement scheduling and processing aspects that were assumed for the performance evaluation.

Two algorithms for tracking data processing were considered: sequential and sliding batch. In the sequential case, estimated parameters (e.g., position & velocity; clock bias & drift) are updated after each measurement and propagated forward between measurements and/or tracking passes. For this analysis an extended Kalman filter was assumed to be employed. In the sliding batch case, selected parameters are estimated for a prescribed epoch via standard weighted least squares processing of tracking observations taken over a given data span (T). Current estimates are derived by propagating the epoch solution over a specified interval (P) beyond the end of tracking and whatever computation/data handling interval (C) is required. In other words, current estimates are predictions in the interval, C to C+P, beyond the end of tracking. For each successive batch the process is repeated with the epoch and tracking interval advanced by P.*

Table 5-1 lists the tracking algorithm and measurement scheduling options considered in the performance evaluation for each alternative. Only sequential processing was assumed for FLBT, since the sliding batch approach was felt to be inappropriate for on-board OD/TD in view of the tracking data volume and associated computation/data handling requirements. For FLST and RLST, two tracking schedule types were considered based on acquiring data every other orbit (Schedule I) and every orbit (Schedule II).

* Since $P \geq C$, predictions for all batches extend at least 2C beyond the data span. In a sense, 2C is a measure of estimate "staleness".

TABLE 5-1: TRACKING ALGORITHM & MEASUREMENT SCHEDULING OPTIONS CONSIDERED

TRACKING ALTERNATIVE	DATA PROCESSING ALGORITHM	TRACKING SCHEDULE* I	TRACKING SCHEDULE* II	TRACKING SCHEDULE* BEACON	DATA SPAN	DATA TYPES
FORWARD LINK BEACON TRACKING (FLBT)	SEQUENTIAL	–	–	CONTINUOUS FOR (SELECTED TDAS)	–	$R, \dot{R}$ (ALL)
FORWARD LINK SCHEDULED TRACKING (FLST)	SEQUENTIAL	ONE 10 MIN. PASS PER TDAS EVERY OTHER ORBIT	ONE 10 MIN. PASS PER TDAS EVERY ORBIT	–	–	↓
	SLIDING BATCH	↓	↓	–	6-24 HOURS	↓
RETURN LINK SCHEDULED TRACKING (RLST)	SEQUENTIAL	↓	↓	–	–	↓
	SLIDING BATCH	↓	↓	–	6-24 HOURS	↓

* $(R, \dot{R})$ MEASUREMENTS AT 3/MINUTE RATE THROUGHOUT A TRACKING PASS.

For sliding batch uses, the tracking data span was considered as a parameter to be selected with possible values ranging from 6-24 hours.

5.3 TRACKING ERROR MODELING AND COMPUTATION

In this study user navigation was evaluated from OD/TD error covariance computations using the SEA and RDGTDS programs [22, 23]. Figure 5-4 illustrates some hypothetical error profiles which indicate the peak errors and time intervals of interest for the options considered:

- Sequential Processing - For FLBT and FLST, user OD/TD accuracy was defined as the peak error occuring over 24 hours with tracking intervals scheduled according to Table 5-1. For RLST, this criterion also applies to ground-based operations, but not necessarily for on-board navigation. Since navigation data updates would be available only on a recurring basis, user OD/TD accuracy was defined instead as the peak error in a prediction-only mode between uploads.

- Sliding Batch Processing - For FLST and RLST, user OD/TD accuracy was defined as the peak error occurring over 24 hours in a series of batch-derived prediction intervals (P), see Figure 5-4. This is defined by the number of batches/day for FLST and by the navigation data upload rate for RLST. In either case, the minimum interval for P is governed by the OD/TD computation/data handling time (C) from the end of any tracking span.*

To obtain user OD/TD uncertainties as a function of various parameters the SEA program was utilized for sequential processing cases and the RDGTDS program for batch processing. Error covariances and budgets were computed given the following input data (see Figure 5-5):

---

* In Figure 5-4, C=10 minutes (for RLST) is based on anticipated ground-system processing capabilities [4]; C=90 minutes (for FLST) is based on LSI-11 type on-board computing capabilities planned for evaluation in a TDRSS forward link doppler tracking experiment [7].

FIGURE 5-4: PERFORMANCE DEFINITIONS FOR OD/TD

ORIGINAL PAGE IS
OF POOR QUALITY

SEQUENTIAL PROCESSING:

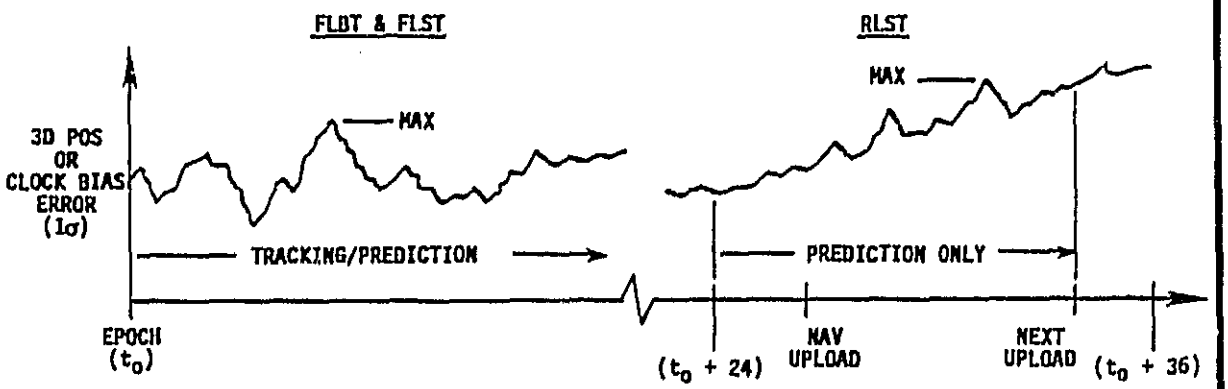

SLIDING BATCH PROCESSING:

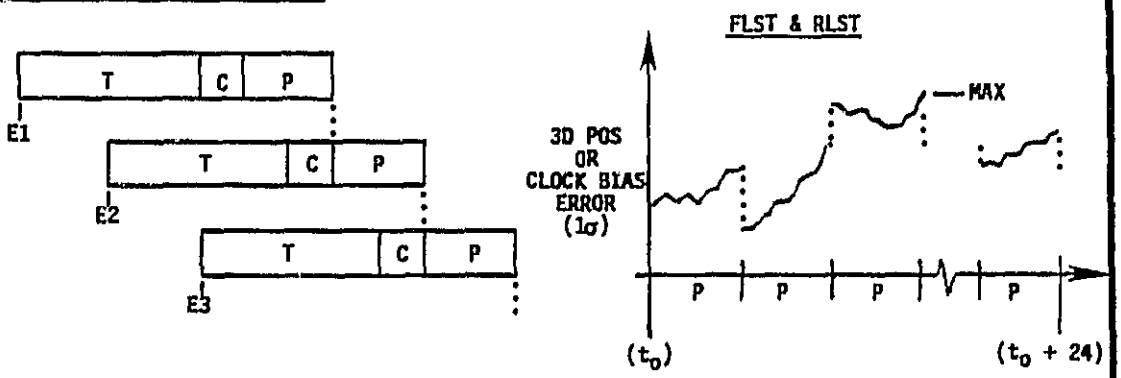

T = TRACKING DATA SPAN
C = COMPUTATION/DATA HANDLING INTERVAL { 10 MIN RLST / 90 MIN FLST
P = BATCH INTERVAL $\geq$ C
E_i = CURRENT EPOCH = E_{i-1} + P
24/P = NO. OF BATCHES PER DAY (FLST)
= NAV UPLOAD RATE PER DAY (RLST)
C+P = TOTAL PREDICTION INTERVAL PER BATCH

STANFORD
TELECOMMUNICATIONS INC.

FIGURE 5-5: TRACKING ACCURACY EVALUATION - OVERVIEW

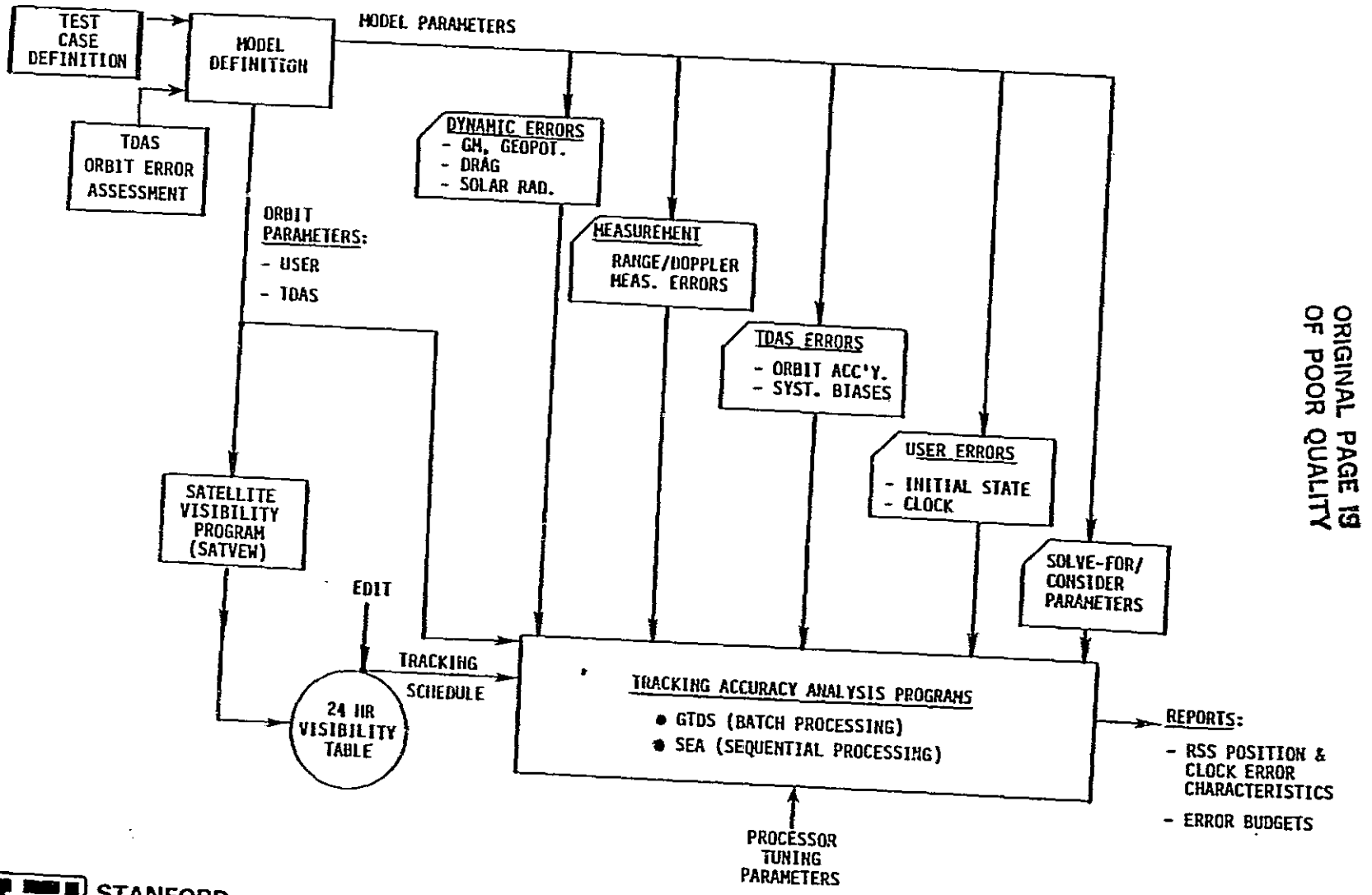

STANFORD TELECOMMUNICATIONS INC.

- User Location - A user was assumed to be in one of the orbits (A-F) indicated in Figure 5-2 with an initial location at 0°N, 0°E for the orbit selected.

- TDAS Location - All TDAS were assumed to be in 5° circular, geosynchronous orbits with initial location at the nominal longitude indicated in Figure 5-1 for the selected constellation option (1, 2, or 3).

- Tracking Schedule - $(R,\dot{R})$ measurement times were set up to occur at the rate defined in Table 5-1.

- Tracking Model Parameters - Values are stated in Table 5-2

TDAS users were assumed to estimate, as a minimum, 8 basic parameters: 3 position and 3 velocity states and two clock states, bias and drift. Unestimated parameters were treated as systematic (consider) error sources in the analysis. Since the analysis is linear, the results for any particular error source may be scaled up or down to note the impact of different a priori uncertainties.

Errors due to atmospheric drag were modeled with two interpretations of uncertainty in the drag coefficient (C_D). For the highest altitude orbits C_D was assumed not to be estimated, so 25% of the nominal value was taken as the consider error, a typical choice [24,33,34]. At altitudes where effects may be significant (e.g., orbits A,B,D,E) C_D was assumed to be estimated, but imperfectly. The residual component was treated as a consider error with a 1σ value equal to 2.5% of the nominal C_D. In other words reducing the a priori uncertainty by estimating C_D was assumed only 90% effective.

Values for uncertainties in the other dynamic parameters (GM, gravitational harmonics and solar pressure coefficient) are undoubtedly conservative for the TDAS time frame. Sequential processing results are based on the GEM9 error model [35], resident in the SEA program. Sliding batch results were

TABLE 5-2: TRACKING MODEL PARAMETERS

PARAMETER		A PRIORI UNCERTAINTY
ESTIMATED	USER ORBIT $\{H, C, L$ / $\dot{H}, \dot{C}, \dot{L}$	500 M 1 M/SEC
	USER CLOCK $\{B$ / $\dot{B}$	1 MSEC 200 NSEC/SEC
UNESTIMATED (SYSTEMATIC) ERRORS	DRAG (C_D) USER ORBITS C,F	25%
	DRAG (C_D) USER ORBITS A,B,D,E	2.5%*
	GRAV. CONST, GM	0.25 PPM
	GRAV. HARMONICS (LUMPED) (12 x 12)	100% GEM9 ERROR OR • (GEM9-GEM7)
	SOLAR RADIATION, C_R	10%
	SYSTEM BIASES R / $\dot{R}$	10 M 1 MM/SEC
	TDAS ORBIT $\{H, C, L$ / $\dot{H}, \dot{C}, \dot{L}$	25, 23, 40 M 3, 2, 3 MM/SEC
	USER OSC. DRIFT $\ddot{B}$	10^{-10} PARTS/DAY
RANDOM MEASUREMENT ERRORS	RANGE σ_R	5 M
	RANGE RATE $\sigma_{\dot{R}}$	5 MM/SEC

PARAMETER		VALUE
TRACKING PROCESSOR TUNING PARAMETERS	SEQUENTIAL:	ORBIT:
	- USER VEL. STATE NOISE	$\{10^{-8}$ M^2/SEC^3 (A,D) $\{10^{-12}$ M^2/SEC^3 (B,C,E,F)
	- CLOCK RATE STATE NOISE	10^{-6} $NSEC^2/SEC^3$ (ALL)
	BATCH:	
	- TRACKING INTERVAL	6, 12, 18, 24 HOURS

* DRAG COEFFICIENT (C_D) IS ASSUMED TO BE PARTIALLY ESTIMATED WITH A RESIDUAL UNCERTAINTY TREATED AS A CONSIDER PARAMETER.
(NOMINAL C_D = 2.0, USER AREA/WEIGHT = .00272 M^2/KG)

derived with the GEM9-GEM7 error model, the closest option resident in RDGTDS.

Constant values assumed for TDAS orbit uncertainty correspond to 1σ errors of approximately 50 m in position and 5 mm/sec in velocity. Results given in Section 4.2 indicate that this accuracy level would still be fairly conservative based on VLBI tracking for TDAS. It would be optimistic by at least 2:1 for BRTS tracking*.

Errors in the tracking measurements $(R,\dot{R})$ were defined in terms of random errors and system biases. Values used for the random errors and the range bias error are representative of the results given in Section 3 (see Table 3-3). The 1 mm/sec for range-rate bias was included only to observe potential sensitivity.

Frequency drift in the user's reference oscillator appears as a doppler rate error which affects range-rate measurement accuracy and as a clock bias acceleration error $(\ddot{B})$ which affects ranging accuracy. Oscillator drift was defined as a consider error with a 1σ value of 10^{-10} parts/day, a level consistent with currently existing quartz oscillator technology.[32]

Other modelling parameters involved in the analysis pertain to tracking data processor tuning for achieving "best" performance in some sense. In the sequential case, state noise parameters are used as an artifice for adjusting the Kalman filter gains to control the weight given to prior estimates. The objective is to achieve a balance between uncertainties introduced by new measurements and those caused by propagating prior estimates with an imperfect dynamical model. The values shown in Table 5-2 were found to give good results in various test runs** and were adopted

---

* This assumes the minimal BRTS tracking configuration using two stations per TDAS (see Figure 4-3).

** As implemented in the SEA program [22], state noise has no connection with physical disturbance phenomena acting on the user spacecraft or clock, although in theory, there could be.

as a baseline set for most cases considered. In the sliding batch case, the tracking interval choice can be made with the same objective in mind. Four durations given in Table 5-2 were considered in each case and the one yielding the lowest peak error in a 6 hour prediction interval from end of tracking was selected.

5.4 NAVIGATION PERFORMANCE RESULTS

TDAS user navigation performance was evaluated in terms of potential OD/TD accuracy for each of the one-way tracking alternatives. Results were obtained as a function of user orbit type, TDAS constellation option, tracking schedule and two processing algorithms. This section presents a summary and interpretation of the significant data. More detailed information can be found in Appendices D and E.

5.4.1 Evaluation Cases

Potential cases for evaluation were defined by the six user orbit types in Figure 5-2 and three constellation options in Figure 5-3. For each case, five subcases were defined based on processor type (sequential or sliding batch) and tracking schedule (I, II or beacon).* Altogether, 90 combinations were identified and 48 of these were evaluated as indicated in Table 5-3.

For each case, user position and time error profiles were computed for a 36 hour period (the last 12 hours in predict-only mode). From these the peak errors for assessing performance were determined as defined in Section 5.3 and Figure 5.4. Appendix D presents error profiles and corresponding tracking schedules for sequential processing. Appendix E has corresponding results for sliding batch processing. Results for all cases were based on the nominal model parameters given in Table 5-2 except for certain processor tuning parameters noted specifically on error profile plots in Appendices D and E.

* Recall Table 5-1.

TABLE 5-3: CASES CONSIDERED FOR NAVIGATION PERFORMANCE EVALUATION*

USER ORBIT	TDAS CONSTELLATION		
	1 TWO FRONTSIDE (171°W/41°)	2 1 FRONT/1 BACK (100°W/98°E)	3 2 FRONT/1 BACK (171°W/41°W/74°E)
A 28°, 200 KM	S(3)	S(3), B(2)	S(3)
B 28°, 600 KM			
C 28°, 1000 KM			
D 97°, 200 KM	S(3), B(2)	S(3), B(2)	S(3)
E 98°, 600 KM	S(3), B(2)	S(3), B(2)	S(3)
F 98°, 1000 KM	S(3)	S(3), B(2)	S(3)
NO. CASES	30	30	30

*S( ) OR B( ) INDICATES NO. OF CASES COMPLETED WITH TRACKING BASED ON SEQUENTIAL (S) OR SLIDING BATCH (B) PROCESSING.

5.4.2 Sequential Data Processing Results

Navigation performance data based on the error analysis results in Appendix D are presented in terms of user position and time accuracies as summarized in Figures 5-6 and 5-8. Corresponding position and time error budgets are given in Figures 5-7 and 5-9.

5.4.2.1 User Position Accuracy. Figure 5-6 illustrates that in low altitude orbits where drag is a factor, performance depends heavily on frequent data availability. Beacon tracking is clearly superior in this respect. At higher altitudes this is not the case and all three tracking alternatives can given comparable performance.

With respect to the various TDAS constellations, Option 3 gives typically better performance due to better geometric distribution of the tracking data available with three satellites. In the two satellite constellations, Option 1 with (130° spacing) is better in the high inclination orbits, while Option 2 (with 162° spacing) is better in low inclination orbits. Although Option 2 provides nearly full coverage ($\geq$ 98%), the performance for high inclination users is sensitive to poor geometry conditions for doppler tracking. This occurs twice a day when the user orbit normal points in the general direction of each TDAS. Consequently a tradeoff exists between maximum TDAS spacing (162°) for best coverage and lower spacing to achieve better OD performance.

Figure 5-7 indicates the major error components affecting OD performance. Those due to unestimated (consider) parameters are: gravitational harmonics (H), drag (D) and TDAS ephemerides (E). The noise component (N) is the random error in user position which is controllable by filter tuning parameters.* Ideally the filter should be tuned to reduce the impact

---

* By adjusting filter gains to partially deweigh prior estimates random errors arising from measurement and a priori uncertainties do not continuously decrease as the number of measurements increases. Rather a "noise floor" (not necessarily constant over time) is reached, which is controllable using velocity state noise tuning parameters. [22, 37]

FIGURE 5-6: TDAS USER POSITION ACCURACY VS TRACKING ALTERNATIVES (SEQUENTIAL PROCESSING)

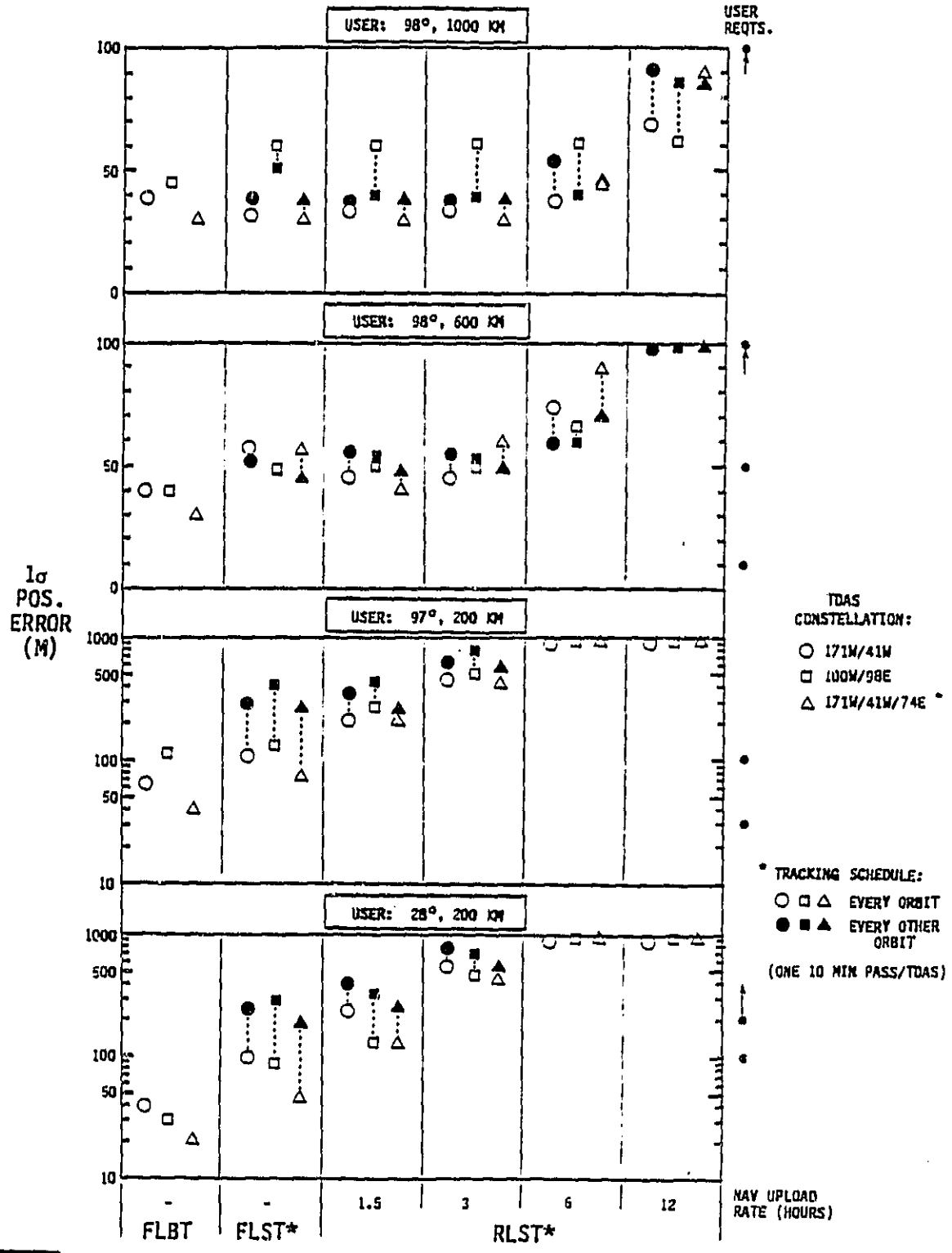

FIGURE 5-7: MAXIMUM USER POSITION ERROR CONTRIBUTORS OVER 24 HOURS VS TDAS CONSTELLATION AND TRACKING ALTERNATIVE (SEQUENTIAL PROCESSING)

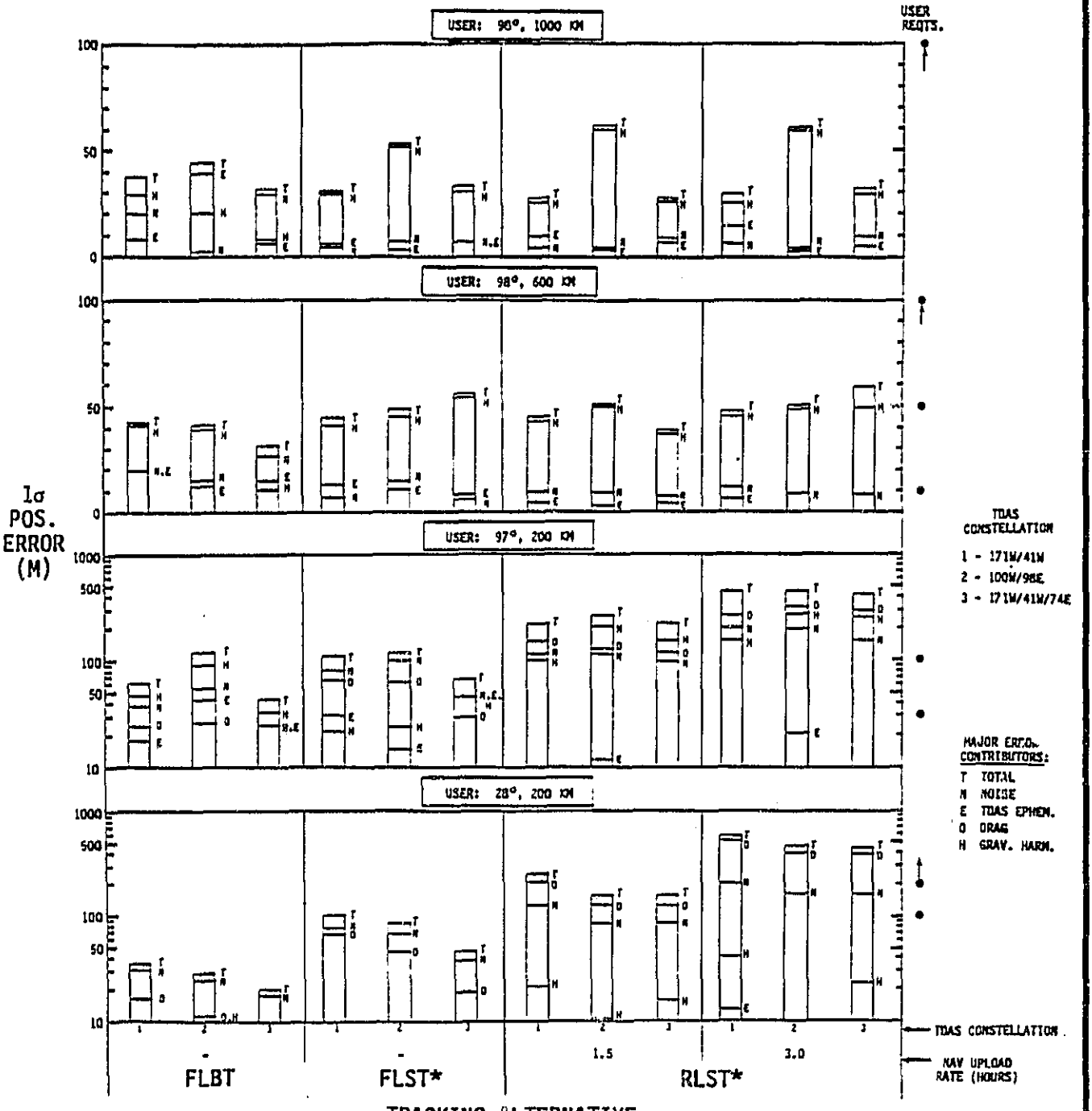

STANFORD TELECOMMUNICATIONS INC.

*ONE 10 MIN PASS/ORBIT/TDAS

of the dominant consider parameter(s) without excessively increasing the noise component. Figure 5-7 suggests that the modelled filter is somewhat overtuned for the 28°, 200 km orbit, about right for the 97°, 200 km orbit and undertuned for the higher altitude orbits.

In the high inclination, high altitude orbits (98°, 600/1000 km) gravitational harmonic modelling uncertainty is typically the dominant error contributor. This is also the case at low altitude with beacon tracking since filter tuning acts more to suppress the drag contribution. At low altitudes with scheduled tracking, drag is the dominant contributor in all cases. TDAS ephemeris error is typically a secondary contributor. All of the other consider error sources identified in Table 5-2 are comparatively insignificant including user oscillator drift.

Also indicated in Figures 5-6 and 5-7 are user requirements extracted from the TDAS mission model (see Appendix A). Most would be met with beacon tracking and in many cases with scheduled tracking based on error analysis results using the assumed models. Meeting the more stringent requirements would imply some improvement in key error sources. For example, in the 98°, 600 km orbit with TDAS Constellation Option 1, the impact of gravitational harmonic modelling errors would have to decrease by at least 5:1 and TDAS ephemeris error by 2:1. Filter retuning would decrease the noise component so the net effect of all contributors would be $\leq$ 10 m. Such reductions could also lead to meeting the most stringent requirement (30 m) at a lower altitudes assuming no change in the modelled drag uncertainty.

5.4.2.2 User Time Accuracy

Figure 5-8 indicates that TD performance is uniformly better with beacon tracking ($\leq$ .25 μsec) than with scheduled tracking in all four orbits. Nevertheless, performance with the scheduled alternatives is sufficient to meet the most stringent user time requirement (1 μsec) identified in the TDAS mission model.

FIGURE 5-8: TDAS USER TIME ACCURACY VS TRACKING ALTERNATIVES (SEQUENTIAL PROCESSING)

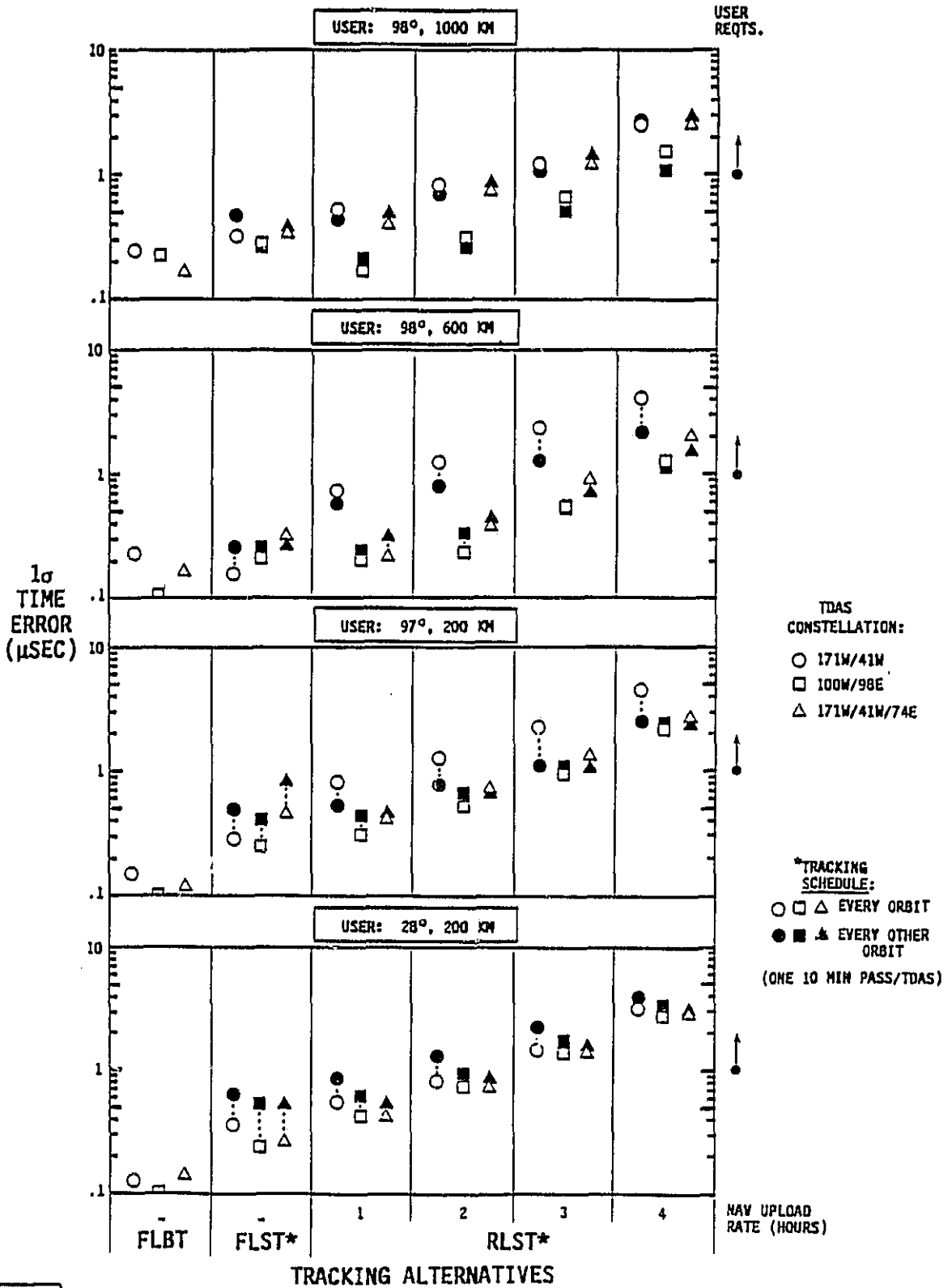

STANFORD TELECOMMUNICATIONS INC.

Figure 5-9 shows the error contributors affecting TD performance. With FBLT, TDAS ephemeris errors tend to dominate. With FLST and RLST, in the high altitude orbits, gravitational harmonic errors are also a primary contributor. In the lower altitude orbits the TD errors due to the drag uncertainty increase but are still secondary. User oscillator drift is also a secondary source in all cases except for RLST if the interval between navigation data uploads begins to exceed 3 hours.

5.4.3 Sliding Batch Data Processing Results

Navigation performance data based on the error analysis results in Appendix E are presented in terms of user position and time accuracies as summarized in Figures 5-10 and 5-12. Corresponding position and time error budgets are given in Figures 5-11 and 5-12. FLST results are shown for batch intervals (P) of 1.5 and 3 hours.* RLST results correspond to navigation data uploads at $\sim$ 1, 2 or 3 orbit intervals.

5.4.3.1 User Position Accuracy. Figure 5-10 indicates that user position errors in low altitude orbits are substantially higher than the sequential provessing results. At higher altitudes however, OD performance is comparable. In either case no significant OD performance difference was observed with respect to the two satellite constellation options (1 and 2) studied.

Figure 5-11 indicates the major error contributors affecting OD performance. At low altitudes drag is dominant even though a tracking interval of only 6 hours was used. For the higher altitude orbits a longer tracking interval (18 hours) was found to give better performance; consequently user oscillator drift became a significant contributor along with gravitational harmonic error.

---

* See Figure 5-4. The assumed computation/data handling interval (C) was 1.5 hours for FLST and 10 minutes for RLST as discussed in Section 5.3.

FIGURE 5-9: MAXIMUM USER TIME ERROR CONTRIBUTORS OVER 24 HOURS VS TDAS CONSTELLATION AND TRACKING ALTERNATIVE (SEQUENTIAL PROCESSING)

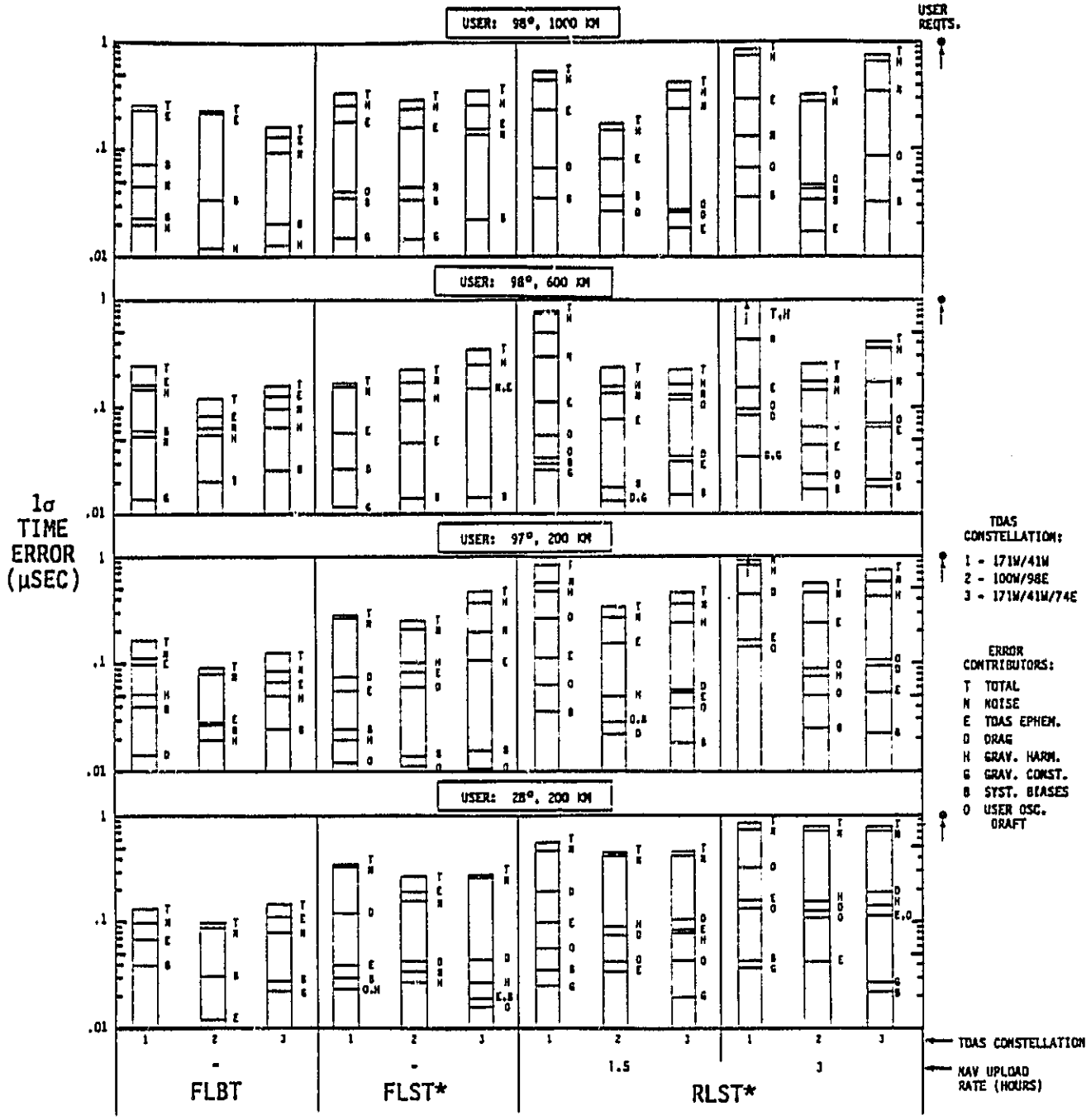

STANFORD TELECOMMUNICATIONS INC.

*ONE 10 MIN PASS/ORBIT/TDAS

FIGURE 5-10: TDAS USER POSITION ACCURACY VS TRACKING ALTERNATIVES (SLIDING BATCH PROCESSING)

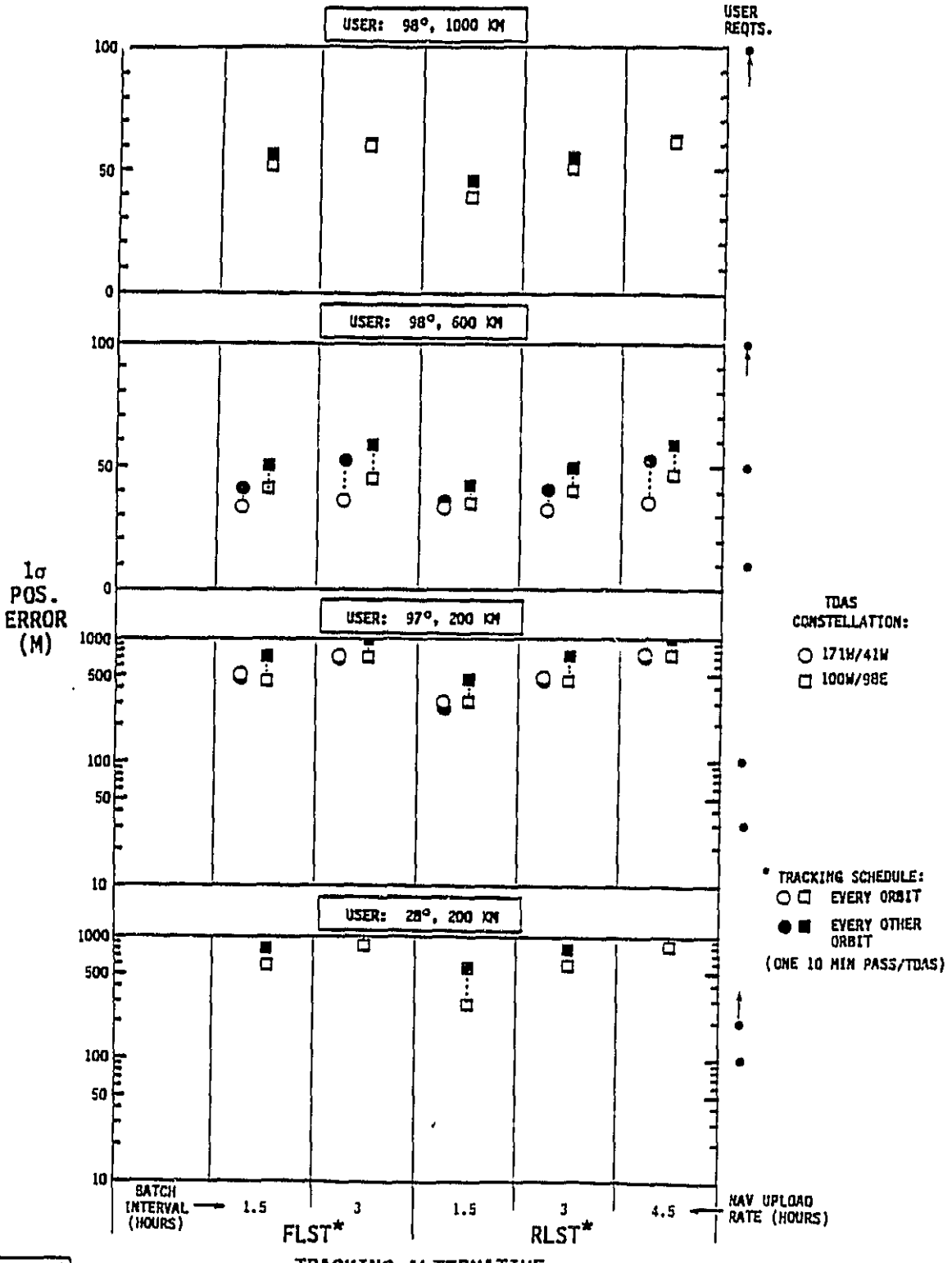

FIGURE 5-11
MAXIMUM USER POSITION ERROR CONTRIBUTORS OVER 24 HOURS VS TDAS CONSTELLATION AND TRACKING ALTERNATIVE (SLIDING BATCH PROCESSING)

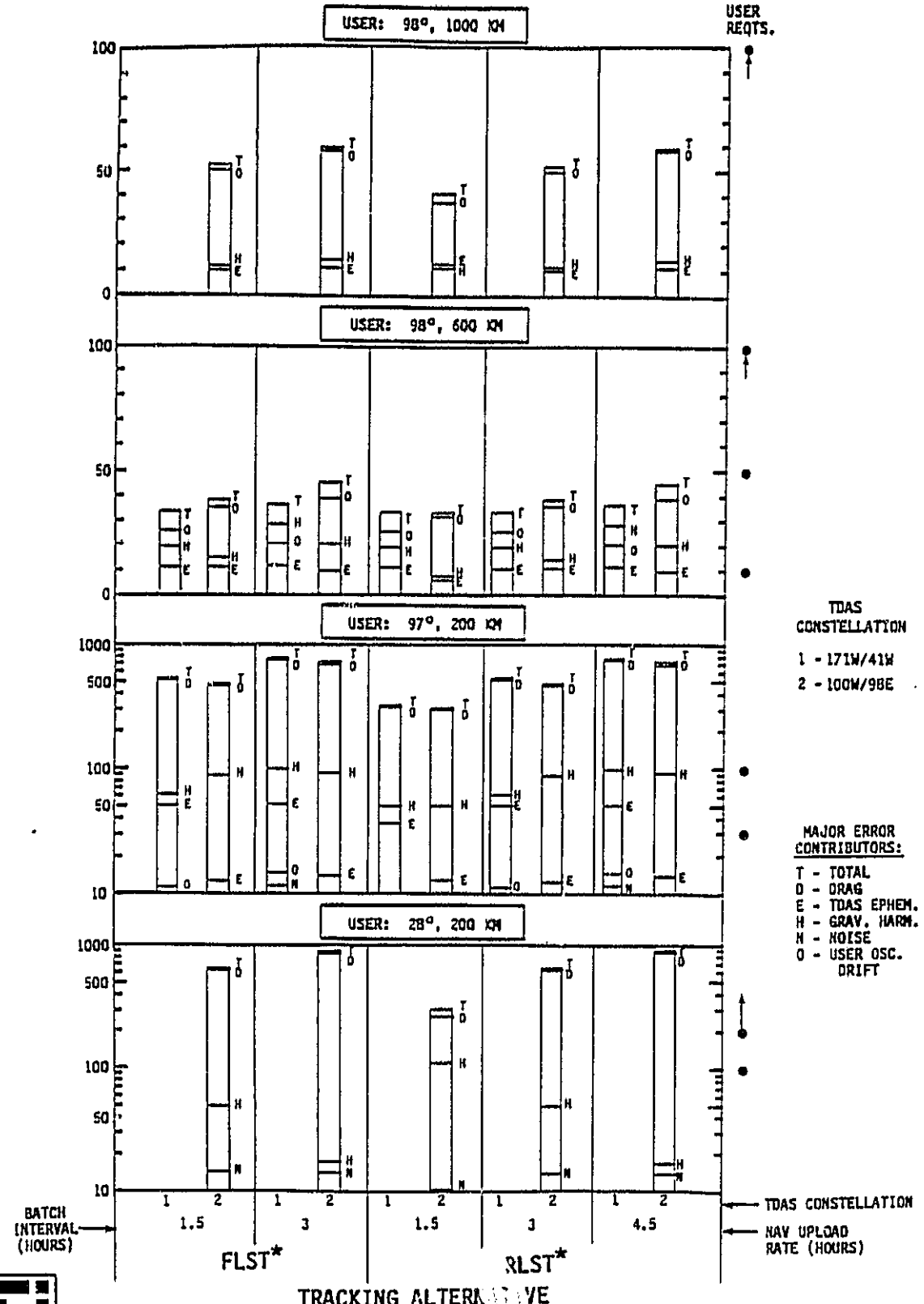

* ONE 10 MIN PASS/ORBIT/TDAS

With respect to meeting user requirements these alternatives would not be good candidates in low altitude orbits. However, at the higher altitudes all but the most stringent requirement (10 m) could be met based on the error analysis results. Metting the 10M requirement would imply some improvement in key error sources, e.g., a decrease in gravitational harmonic errors by at least 4:1, TDAS ephemeris error by 1.5-2:1 and user oscillator drift by 5:1.

5.4.3.2 User Time Accuracy. Figure 5-12 indicates that TD performance is at best 2.5-3 μsec. This is significantly lower than with sequential processing and would not meet the most stringent time requirement of 1 μsec.

Figure 5-13 shows that the dominant error contributors are the same as for user position error -- drag at low altitudes and user oscillator drift at high altitudes.

5.4.4 Observations

A summary of user navigation performance based on the error analysis results is given in Table 5-4. In addition, the following observations can be made:

- Sequential Processing

  - At low altitudes (e.g. $\leq$400 km) beacon tracking (FLBT) provides significantly better orbit determination (OD) accuracy than scheduled alternatives (FLST, RLST). The latter are both highly sensitive to tracking frequency and RLST to NAV upload rate.

  - At higher altitudes all three alternatives provide compairable OD performance.

FIGURE 5-12: TDAS USER TIME ACCURACY VS TRACKING ALTERNATIVES (SLIDING BATCH PROCESSING)

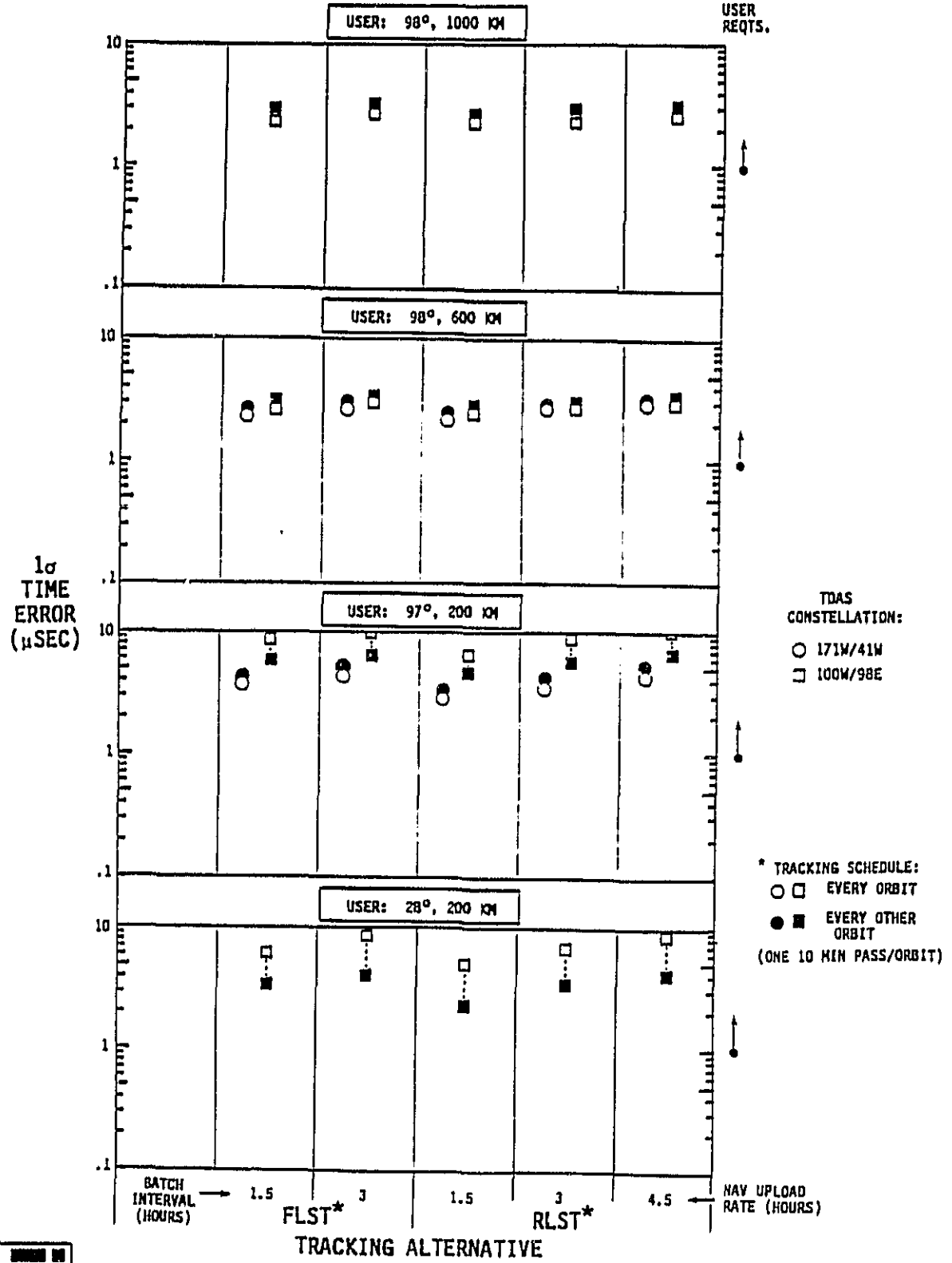

FIGURE 5-13

MAXIMUM USER TIME ERROR CONTRIBUTORS OVER 24 HOURS VS TDAS CONSTELLATION AND TRACKING ALTERNATIVE (SLIDING BATCH PROCESSING)

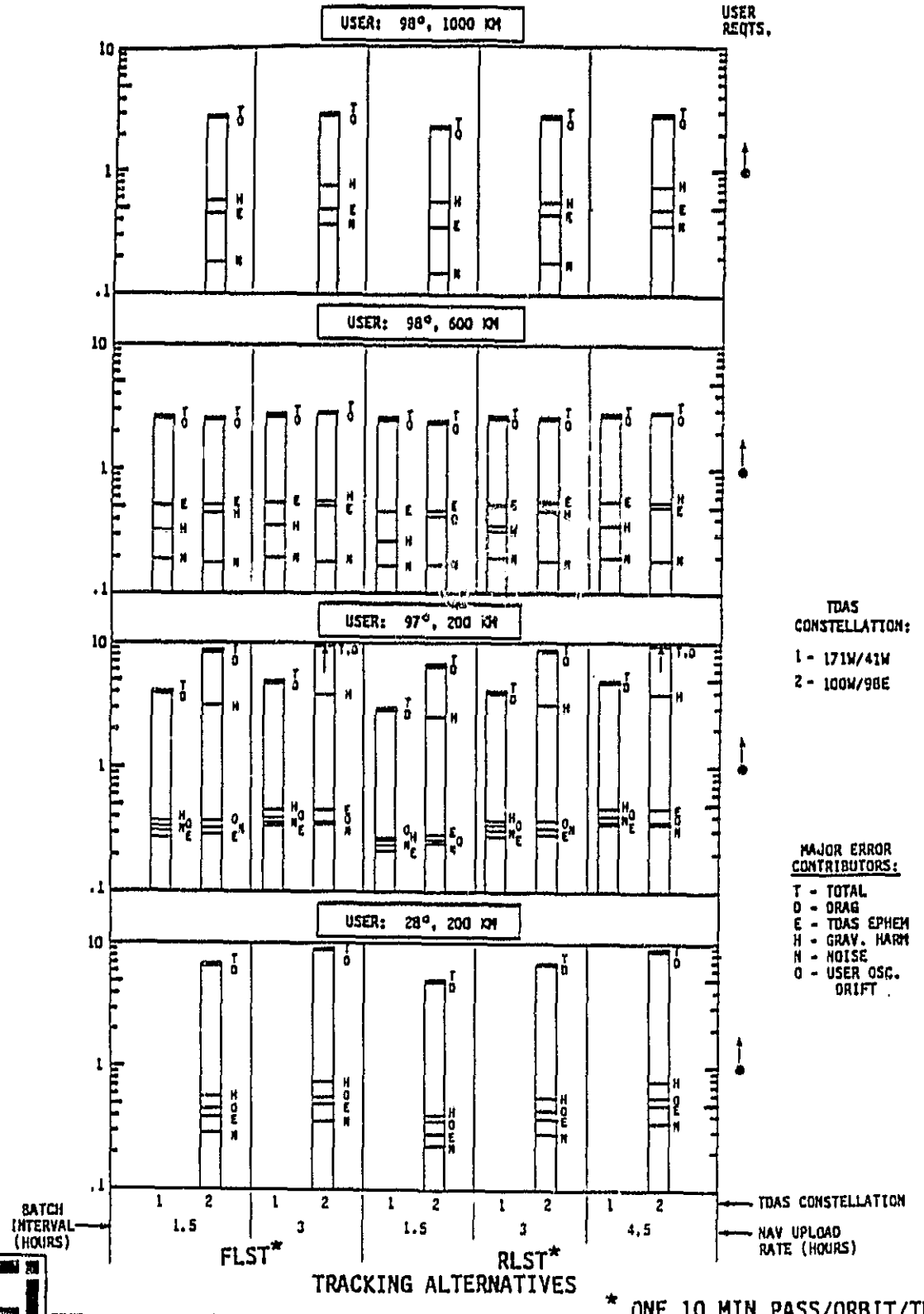

- Performance projections based on error source improvements indicate that FLBT could satisfy all users in the TDAS mission model with position accuracy reqts. down to 10m. For this accuracy error sources requiring improvement include:
  - -- gravitational harmonic modeling ($\geq$ 5:1 reduction in GEM-9 errors)
  - -- TDAS tracking accuracy (to 25m - pos., 2.5 mm/s - vel.)

- Time determination (TD) is better than 0.25 μsec with FLBT and better than 1 μsec with FLST and RLST.

• Sliding Batch Processing

- Results for FLST and RLST indicate that compared to sequential processing:
  - -- OD performance tends to be worse for low altitude orbits (< 400 km) where drag is the dominant error source and comparable to or slightly better in higher orbits where user oscillator drift is also a major error source.
  - -- TD performance is worse ($\geq$ 2.5 μsec) for all orbits considered and particularly sensitive to the tracking interval duration.

TABLE 5-4

COMPARISON OF USER NAVIGATION PERFORMANCE (ERROR ANALYSIS)

SUMMARY OF USER NAVIGATION PERFORMANCE EVALUATION

TRACKING DATA PROCESSING ALGORITHM	EVALUATION ITEMS	USER ORBIT: 200 KM, 28°	USER ORBIT: 200 KM, 97°	USER ORBIT: 600/1000 KM, 98°
SEQUENTIAL (FLBT, FLST, RLST)	ORBIT ACCURACY	• FLBT IS SIGNIFICANTLY BETTER THAN FLST & RLST • FLBT COULD MEET ALL REQUIREMENTS IN TDAS MISSION MODEL DEPENDING ON CONSTELLATION USED.		• FLBT, FLST & RLST CAN GIVE COMPARABLE RESULTS WITH APPROPRIATE FILTER TUNING • ALL COULD MEET REQUIREMENTS > 30 M
	TDAS CONSTELLATION* IMPACT	• ALL OPTIONS MEET ACCURACY REQUIREMENTS • OPTION 3 OFFERS UP TO 2:1 ADVANTAGE	• PERFORMANCE DEGRADES SIGNIFICANTLY FOR OPTION 2 DUE TO POOR GEOMETRY RECURRING TWICE PER DAY	• OPTION 3 HAS SLIGHT ACCURACY ADVANTAGE WITH FLBT; OTHERWISE ALL OPTIONS ARE COMPARABLE
	LEADING ERROR CONTRIBUTORS**	M, H	M, H, E, O	H, M, E
	TIME ACCURACY	• FLBT IS SUPERIOR FOR ALL CASES (MINIMUM ACCURACY ≤ 0.25 μSEC) • FLST & RLST (WITH UPLOAD RATE ≤ 3 HOURS) ALSO MEET MOST STRINGENT REQUIREMENT (1 μsec)		
	TDAS CONSTELLATION* IMPACT	• ALL OPTIONS GIVE COMPARABLE RESULTS FOR A GIVEN TRACKING ALTERNATIVE		
	LEADING ERROR CONTRIBUTORS**	M, E	M, E, H	M, E, H
SLIDING BATCH (FLST, RLST)	ORBIT ACCURACY	• NEITHER FLST OR RLST MEET TDAS MISSION MODEL REQUIREMENTS		• BOTH FLST & RLST COULD MEET REQUIREMENTS > 30 M
	LEADING ERROR CONTRIBUTORS**	O		O, E, H
	TIME ACCURACY	• MAXIMUM ACCURACY FOR ANY ALTERNATIVE IS 2.5 μSEC		
	LEADING ERROR CONTRIBUTORS**	O		O, E, H

* OPTION 1 (2 S/C, 130° APART); OPTION 2 (2 S/C, 162° APART); OPTION 3 (3 S/C).

** ERROR SOURCES: M = MEASUREMENT NOISE; E = TDAS ORBIT UNCERTAINTY; O = RESIDUAL DRAG MODELLING ERROR, H = GRAVITATIONAL HARMONICS MODELLING ERROR, O = USER OSCILLATOR DRIFT. (ARRANGEMENT IN TABLE NOT NECESSARILY IN ORDER OF SIGNIFICANCE.)

SECTION 6

STUDY SUMMARY AND CONCLUSIONS

The TDAS navigation architecture study has focused on three TDAS-based one-way tracking alternatives for providing user orbit and time determination (OD/TD). This section presents a functional overview and requirements summary for each alternative, summaries of potential user navigation performance and TDAS tracking accuracy, and the conclusions reached from the study.

6.1 FUNCTIONAL OVERVIEWS AND REQUIREMENTS SUMMARY (2, 3)*

The proposed TDAS architecture design [1a] would extend TDRSS navigation and data relay capabilities to support:

- beacon tracking (FLBT) via an independent beacon signal, and
- scheduled one-way tracking (FLST, RLST) via enhanced multiple and single access (MA, SA) services.

A functional overview of each alternative is presented in Figure 6-1.

The beacon signal is assumed to be generated by a TDAS ground terminal for broadcast by each TDAS satellite using a single element of the S-band MA antenna array. Users would receive continuous tracking signals while within a beacon antenna's ±13° field of view. The corresponding upper limit on user altitude for 100% coverage exceeds 3100 km for all TDAS constellations considered. Lower altitude coverage is governed by the zone of exclusion (ZOE) size for a given constellation.

In the scheduled modes, signals for tracking are available only during an allocated contact period as part of normal MA or SA service. Since each

* Numbers in brackets ( ) refer to preceding sections with full details.

FIGURE 6-1: ONE-WAY NAVIGATION ALTERNATIVES - FUNCTIONAL OVERVIEW

FORWARD LINK BEACON TRACKING (FLBT)

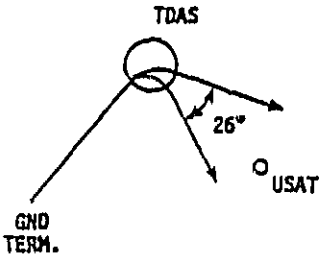

FORWARD LINK SCHEDULED TRACKING (FLST)

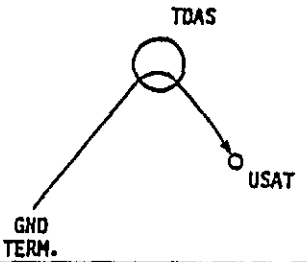

ELEMENTS	MAJOR FUNCTIONS	
	FORWARD LINK BEACON TRACKING (FLBT)	FORWARD LINK SCHEDULED TRACKING (FLST)
TDAS GROUND SEGMENT	TRACKING SIGNAL & ANCILLARY DATA* GENERATION AND UPLINK	
	CONTINUOUS TRANSMISSION	TRANSMISSIONS DURING SCHEDULED SERVICE ONLY
TDAS SATELLITES	BENT PIPE RELAY FOR SMA USERS ONLY (VIA BROADBEAM ANTENNA-SINGLE SMA ELEMENT)	BENT PIPE RELAY FOR ALL SERVICES (SMA, KSA, WSA, LSA)
USERS	• RANGE/DOPPLER DATA MEASUREMENT • ON-BOARD ORBIT/TIME DETERMINATION	

* TDAS S/C ORBITS, RANGE/DOPPLER CORRECTION DATA, ETC.

RETURN LINK SCHEDULED TRACKING (RLST)

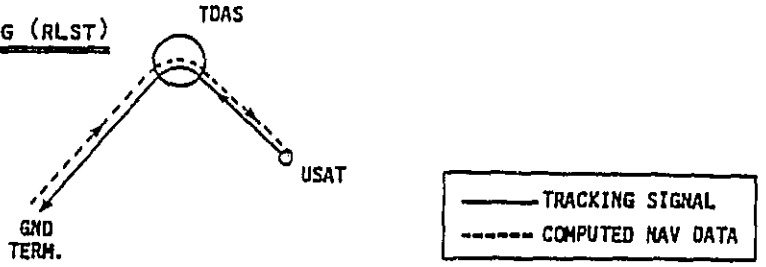

ELEMENTS	MAJOR FUNCTIONS
USERS	• TRACKING SIGNAL GENERATION AND TRANSMISSION DURING SCHEDULED RETURN LINK SERVICE • RECEIVE AND PROCESS GROUND-DERIVED DATA FOR ORBIT/CLOCK STATE PREDICTION UNTIL NEXT UPLOAD VIA SCHEDULED FORWARD LINK COMM. SERVICE
TDAS GROUND SEGMENT	• RANGE/DOPPLER DATA MEASUREMENT • USER ORBIT DETERMINATION AND CLOCK (OSC.) CALIBRATION • ORBIT PREDICTION DATA GENERATION AND TRANSMISSION TO USER AT SCHEDULED INTERVALS
TDAS SATELLITES	BENT PIPE RELAY FOR ALL SERVICES (SMA, KSA, WSA, LSA)

TDAS can support two S-Band MA forward channels and eight SA channels, up to 20 simultaneous users theoretically could be supported for FLST with a two satellite TDAS constellation depending on channel scheduling policy. Similarly, for RLST up to 20 simultaneous MA users theoretically could be accomodated, since each TDAS can support ten return S-Band MA channels.

Table 6-1 lists various system requirements for supporting each 1-way alternative. Table 6-2 summarizes characteristics of the tracking signals assumed in each case including estimates of metric tracking data (R, $\dot{R}$) accuracies based on transmission link performance analyses.

The multiple beam antenna and switch enhancements for TDAS spacecraft provide the capability for simultaneous, direct transmissions between the space segment and several ground stations [1d,e]. This provides possibilities for direct control of user spacecraft by the mission control centers (MCC) instead of interfacing through the White Sands (WSN) terminal and/or Network Control Center (NCC) as in TDRSS.

Figure 6-2 illustrates options for tracking signal and navigation data flow with each of the one-way alternatives. Since the beacon signal for FLBT is a general resource, it is assumed to originate at WSN, the assumed control point for TDAS spacecraft. Navigation data computed on-board can be received by a TDAS ground terminal at the NCC directly and by MCCs with direct space/ground access. Additional interfacility transfer of data can occur to support MCCs without direct space/ground access or for general coordination and/or verification functions. The latter includes WSN which has control of TDAS spacecraft facilities (e.g., SA antenna/telescope pointing).

With FLST (see Figure 6-2b) the user tracking signal is imbedded in the normal uplink data communication traffic so it can emanate from either the NCC or a cognizant MCC. Navigation data computed on-board can be distributed in the same manner discussed above for FLBT.

TABLE 6-1

SUMMARY OF ADDITIONAL SYSTEM REQUIREMENTS FOR 1-WAY NAVIGATION ALTERNATIVES SUPPORT

SYSTEM ELEMENT	SYSTEM REQUIREMENT	APPLICABLE NAV ALTERNATIVE		
		FLBT	FLST	RLST
GROUND	• BEACON SIGNAL GENERATION	✓		
	• ANCILLARY NAV DATA GENERATION & TRANSMISSION	✓	✓	
	• USER OD/TD* COMPUTATION & NAV DATA UPLOAD			✓
SPACE	• DEDICATED HARDWARE:			
	– TWTA & K_U-TO-S BAND REPEATER	✓		
	– SMA ANTENNA ELEMENT	✓		
USER	• DEDICATED RECEIVER CHANNEL	✓		
	• STABLE FREQUENCY STANDARD	✓	✓	✓
	• R,$\dot{R}$ EXTRACTOR	✓	✓	✓
	• NAV DATA DECODER	✓	✓	✓
	• ANCILLARY DATA GENERATION			
	• ON-BOARD COMPUTING FACILITY:			
	– FULL OD/TD* COMPUTATION	✓	✓	
	– ORBIT/TIME PROPAGATION ONLY			✓

* OD/TD – ORBIT DETERMINATION AND TIME DETERMINATION

TABLE 6-2

SUMMARY OF TRACKING SIGNAL CHARACTERISTICS

SIGNAL CHARACTERISTICS	BEACON (FLBT)	SCHEDULED (FLST)	SCHEDULED (RLST)
TYPE	• PN MODULATED BPSK DATA	• STAGGERED QUADRIPHASE PN (SQPN) (COMMAND & RANGE CHANNELS PER TDRSS)	• STAGGERED QUADRIPHASE PN (SQPN) (PER TDRSS DGI-MODE2/ NONCOHERENT)
CODE(S)	• UNIQUE 1023-CHIP GOLD CODE • 3.0778×10^6 CHIPS/SEC • 2.6 NS GRANULARITY (VIA INTERPOLATION TO 1/128 CHIP	• SHORT CODE (COMMAND CHANNEL/ 1023 CHIP GOLD CODE) • LONG CODE (RANGE CHANNEL/ 256 x 1023 CHIPS USED TO RESOLVE RANGE AMBIGUITY • 3.0778×10^6 CHIPS/SEC	• 2047 CHIP GOLD CODES ON I AND Q CHANNELS (OFFSET $\geq$ 20,000 CHIPS) • 3.0778×10^6 CHIPS/SEC
DATA*	• INCLUDES ANCILLARY DATA (E.G., TDAS EPHEMERIS, TIME REFERENCE AND PN EPOCH) $\leq$ 1000 BITS/FRAME • CONVOLUTIONALLY-CODED (RATE ½) • DATA RATE ~ 100 BPS • ASSEMBLED INTO 1000 BIT FRAMES (10 SECONDS) • SYNC WORD IN EACH FRAME RESOLVES AMBIGUITY	• INCLUDES ANCILLARY DATA (SIMILAR TO FLBT) • CONVOLUTIONALLY-CODED (RATE ½)	• INCLUDES USER ANCILLARY DATA (E.G., PN CODE EPOCH, CURRENT TIME REFERENCE AND SYNCH WORD FOR AMBIGUITY RESOLUTION) • CONVOLUTIONALLY-CODED (RATE ½)
DOPPLER COMPENSATION	• NONE (NOT FEASIBLE FOR MULTIPLE USER SUPPORT, BUT COORDINATION WITH FLST ENABLES REDUCTION OF DOPPLER UNCERTAINTY FOR INITIAL BEACON ACQUISITION	• PROVIDED FOR SIGNAL ACQUISITION	
TRACKING DATA ACCURACY — R (RANDOM)	5 M	1 M	2.5 M
TRACKING DATA ACCURACY — R (SYSTEM)	10 M**	10 M**	10 M**
TRACKING DATA ACCURACY — $\dot{R}$ (RANDOM)	6 MM/SEC	3 MM/SEC	7 MM/SEC

* MODULO – 2 ADDED ASYNCHRONOUSLY TO PN CODE(S)

** PROJECTED SYSTEMATIC DELAY (WITH CALIBRATION) [15]

FIGURE 6-2: TRACKING SIGNAL AND DATA HANDLING INTERFACES (ONE-WAY TRACKING ALTERNATIVES)

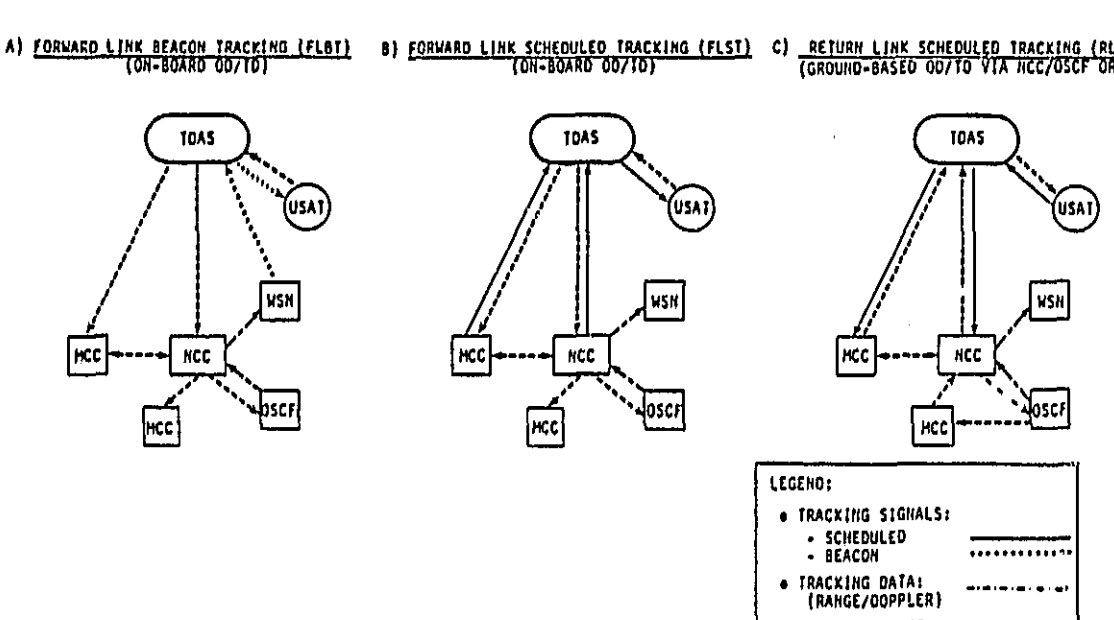

STANFORD TELECOMMUNICATIONS INC.

FIGURE 6-3: TDAS TRACKING SIGNAL AND DATA HANDLING INTERFACES (TWO-WAY TRACKING ALTERNATIVES)

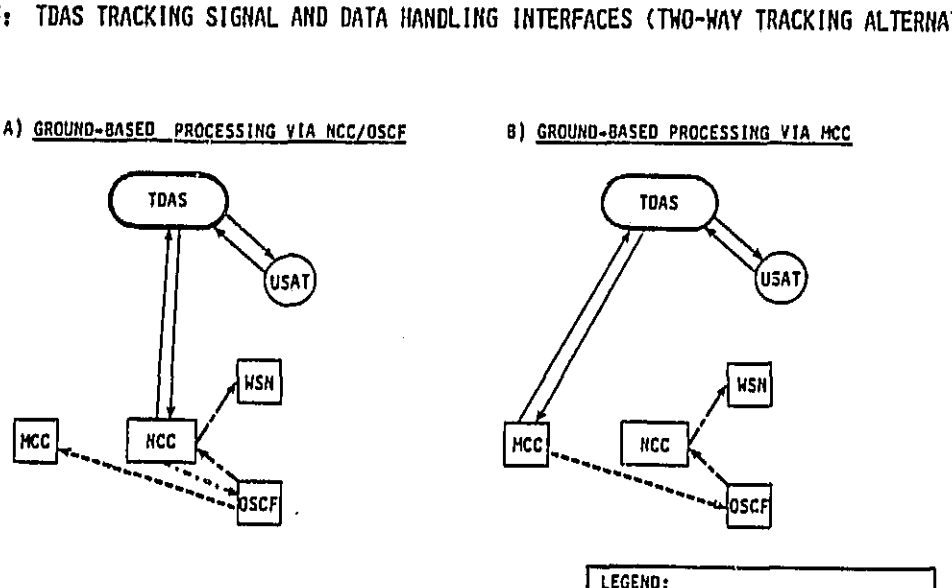

STANFORD TELECOMMUNICATIONS INC.

With RLST (see Figure 6-2c) the user tracking signal is imbedded in the normal downlink data communication traffic, so it can be received by either the NCC or cognizant MCC. Ground processing for user OD/TD can occur at the Orbit Support Computing Facility (OSCF) or at the MCC with subsequent interfacility data transfer as noted above. Since two-way tracking with ground-based processing is also a TDAS alternative, Figure 6-3 provides a comparison with the RLST data flow.

6.2 USER NAVIGATION PERFORMANCE SUMMARY

To assess the potential navigation performance with each of the one-way alternatives, user OD/TD accuracy was evaluated as a function of various parameters and compared with requirements in the TDAS mission model. Figure 6-4 gives an overview of the elements involved in the analysis.

User Orbits and TDAS Constellations (5.2) - Options considered are shown in Figure 6-5. Constellation Option 1 is analogous to TDRSS with two satellites spaced 130° apart which provides 85-100% coverage at altitudes down to 200 km. Option 2 also uses two satellites, but with the maximum allowable spacing, 162°, which yields 98-100% coverage. Option 3 has three satellites, two deployed as in Option 1 and a third on the backside, which together provide 100% coverage.

The low altitude (high drag) user orbit types are of interest to determine whether more frequent tracking data, available with FLBT, is of significant benefit. The high and low inclination orbit types are of interest, since their coverage and geometrical properties can differ significantly.

Tracking Schedules/Processing Algorithms (5.2) - For the FLBT mode, the schedule was assumed to be continuous for a selected TDAS with metric tracking data $(R,\dot{R})$ processed sequentially. For the FLST and RLST modes, the tracking schedule impact was assessed based on tracking every orbit and every other orbit during a 10 min pass/TDAS. Also, navigation performance was evaluated for both sequential and sliding batch* data processing.

Error Modelling - User OD/TD error was computed via covariance analysis programs [22,23] given nominal TDAS and user orbits, a tracking schedule and processing approach, and appropriate models of the tracking error sources. The latter comprised measurement errors and various systematic errors, e.g., gravitational harmonic modelling error, drag modelling error, TDAS ephemeris error, user oscillator drift effects, etc.

* Details are given in Section 5.

FIGURE 6-4: NAVIGATION PERFORMANCE EVALUATION - OVERVIEW

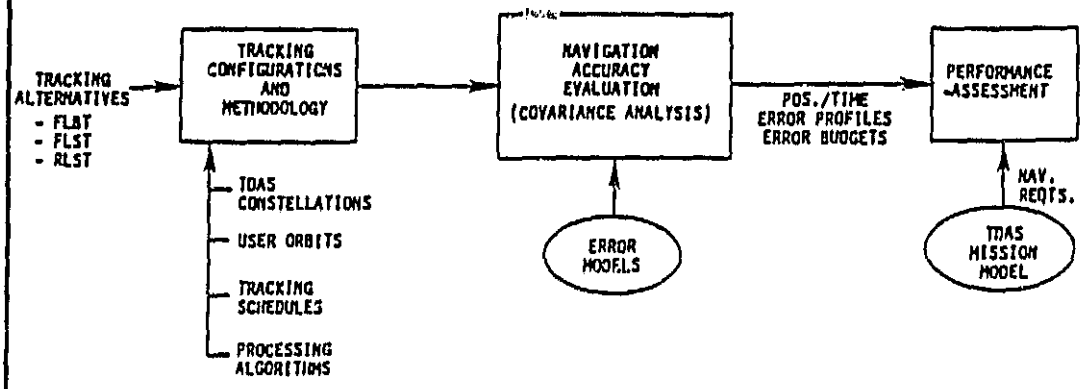

STANFORD TELECOMMUNICATIONS INC.

FIGURE 6-5: USER ORBITS AND TDAS CONSTELLATIONS CONSIDERED

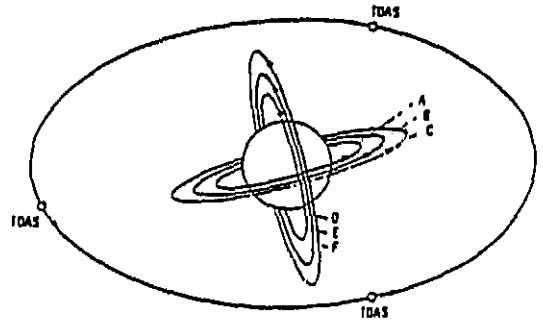

USER ORBITS

TYPE	INCLINATION	ALTITUDE
A	28°	200 KM
B	"	600
C	"	1000
D	97°	200
E	98°	600
F	"	1000

OPTION 1: TWO FRONTSIDE TDAS

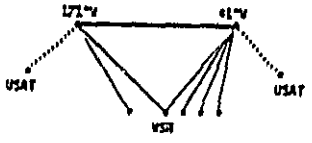

OPTION 2: ONE FRONTSIDE/ONE BACKSIDE TDAS

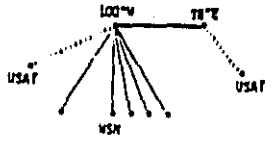

OPTION 3: TWO FRONTSIDE/ONE BACKSIDE TDAS

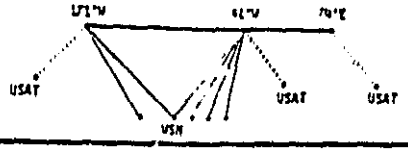

STANFORD TELECOMMUNICATIONS INC.

Table 6-3 lists the baseline modelling assumptions made for these particular error sources and their relative impact on achieving a 40 M OD accuracy with beacon tracking in the user orbits considered. In this case gravitational harmonic error dominates, so TDAS ephemeris error is only a secondary effect. The projected requirements indicate the gravitational model improvement required (in terms of GEM-9 errors) to achieve 10 M and 30 M accuracies in the noted orbits. At this level, the modeled TDAS ephemeris error would also be significant so a reduction of ~2:1 is indicated.

Navigation Performance With Sequential Processing (5.4.2) - Figure 6-6 shows the OD performance (max error over 24 hours) with beacon tracking for each TDAS constellation option along with user requirements identified in the TDAS mission model (see Appendix A). Higher errors tend to occur for Option 2 in near polar orbits particularly at low altitudes due to recurring poor geometry.*

Error analysis results correspond to the basic modelling assumptions and the projected results to the improved errors indicated in Table 6-3. Thus, beacon tracking is projected to satisfy all user requirements in the TDAS mission model down to 10 M.

Figure 6-7 shows the navigation performance with FLST for two assumed tracking schedules and sequential processing. In contrast to beacon tracking, the performance in low orbits is drag dominated and substantially worse. At higher altitudes, results are comparable.

Figure 6-8 shows the navigation performance with RLST for the same tracking schedules and two different nav data upload rates - 1.5 hours and 3 hours. Again, performance is worse in low orbits (drag dominated), but is comparable at higher altitudes.

* This occurs about twice a day when the orbit normal points toward a TDAS thereby limiting the range change over the pass (poor doppler characteristic).

TABLE 6-3

ERROR CONTRIBUTOR SUMMARY FOR BEACON TRACKING
(SEQUENTIAL DATA PROCESSING)

ERROR CONTRIBUTOR	MODELING ASSUMPTIONS FOR ANALYSIS	ORBIT DETERMINATION IMPACT FOR 40 m ACCURACY	PROJECTED REQTS. FOR 10 m ACCY.* 30 m ACCY.**	COMMENTS
GRAVITATIONAL HARMONICS MODEL	100% GEM-9 ERROR	MAJOR	20% GEM-9 ERROR	≥ 10:1 IMPROVEMENT ANTICIPATED BY EARLY 1990'S [36]
DRAG COEFFICIENT (C_D) (<600 Km ORBITS)	2.5% OF NOMINIAL C_D (RESIDUAL ERROR)	SECONDARY	SAME AS MODEL	OPTIMIZE PROCESSOR TUNING PARAMETERS
TDAS ORBIT ERROR	50 m POS. 5 mm/s VEL.	SECONDARY	25 m POS. 2.5 mm/s VEL.	- MINIMAL BRTS CONFIG. CANNOT MEET PROJECTED REQT. - VLBI TRACKING MEETS PROJECTED REQT.
USER OSC. DRIFT	10^{-10}/DAY	NEGLIGIBLE	SAME AS MODEL	CURRENTLY AVAILABLE CAPABILITY

*98°, 600 KM ORBIT
**98°, 200 KM ORBIT

+ GEM-9 = GODDARD EARTH MODEL 9 (1979)

FIGURE 6-6

USER NAVIGATION PERFORMANCE SUMMARY - BEACON TRACKING (SEQUENTIAL PROCESSING)

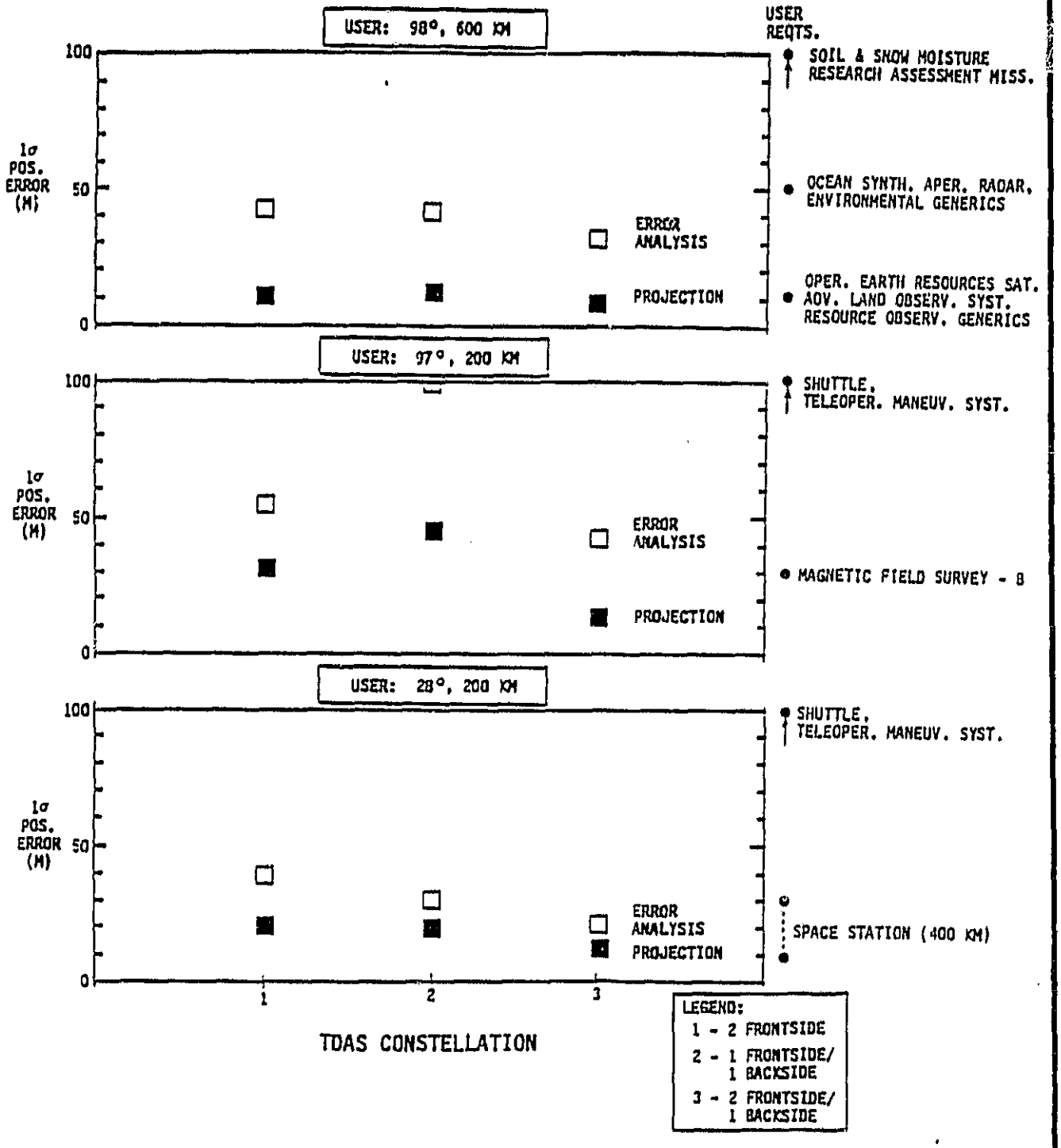

STANFORD TELECOMMUNICATIONS INC.

FIGURE 6-7

USER NAVIGATION PERFORMANCE SUMMARY - FORWARD LINK SCHEDULED TRACKING
(SEQUENTIAL PROCESSING)

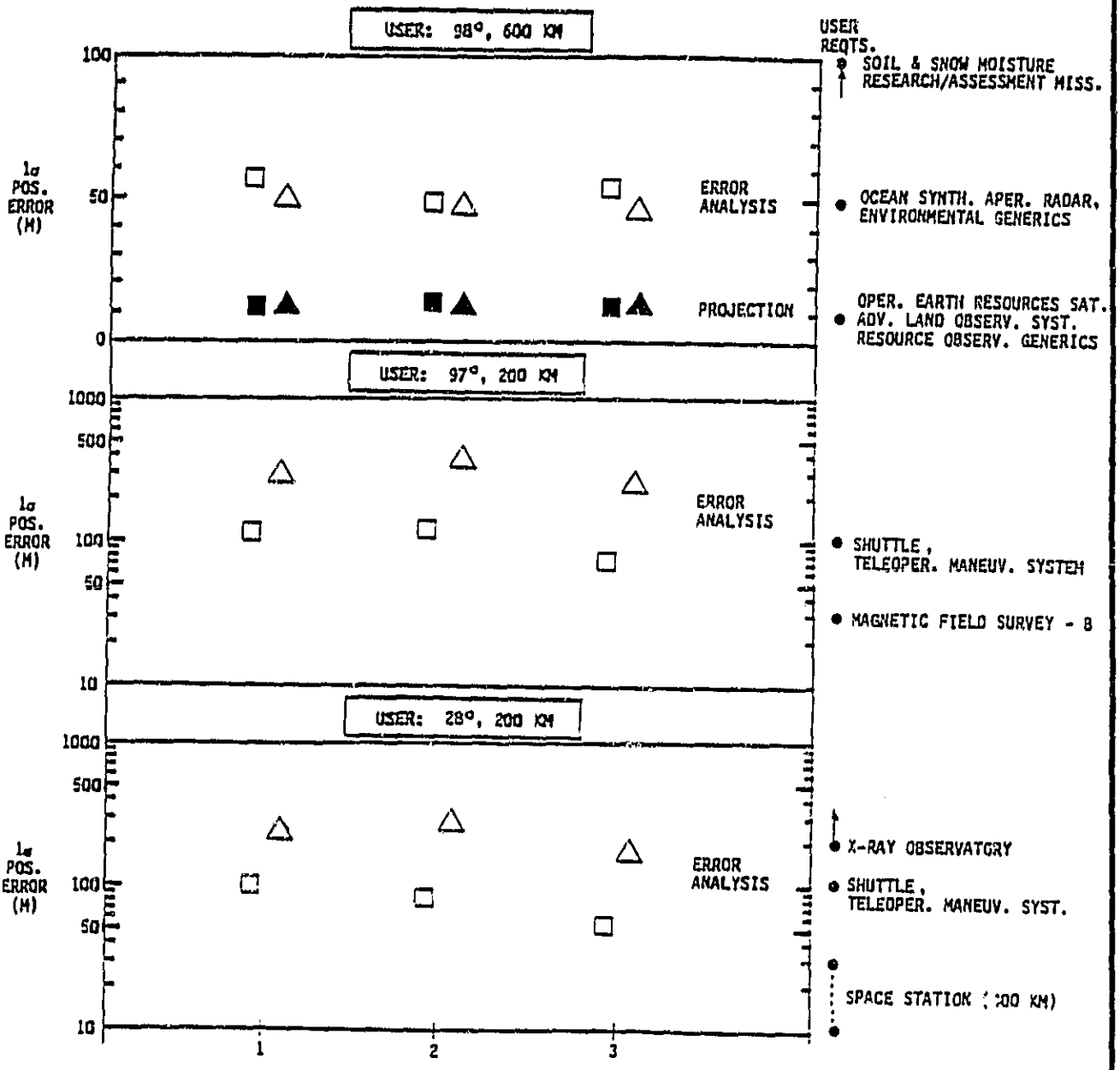

STANFORD TELECOMMUNICATIONS INC.

FIGURE 6-8

USER NAVIGATION PERFORMANCE SUMMARY - RETURN LINK SCHEDULED TRACKING (SEQUENTIAL PROCESSING)

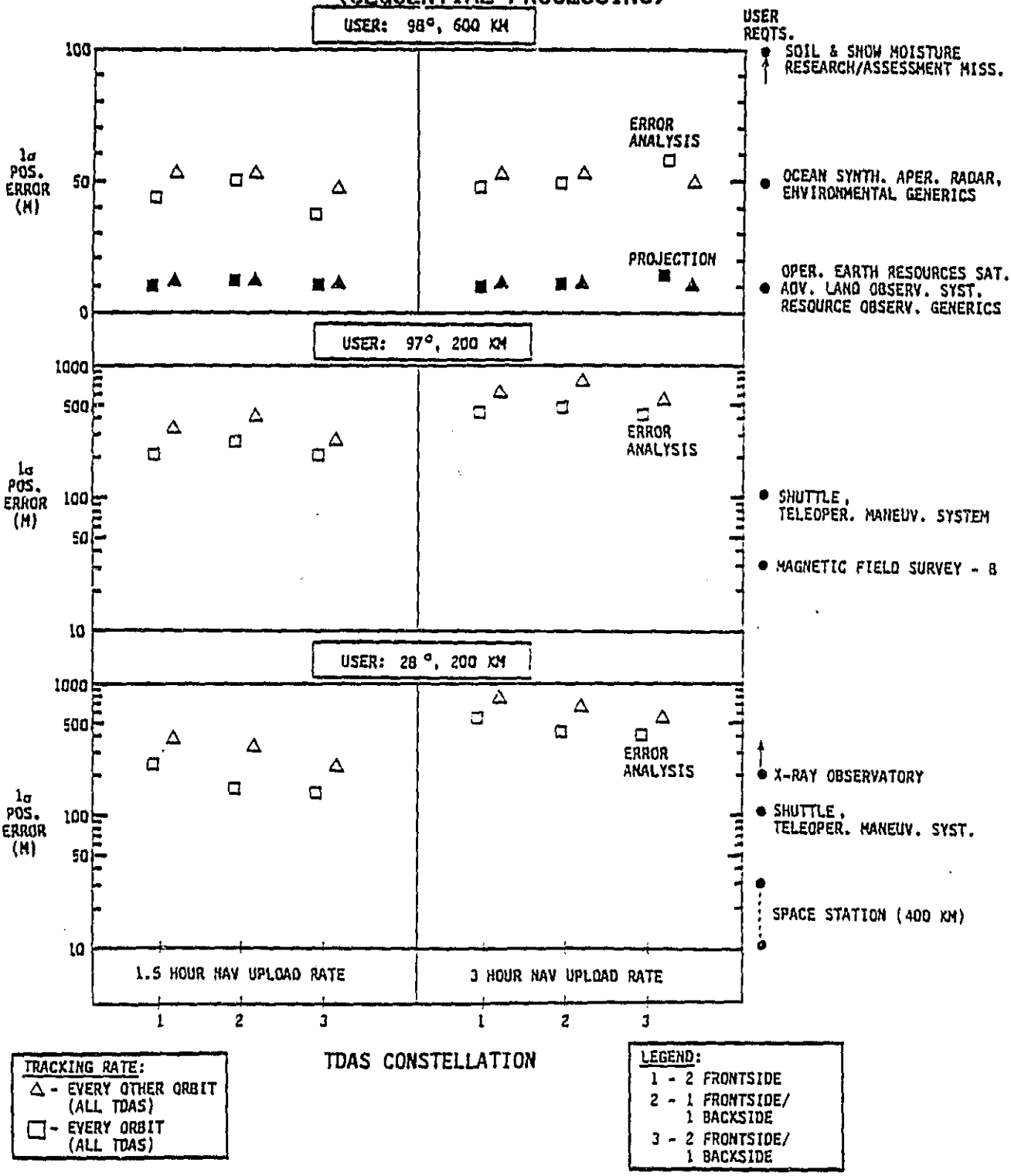

STANFORD TELECOMMUNICATIONS INC.

TD accuracy results* indicate that performance is uniformly better with beacon tracking ($\leq$ .25 μsec) than with scheduled tracking in all orbits considered. Nevertheless, performance with the scheduled alternatives is sufficient to meet the most stringent user time requirement (1 μsec) identified in the TDAS mission model.

Navigation Performance With Sliding Batch Processing (5.4.3) - Results for FLST and RLST indicate that compared to sequential processing:

- OD performance tends to be worse for low altitude orbits (< 400 km) where drag is the dominant error source and comparable to or slightly better in higher orbits where user oscillator drift is also a major error source.

- TD performance is worse ($\geq$ 2.5 μsec) for all orbits considered and particularly sensitive to the tracking interval duration.

* See Section 5.4.

6.3 TDAS TRACKING ANALYSIS SUMMARY

Information about TDAS orbits is assumed to be provided for user OD/TD on a recurring basis. User navigation performance is then a function of TDAS orbit uncertainties in the interval between updates (i.e., prediction interval errors). To assess potential orbit prediction errors, an accuracy analysis was made of TDAS tracking with the BRTS and VLBI techniques. An overview of the elements considered in pursuing this analysis is given in Figure 6-9.

Tracking Configurations (4.1) - In terms of TDAS tracking, the various constellations reduce to two situations: frontside and backside satellites. Figure 6-10 illustrates configuration options for acquiring TDAS tracking data with each technique.

With BRTS tracking, two-way range and range-rate ($R,\dot{R}$) data are acquired from transmissions originating at White Sands (WHS). These are returned by bilateration ranging transponders (BRTs) operating at pairs of automated ground stations (one pair per TDAS in the minimal configuration). For the backside TDAS, transmissions are also relayed via the crosslink which impacts tracking accuracy since measurements are affected by uncertainties in the frontside satellite orbit.

With VLBI tracking, the fundamental measurement data type is the difference in range (ΔR) between a signal source and two receivers displaced along a known baseline. For the TDAS application, signals received at each automated station would be returned to WHS for processing. Typically, one processed pair of VLBI observations per hour per station set (three per TDAS) would be needed. Crosslink uncertainties are not a factor due to the inherent differencing of common path components.

Error Modelling (4.2.1) - TDAS OD was assumed to employ batch processing of tracking observations taken over a given tracking interval. Orbit prediction errors beyond the end of tracking were evaluated via a covariance

FIGURE 6-9: TDAS TRACKING ANALYSIS - OVERVIEW

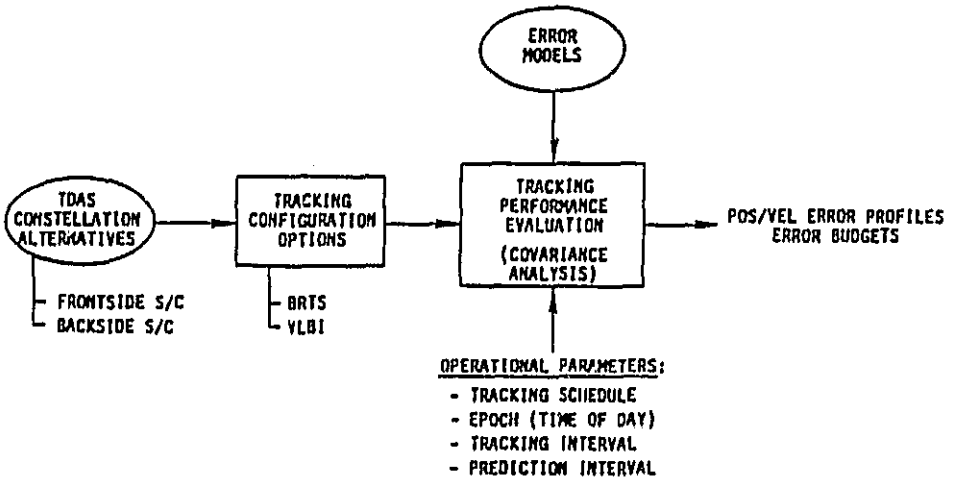

STANFORD TELECOMMUNICATIONS INC.

FIGURE 6-10: BRTS AND VLBI CONFIGURATIONS FOR TDAS TRACKING

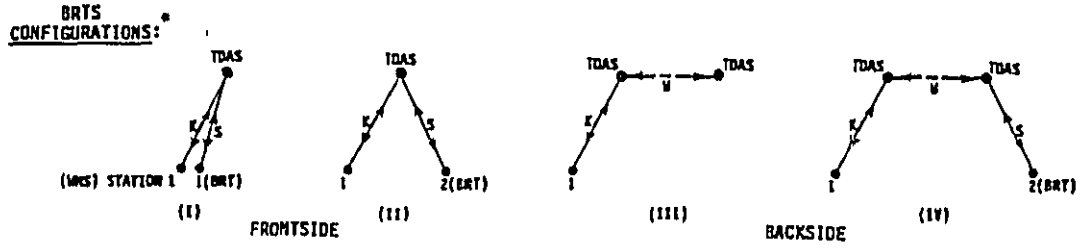

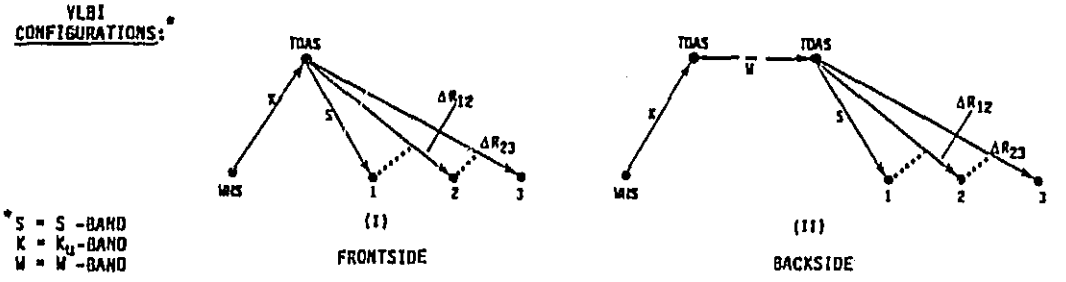

*S = S -BAND
K = K_u-BAND
W = W -BAND

STANFORD TELECOMMUNICATIONS INC.

analysis program [16] given a nominal orbit, tracking station locations, tracking schedule and appropriate models of significant tracking error sources (measurement noise and bias, station survey, solar pressure and tropospheric uncertainties).

BRTS measurement errors were assumed consistent with TDRS OD analyses [18]. VLBI measurement errors were considered at two levels: a conservative baseline model consistent with values used in studies of a Deep Space Network (DSN) tracking application to TDRS [19] and a more optimistic reduced model which reflects achieved capabilities with VLBI stations observing celestial radio sources [20]. Station errors were taken to be the same as BRTS for the baseline model and an order of magnitude better for the reduced model.

TDAS Tracking Accuracy (4.2.2) - For evaluating performance, the first criterion considered was the peak error over a 24 hour continuous prediction interval from the end of tracking. Analysis results indicate, however, that since solar pressure is so dominant, OD accuracy can be significantly affected by the choice of reference epoch and duration of the tracking interval and prediction interval. Thus, in both BRTS and VLBI analyses efforts were made to identify multiple combinations (epoch/tracking interval/prediction interval) which, taken together, yield better accuracy over a 24 hour period than any one combination alone.

Table 6-4 gives results for both frontside and backside TDAS OD accuracy via BRTS tracking using one 24 hour prediction interval and two concatenated 12 hour intervals. Multiple segments are effective for the frontside TDAS but not the backside which is >2.5:1 higher. The prediction error is due primarily to the impact of the frontside TDAS position uncertainty assumed to be 100 M.

Table 6-5 and Figure 6-11 present the results for TDAS OD accuracy with VLBI tracking for both baseline and reduced error models. The reduced

TABLE 6-4

MAXIMUM TDAS POSITION ERROR IN 24 HOUR PREDICTION INTERVAL WITH BRTS TRACKING

TDAS	TRACKING INTERVAL (HOURS)	PREDICTION INTERVAL(S) (HOURS)	MAXIMUM POSITION ERROR (M)	PRIMARY ERROR CONTRIBUTORS* (M)
FRONTSIDE 100°W	18	24	175	150 (SP) 80 (B) 40 (S)
	18	12 + 12**	110	80 (B) 60 (SP) 45 (S)
BACKSIDE 98°E	36	24	290	230 (S') 175 (SP) 25 (B)
	36	12 + 12**	280	220 (S') 165 (SP) 25 (B)

* LEGEND: SP - SOLAR PRESSURE; B - BRT BIAS; S - STATION SURVEY;
S' - STATION SURVEY + T100 LOCATION (TDAS 100°W).

** CONCATENATED INTERVALS BASED ON TRACKING INTERVAL EPOCHS SPACED ~12 HOURS APART.

STANFORD TELECOMMUNICATIONS INC.

TABLE 6-5

MAXIMUM TDAS POSITION ERROR IN 24 HOUR PREDICTION INTERVAL WITH VLBI TRACKING

VLBI ERROR MODEL	TRACKING INTERVALS (HOURS)	PREDICTION INTERVAL NO. SEGMENTS	PREDICTION INTERVAL LENGTH (HOURS)	MAXIMUM POSITION ERROR* (M)	PRIMARY ERROR CONTRIBUTORS** (M)
BASELINE	18/36	4	9/3	87	72 (SP) 45 (VB) 25 (S)
BASELINE (WITH BIAS ESTIMATED)	18/12	4	6/6	72	56 (SP) 45 (VN) 20 (S)
REDUCED	6	24	1	12	10 (TR) 6 (SP) 4 (S)
REDUCED (W. 5% TROPO)	6	24	1	8	6 (SP) 4 (S) 3 (TR)

* TDAS @ 100°W; STNS: WHS-AGO, WHS-HAW; DATA RATE = 1/HR

** LEGEND: SP - SOLAR PRESSURE
S - STATION SURVEY
VB - VLBI MEAS. BIAS
VN - VLBI MEAS. NOISE
TR - TROPOSHERE

STANFORD TELECOMMUNICATIONS INC.

FIGURE 6-11: TDAS POSITION UNCERTAINTY IN 24 HOUR PREDICTION INTERVAL (BASED ON MULTIPLE VLBI TRACKING SEGMENTS)

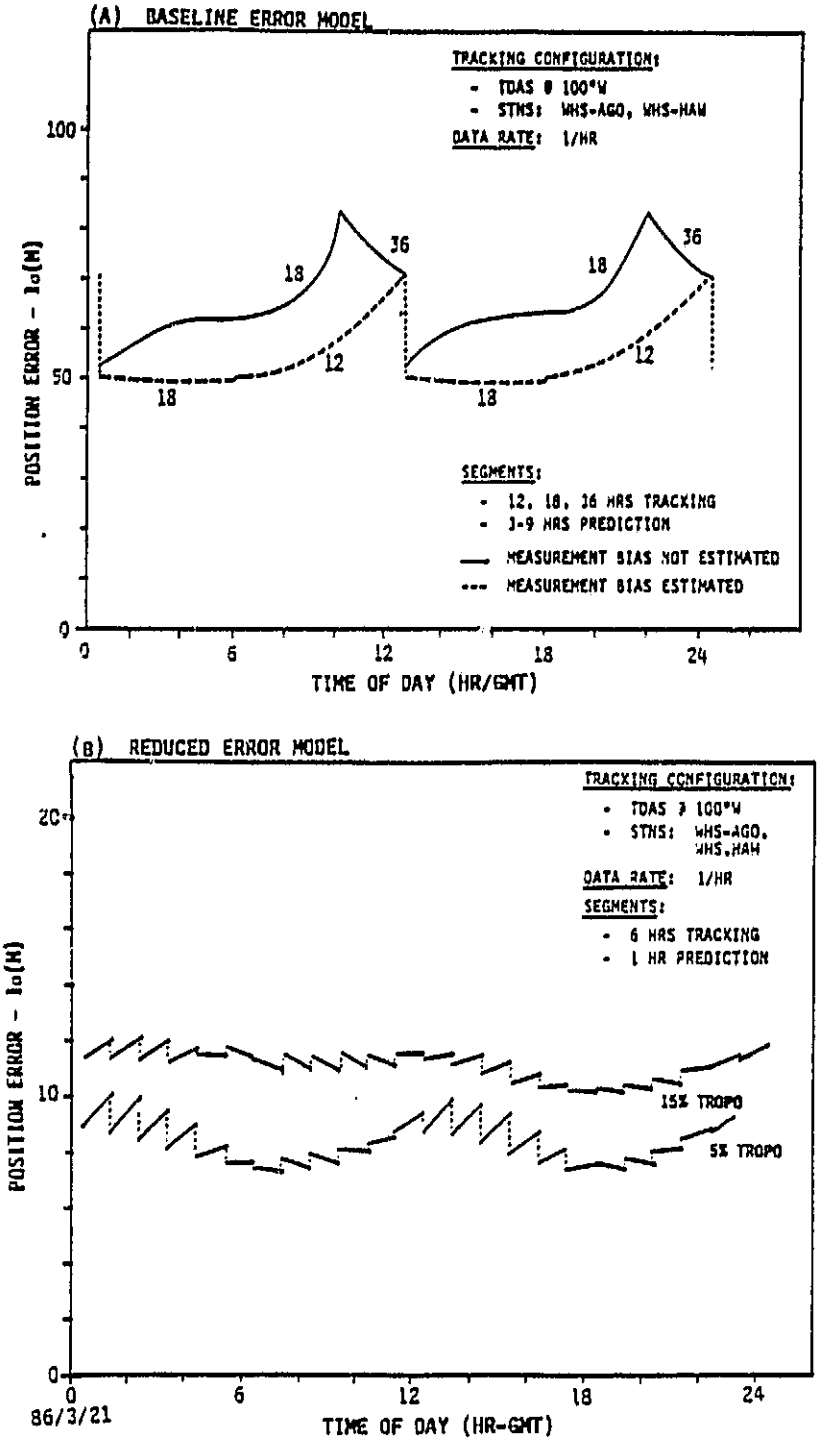

model results illustrate dramatically the benefit of more accurate measurements since shorter tracking and prediction intervals can be used to offset the pervasive influence of solar pressure errors. Additional improvement to the 5-8 M level would be possible if better tropospheric correction ($\leq$ 5%) can be achieved.

Results of the TDAS tracking analysis lead to the following observations:

- Orbit determination error for backside TDAS satellite tracking via BRTS is significantly higher ($\sim$ 2-3:1) than for frontside tracking based on two BRT sites per satellite.

- VLBI tracking offers the potential for significantly improved TDAS orbit accuracy (< 10m) for both front and backside satellites
  - This method is not sensitive to cross-link uncertainties, but tracking data from three stations would be required for each satellite
  - Realization of potential VLBI tracking accuracy requires:
    -- Calibration of tracking biases and station location/baseline uncertainties (e.g., using ΔVLBI data)
    -- Judicious selection of epoch (time of day), tracking interval, and prediction interval combinations.

- Preliminary results for VLBI tracking with Conus-based sites also indicate increased accuracy, although the shorter baselines may reduce the potential improvement compared to that with intercontinental baselines.

6.4 CONCLUSIONS

Analysis of the study results leads to the following key findings:

- TDAS beacon tracking (FLBT) will satisfy all users in the TDAS mission model with position accuracy requirements down to 10 M.

- Scheduled tracking alternatives (FLST, RLST) can also meet the accuracy requirements except at low altitudes where performance is highly sensitive to:
  - Drag uncertainty
  - Frequency of tracking passes, and/or
  - Frequency of navigation data uploads (RLST/only).

- A two or three satellite TDAS constellation impacts performance as follows:
  - Selecting 2 satellites leads to a tradeoff between coverage and accuracy. Increased satellite spacing improves coverage, but a point is reached where performance in high inclination orbits begins to degrade (130° spacing appears better than 162°).

  - Selecting 3 satellites provides full coverage and up to a 2:1 advantage in navigation accuracy over two satellites.

- Projected TDAS tracking accuracy requirements (25 M-POS. & 2.5 MM/SEC-VEL.) can be met with VLBI tracking but not with a minimal* BRTS configuration.

6.5 RECOMMENDATION

Based on the study results beacon tracking is recommended as the prime approach for routine navigation support. Scheduled tracking alternatives, one-way and two-way, should also be considered for supporting user navigation functions, as proposed in Table 6-6.

* 2 BRTS sites/TDAS.

TABLE 6-6

SUMMARY OF PROPOSED TDAS NAVIGATION FUNCTIONS

- TDAS ARCHITECTURE WILL ACCOMODATE ALL ONE-WAY AND TWO-WAY TRACKING TECHNIQUES.

USER SUPPORT FUNCTION		PROPOSED TECHNIQUE	RATIONALE
NAVIGATION	ROUTINE	BEACON TRACKING	- MAX. AVAILABILITY - MEETS REQUIREMENTS
	INITIAL ACQUISITION	SCHEDULED TRACKING (FORWARD LINK)	DOPPLER COMPENSATION AVAILABLE
	BACKUP	SCHEDULED TRACKING FWD. LINK / RTN. LINK / OR 2-WAY	PROVIDE REDUNDANCY VIA COMM. CHANNELS
	VERIFICATION	SCHEDULED TRACKING (2-WAY)	- GROUND-BASED OPNS. - QUALITY CONTROL
COMM./NAV.	TDAS ANTENNA POINTING	SCHEDULED TRACKING (RETURN LINK) OR BEACON TRACKING	- GROUND-BASED OPNS. - ACCURACY SUFFICIENT - DIRECT DOWNLINK TO NCC

APPENDIX A

TDAS MISSION MODEL

In Task 1 of the TDAS study [1b], a screened baseline of NASA plans was used to generate scenarios of experiments/missions for the 1990 - 2005 time period. An estimated flight schedule was established by first assigning planned experiments, then candidate experiments and finally opportunity experiments. Where planning data for the 1990s was unavailable, generic experiments/missions were developed based on trends established in the 1980's planning data. Table A-1 lists the adopted TDAS mission model and corresponding orbit data.*

Potential navigation accuracy requirements for the various experiments/missions were developed from user community survey data, subsequent conversations with designated points-of-contact and/or independent estimates. Table A-1 lists the position and time accuracy requirements developed in each case. Except for the TOPEX mission, the most stringent position accuracy requirements is 10M. Time accuracy requirements were found to be no less than 1 μsec.

For purposes of comparing user navigation requirements with estimated navigation performance results, user orbits were divided into six categories (A-F). Tables A-2 and A-3 show the distribution by category and number of missions with a given requirement. Some missions are counted more than once, since the orbit range spans more than one category (see Table A-1).

* More detailed information is available in [1b].

TABLE A-1
TDAS MISSION MODEL (1990 - 2005)

EXPERIMENT/MISSION		ALTITUDE (km)	ORBIT* INCLINATION (deg)	CATEGORY	ACCURACY REQUIREMENT POSITION (m)	ACCURACY REQUIREMENT TIME (usec)
ASTROPHYSICS	SPACE TELESCOPE	600	28.8	B	≥ 200	1
	ADVANCED X-RAY ASTROPHYSICS FACILITY (AXAF)	450	28.5	B	> 1000	≥ 1
	ASTROPHYSICS GENERIC (AG) - 1,2,3,4	LEO	28.5	B	"	TBD
	VERY LONG BASELINE RADIO INTERFEROMETER (VLBRI)	400-5000	45	B,C	"	1**
	X-RAY OBSERVATORY	300	28.5	A	≥ 200	≥ 100
	COSMIC OPTICAL SYSTEM OF MODULAR IMAGING COLLECTORS/100 METER THINNED APERATURE TELESCOPE	500	28	B	"	1
	LARGE OPTICAL/ULTRAVIOLET INTERFEROMETER	450	28.5	B	"	"
	ORBITING SUBMILLIMETER TELESCOPE	1000	SUN SYNC	F	"	TBD
	LARGE AMBIENT DEPLOYABLE IR TELESCOPE (LADIR)	400-700	28-50	B	"	≥ 100
SOLAR TERRESTRIAL	SOLAR CYCLE AND DYNAMICS MISSION (SCADM)	575	28 or 98	B or E	≥ 1000	1
	SOLAR TERRESTRIAL GENERIC (SG) - 2	575	28	B	"	"
	SOLAR TERRESTRIAL GENERIC (SG) - 1,3	400	57	B	"	"
GLOBAL ENVIRONMENT	TOPOGRAPHY EXPERIMENT (TOPEX)	1334	63.4	C	3(0.1 ALT)	≥ 100
	ENVIRONMENTAL GENERIC (EG) - 2,5,6	1334	63	C	"	"
	OCEAN SYNTHETIC APERATURE RADAR (OSAR)	790	98	E	50	1
	ENVIRONMENTAL GENERIC (EG) - 1,3,4	790	98	E	"	"
RESOURCE OBSERVATION	SOIL AND SNOW MOISTURE RESEARCH AND ASSESSMENT MISSION	400-700	60-98	B or E	100	"
	OPERATIONAL EARTH RESOURCES SATELLITE/ ADVANCED LAND OBSERVING SYSTEM (OERS/ALOS)	705	99	E	10	"
	RESOURCES GENERIC (RG) - 1,2,3	700	98	E	"	"
	ADVANCED THERMAL MAPPING APPLICATIONS SATELLITE	620	97.8	E	50	"
	MAGNETIC FIELD SURVEY B	300	97	D	30	"
METEOROLOGY	OPERATIONAL METEOROLOGY SATELLITE (2)	830	98.7	F	500	≥ 100
SPACE TRANSPORTATION	SHUTTLE - 1	185-1110	28.5-57	A-C	100	1 (FUTURE)
	SHUTTLE - 2	185-1110	70-104	D-F	"	"
	TELEOPERATOR MANEUVERING SYSTEM (TMS)	185-1000	VARIOUS	A-F	"	TBD
	ORBITAL TRANSFER VEHICLE (OTV)	LEO-GEO	VARIOUS	A-F	"	"
	HEAVY LIFT LAUNCH VEHICLE (HLLV)	200-500	VARIOUS	A,B or D,E	"	"
	MANNED ORBITAL TRANSFER VEHICLE (MOTV)	LEO-GEO	VARIOUS	A-F	"	"
	SPACE STATION/PLATFORM (2)	400	28.5	B	10-30	1

* LEO - Low Altitude Earth Orbit
GEO - Geostationary Earth Orbit

** For Clock Synchronization Only, Needs Hydrogen MASER Stability.

TABLE A-2
USER POSITION ACCURACY REQUIREMENTS AND ORBIT DISTRIBUTION IN TDAS MISSION MODEL

INCLINATION I (DEG)	ALTITUDE, h (km)		
	$h \leq 300$	$300 \leq h < 800$	$h > 800$
$I < 70°$	A 100m - 5 $\geq$ 200m - 1	B $\geq$ 10m - 1 100m - 6 $\geq$ 200m - 4 $\geq$ 1000m - 6	C 3m(.1 Alt) - 2 100m - 4 $\geq$ 1000m - 1
$I \geq 70°$	D 30m - 1 100m - 5	E 10m - 2 50m - 3 100m - 6 $>$ 1000m - 1	F 100m - 4 $\geq$ 200m - 1 500m - 1

TABLE A-3
USER TIME ACCURACY REQUIREMENTS AND ORBIT DISTRIBUTION IN TDAS MISSION MODEL

INCLINATION I (DEG)	ALTITUDE, h (km)		
	h ≤ 300	300 ≤ h ≤ 800	h < 800
I < 70°	A 1 μs - 1 > 100 μs - 1 TBD - 4	B 1 μs - 11 ≥ 100 μs - 1 TBD - 5	C 1 μs - 3 > 100 μs - 1 TBD - 3
I ≤ 70°	D 1μs - 2 TBD - 4	E 1 μs - 8 TBD - 4	F ≥ 100 μs - 1 TBD - 5

APPENDIX B

TRACKING DATA MEASUREMENT ERRORS: RANDOM COMPONENT

Random errors in the range and Doppler measurement data arise due to noise in the tracking link. This appendix estimates these errors for the three one-way tracking alternatives based on the signal definitions and assumptions in Section 3. Parametric results are presented where applicable to indicate the sensitivity to design parameters; e.g., TDAS EIRP and user G/T or user EIRP. The results are presented as follows:

B.1 Thermal Noise in Range Measurements
B.2 Thermal Noise in Range-Rate Measurements
B.3 Phase Noise in Range-Rate Measurements

B.1 THERMAL NOISE IN RANGE MEASUREMENTS

The measurement of range in the systems considered here relies upon the acquisition and tracking of a pseudonoise (PN) ranging code. In all the one-way navigation modes, the receivers exploit the correlation properties of PN codes to produce an error signal which directs the timing correction. The principal figure of merit is the variance of the timing error as a function of the input ratio of signal power to noise density, C/N_0.

B.1.1 Forward Link Tracking

The Motorola 2nd generation TDRSS user transponder design [14] is assumed to apply to the users to be supported in the TDAS era. The design's code tracking loop is a digital implementation of a 2nd order type II tau-dither loop; a rate aided tracking loop configuration is also present, providing a 1st order tau-dither loop with frequency tracking from the carrier loop. Motorola expresses the variance of the tracking jitter due to thermal noise as

$$\sigma_\tau^2 \leq \frac{B_L}{C/N_0}\left[1 + 2\,\frac{B_{IF}}{C/N_0}\right] \quad (\text{chips})^2 ,$$

where B_L is the closed loop bandwidth of the loop, either 1 Hz for the independent tracking mode or .125 Hz with rate aiding, and B_{IF} is the IF filter bandwidth of 4 kHz. This result can be seen to stem from Hartmann's analysis [25] of the tau-dither loop where the incoming PN coded signal is alternately correlated with early and late versions of a locally generated code replica.

Based on the forward link budget in Figure 3-1, Figure B-1 shows the RMS range error σ_R in meters as a function of the user G/T, parameterized by the TDAS EIRP. The mean square range error σ_R^2 is derived from the mean square timing error σ_T^2 by the simple conversion

$$\sigma_R^2 = (c\ T_c\ \sigma_T)^2 = (d_c\ \sigma_T)^2 \quad (\text{meters})^2,$$

where c is the speed of light and T_c is, again, the chip duration, assumed here to be 1/3.0778 Mcps. From these curves the forward link range errors due to thermal noise are extracted for a user with G/T = -27 dB/°K for both FLBT and FLST modes.

B.1.2 Return Link Tracking

For return link tracking, a ground receiver incorporating the Harris wide dynamics demodulator (WDD) is envisioned. The WDD uses a delay-locked loop to track the PN coded signal: early and later versions of the local PN code are correlated simultaneously with the input PN code sequence. An analysis of the exact implementation used in the WDD is not readily available, but work by Simon [26] provides results applicable to a delay-locked loop where the bandpass arm filters have bandwidths on the order of the data rate. A linear analysis for the mean-square timing jitter, assuming a large equivalent loop signal-to-noise ratio yields

$$\sigma_T^2 = \frac{B_L}{2\ C/N_0} \cdot \frac{1}{S_L} \quad (\text{chips})^2,$$

FIGURE B-1: TDAS SMA FORWARD LINK: RANGE ERROR DUE TO THERMAL NOISE

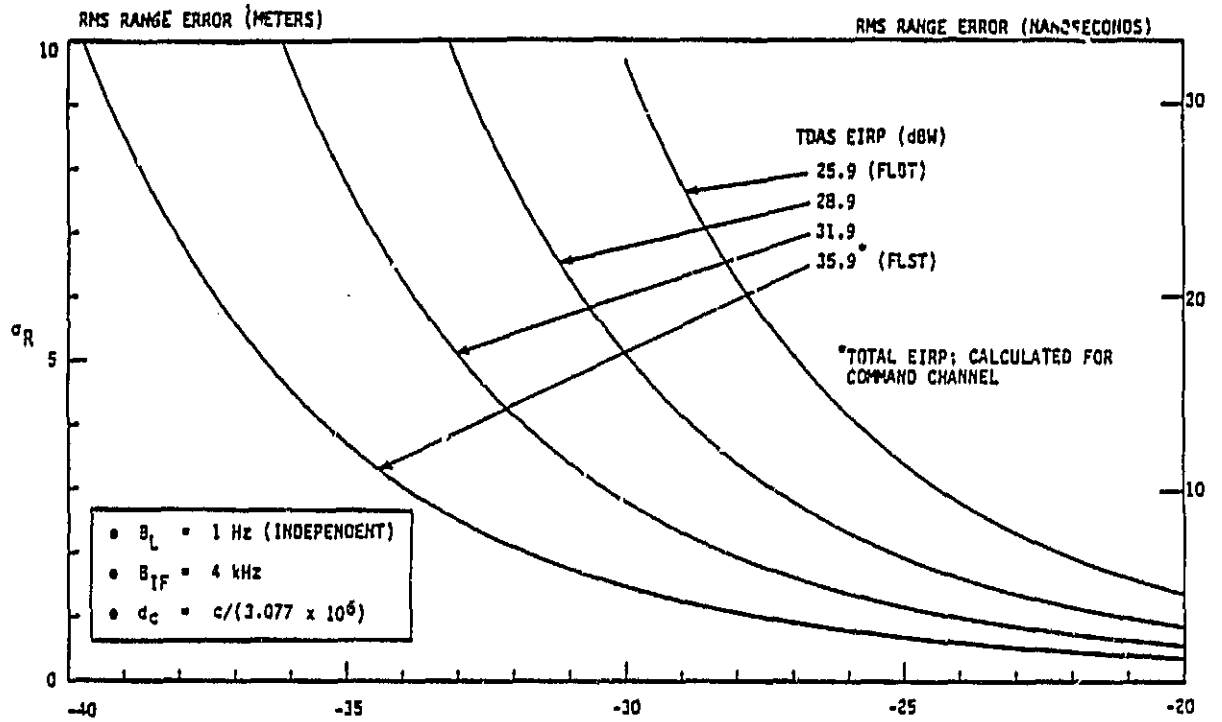

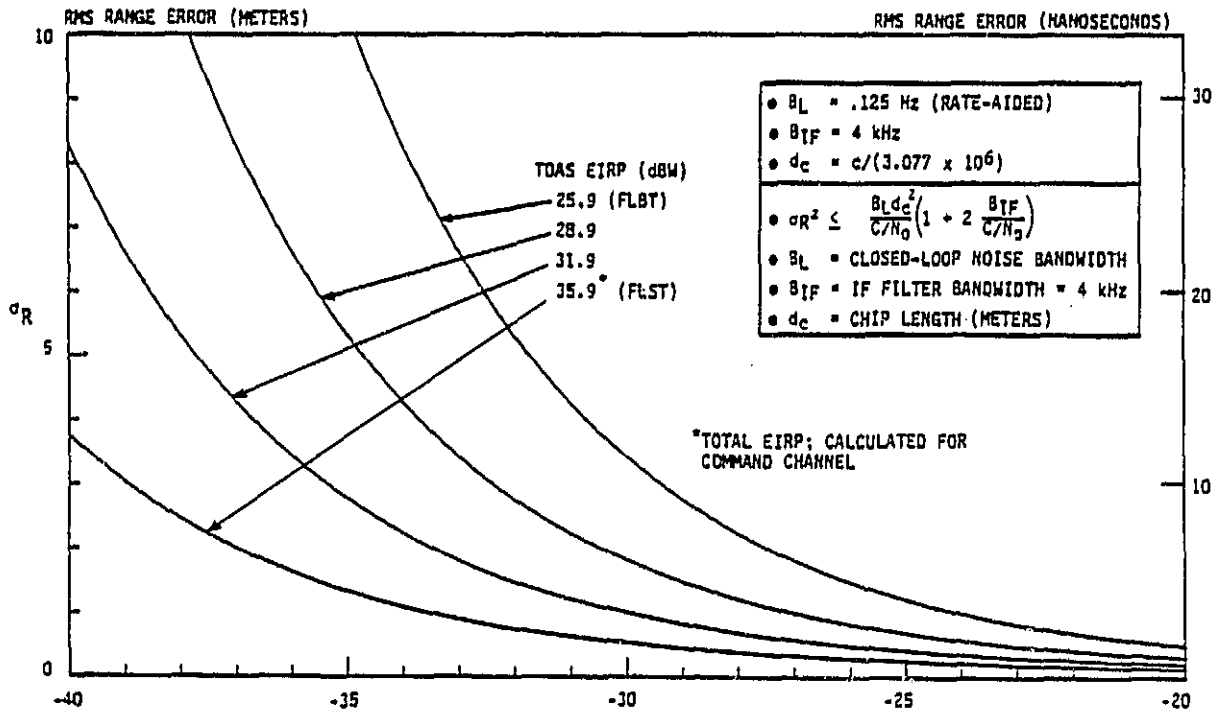

STANFORD TELECOMMUNICATIONS INC.

where B_L is the single-sided tracking loop bandwidth and S_L is the squaring loss of the delay-locked loop. Simon shows that

$$S_L = \frac{D_m}{K_D + K_L\left[\frac{2B_{arm}/R_s}{R_d D_m}\right]}$$

where

R_s = data symbol rate = $1/T_s$,

B_{arm} = 2-sided arm filter noise bandwidth

R_d = symbol SNR = $\frac{C}{N_0} T_s$,

$$D_m = \int_{-\infty}^{+\infty} S_d(f)|H(f)|^2\, df,$$

$$K_D = \frac{\int_{-\infty}^{+\infty} S_d(f)|H(f)|^4\, df}{\int_{-\infty}^{+\infty} S_d(f)|H(f)|^2\, df},$$

$$K_L = \frac{\int_{-\infty}^{+\infty} |H(f)|^4\, df}{\int_{-\infty}^{+\infty} |H(f)|^2\, df},$$

$S_d(f)$ = baseband power spectral density of the data,

and $H(f)$ = transfer function of the arm filter.

In keeping with the WDD parameters, it is assumed that B_L = 4 Hz in the tracking mode and that 1-pole arm filters are used. The symbol rate used for the calculation is assumed to be the maximum achievable data rate for a given user spacecraft EIRP, as detailed in Section 3.2.2 and shown in Figure 3-5. With the anticipated rate 1/2 convolutional coding, the symbol rate R_s is found as twice the achievable data rate. The tracking filters used in the WDD are chosen on the basis of symbol rate to optimally bandlimit the input noise. The 3 dB bandwidth f_c for the WDD is thus

$$f_c = \begin{cases} 8 \text{ kHz for all } R_s < 4 \text{ ksps} \\ 39 \text{ kHz for all } R_s < 26 \text{ ksps} \\ 300 \text{ kHz for all } R_s \leq 300 \text{ ksps} \end{cases}$$

where $B_{IF} = \pi f_c$ for a 1-pole filter, $H(f) = \frac{1}{1+jf/f_c}$. The parameter K_L for a 1-pole filter is found as:

$$K_L = \frac{f_c \frac{\pi}{2}}{f_c \pi} = \frac{1}{2}$$

The other parameters in Simon's expression depend on the data modulation format as well as the arm filter transfer function. Assuming equiprobable independent transmitted symbols — an assumption not strictly valid with coding — the power density for the NRZ signalling format is given by

$$S_d(f) = T_s \frac{\sin^2(\pi f T_s)}{(\pi f T_s)^2} \quad ;$$

for biphase (Manchester) coding, $B_d(f) = T_s \frac{\sin^4(\pi f T_s/2)}{(\pi f T_s/2)}$. It can be shown that

$$D_m = \begin{cases} 1 - \frac{1}{2\pi R'}(1-e^{-2\pi R'}) & \text{for NRZ coding} \\ 1 - \frac{1}{2\pi R'}(3-4e^{-\pi R'} + e^{-2\pi R'}) & \text{for biphase coding} \end{cases}$$

$$K_D = \begin{cases} \dfrac{1 - \frac{[3-(3+2\pi R')e^{-2\pi R'}]}{4\pi R'}}{D_m} & \text{for NRZ coding} \\ \dfrac{1 - \frac{[9-4(3+\pi R')e^{-\pi R'} + (3+2\pi R')e^{-2\pi R'}]}{4\pi R'}}{D_m} & \text{for biphase coding} \end{cases}$$

where $R' = f_c T_s$.

Figure B-2 shows the above results expressed as an RMS range error in meters versus the user EIRP corresponding to the return link budget in Figure 3-5. The discontinuities appearing on the graph result from the change in arm filter bandwidth with data rate. A user EIRP of 2 dBW is assumed as a baseline value.

B.2 THERMAL NOISE IN RANGE-RATE MEASUREMENTS

Range-rate is estimated on the basis of a signal's observed doppler shift in frequency due to the relative motion between the transmitter and receiver. A carrier-tracking loop in the receiver provides the means to extract the phase ϕ (in radians) of the received signal and thus the received frequency, since $\phi = 2\pi$ ft. By counting positive-going zero-crossings, $N(t)$, over the averaging time T_{av}, an estimate $\hat{\dot{R}}$ of the range rate $\dot{R}$ is derived as

$$\hat{\dot{R}} = \lambda \left[\frac{N(t+T_{av}) - N(t)}{T_{av}} \right] = \dot{R} + \frac{\lambda}{2\pi} \frac{\delta\phi(t+T_{av}) - \delta\phi(t)}{T_{av}} ,$$

where $\delta\phi(t)$ represents noise in the phase measurement and λ is the carrier wavelength, assumed to be known a priori for one-way navigation. Assuming T_{av} is long enough so that the phase samples are independent and identically distributed, the RMS range-rate error is given by

$$\sigma_{\hat{\dot{R}}} = \frac{\lambda}{2\pi T_{av}} \sqrt{\sigma^2_{\phi(t+T_{av})} + \sigma^2_{\phi(t)}} = \frac{\lambda}{2\pi T_{av}} \sqrt{2}\, \sigma_\phi$$

Here σ_ϕ is the RMS phase error in radians and one may identify $\sqrt{2}\sigma_\phi$ as the RMS doppler phase error. The performance of the carrier-tracking loop in the receiver thus determines the range-rate error due to thermal noise. In the results presented here, the doppler averaging time T_{av} is assumed to be 1 second.

FIGURE B-2: TDAS RLST: RANGE ERROR DUE TO THERMAL NOISE

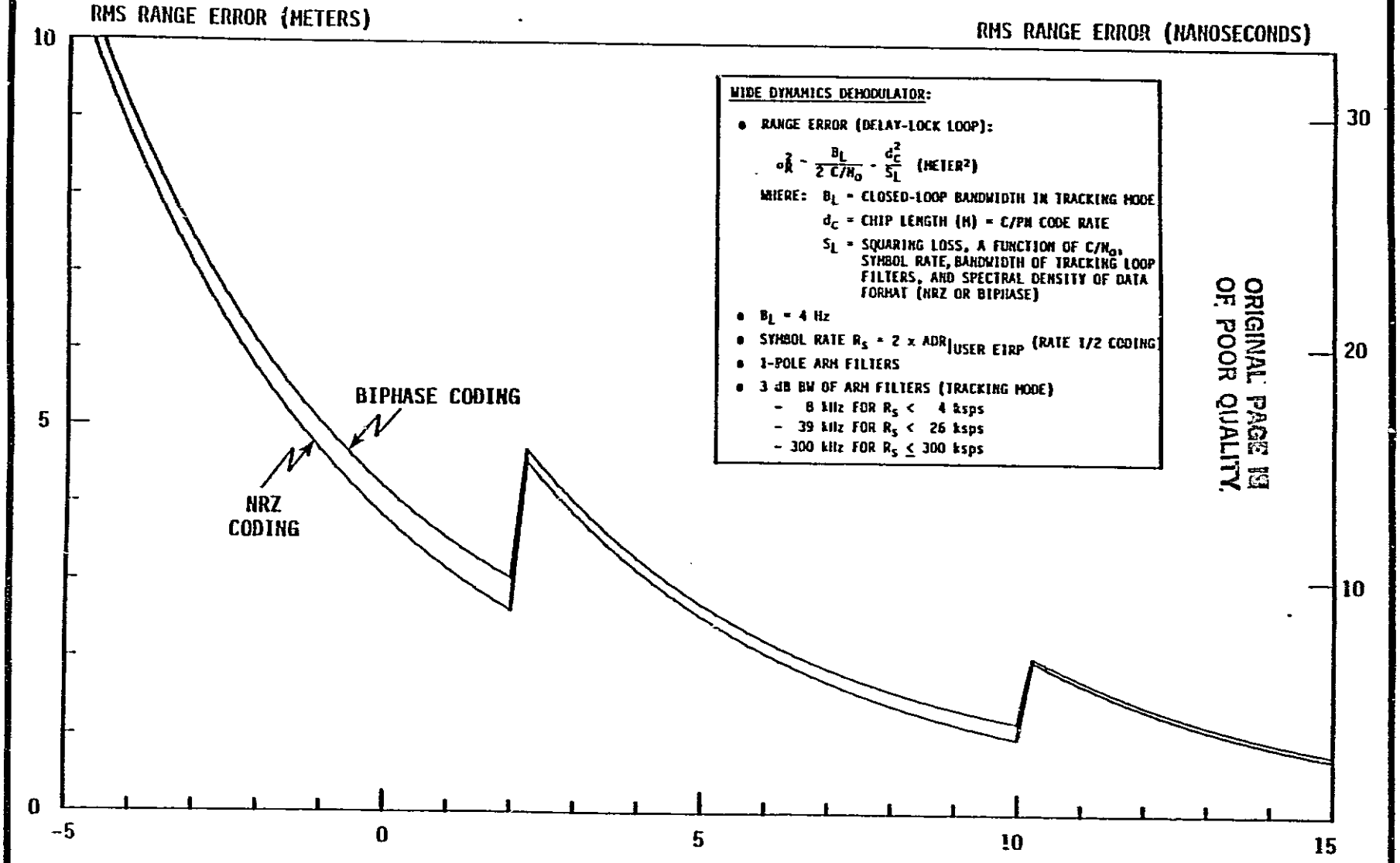

ORIGINAL PAGE IS
OF POOR QUALITY

STANFORD TELECOMMUNICATIONS INC.

B.2.1 Forward Link Tracking

The Motorola 2nd generation TDRSS user transponder's carrier-tracking loop is a 2nd order type II modified Costas loop. For Costas loops in general, the mean square phase error is given by [27, 28]:

$$\sigma_\phi^2 = \frac{4B_L}{C/N_0} \cdot \frac{1}{S_L} \text{ (radians)}^2 ,$$

where B_L is the loop noise bandwidth and S_L is the Costas loop squaring loss. The phase of a Costas loop, however, is twice the received signal phase, so the thermal noise phase jitter σ_ϕ that is of concern here is

$$\sigma_\phi^2 = \frac{B_L}{C/N_0} \cdot \frac{1}{S_L}$$

For the Motorola design, B_L = 40 Hz and S_L = .73. With these parameters, Figure B-3 shows the RMS one-way range-rate error anticipated for forward link tracking assuming the link budget of Figure 3-1 and the various possible TDAS EIRP values. As before, a user G/T value of -27 dB/°K is used as a baseline.

B.2.2 Return Link Tracking

The wide dynamics demodulator's 1st order carrier-tracking loop, shown in Figure B-4a, has been analyzed by Weinberg [29], yielding the following expression for the received mean square phase error:

$$\sigma_\phi^2 = \frac{B_L T_S}{\alpha\beta\, E_b/N_0} \left[\frac{1}{1 - \frac{2\, B_L T_S}{\beta}} \right] \text{(radians)}^2$$

Here

T_S = symbol duration,

$\frac{E_b}{N_0}$ = symbol SNR = $\frac{C}{N_0} T_S$,

$\alpha = 1 - 2\, Q(\sqrt{2\, E_b/N_0}) + \sqrt{\frac{1}{\pi\, E_b/N_0}}\; e^{-E_b/N_0}$,

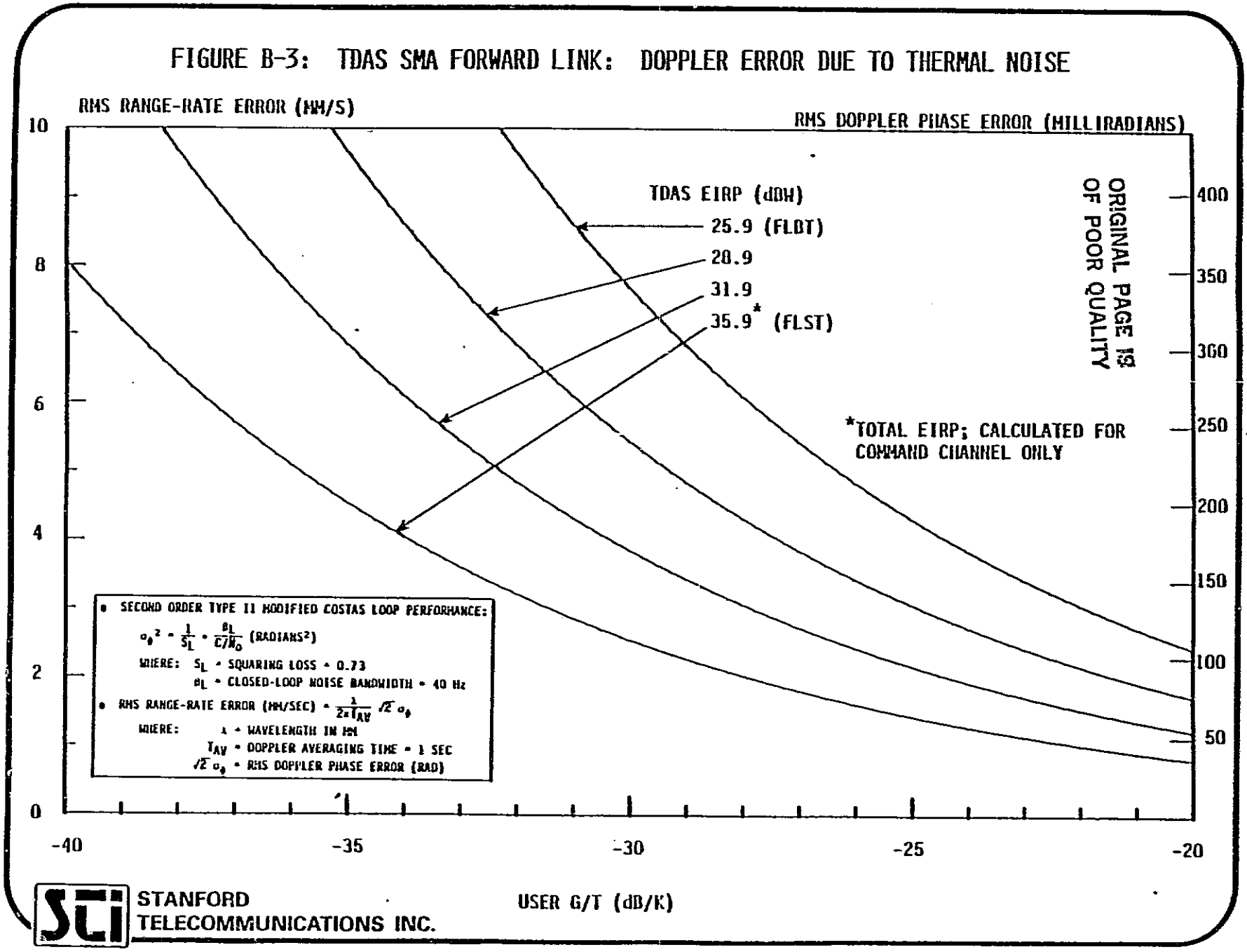
FIGURE B-3: TDAS SMA FORWARD LINK: DOPPLER ERROR DUE TO THERMAL NOISE
RMS RANGE-RATE ERROR (MM/S)
RMS DOPPLER PHASE ERROR (MILLIRADIANS)
TDAS EIRP (dBW)
25.9 (FLBT)
28.9
31.9
35.9* (FLST)
*TOTAL EIRP; CALCULATED FOR COMMAND CHANNEL ONLY
ORIGINAL PAGE IS OF POOR QUALITY
• SECOND ORDER TYPE II MODIFIED COSTAS LOOP PERFORMANCE:
$\sigma_\phi^2 = \frac{1}{S_L} \cdot \frac{B_L}{C/N_0}$ (RADIANS²)
WHERE: S_L = SQUARING LOSS = 0.73
B_L = CLOSED-LOOP NOISE BANDWIDTH = 40 Hz
• RMS RANGE-RATE ERROR (MM/SEC) = $\frac{\lambda}{2\pi T_{AV}} \sqrt{2}\,\sigma_\phi$
WHERE: λ = WAVELENGTH IN MM
T_{AV} = DOPPLER AVERAGING TIME = 1 SEC
$\sqrt{2}\,\sigma_\phi$ = RMS DOPPLER PHASE ERROR (RAD)
10
8
6
4
2
0
400
350
300
250
200
150
100
50
-40
-35
-30
-25
-20
USER G/T (dB/K)
STANFORD TELECOMMUNICATIONS INC.

FIGURE B-4: RLST: CARRIER TRACKING LOOP ERROR DUE TO THERMAL NOISE

A) WDD CARRIER TRACKING LOOP

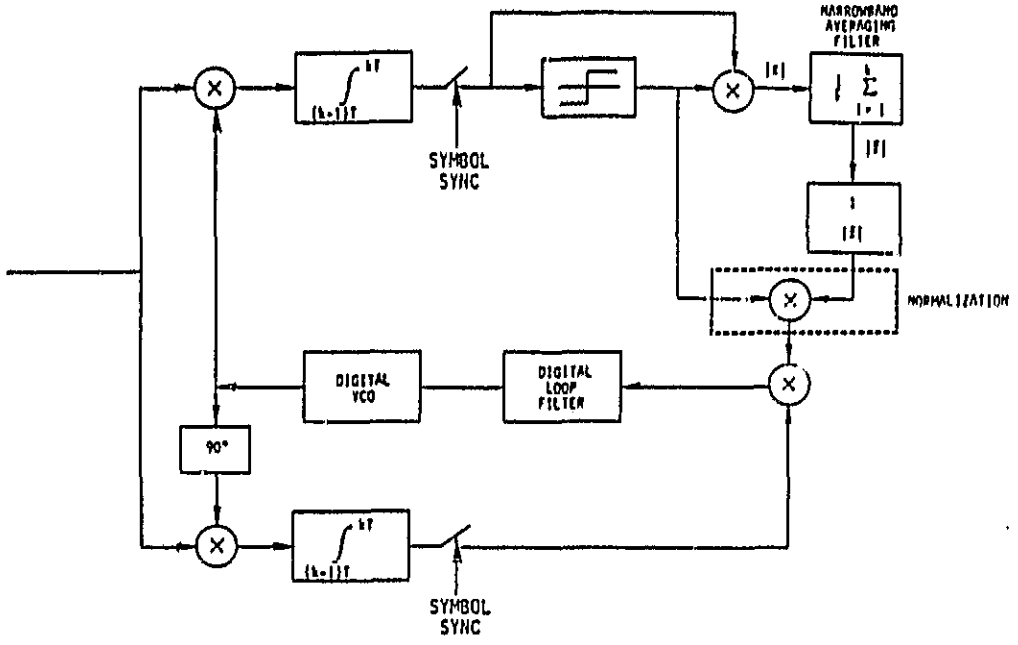

B) THERMAL NOISE PERFORMANCE

PERFORMANCE MEASURES	RESULTS*
WIDE DYNAMICS DEMODULATOR (PLL) PHASE ERROR, $\sigma_\phi = \sqrt{\frac{K}{E_B/N_O}}$	109 MRAD (6.2°)
DOPPLER PHASE ERROR = $\sqrt{2}\ \sigma_\phi$	154 MRAD (8.8°)
RANGE-RATE ERROR = $\frac{\lambda}{2\pi T_{AV}} \sqrt{2}\ \sigma_\phi$ (1-WAY)	3.5 MM/SEC

* ASSUMPTIONS:

- BER = 10^{-5}, 3 DB MARGIN, 5 DB CODING GAIN
- E_B/N_O = 4.3 DB (WORST CASE) = (C/N_O)/SYMBOL RATE
- K = .032, A FUNCTION OF E_B/N_O, LOOP BANDWIDTH AND SYMBOL RATE
- T_{AV} = 1 SEC, DOPPLER AVERAGING TIME
- λ = SMA WAVELENGTH (MM)

$$\beta = 1 - Q(\sqrt{2\,E_b/N_0}),$$

and $Q(x)$ = complementary Gaussian distribution function

$$= \frac{1}{\sqrt{2\pi}} \int_x^\infty e^{-u^2/2}\, du$$

In the WDD, the loop bandwidth is adjusted proportional to the symbol rate; for this calculation, it is assumed that $B_L T_S \approx .03$. If worst-case operation is assumed and the maximum achievable data rate is used for all values of user EIRP, then Figure 3-5 shows that E_b/N_0 is constant at 4.3 dB-Hz. Consequently, the carrier tracking error is constant, as summarized in Figure B-4b.

B.3 PHASE NOISE IN RANGE-RATE MEASUREMENTS

Additive thermal noise introduced by the channel is not the sole source of random fluctuations that affect range-rate measurement precision. A system's transmitting and receiving oscillators, system mixing chains, AM to PM conversion in the channel, spurious vibrations, etc. all introduce phase noise components into the signal which degrade the carrier-tracking loop performance of the receivers. To estimate the impact of phase noise on one-way navigation, consider first the doppler measurement process: the phase value ϕ extracted by the carrier-tracking loop is sampled at time $t-T_{av}$ and at time t and then differenced. That difference $\Delta\phi$ is related to the range-rate $\dot{R}$ as $\dot{R} = (\lambda/2\pi T_{av})\Delta\phi$. Since $\Delta\phi = \phi(t) - \phi(t - T_{av})$, the transfer function describing the operation is simply $F(f) = 1-e^{-j2\pi f T_{av}}$. If the input to the doppler extractor has single-sided phase noise spectral density $S_\phi(f)$, then the spectral density of $\Delta\phi$ is given by

$$S_{\Delta\phi}(f) = |F(f)|^2\, S_\phi(f) = 4 \sin^2 (\pi f T_{av})\, S_\phi(f).$$

Since $\sigma^2_{\Delta\phi} = 2\int_0^\infty S_{\Delta\phi}(f)\, df$, the input spectral phase noise density $S_\phi(f)$

contributed by the system can be seen to determine the range-rate mean square error due to phase noise.

In this analysis, only the effects of phase noise in the system oscillators and VCO's as propagated through the system mixing chain are considered. The key to the analysis, as discussed in [30], lies in characterizing a carrier-tracking loop by its closed loop transfer function H(f). A linear analysis of the carrier loop shows that the loop's VCO output tracks the carrier with noise contributions from two sources. One is the input phase jitter lowpass filtered by H(f), the other, the VCO's own phase jitter highpass filtered by 1-H(f). In other words, if the input phase noise spectral density is $S_\theta(f)$ and the phase noise spectral density of the VCO itself is $S_\theta'(f)$, then the coherent reference provided by the tracking loop has phase noise spectral density $S_\theta(f) = |H(f)|^2 S_\theta(f) + |1-H(f)|^2 S_\theta'(f)$. The simple analysis explained here has been validated by extending it to model the two-way doppler tracking of TDRSS; the results are consistent with other estimates of the doppler measurement error due to phase noise.

The forward and return links are modeled in terms of the ground and user oscillators, the tracking loops and their VCO's, and the frequency multiplies comprising the mixing chains. It is assumed that TDAS satellites will operate in the same fashion as do TDRSS satellites: a ground-generated pilot tone is tracked on-board the TDAS satellite to provide the reference tone for frequency-transition of the relayed signals. TDRSS uses a K_u-band space-to-ground link; in TDAS, both K_u- and K_a-band frequencies are being considered. Figure B-5 shows the models used here for the forward and return links, respectively. Both the user and ground station's oscillators are assumed to be 5 MHz standards; the frequency multiplies required to support return and forward link service and a K_u- or K_a-band space-to-ground link are shown in the diagrams. The K_u-band uplink, downlink, and pilot frequencies are taken from TDRSS; those for K_a-band are chosen arbitrarily. S-band forward link service centered at 2106.406 MHz (as in TDRSS) and an assumed IF frequency at the user spacecraft of 9.5 MHz yield a fixed multiply value at the user oscillator, as shown in Figure B-5a. S-band return link service centered at 2287.5 MHz similarly requires a fixed

FIGURE B-5: PHASE NOISE MODELS FOR TDAS FORWARD AND RETURN LINKS

A) FORWARD LINK:

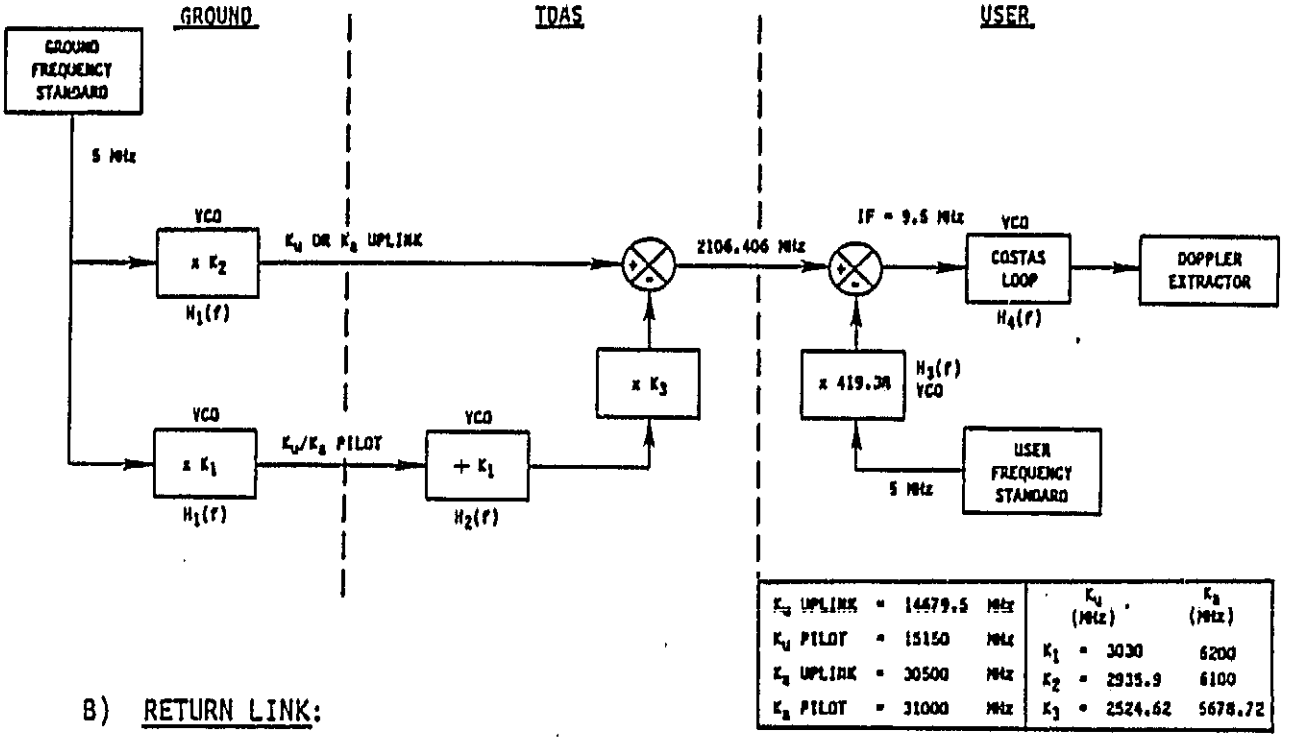

				K_u (MHz)	K_a (MHz)
K_u UPLINK	=	14479.5	MHz		
K_u PILOT	=	15150	MHz		
K_a UPLINK	=	30500	MHz		
K_a PILOT	=	31000	MHz		
				K_1 = 3030	6200
				K_2 = 2935.9	6100
				K_3 = 2524.62	5678.72

B) RETURN LINK:

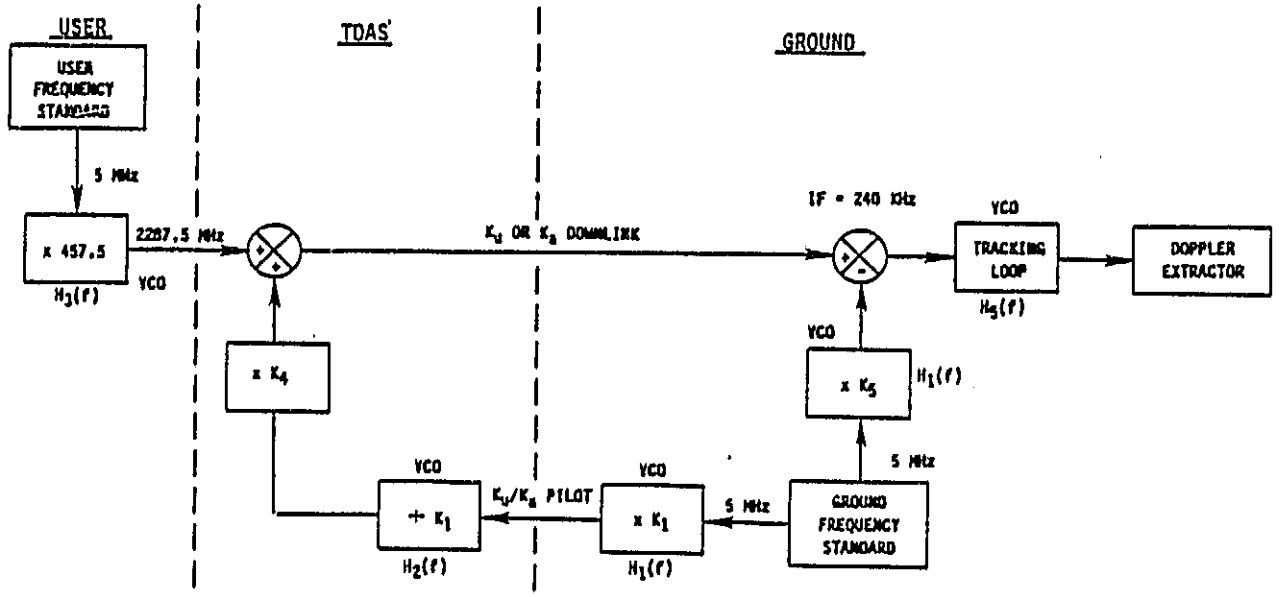

				K_u (MHz)	K_a (MHz)
K_a = DNLINK	=	13677.5	MHz		
K_u = PILOT	=	15150	MHz		
K_a = DNLINK	=	20700	MHz		
K_a = PILOT	=	31000	MHz		
				K_1 = 3030	6200
				K_4 = 2278	3682.5
				K_5 = 2735.45	4139.95

STANFORD TELECOMMUNICATIONS INC.

multiply value at the user oscillator in Figure B-5b. For return link tracking, an IF of 240 kHz into the ground carrier-tracking loop is assumed.

The generation of high-frequency signals from the ground and user frequency standards is pessimistically assumed to require frequency synthesizers and hence tracking loops and their VCO's. Noise from VCO's, of course, is also introduced at the pilot tracking loop on-board the TDAS satellite and at the ground and user receivers' tracking loops. For simplicity, all the tracking loops are assumed to be 2nd order with closed loop transfer function

$$H(w) = \frac{w_n^2 + j\sqrt{2}\, w_n w}{w_n^2 + j\sqrt{2}\, w_n w - w^2}$$

where $w = 2\pi f$, w_n is the loop natural frequency, and the single-sided loop noise bandwidth $B_L \approx \frac{3w_n}{4\sqrt{2}}$. Each of the tracking loops may thus be parameterized by its loop bandwidth. The following values are chosen on the basis of present TDRSS practice, the Motorola 2nd generation TDRSS user transponder design, and arbitrary selection:

$H_1(f)$ (ground frequency system): B_L = 700 Hz,
$H_2(f)$ (TDAS frequency system): B_L = 262 Hz,
$H_3(f)$ (user frequency system): B_L = 700 Hz,
$H_4(f)$ (user tracking loop): B_L = 40 Hz,
$H_5(f)$ (ground tracking loop): B_L = 70 Hz.

To complete the model, the single-sided phase noise spectral densities of the ground and user frequency standards and the VCO's are approximated as shown in Figure B-6. As in TDRSS, the ground frequency standard is assumed to be an HP 5061A+004 cesium oscillator with its phase noise spectral density derived from the manufacturer's specifications [31]. The user frequency standard is assumed to be a precision quartz oscillator; its phase noise spectrum is estimated from the specifications for the FTS 1150 quartz standard [32]. Note that while the cesium oscillator provides superior long term stability, its short term phase fluctuations are more

FIGURE B-6

SINGLE-SIDED PHASE NOISE SPECTRUM OF OSCILLATORS IN TDAS FORWARD AND RETURN LINKS*

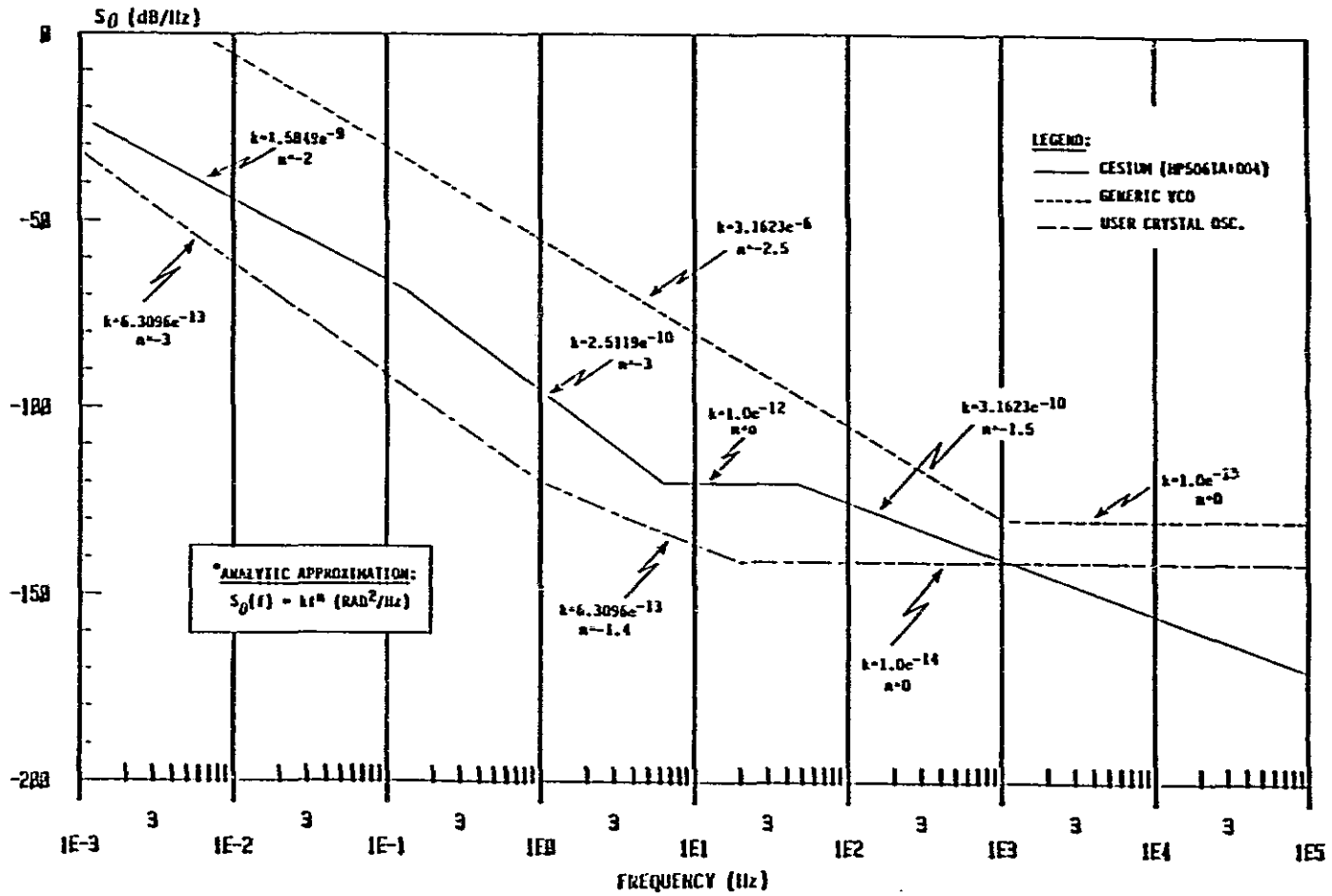

STANFORD TELECOMMUNICATIONS INC.

severe than those of the quartz oscillator. In all the figures, the spectral density is assumed to extend for offset frequencies beyond those shown in the same manner as immediately before the end of the depicted range. Only for the VCO spectral density will these high offset frequencies be significant since only the VCO output is highpass filtered by transfer functions of the form 1-H(f).

B.3.1 Forward Link Tracking

Figure B-7a explicitly shows the various filtering operations to which the phase processes ϕ_{CESIUM}, ϕ_{VCO}, and ϕ_{XTAL} in the forward link are subjected. The ground-to-TDAS delay τ_1 and TDAS-to-user delay τ_2 are accounted for by the appropriate phase shifts; τ_1 and τ_2 are approximated here as .14 seconds, corresponding to distances of 42000 kilometers. Inspection of the diagram allows the transfer functions associated with the ground, TDAS, and user segments to be identified separately. This yields the component single-sided phase noise spectral densities at the input to the user's doppler extractor:

$$S_{\phi_{GND}}(f) = S_{\phi_{CESIUM}}(f)|H_4(f)H_1(f)e^{-jw(\tau_1 + \tau_2)}(K_2-K_3H_2(f))|^2$$

$$- S_{\phi_{VCO}}(f)|(1-H_1(f))H_4(f)e^{-jw(\tau_1 + \tau_2)}(K_2-K_3H_2(f))|^2$$

$$= \left[S_{\phi_{CESIUM}}(f)|H_1(f)|^2 + S_{\phi_{VCO}}(f)|1-H_1(f)|^2\right]x$$

$$|H_4(f)|^2\left[K_2^2 - 2K_2K_3Re\{H_2(f)\} + K_3^2|H_2(f)|^2\right];$$

$$S_{\phi_{TDAS}}(f) = S_{\phi_{VCO}}|(1-H_2(f))K_3\ H_4(f)|^2;$$

$$S_{\phi_{USER}}(f) = \left[S_{\phi_{XTAL}}(f)|H_3(f)|^2 + S_{\phi_{VCO}}(f)|1-H_3(f)|^2\right](419.38)^2|H_4(f)$$

$$+ S_{\phi_{VCO}}(f)|1-H_4(f)|^2;$$

where Re{•} denotes "the real part of {•}".

FIGURE B-7: DERIVATION OF TRANSMISSION LINK TRANSFER FUNCTIONS

A) FORWARD LINK:

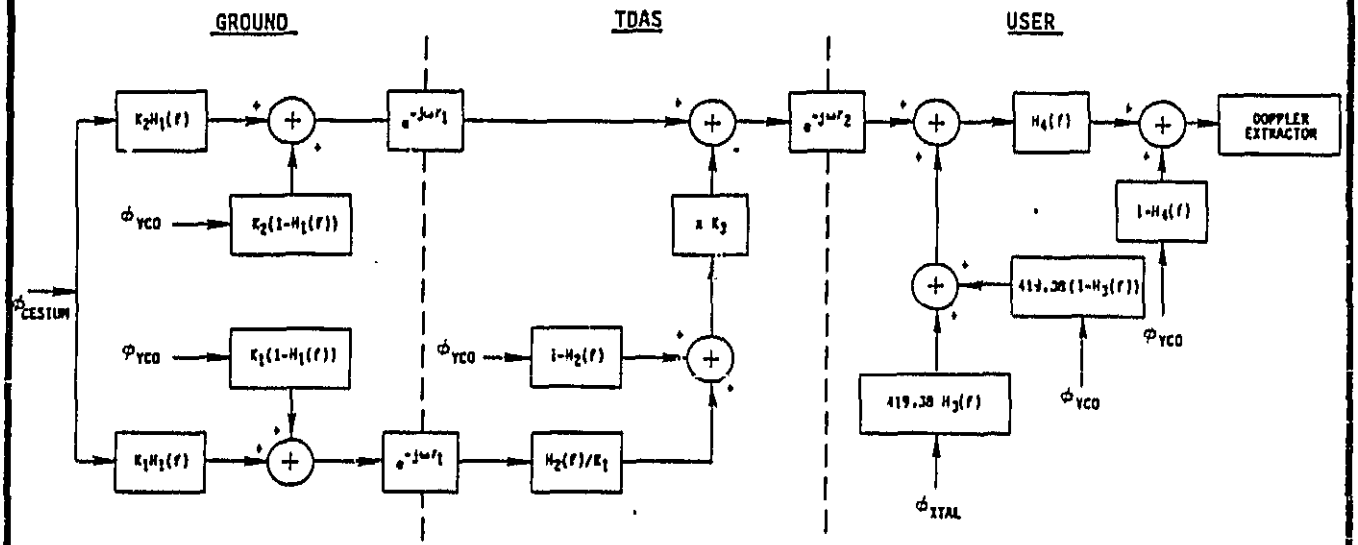

B) RETURN LINK:

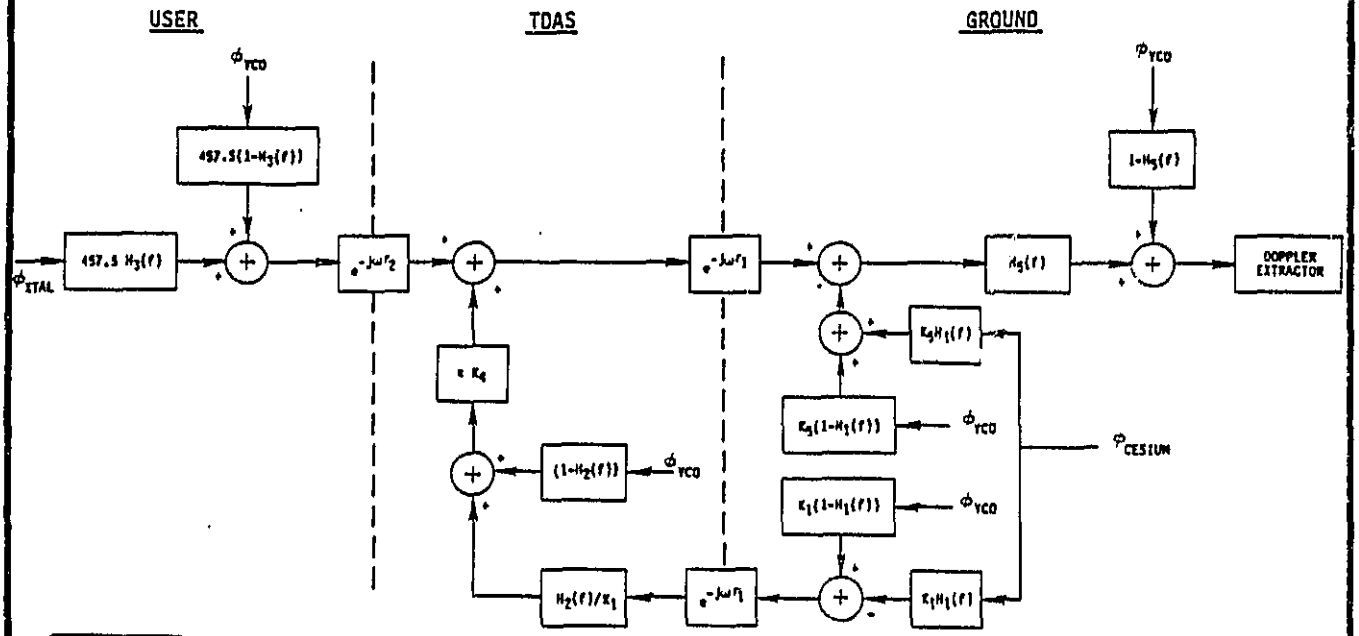

STANFORD TELECOMMUNICATIONS INC.

The phase noise variances corresponding to each of these densities is obtained as simply $\sigma^2_{\phi_X} = 2\int_0^\infty S_{\phi_X}(f)\,df$; the range-rate variance due to each component is similarly obtained as

$$\sigma^2_{\dot{R}_X} = 2\int_0^\infty S_{\phi_X}(f)\; 4\sin^2(\pi f T_{av})df$$

The results obtained from numerical integration are reported in Table 3-3.

B.3.2 RETURN LINK TRACKING

The necessary transfer functions are found from Figure B-7b in the same way as in the preceding section. As previously, the single-sided phase noise spectral density at the input to the doppler extractor may be broken into its component elements accoraing to the phase noise sources:

$$S_{\phi_{USER}}(f) = \left[S_{\phi_{XTAL}}(f)\,|H_3(f)|^2 + S_{\phi_{VCO}}(f)\,|1-H_3(f)|^2\;(457.5)^2\right]|H_s(f)|^2;$$

$$S_{\phi_{TDAS}}(f) = S_{\phi_{VCO}}(f)|(1-H_2(f))K_4\,H_5(f)|^2;$$

$$S_{\phi_{GND}}(f) = \left[S_{\phi_{CESIUM}}|H_1(f)|^2 + S_{\phi_{VCO}}|1-H_1(f)|^2\right]x$$

$$|H_5(f)|^2\Big\{K_4^2|H_2(f)|^2 + K_5^2 - K_5K_4[2\,\mathrm{Re}\{H_2(f)\}\cos 2w\tau_1$$

$$+ 2\,\mathrm{Im}\{H_2(f)\}\sin 2w\tau_1]\Big\}$$

$$+ S_{\phi_{VCO}}(f)|1-H_5(f)|^2;$$

where Im {•} denotes "the imaginary part of {•}".

Again, the range-rate variance $\sigma^2_{\dot{R}_X}$ due to each component is

$$\sigma^2_{\dot{R}_X} = 2\int_0^\infty S_{\phi_X}(f)\; 4\sin^2(\pi f T_{av})df.$$

The results from numerical integration are shown in Table 3-5.

APPENDIX C

TDAS TRACKING ANALYSIS - SUPPLEMENTARY RESULTS

C.1 INTRODUCTION

An evaluation of the potential tracking accuracy for TDAS satellites was made based on BRTS and VLBI tracking techniques. Section 4 presented a brief description of each technique, possible tracking configurations to support frontside and backside satellites, and the error analysis modeling approach and major results. This appendix provides supplementary results for BRTS tracking in Section C.2 and VLBI tracking in Section C.3. Relevant modelling data used in the analysis are given in Section C.4.

C.2 BRTS RESULTS

TDAS position errors in the prediction interval are presented in Figures C-1 through C-4 as a function of BRTS tracking epoch and tracking interval.

Figure C-1 (Frontside TDAS) illustrates the sensitivity of TDAS position errors in the prediction interval as a function of epoch time. In all cases, the minimum error bound is about 100 m, regardless of epoch time. However, the maximum error bound is cyclic with roughly a 12 hour period, and the peak to peak variation diminishes with longer tracking intervals. To minimize the position error in the 12 hour prediction interval, an epoch is chosen at the valley of the maximum error bound. Note that the valley epochs shift as the tracking interval changes. Of the four tracking intervals shown (18, 24, 30, and 36 hours), the 18 hour case has the lowest valleys (110 m), which occur near 18^H30^M GMT and 5^H30^M GMT. The 24, 30, and 36 hour cases all have valleys on the maximum error bound greater than 125 m, which occur at epochs different from the 18 hour case. For example, the valleys for the 24 hour case occur near 0^H30^M and 12^H30^M GMT, with a magnitude of 140 m. For the 24 hour prediction interval, the valleys in the maximum

FIGURE C-1: TDAS POSITION ERROR BOUNDS IN 12 AND 24 HOUR PREDICTION INTERVALS VS. TRACKING EPOCH (BRTS TRACKING - FRONTSIDE TDAS)

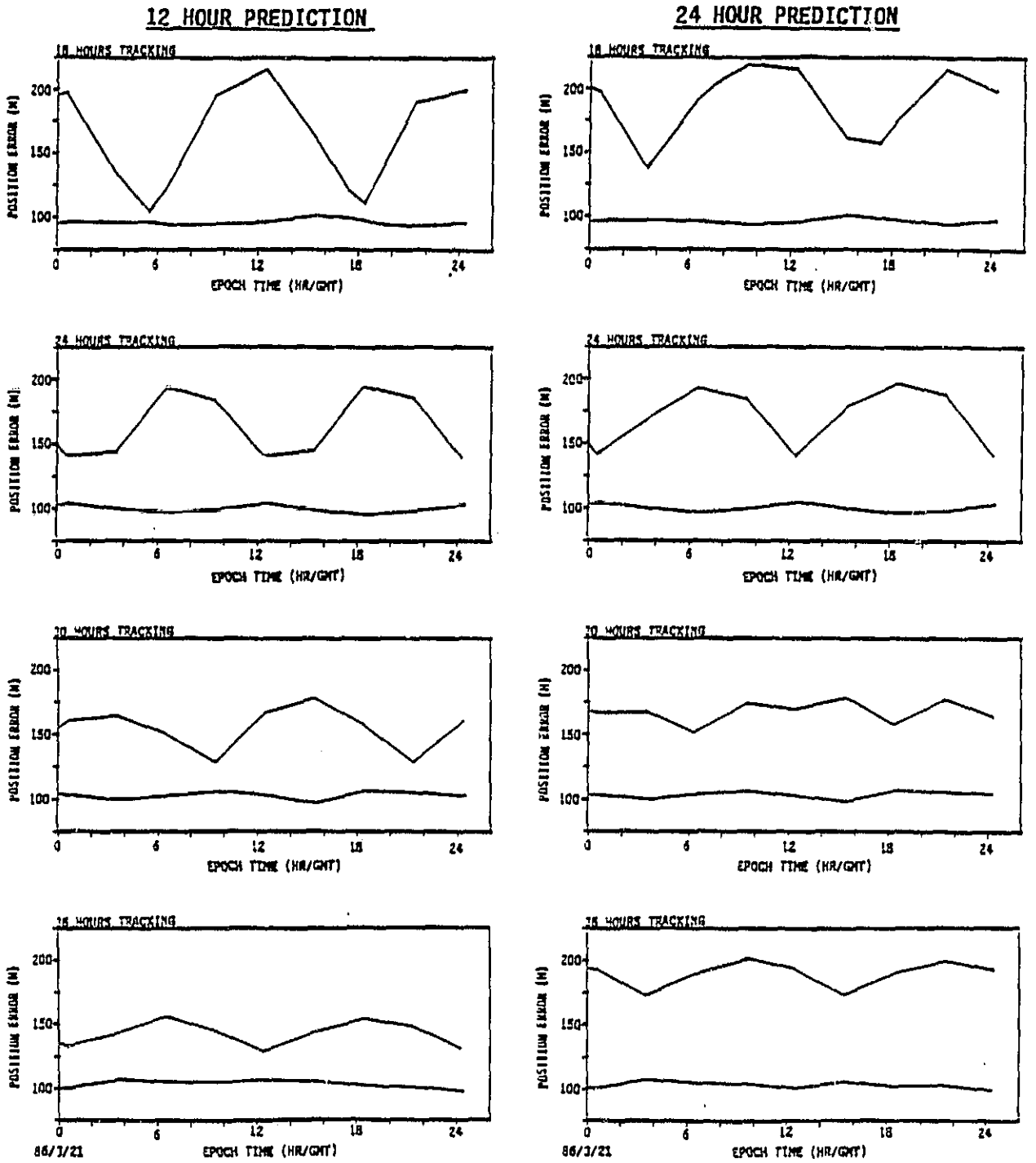

STANFORD TELECOMMUNICATIONS INC.

FIGURE C-2: TDAS POSITION ERROR BOUNDS IN 12 AND 24 HOUR PREDICTION INTERVALS VS TRACKING EPOCH (BRTS TRACKING - BACKSIDE TDAS)

12 HOUR PREDICTION

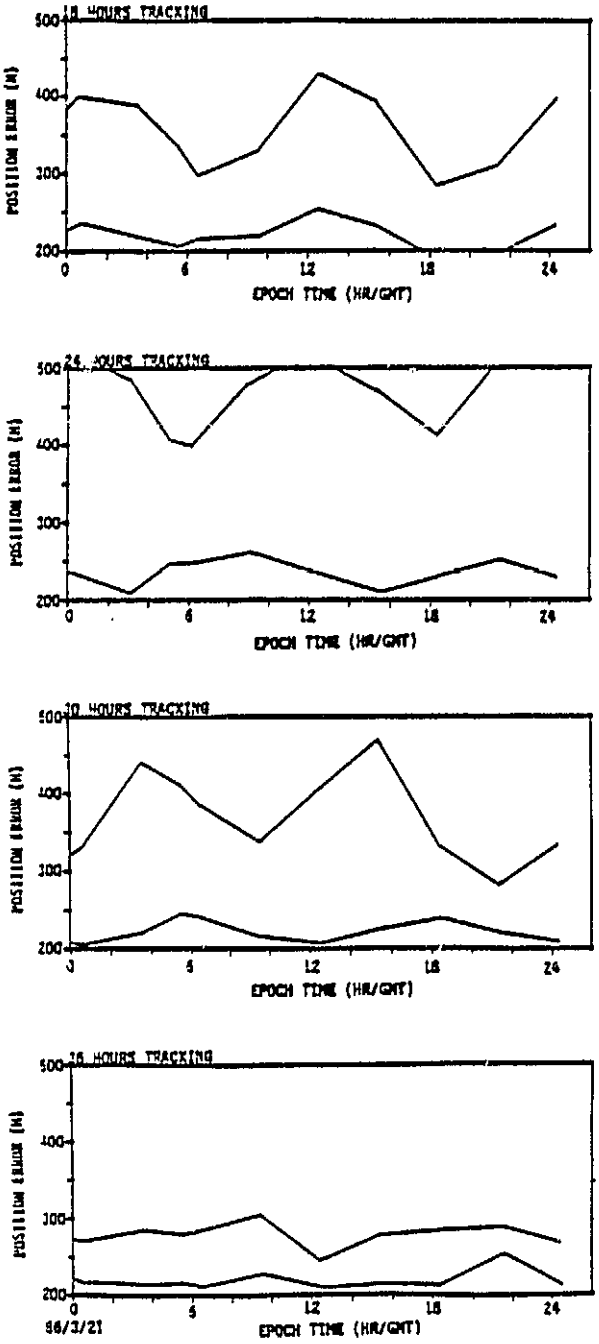

24 HOUR PREDICTION

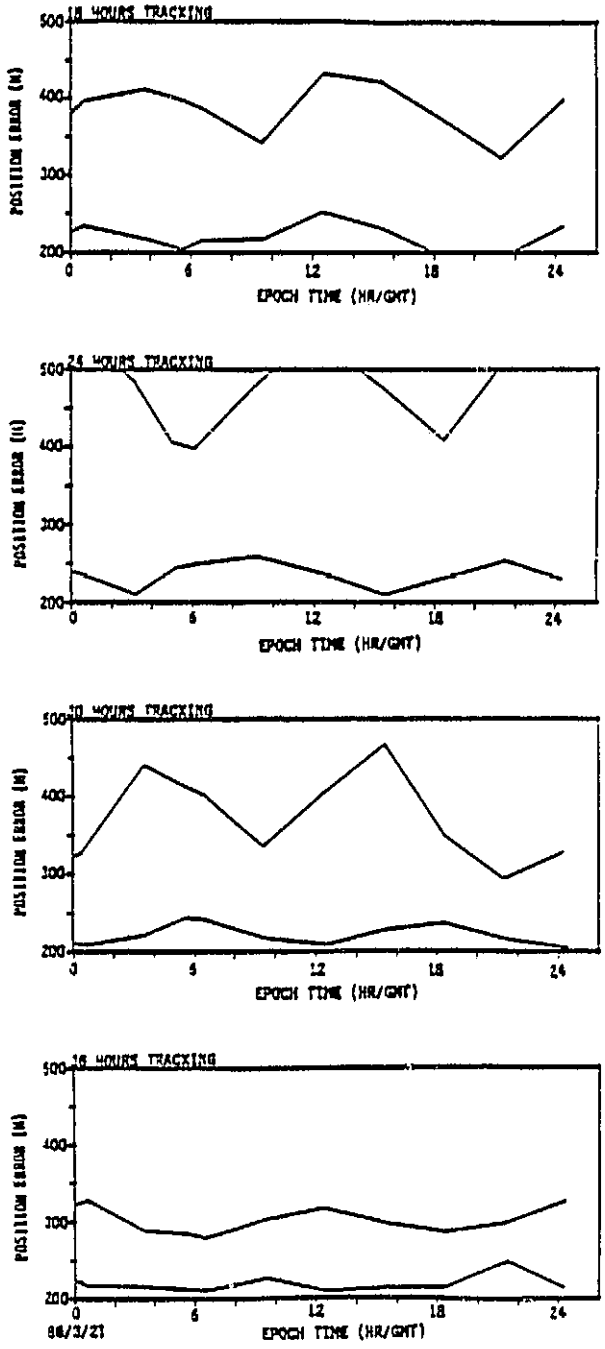

TRACKING CONFIGURATION:
- TDAS @ 98°E
- STNS: T100-T100, T100-OGA
- DATA RATE: 1/MIN FOR 5 MIN/HR

STANFORD TELECOMMUNICATIONS INC.

FIGURE C-3
TDAS POSITION UNCERTAINTY IN PREDICTION INTERVAL VS. BRTS TRACKING INTERVAL

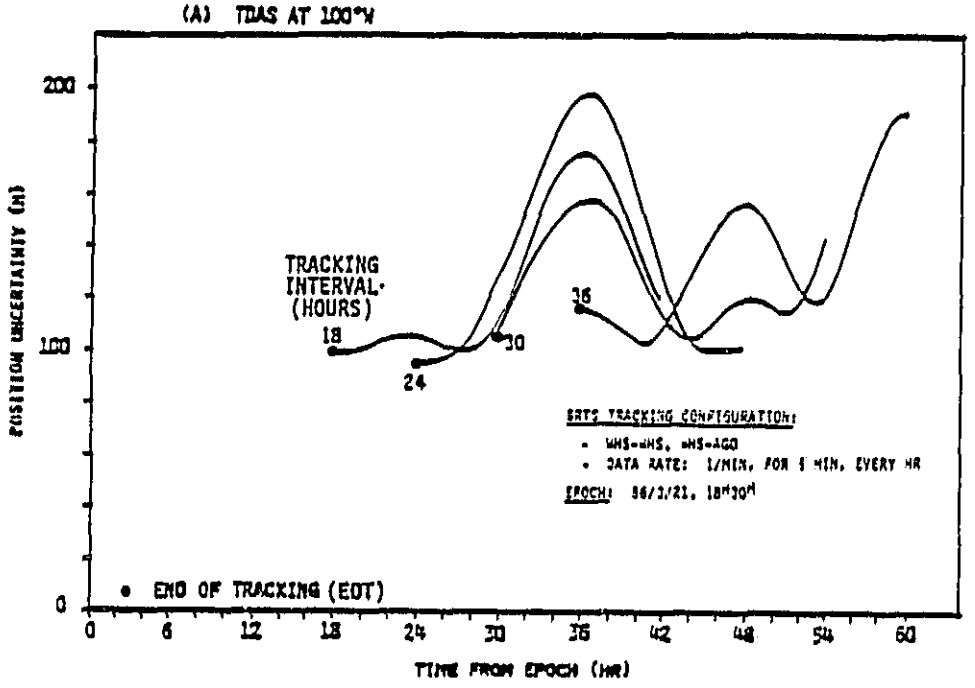

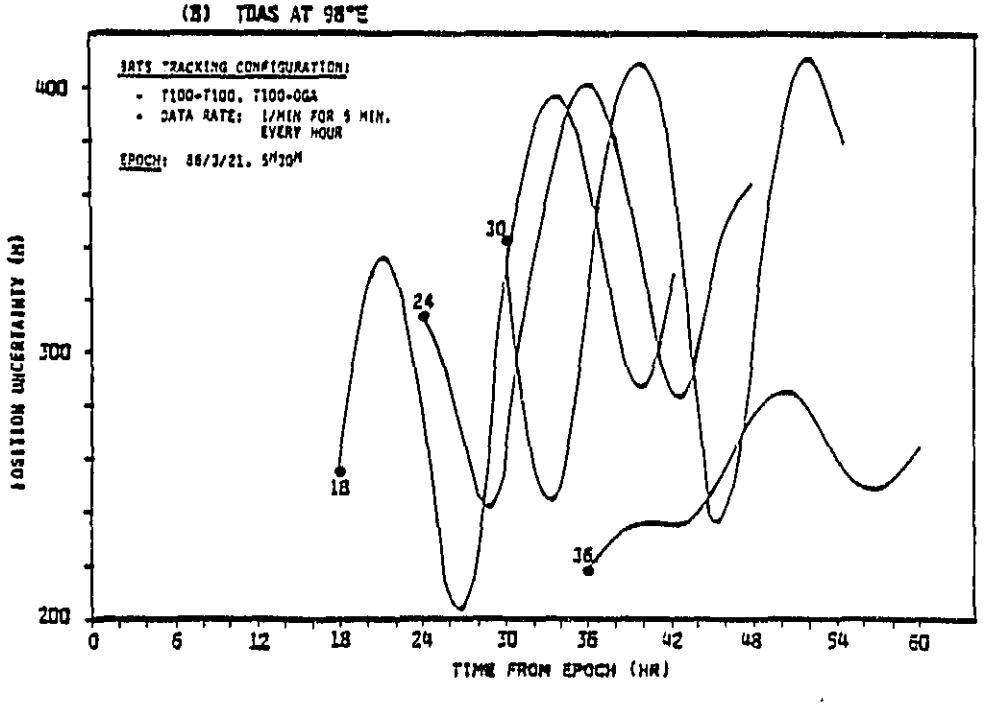

STANFORD TELECOMMUNICATIONS INC.

FIGURE C-4
TDAS MAXIMUM POSITION ERROR CONTRIBUTORS IN 12 HOUR PREDICTION INTERVAL VS. BRTS TRACKING INTERVAL

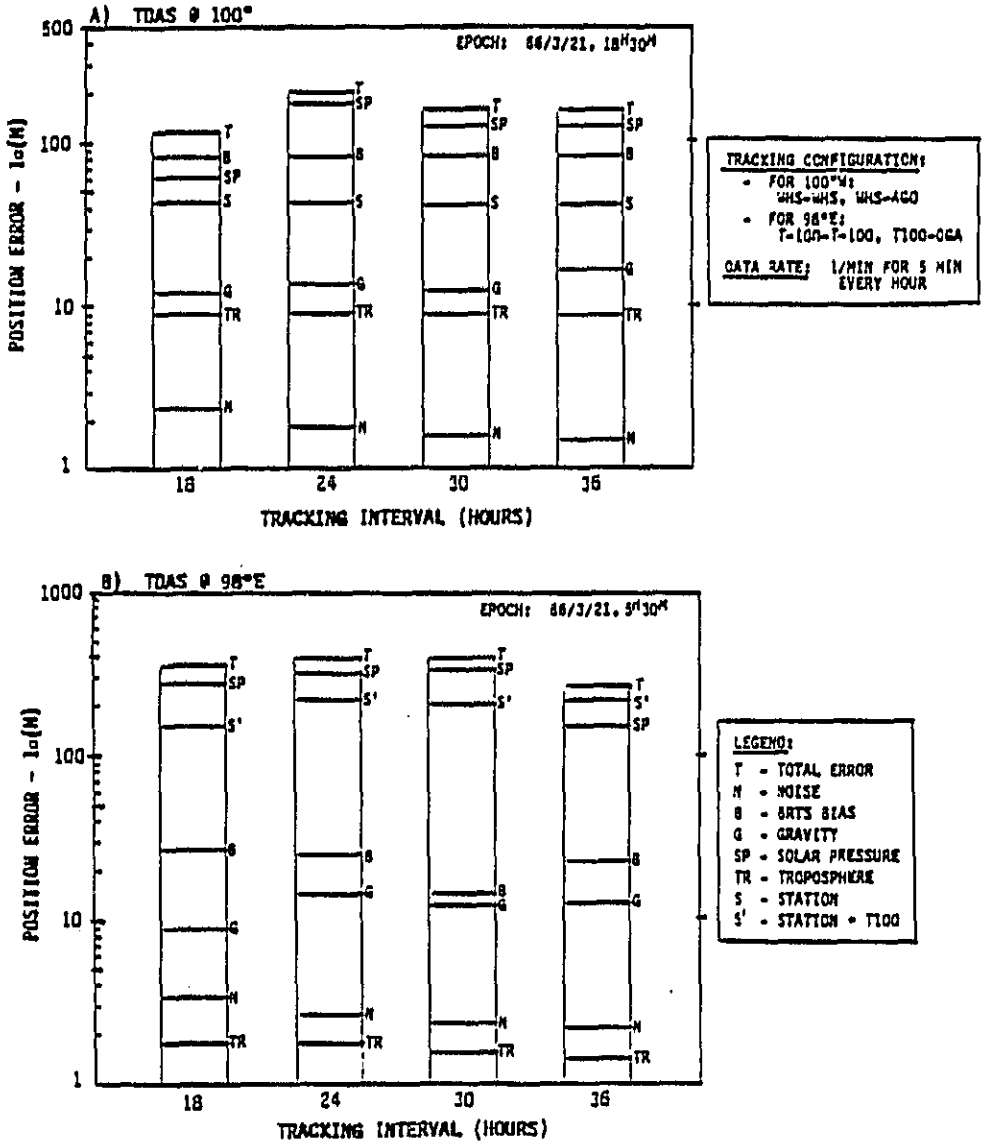

STANFORD TELECOMMUNICATIONS INC.

error bound are all above 140 m for all tracking intervals. Thus, for the frontside TDAS (at 100°W), the best choice is 18 hour tracking, 12 hour prediction, and epoch of 18^H30^M, resulting in TDAS 1σ position errors between 100 and 110 m.

Figure C-2 demonstrates the same relationships for the backside TDAS at 98°E, for which the best choice is 36 hour tracking, 12 hour prediction, and epoch of 12^H30^M, resulting in TDAS 1σ position errors between 210 and 250 m. However, note that the maximum error bound is relatively flat for the 36 hour tracking interval and remains below 300 m over all epochs. Thus, the epoch is not as critical for the 36 hour tracking case as it is for 18, 24, and 30 hour tracking cases in which the maximum errors fluctuate widely (exceeding 400 m).

Figure C-3 illustrates the TDAS position errors from the end of tracking to the end of prediction for a fixed epoch time. Figure C-3a is for TDAS at 100°W, with a tracking configuration using transponders at White Sands (WHS) and Santiago (AGO). WHS-WHS denotes a roundtrip path from WHS transmitter-to TDAS to WHS ground transponder and return to TDAS to WHS receiver. Similarly, WHS-AGO denotes a roundtrip path from WHS transmitter to TDAS to AGO transponder and return to TDAS to WHS receiver. The TDAS position errors are plotted for 18, 24, 30, and 36 hour tracking intervals, all for 24 hour prediction intervals, based on an epoch time of 18^H30^M GMT. Again, note the best prediction interval occurs during the 12 hours after the end of the 18 hour tracking. Figure C-3b is for TDAS at 98°E with transponders on the 100°W TDAS (T100) and at Diego Garcia (DGA). T100-T100 represents a roundtrip path from T100 to TDAS (98°E) and return to T100.* T100-DGA represents a roundtrip path from T100 to TDAS to DGA transponder and return via TDAS to T100.* The best prediction interval for the backside TDAS is during the 12 hours after the end of the 36 hour tracking.

---

* For error analysis with existing ORAN capabilities the WHS-T100 link was not modelled. Instead, separate WHS-T100 path delay measurements were assumed to be subtracted from backside two-way BRTS measurements made at WHS. ORAN was set up to use T100 as the terminal location (analogous to WHS) with station errors equal to the position accuracy for frontside TDAS tracking.

Figure C-4 presents the TDAS maximum error contributors in the 12 hour prediction intervals for 18, 24, 30, and 36 hour tracking intervals. Note the position error scale is a log scale. Figure C-4A is for TDAS at 100°W, and shows solar pressure, VLBI measurement bias, and station survey errors as dominant, with magnitudes greater than 40 m. Figure C-4B is for TDAS at 98°E, and shows station errors and solar pressure uncertainties as the dominant error sources, with each contributing well above 100 m. Note that the station error reflects uncertainty due to the frontside TDAS (T100) tracking error assumed to be a constant 105 m (H = 26 m, C = 28 m, L = 98 m).

C.3 VLBI TRACKING

This section presents TDAS tracking accuracy results based on the VLBI tracking technique. Subsections C.3.1 and C.3.2 discuss results generated for the baseline and reduced error models defined in Section 4 (Table 4-1). Subsection C.3.3 presents some preliminary results for frontside TDAS tracking using VLBI stations located only in CONUS. These three subsections show the effects of tracking interval, epoch time, prediction interval, VLBI bias estimation, error sources, and data rate on TDAS uncertainty.

C.3.1 Baseline Error Model Results

A composite plot of TDAS 1σ position uncertainty during the prediction interval is shown in Figure C-5 for several tracking intervals - 3, 6, 12, 18, 24, 30, 36, and 42 hrs, all using a fixed epoch time of $18^{H}30^{M}$ GMT. Figure C-5A shows the error profile without VLBI bias estimation. For the 3, 6, 12, 24, 30, and 42 hr tracking, the position uncertainties rise above 100 m after a few hours in the prediction interval. Only for the 18 and 36 hr tracking does the position uncertainty remain below 100 m for several hours in the prediction interval. As will be shown later, concatenation of several 18 and 36 hr tracking segments may provide 24 hours of prediction below the 100 m level.

Figure C-5B shows the same cases as C-5A except VLBI bias is estimated. The best choices of prediction intervals are those following the 12 and 18 hr tracking. These may be concatenated to provide 24 hours of prediction below the 100 m level. Note that the position error is close to 200 m at the end of the 36 hr tracking interval.

FIGURE C-5
TDAS POSITION UNCERTAINTY IN PREDICTION INTERVAL VS VLBI TRACKING INTERVAL

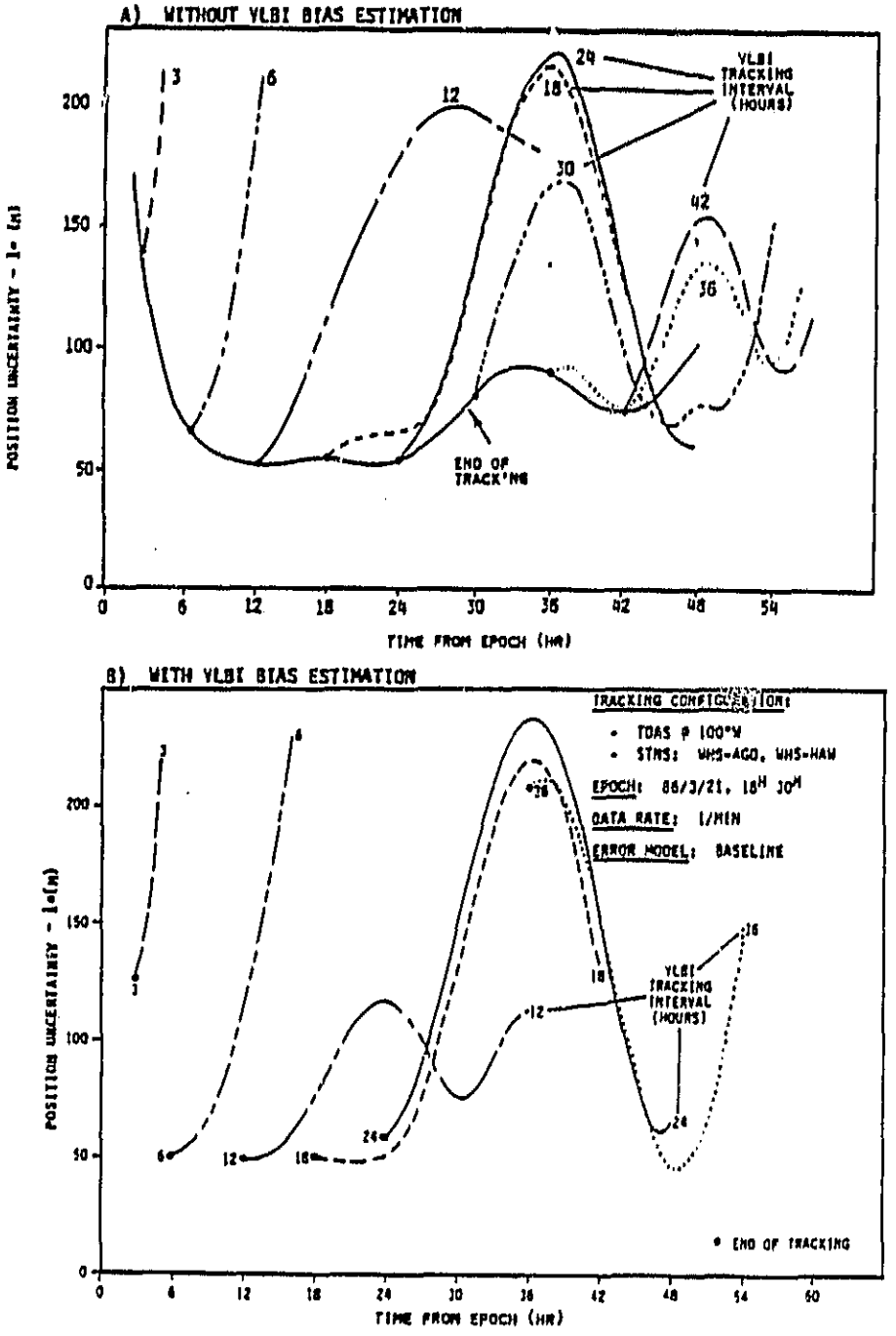

STANFORD TELECOMMUNICATIONS INC.

Figures C-6 and C-7 display the TDAS maximum error contributors for various prediction and tracking intervals with and without VLBI bias estimation. As mentioned above, the 18 and 36 hr tracking intervals are the best choices for either 6 or 12 hr prediction intervals. In Figure C-6A for 6 hr tracking note that VLBI bias station survey and noise errors are dominant, while for long tracking intervals (24, 30, and 36 hrs) solar pressure error is dominant. For intermediate tracking intervals (12, 18 hrs) VLBI bias, solar pressure, and station survey errors are dominant. As the prediction interval increases, however, solar pressure ultimately dominates. Note that in all of these cases, the gravity and tropospheric effects are relatively insignificant (less than 20 m).

Figure C-7 is based on VLBI tracking with bias estimation. As noted before, the 12 and 18 hr tracking intervals are the best choices for either 6 or 12 hr prediction intervals. With VLBI bias estimated, other related errors (station survey and tropospheric errors) are also reduced whereas noise and solar pressure error increase, particularly noise. The overall result, however, is a decrease in the total error.

Figure C-8 shows the sensitivity of the TDAS position error profile to epoch time of day at the beginning of an 18 hr tracking interval with VLBI bias estimation. For each prediction interval (1, 3, or 6 hr), the minimum and maximum error bounds are plotted. The best epoch choices are $6^{H}30^{M}$ GMT (TDAS local midnight) and $18^{H}30^{M}$ GMT (TDAS local noon). The minimum error bound is in the 48-55 m range for all three prediction intervals. The maximum error bound increases dramatically from 1 hr prediction to 6 hr prediction when the epoch is not near $6^{H}30^{M}$ or $18^{H}30^{M}$. For these best epochs, there is little change in maximum error bound as the prediction interval increases from 1 to 6 hr.

FIGURE C-6
TDAS MAXIMUM POSITION ERROR CONTRIBUTIONS VS VLBI TRACKING INTERVAL (WITHOUT VLBI BIAS ESTIMATION)

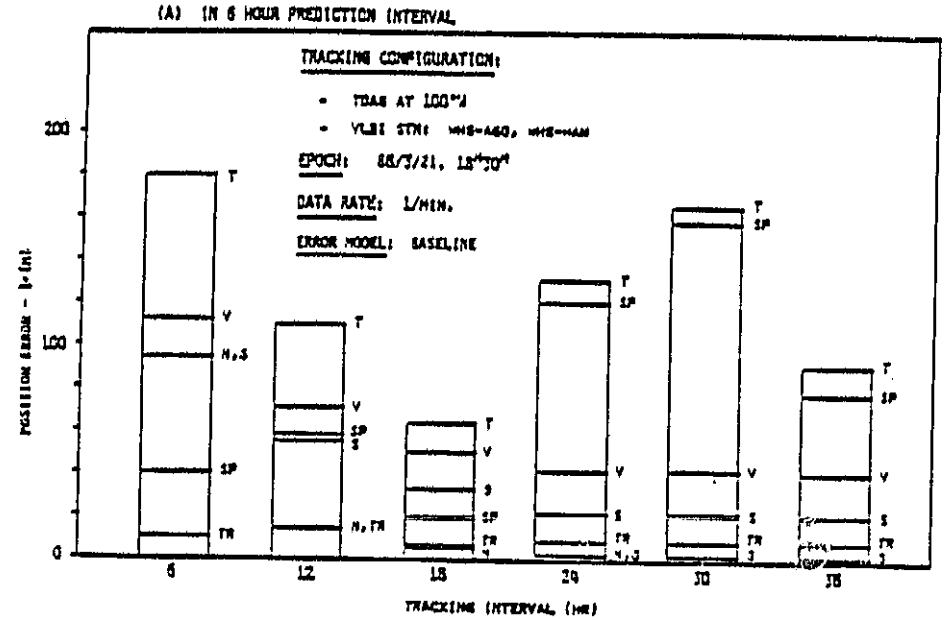

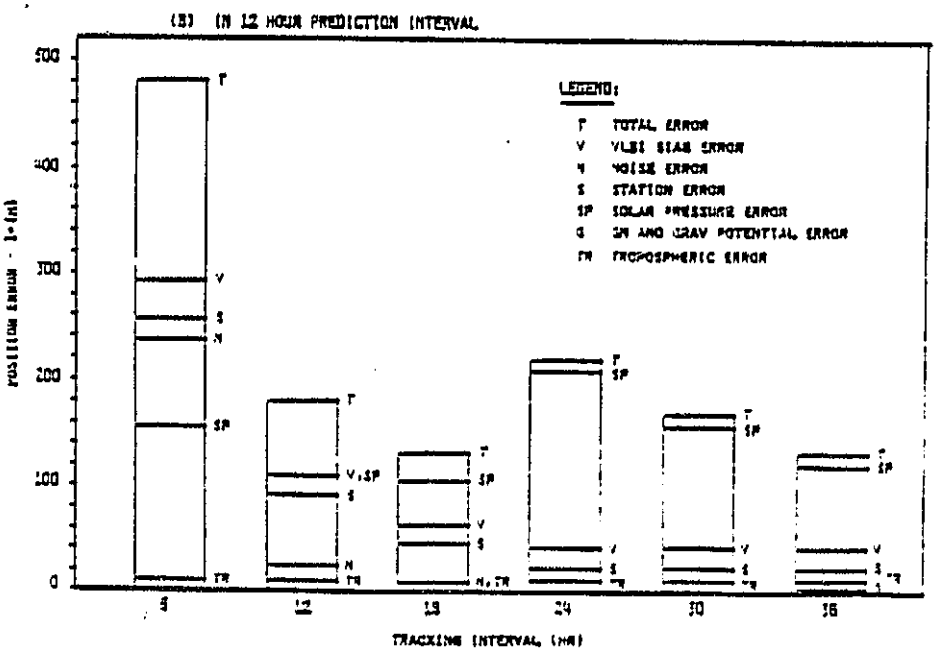

FIGURE C-7
TDAS MAXIMUM POSITION ERROR CONTRIBUTIONS VS VLBI TRACKING INTERVAL (WITH VLBI BIAS ESTIMATION)

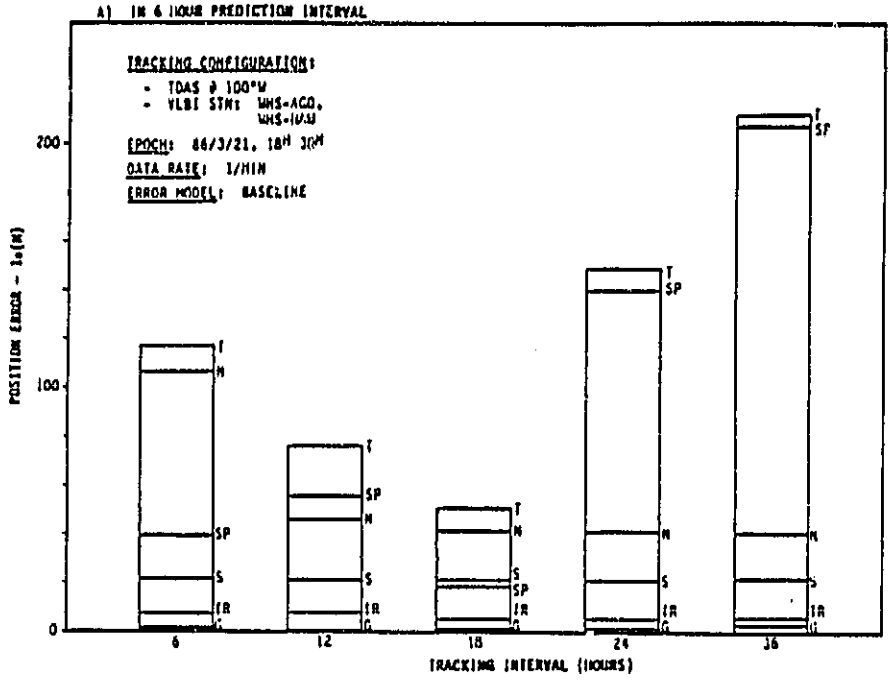

STANFORD TELECOMMUNICATIONS INC.

FIGURE C-8
TDAS POSITION ERROR BOUNDS WITHIN PREDICTION INTERVAL VS. TRACKING EPOCH TIME

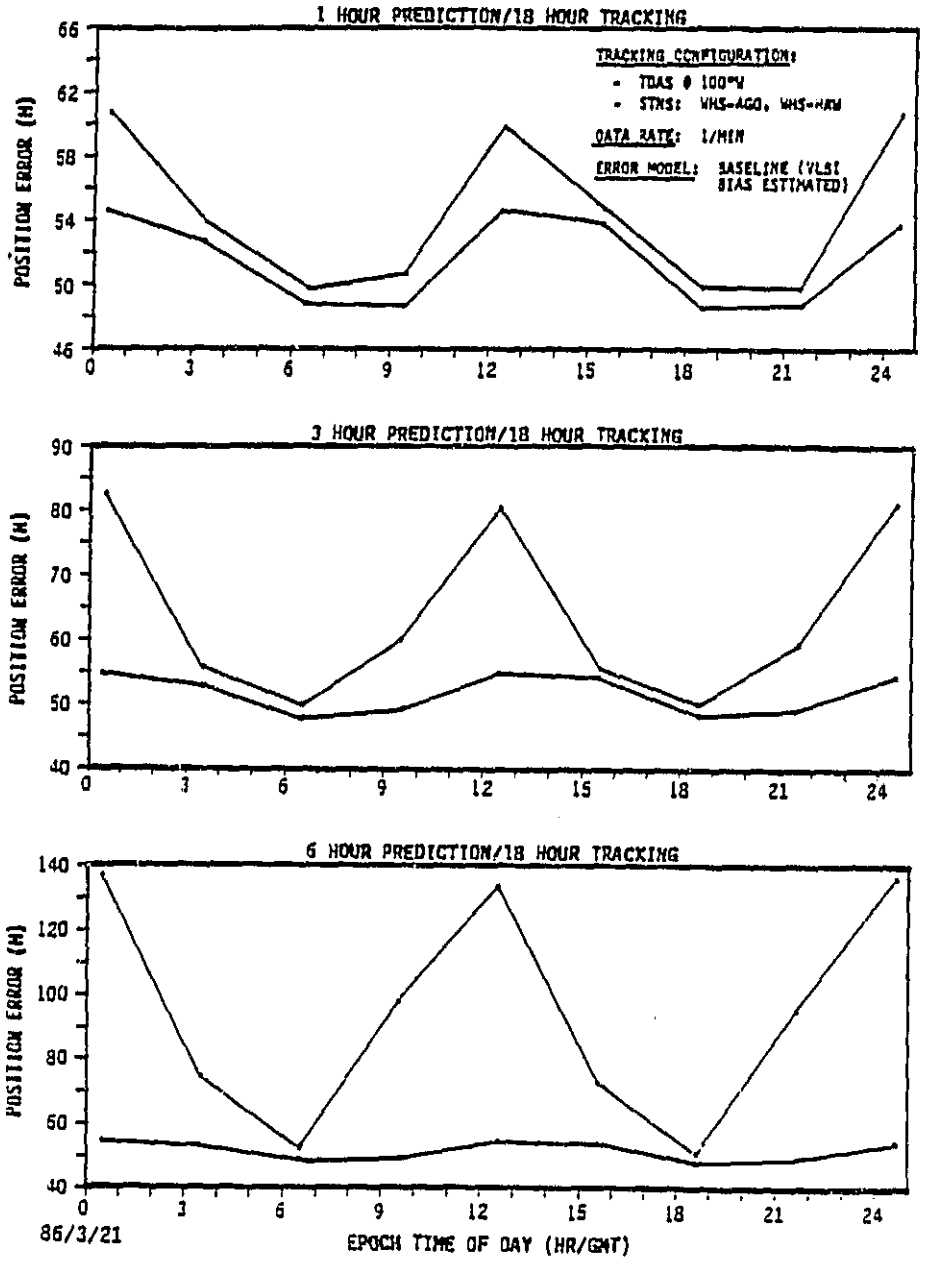

STANFORD TELECOMMUNICATIONS INC.

C.3.1.1 Impact of TDAS Location. Figure C-9 illustrates that TDAS position uncertainty is insensitive to TDAS geographic location. Four prediction profiles are plotted, based on TDAS longitudes of 100°W, 98°E, 171°W, and 41°W. Both the 18 and 36 hr tracking cases are shown. The small differences among each set of four profiles can be attributed to geometrical differences in the tracking station configurations.

C.3.1.2 Effect of VLBI Data Rate. Table C-1 is a tabulation of minimum and maximum TDAS position uncertainties as a function of data rate, tracking interval, and prediction interval for an epoch of 18^H30^M GMT. For a 6 hr tracking interval, the effect of data rate is dramatic with the maximum error increasing by more than 2:1 as the data period increases from 60 sec to 3600 sec. For a 12 hr tracking interval, the factor is about 20%. For longer tracking intervals (18, 24, and 36 hours), there are virtually no differences in position errors for data periods of 60, 1800, or 3600 sec. This has significant operational importance since VLBI measurements data collection and processing need occur no more frequently than once per hour.

C.3.1.3 Prediction Interval Concatenation. Figures C-10 and C-11 demonstrate how it is possible to concatenate several prediction segments to achieve better TDAS position performance over a 24 hr period compared with a single segment. The 18 hr tracking segments are shown in Figure C-10A. Two start times are indicated - S/C local midnight and S/C local noon on 3/22. At the end of tracking of these two cases, the 9 hr prediction profiles may be used, i.e., on 3/23 the interval between 0^H30^M and 9^H30^M and the second interval between 12^H30^M and 21^H30^M. Gaps from 9^H30^M to 12^H30^M and from 21^H30^M to 24^H30^M may be filled using prediction intervals based on 36 hr tracking starting at S/C local noon and S/C local midnight on 3/21 and 3/22, respectively (see Figure C-10B). When all these segments are concatenated in Figure C-11A, the result is a 24 hr prediction interval in which the TDAS position error remains below 85 m.

The same procedure may be used when the VLBI bias is estimated (see Figure C-11B). By concatenating multiple prediction segments following 18 and

FIGURE C-9
TDAS POSITION UNCERTAINTY IN PREDICTION I. .RVAL VS TDAS LOCATION

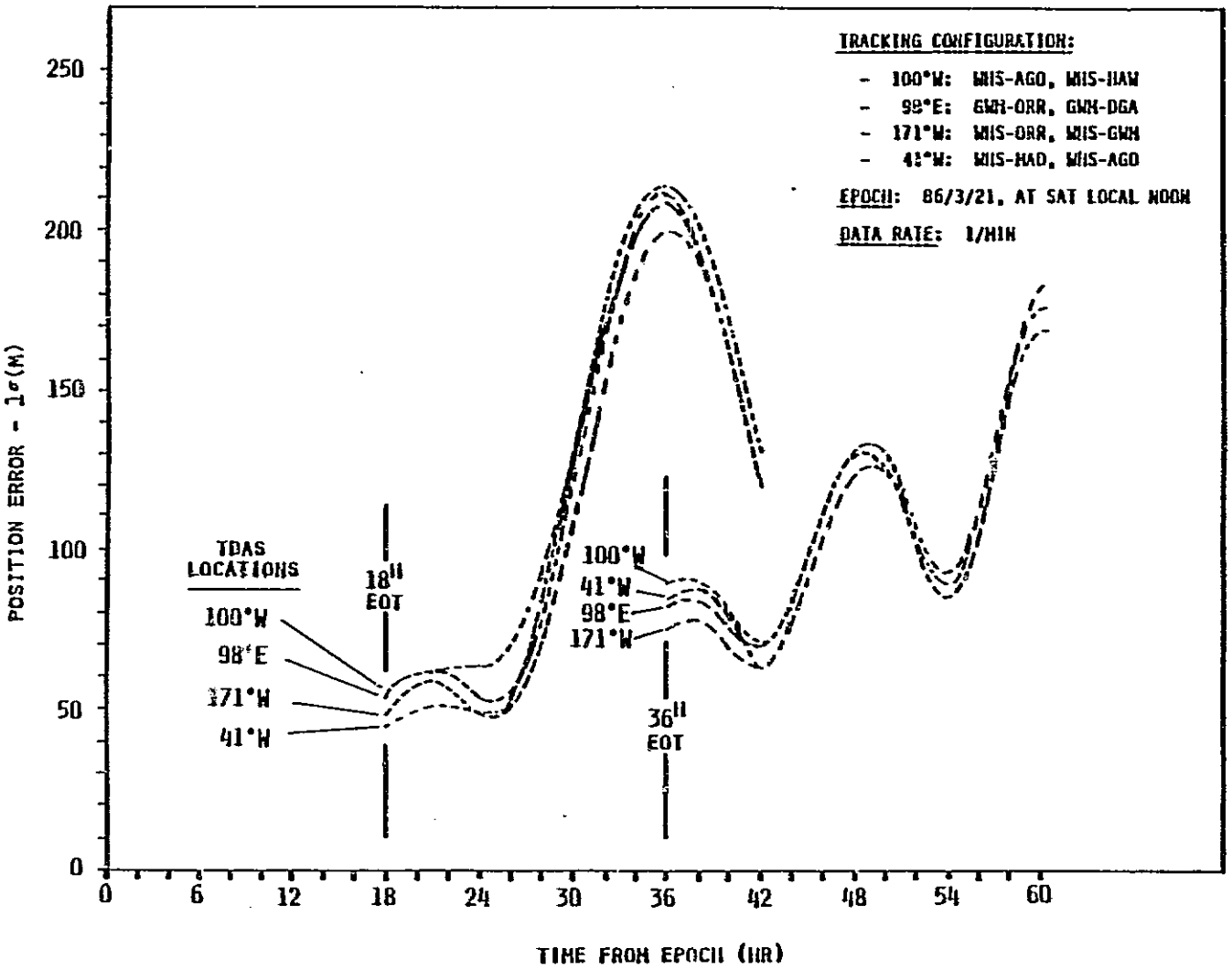

STANFORD TELECOMMUNICATIONS INC.

TABLE C-1
MIN/MAX POSITION UNCERTAINTY (M) IN PREDICTION INTERVAL VS. VLBI DATA RATE AND TRACKING INTERVAL*

WITH BASELINE ERROR MODEL

PREDICTION INTERVAL (HOURS)	TRACKING INTERVAL (HOURS)	VLBI DATA RATE (SEC)		
		60	1800	3600
6	6	66/180	92/437	101/520
	12	49/110	52/127	53/136
	18	53/63	53/65	53/67
	24	53/131	53/128	53/126
	36	71/92	71/90	71/89
12	6	66/481	92/1108	101/1318
	12	49/180	52/210	53/227
	18	53/131	53/130	53/129
	24	53/219	53/217	71/134
	36	71/131	71/133	71/134

* TRACKING CONFIGURATION: TDAS @ 100°W; STNS: WHS-AGO, WHS-HAW
EPOCH: 86/3/21, 18^H30^M

FIGURE C-10
TDAS POSITION UNCERTAINTY VS TIME AND VLBI TRACKING EPOCH

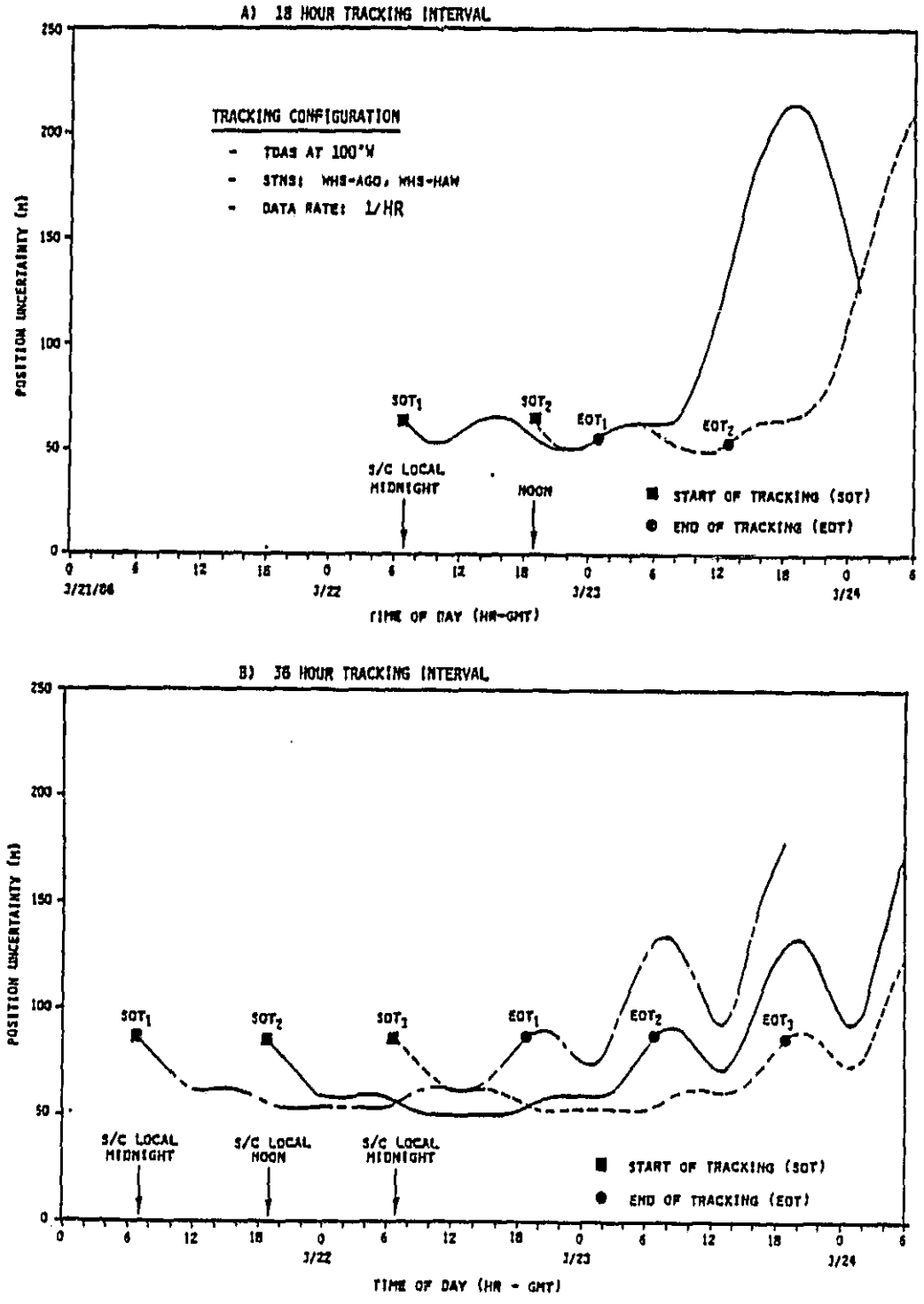

STANFORD TELECOMMUNICATIONS INC.

FIGURE C-11
TDAS POSITION UNCERTAINTY IN 24 HOUR PREDICTION INTERVAL
(BASED ON MULTIPLE VLBI TRACKING SEGMENTS)

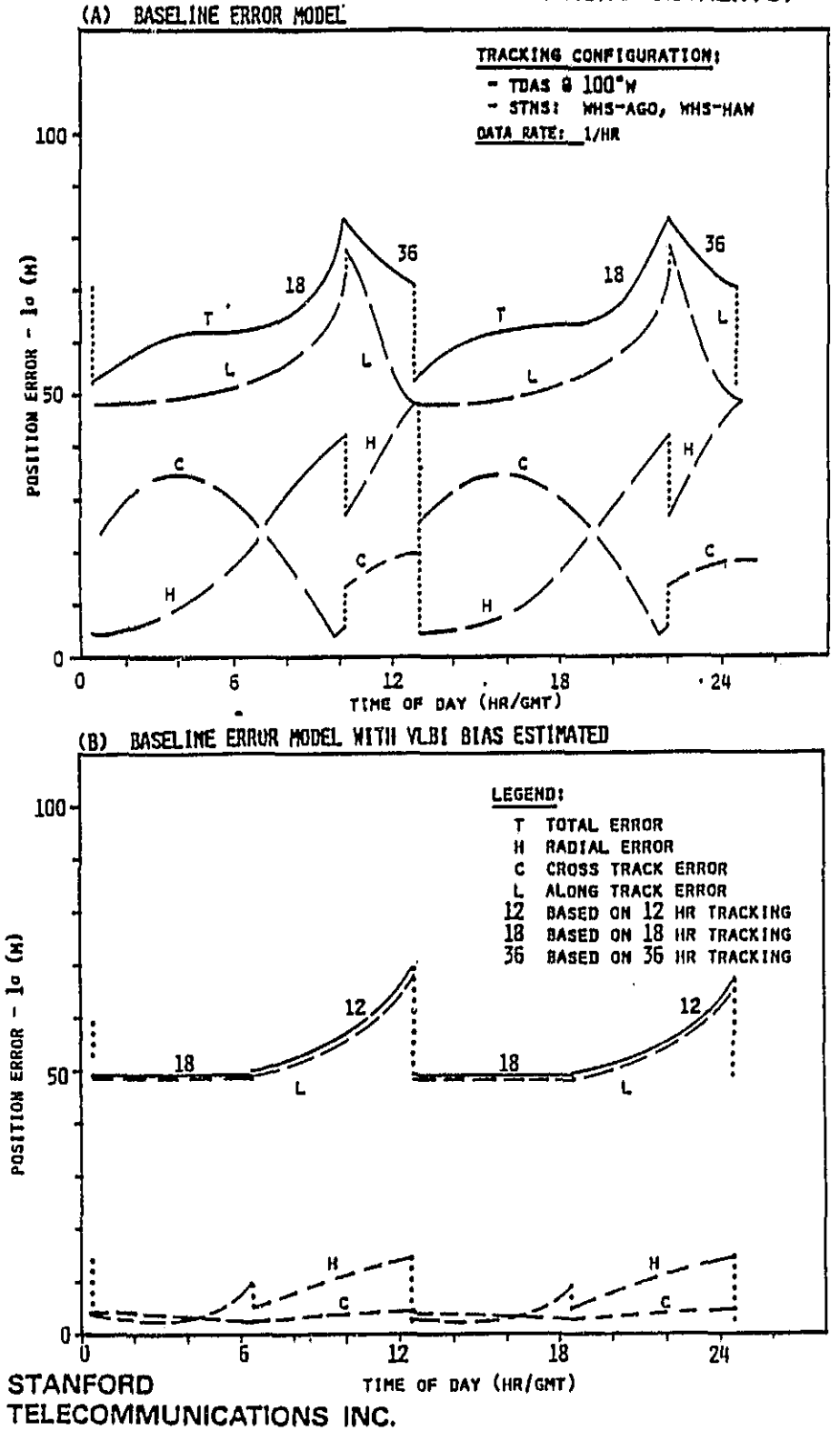

STANFORD TELECOMMUNICATIONS INC.

12 hr tracking intervals, an error profile that remains below 70 m can be obtained. Also shown in Figures C-11A and B are the radical, cross track, and along track components of TDAS position error. In both cases, the along track component dominates.

C.3.2 Reduced Error Model Results

TDAS position uncertainties computed from the baseline and reduced error models are compared in Figure C-12. Four tracking intervals were used - 1, 3, 6, and 12 hrs. For the baseline model, longer tracking intervals produce better prediction profiles, as observed in Subsection C.3.1. However, for the reduced error model, shorter tracking intervals appear advantageous. A 6 hr tracking interval followed by a 1 hr prediction interval seems to be an optimal choice. As will be demonstrated later, 1 hr segments may be concatenated to form a 24 hr prediction interval with TDAS position errors between 10 and 12 m, a significant improvement over the baseline model.

TDAS maximum position error contributors are shown in Figure C-13 for the 1, 3, 6, and 12 hr tracking intervals. Note that the tropospheric error contribution is significant here, but decreases, while the solar pressure contribution increases with tracking interval. A crossover between these two error sources occurs around a 6 hr tracking interval. All the other error contributors are relatively small in this region.

C.3.2.1 Impact of Tracking Data Rate. Table C-2 lists minimum and maximum TDAS position uncertainties as a function of data rate, tracking interval, and prediction interval. For 1 hr tracking, the 3600 sec period (1 measurement per hr) is inadequate for orbit estimation (number of measurements less than the number of unknowns being solved for). For 3 hr tracking the 1/hr rate produces a maximum error about twice that of the 1/min rate. For 6 or 12 hr tracking, changing the data rate from 1/min to 1/hr has little impact on the results.

FIGURE C-12
TDAS POSITION UNCERTAINTY IN PREDICTION INTERVAL FOR 1, 3, 6 AND 12 HOUR TRACKING INTERVALS

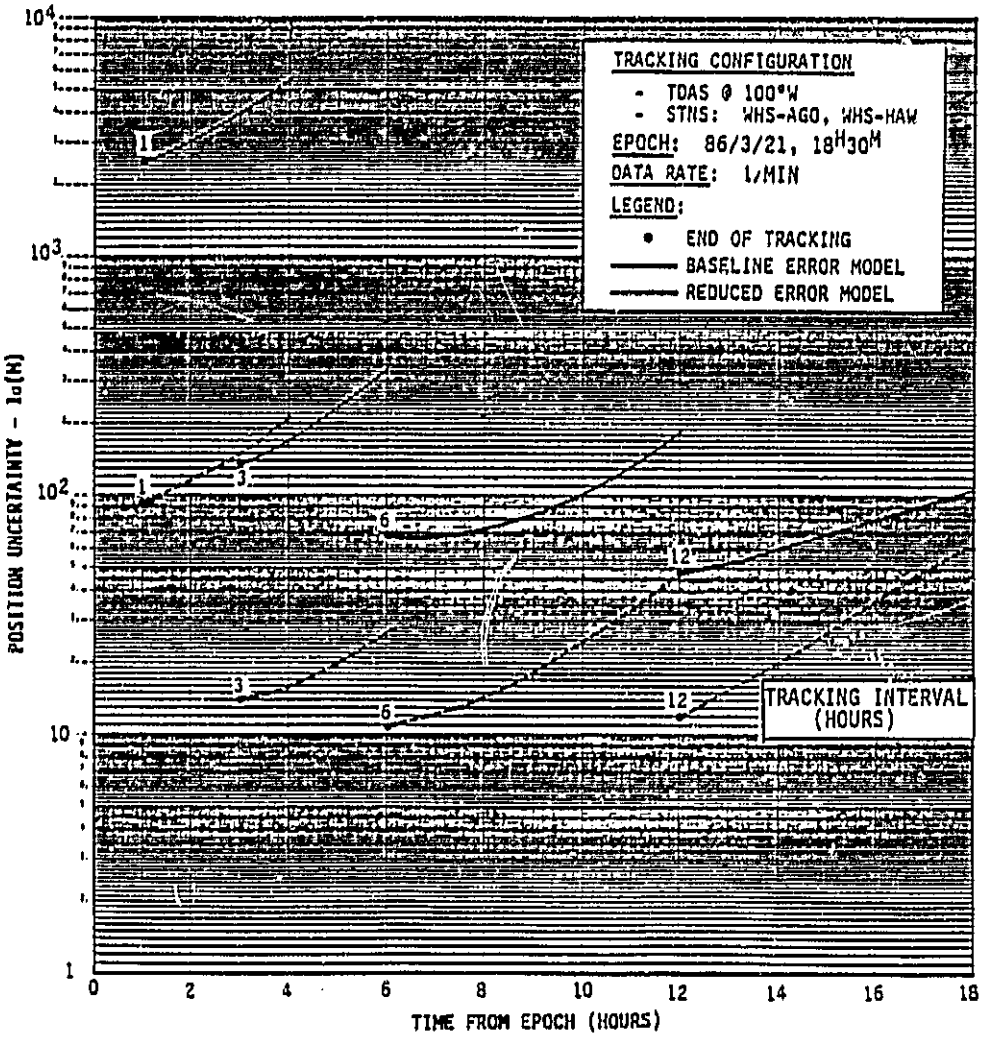

FIGURE C-13
TDAS MAXIMUM POSITION ERROR CONTRIBUTORS VS. VLBI TRACKING INTERVAL FOR THE REDUCED ERROR MODEL

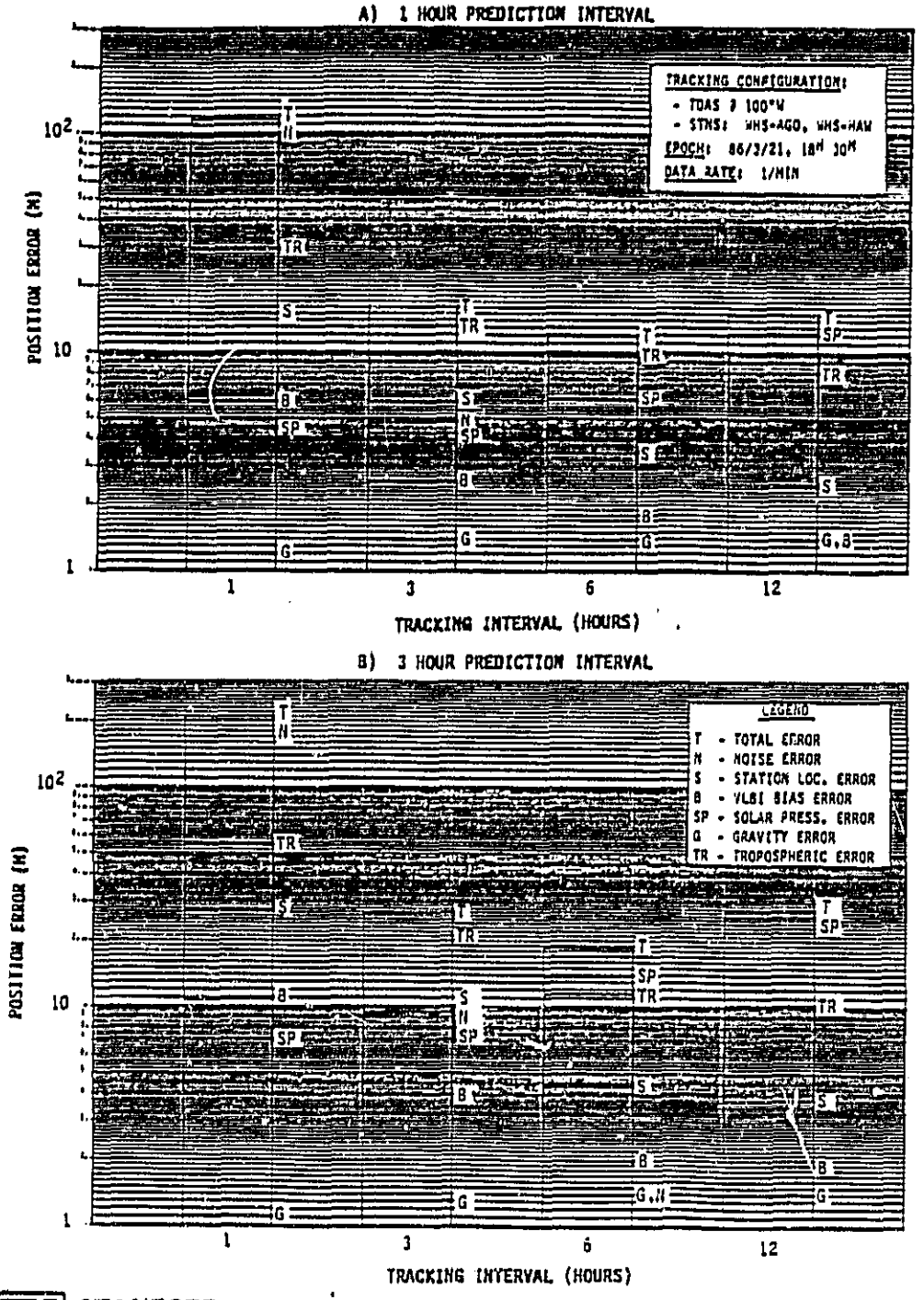

STANFORD TELECOMMUNICATIONS INC.

TABLE C-2
MIN/MAX POSITION UNCERTAINTY (M) IN PREDICTION INTERVAL VS. VLBI DATA RATE AND TRACKING INTERVAL*

WITH REDUCED ERROR MODEL

PREDICTION INTERVAL (HOURS)	TRACKING INTERVAL (HOURS)	VLBI DATA RATE (SEC)		
		60	1800	3600
1	1	96/114	333/398	X
	3	14/16	19/23	23/29
	6	11.5/18.7	11.6/18.9	11.7/19.3
	12	11.6/15.1	11.4/14.7	11.2/14/4
3	1	96/212	333/740	X
	3	14/27	19/43	23/56
	6	11.5/18.7	11.6/18.9	11.7/19.3
	12	11.6/28.2	11.4/27.6	11.2/27.1

* TRACKING CONFIGURATION: TDAS @ 100°W; STNS: WHS-AGO, WHS-HAW
EPOCH: 86/3/21, 18^H30^M

C.3.2.2 Prediction Interval Concatenation. Figure C-14 illustrates how a series of 1 hr prediction segments may be concatenated to form a 24 hr prediction profile. Each segment is based on 6 hours of tracking data. In (A), the dominant error source is the tropospheric error (15%),* and the profile is relatively flat over 24 hours with a mean TDAS position error near 11.5 m. In (B), the effect of a possible reduction in tropospheric error to 5% is shown with TDAS position error reduced to the 5-8 m level. Solar pressure is the dominant contributor as is evident from the 12 hr cycle.

C.3.3 CONUS-Based VLBI Tracking Results

Some preliminary results on TDAS position uncertainty based on CONUS tracking sites rather than global sites are presented in Figures C-15 and C-16. The CONUS sites used were GSFC, HSN (Houston), and SUN (Sunnyvale). Figure C-15A shows the prediction error profiles generated with the baseline model for 6-48 hr tracking intervals in 6 hr steps. As observed in Section C.3.1, longer intervals give better performance than shorter intervals with measurement and station survey errors at the baseline model levels. Figure C-15B indicates that the maximum TDAS position error during a 6 hr prediction interval is dominated by either solar pressure or VLBI bias for the tracking intervals considered.

Figure C-16 demonstrates how several prediction interval segments can be concatenated to form a 24 hour prediction error profile. In (A), with segments based on 24 and 48 hr tracking intervals, the TDAS position uncertainty ranges between 80 and 125 m. In (B), VLBI bias is estimated, and the TDAS position uncertainty decreases to the 50-75 m level.

C.4 MODELLING DATA

Tables C-3 and C-4 list various modelling data used in the analysis.

* A 15% uncertainty in tropospheric delay modelling was assumed in the VLBI error model (Table 4-1).

FIGURE C-14

TDAS POSITION UNCERTAINTY IN 24 HOUR PREDICTION INTERVAL
(BASED ON MULTIPLE VLBI TRACKING SEGMENTS)

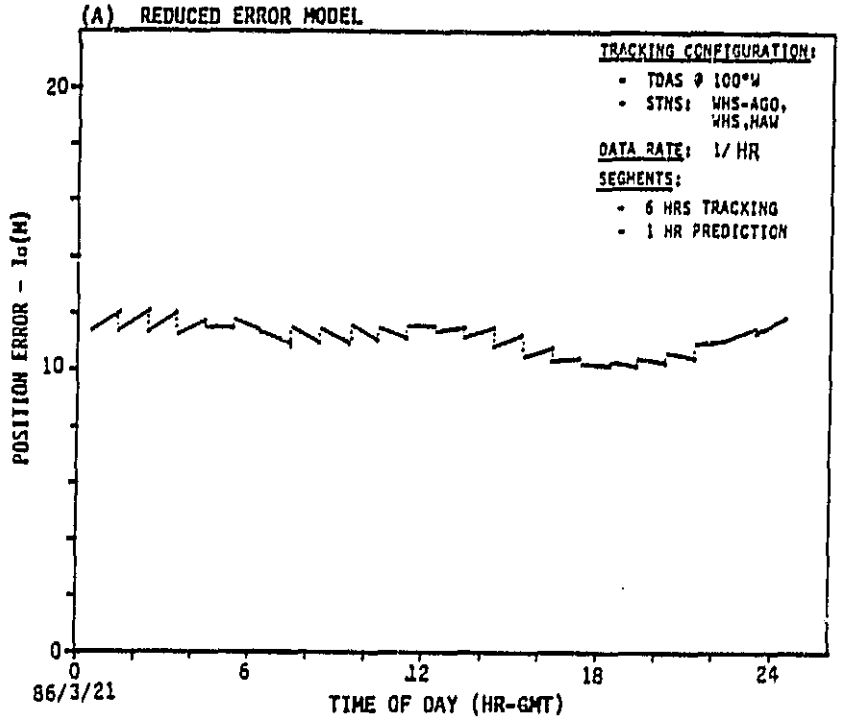

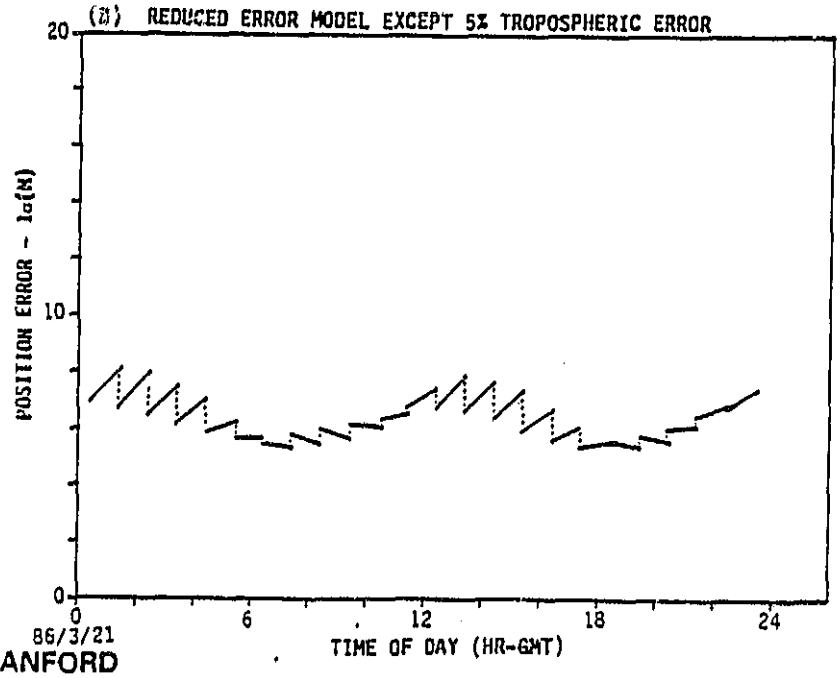

STANFORD TELECOMMUNICATIONS INC.

FIGURE C-15
TDAS POSITION UNCERTAINTY IN PREDICTION INTERVAL AND ERROR CONTRIBUTORS FOR CONUS BASED VLBI TRACKING

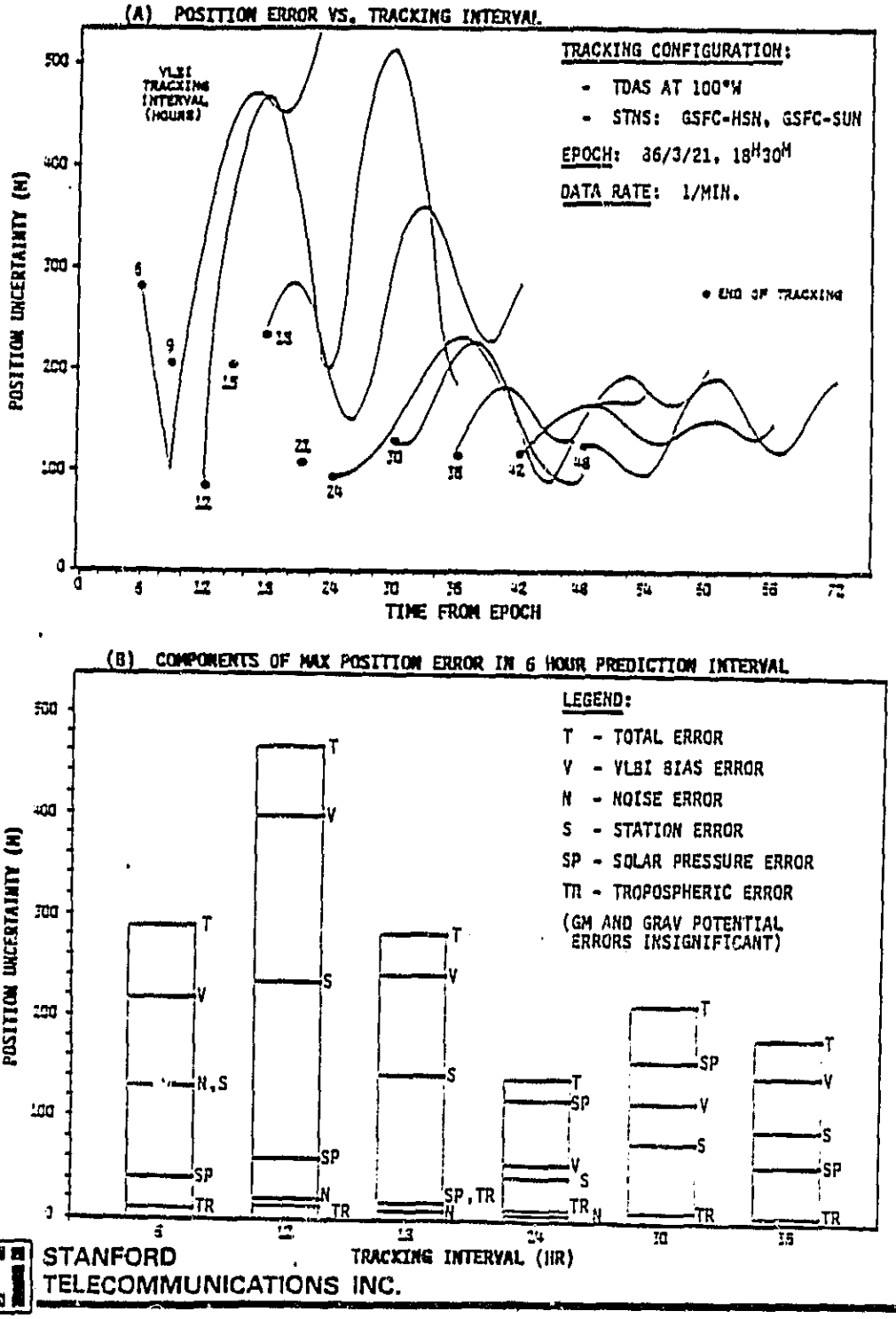

STANFORD TELECOMMUNICATIONS INC.

FIGURE C-16
TDAS POSITION UNCERTAINTY IN PREDICTION INTERVAL WITH 24, 48 HOUR VLBI TRACKING INTERVALS FROM CONUS BASED SITES

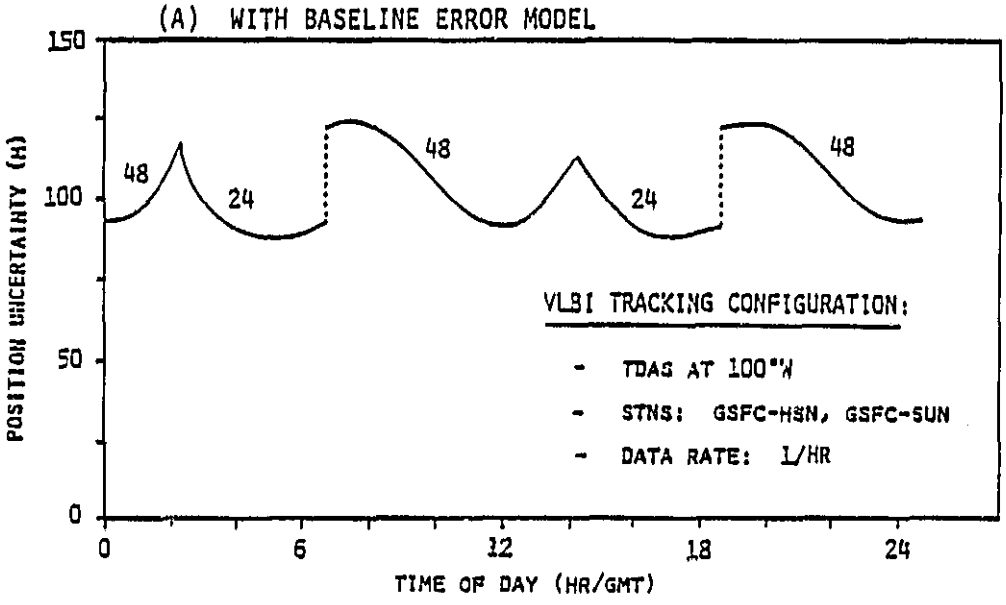

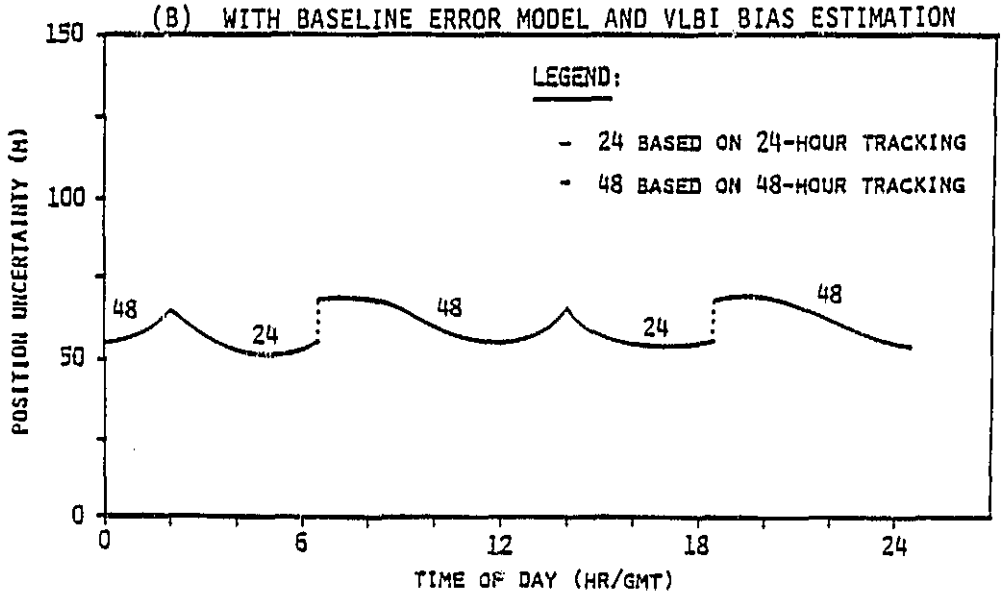

TABLE C-3

TDAS TRACKING ERROR MODEL ASSUMPTIONS

ERROR SOURCE		1σ VALUES		
		BRTS	VLBI (BASELINE MODEL)	VLBI (REDUCED MODEL)
MEASUREMENT - BRTS ($R/\dot{R}$) - VLBI (ΔR)	NOISE	2 M/.13 CM/S	0.9 M	0.03 M
	BIAS	10 M/0 CM/S	3 M	0.1 M
LOCAL	STATIONS (X,Y,Z)	3 M	3 M	0.3 M
	TROPOSPHERIC REFRACTION	15%		
DYNAMIC	GM GRAV. POT.	10^{-7} 100% OF GEM5 - GEM1		
	SOLAR PRESSURE*	10%		

* TDAS AREA/WEIGHT = .042 M^2/KG (SAME AS TDRS).

STANFORD TELECOMMUNICATIONS INC.

TABLE C-4

EXISTING AND POTENTIAL GROUND STATIONS

STATIONS LOCATIONS	STATION CODE	LATITUDE* (DEG.)	LONGITUDE (E) (DEG.)
ASCENSION ISLAND	ACN	-8.0	345.7
SANTIAGO, CHILE	AGO	-33.2	289.3
ALICE SPRINGS, AUSTRALIA	ALS	-23.8	133.9
AMERICAN SAMOA	AMS	-14.3	189.3
JOHANESBURG, S. AFRICA	BUR	-25.9	27.7
DIEGO GARCIA	DGA	-7.0	72.0
EASTER ISLAND	EIL	-27.5	251.0
GODDARD SPACE FLIGHT CENTER	GSFC	39.0	283.2
GUAM	GWM	13.3	144.7
HAWAII	HAW	22.1	200.3
HOUSTON, TEXAS	HSN	29.0	265.0
MADRID, SPAIN	MAD	40.5	355.8
MERRITT ISLAND, FLORIDA	MIL	28.5	279.3
ORRORAL VALLEY, AUSTRALIA	ORR	-35.6	149.0
SUNNYVALE, CALIFORNIA	SUN	37.0	238.0
VANDENBURG, AFB, CALIFORNIA	VAN	34.7	239.5
WHITE SANDS, NEW MEXICO	WHS	32.5	253.4

* A MINUS SIGN (-) INDICATES SOUTH LATITUDE

APPENDIX D

USER NAVIGATION PERFORMANCE RESULTS - SEQUENTIAL DATA PROCESSING

TDAS user navigation performance was evaluated in terms of potential OD/TD accuracy for the three one-way tracking alternatives defined in Section 2. The objective was to assess several user orbit types and the impact of two and three satellite TDAS constellations, the tracking schedule and two algorithms for tracking data processing (sequential and sliding batch). This section contains the detailed performance results based on sequential processing of tracking data*. The error modeling approach and major findings were presented in Section 5.

Cases for evaluation were defined originally for three TDAS constellation options (see Figure 5.2) and six user orbit types (see Figure 5.3). The results that follow cover 12 cases: four of the user orbits (A, D, E and F)** with each of the three TDAS constellations.** Each case is presented in a standard format:

- Tracking Schedule - This shows tracking contact intervals over 24 hours for Schedules I and II and for beacon tracking (see Table 5-1). An accompanying user ground trace indicates coverage outages due to a zone of exclusion (if any).

- User Position & Time Accuracy Profiles - These show the 1σ errors corresponding to the 24 hour tracking schedules and a subsequent 6 or 12 hour prediction-only interval.

Summary tables (D-1 thru D-4) included at the end of Appendix D record the peak errors and identify the major error contributors for each tracking alternative.

---

* Performance results for sliding batch processing are in Appendix E.

** Individual cases are identified by a two element mnemonic; e.g., A2 indicates user orbit Type A and TDAS constellation Option 2. Evaluation of user orbit types, B (28°, 600 km) and C (28°, 1000 km) remains to be completed.

FIGURE D-1
CASE A1 TRACKING SCHEDULES

USER ORBIT (A): 28°, 200 KM
TDAS CONST.(1): 171°W, 41°W

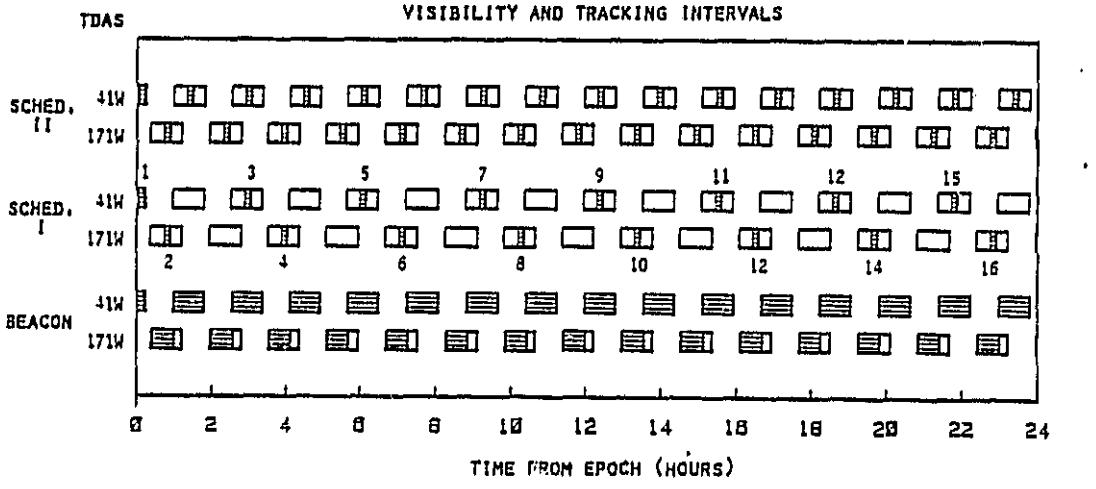

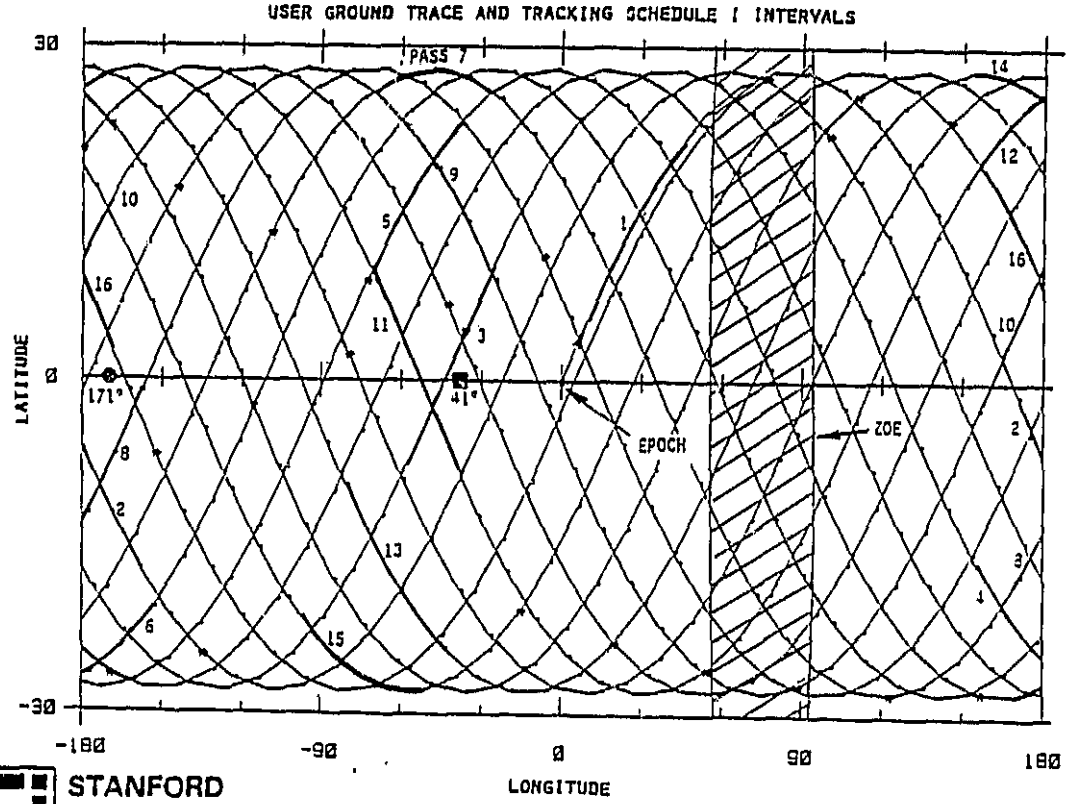

STANFORD TELECOMMUNICATIONS INC.

FIGURE D-2
USER POSITION AND TIME ACCURACY WITH 1-WAY TDAS TRACKING - CASE A1
(SEQUENTIAL DATA PROCESSING)

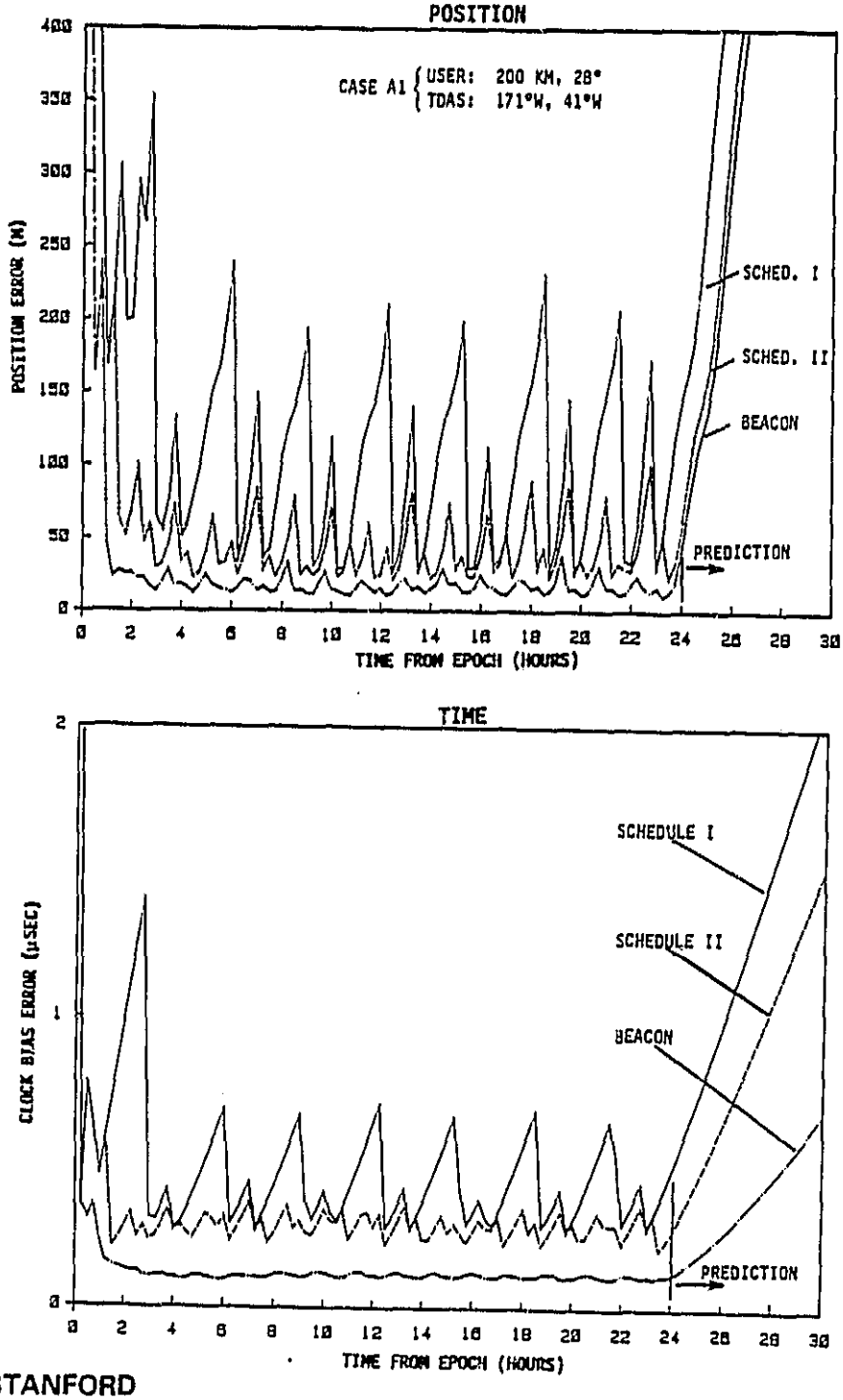

STANFORD
TELECOMMUNICATIONS INC.

FIGURE D-3
CASE A2 TRACKING SCHEDULES

USER ORBIT (A): 28°, 200 KM
TDAS CONST.(I): 100°W, 98°E

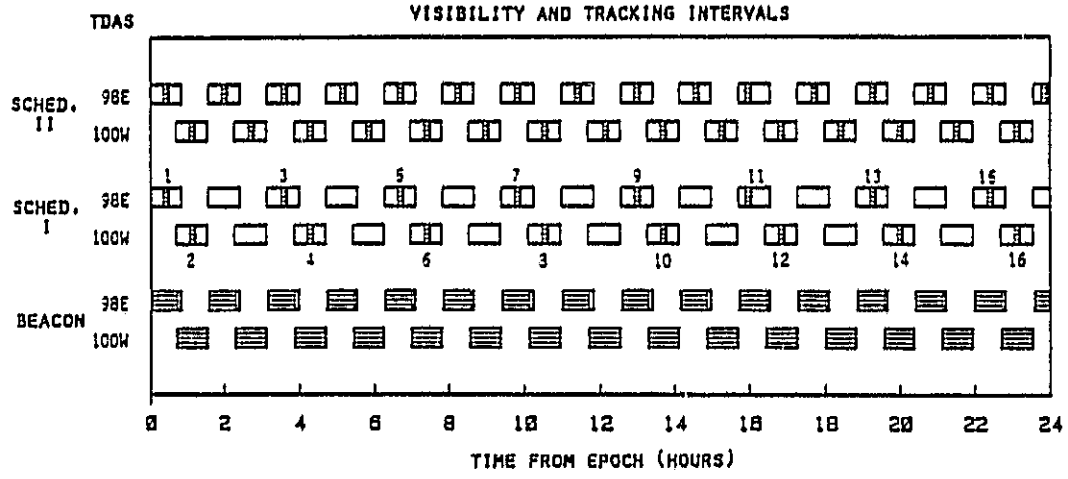

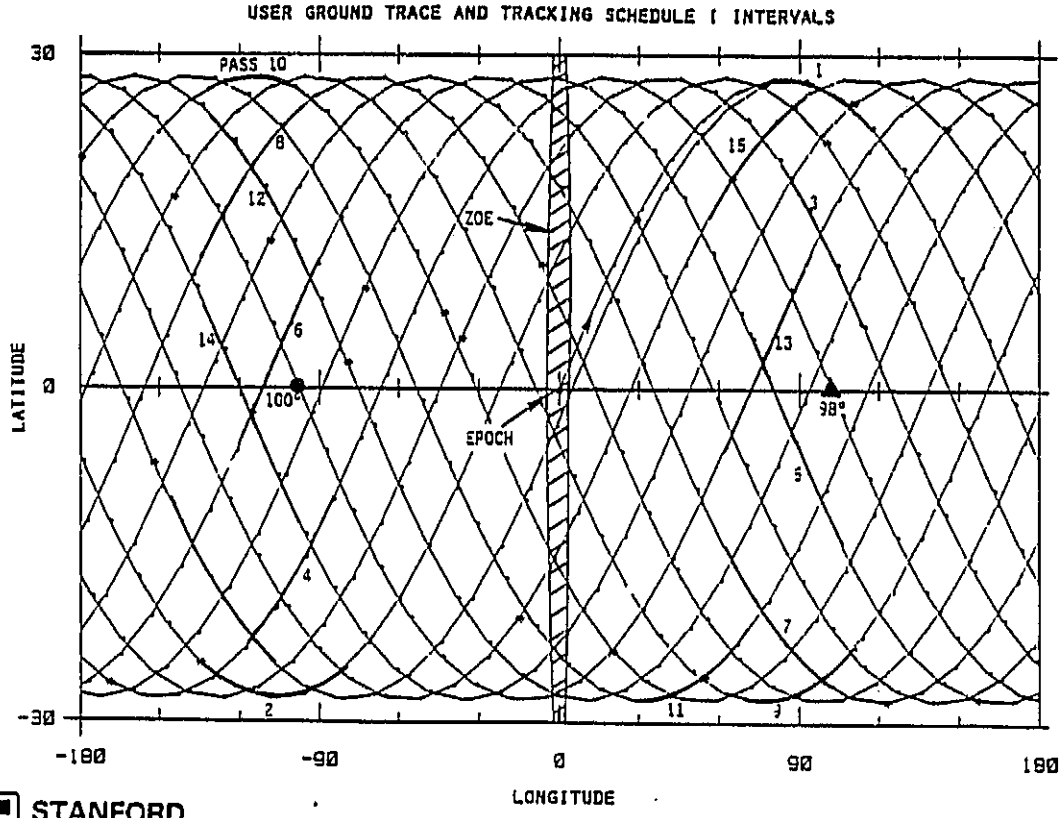

STANFORD TELECOMMUNICATIONS INC.

FIGURE D-4

USER POSITION AND TIME ACCURACY WITH 1-WAY TDAS TRACKING - CASE A2
(SEQUENTIAL DATA PROCESSING)

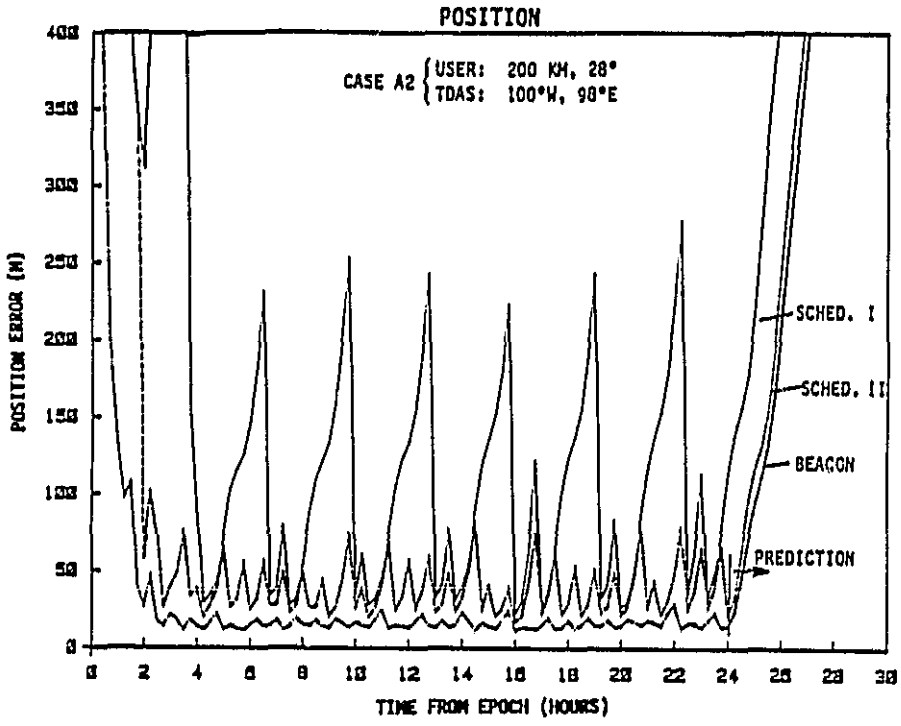

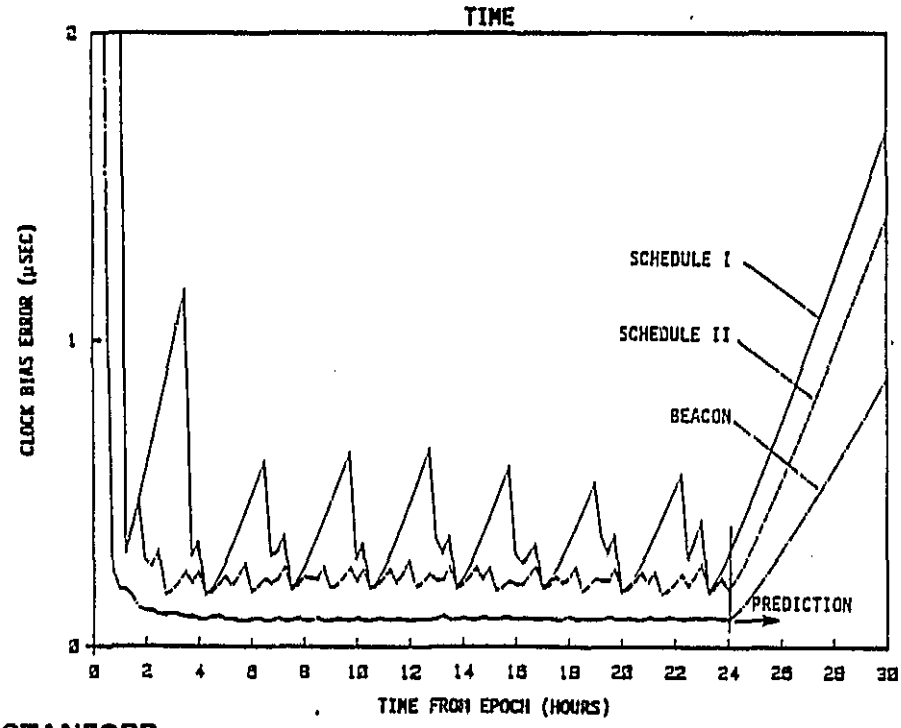

STANFORD
TELECOMMUNICATIONS INC.

FIGURE D-5
CASE A3 TRACKING SCHEDULES

USER ORBIT (A): 28°, 200 KM
TDAS CONST.(3): 171°W, 41°W, 74°E

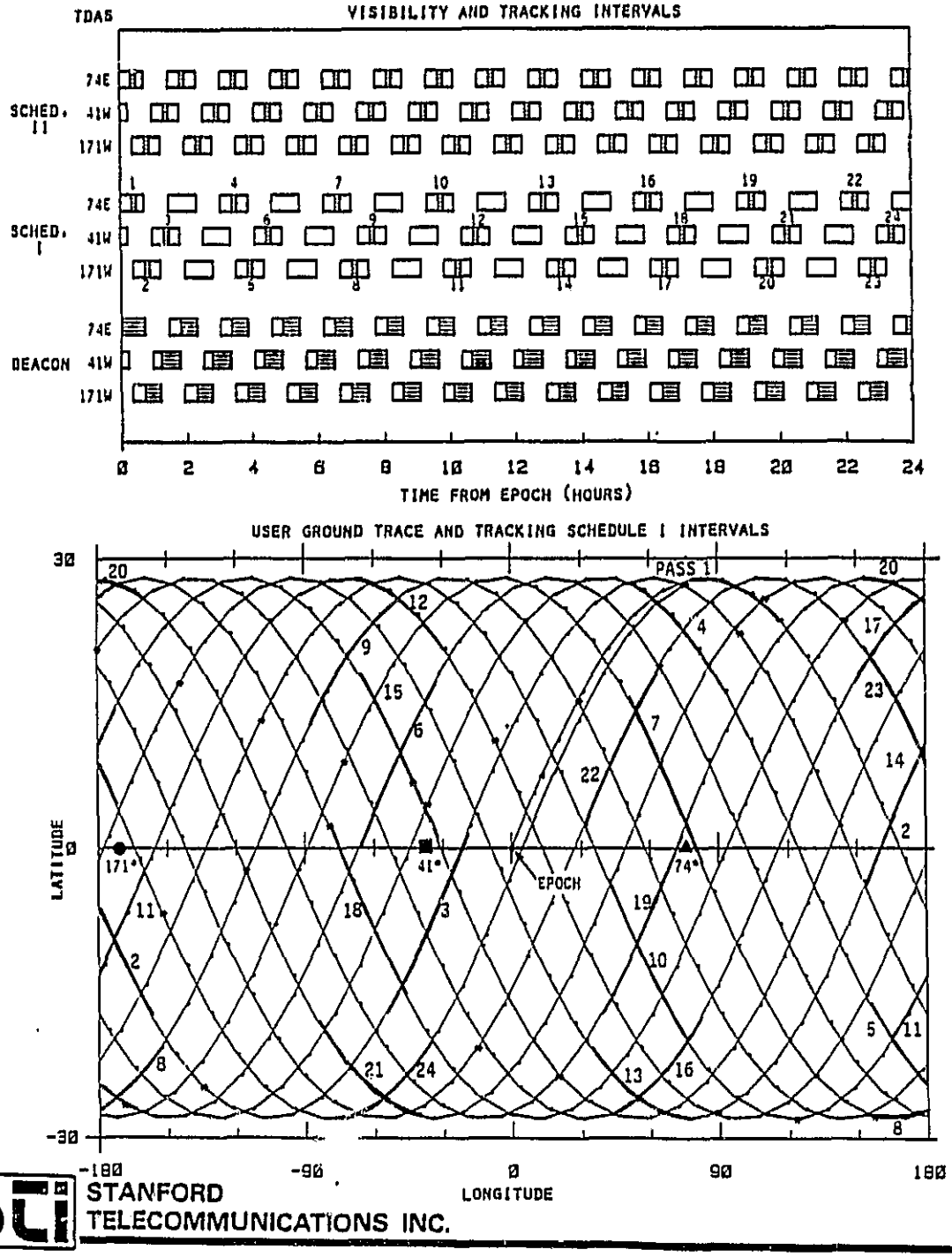

STANFORD TELECOMMUNICATIONS INC.

FIGURE D-6
USER POSITION AND TIME ACCURACY WITH 1-WAY TDAS TRACKING - CASE A3
(SEQUENTIAL DATA PROCESSING)

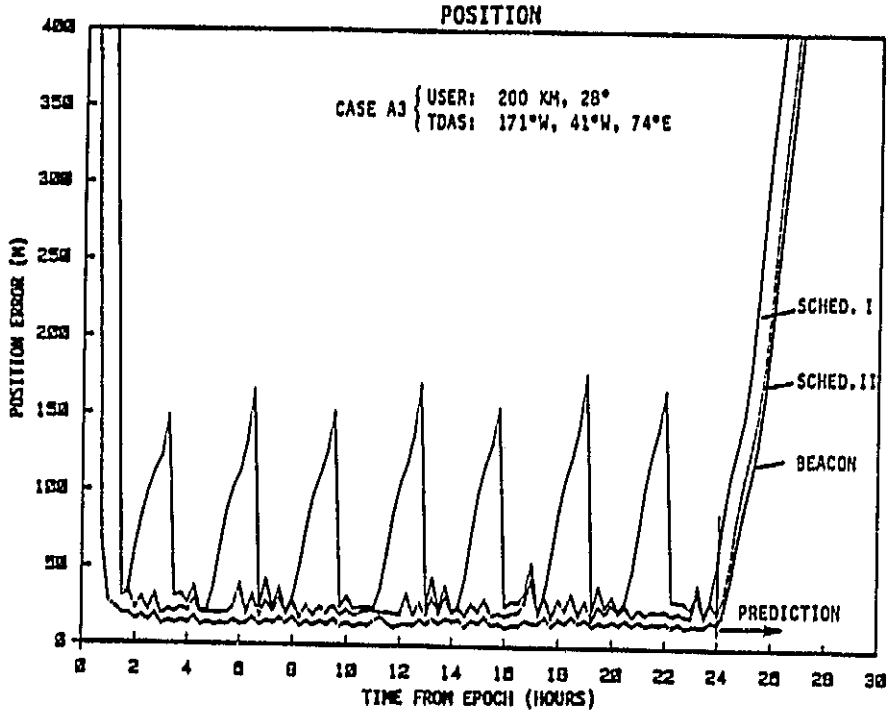

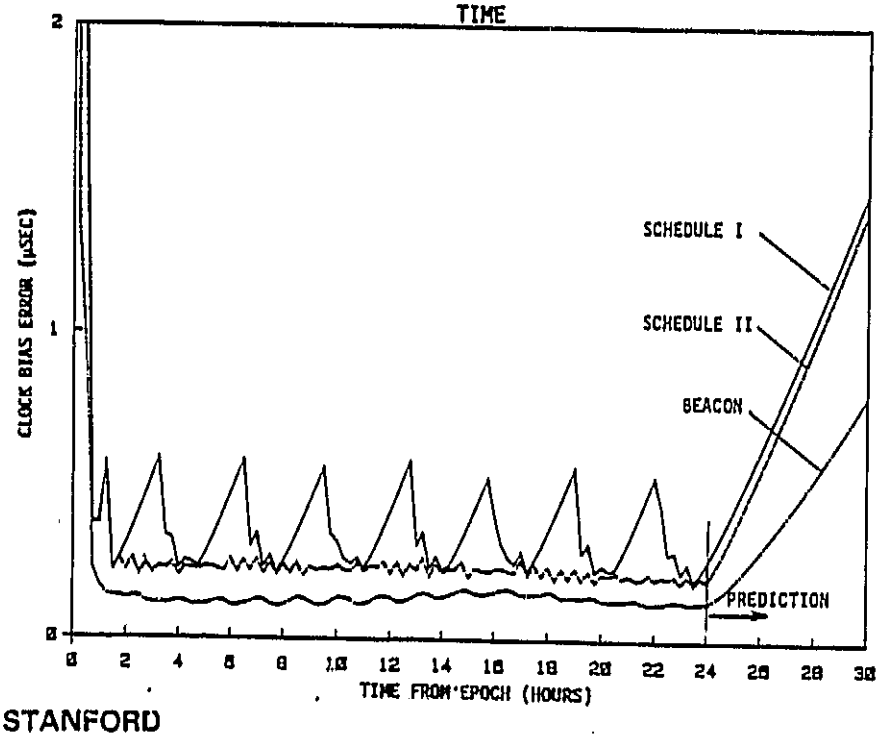

STANFORD
TELECOMMUNICATIONS INC.

FIGURE D-7
CASE D1 TRACKING SCHEDULES

USER ORBIT (D): 97°, 200 KM
TDAS CONST.(1): 171°W, 41°W

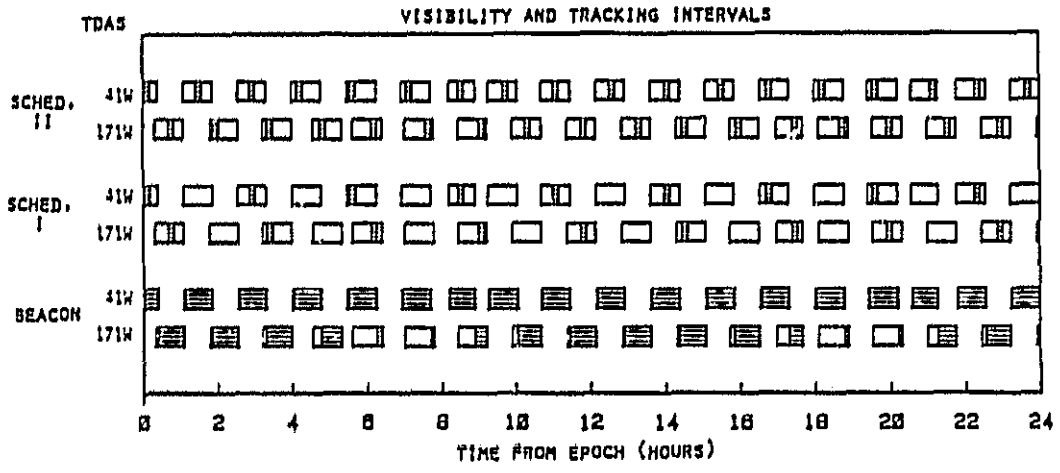

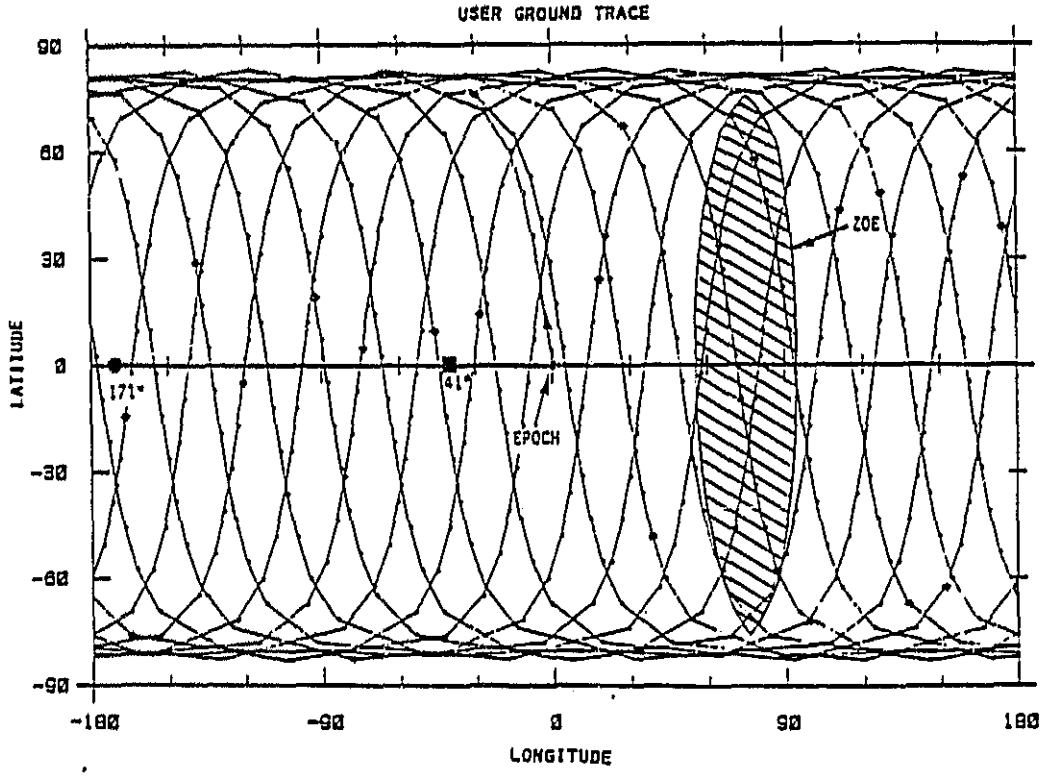

STANFORD TELECOMMUNICATIONS INC.

FIGURE D-8

USER POSITION AND TIME ACCURACY WITH 1-WAY TDAS TRACKING - CASE D1

(SEQUENTIAL DATA PROCESSING)

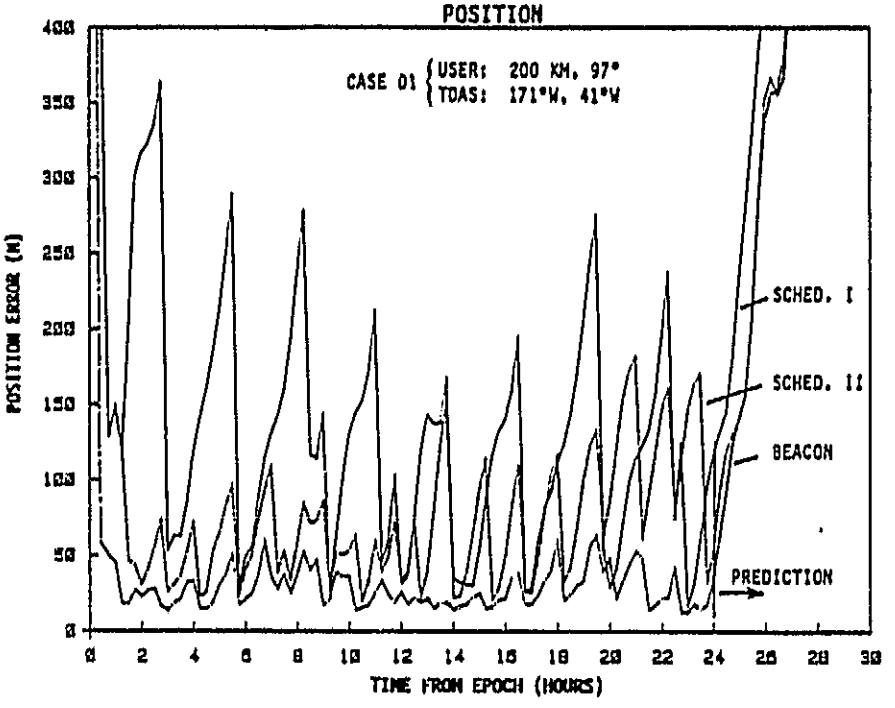

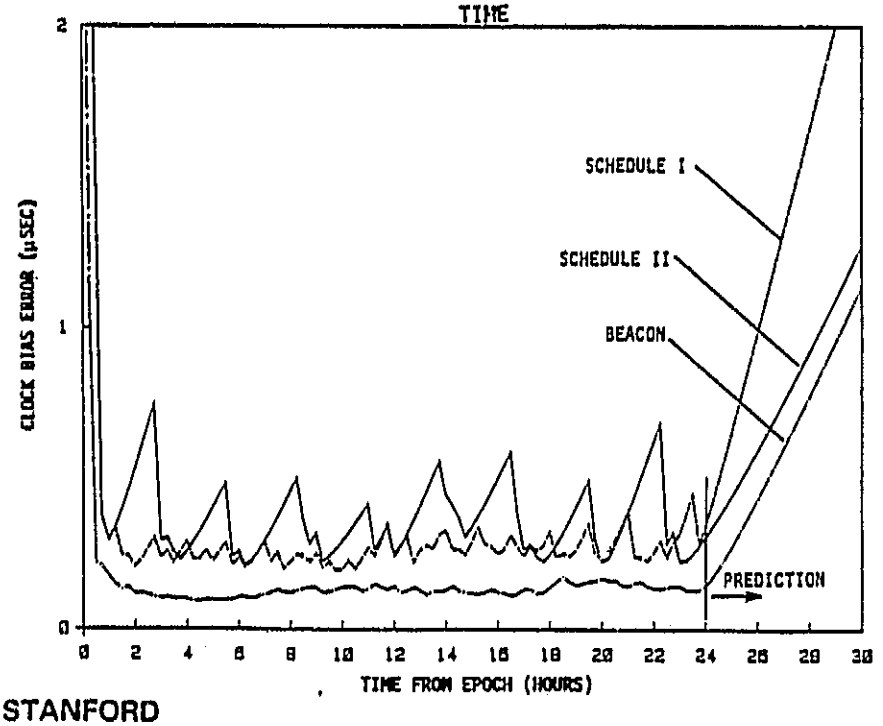

STANFORD TELECOMMUNICATIONS INC.

FIGURE D-9
CASE D2 TRACKING SCHEDULES

USER ORBIT (D): 97°, 200 KM
TDAS CONST.(2): 100°W, 98°E

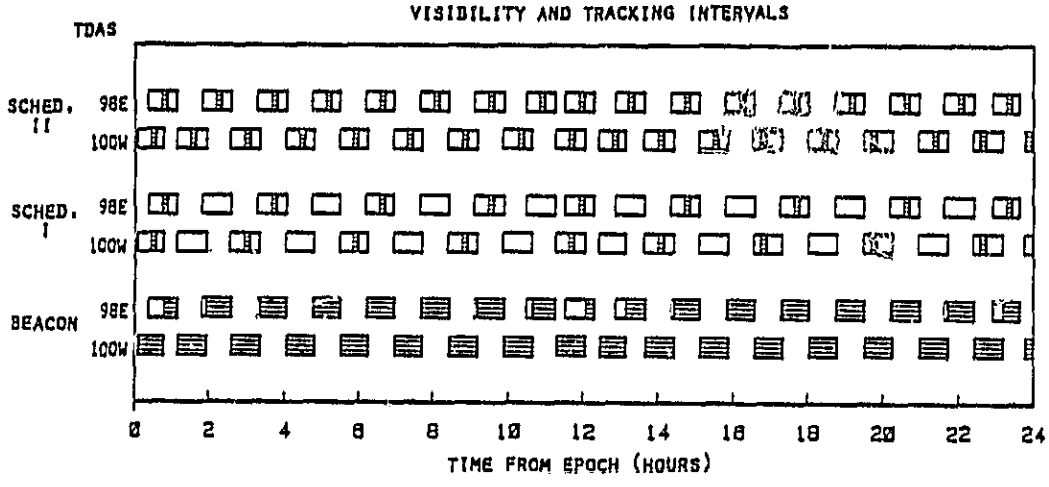

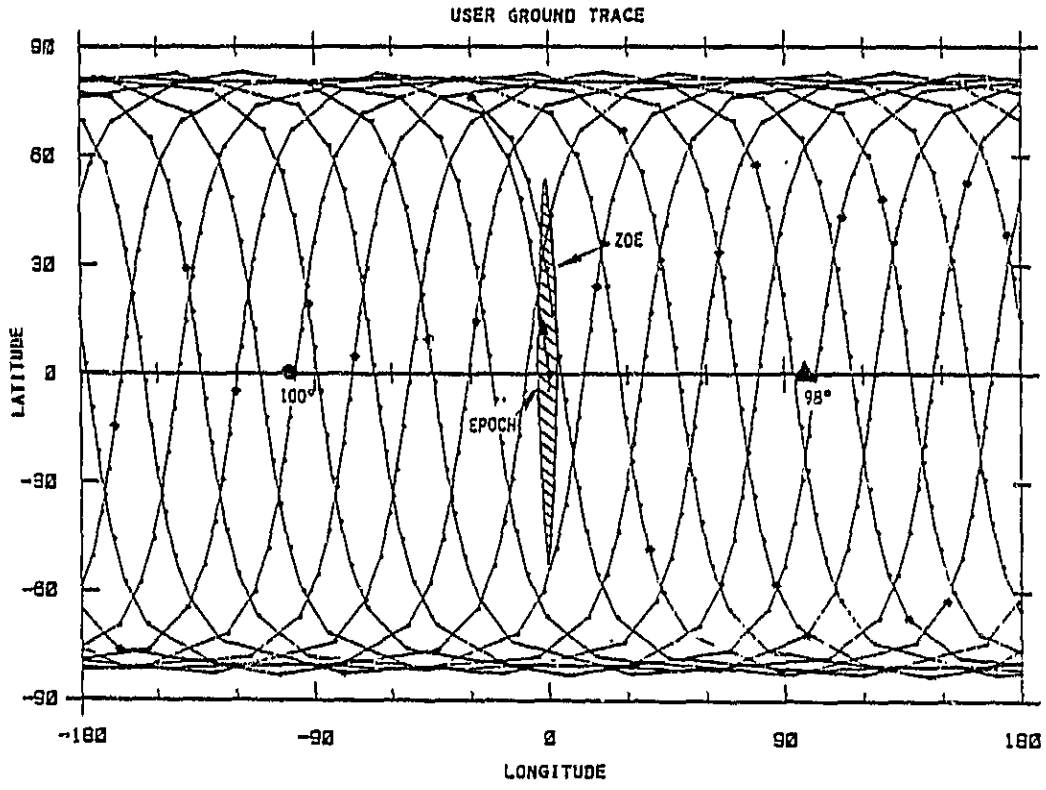

STANFORD TELECOMMUNICATIONS INC.

FIGURE D-10

USER POSITION AND TIME ACCURACY WITH 1-WAY TDAS TRACKING - CASE D2

(SEQUENTIAL DATA PROCESSING)

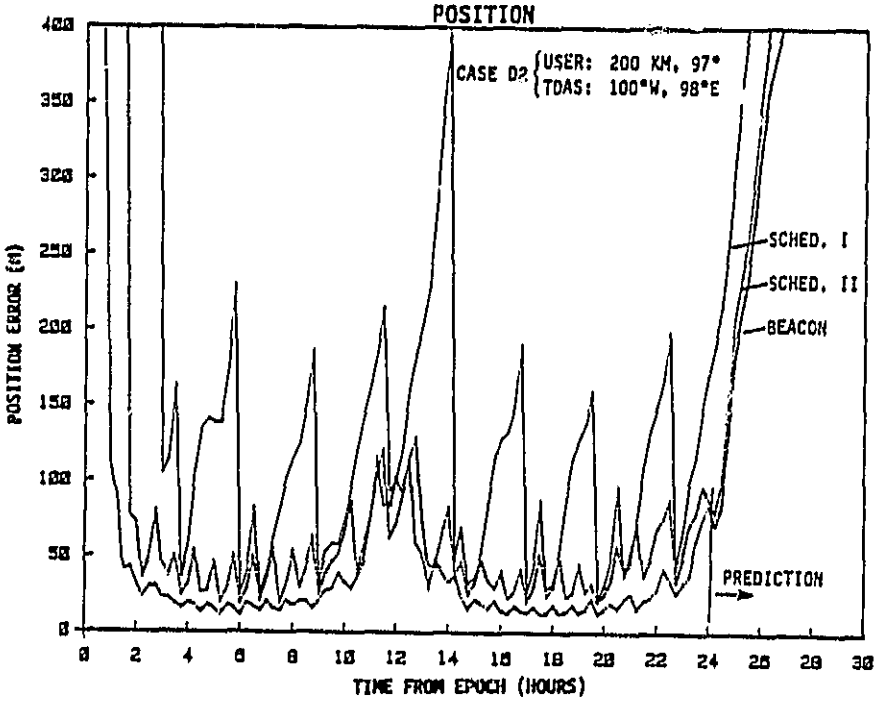

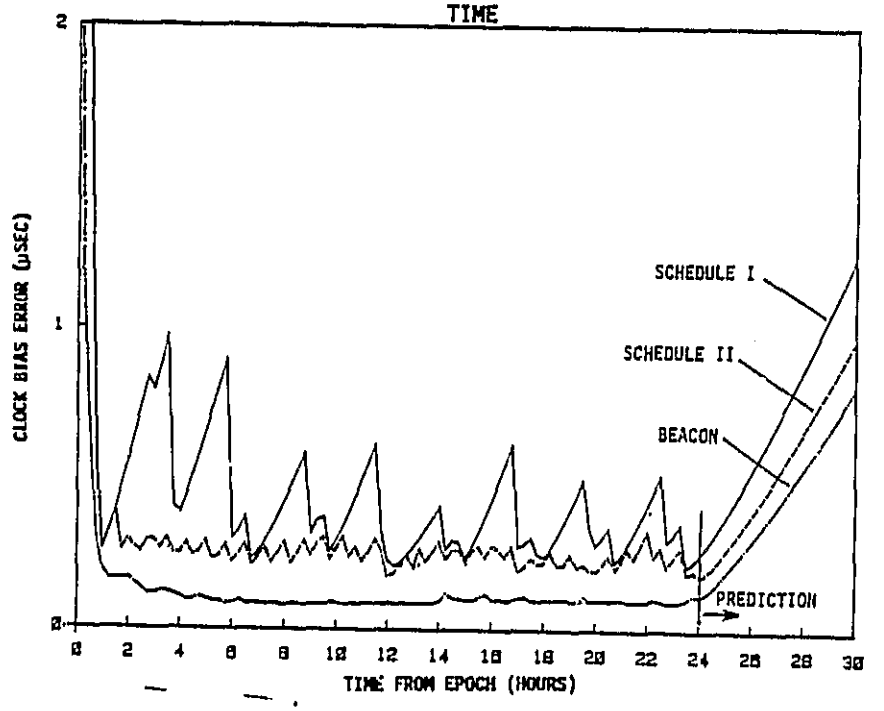

STANFORD TELECOMMUNICATIONS INC.

FIGURE D-11
CASE D3 TRACKING SCHEDULES

USER ORBIT (D): 97°, 200 KM
TDAS CONST. (3): 171°W, 41°W, 74°E

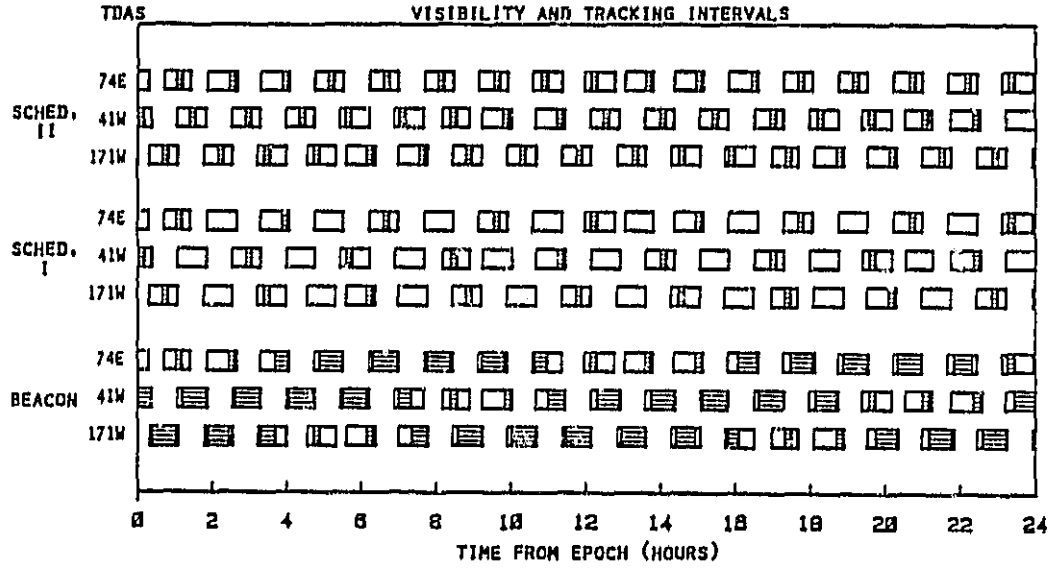

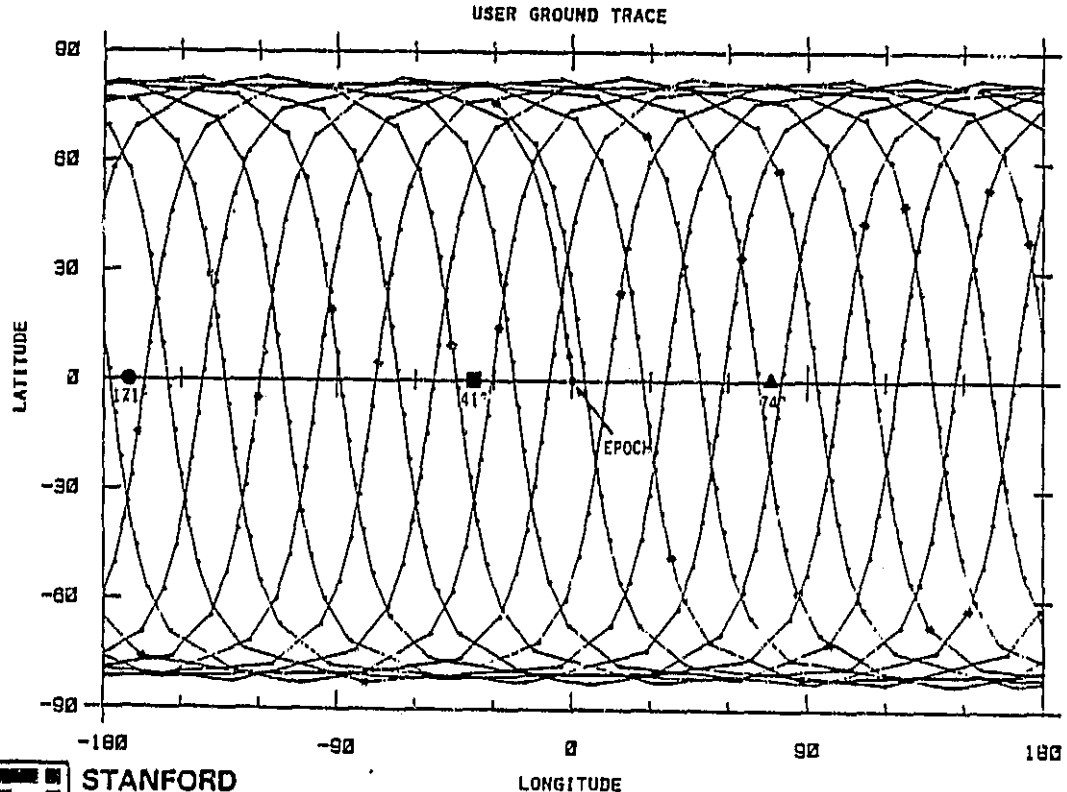

STANFORD TELECOMMUNICATIONS INC.

FIGURE D-12

USER POSITION AND TIME ACCURACY WITH 1-WAY TDAS TRACKING - CASE D3
(SEQUENTIAL DATA PROCESSING)

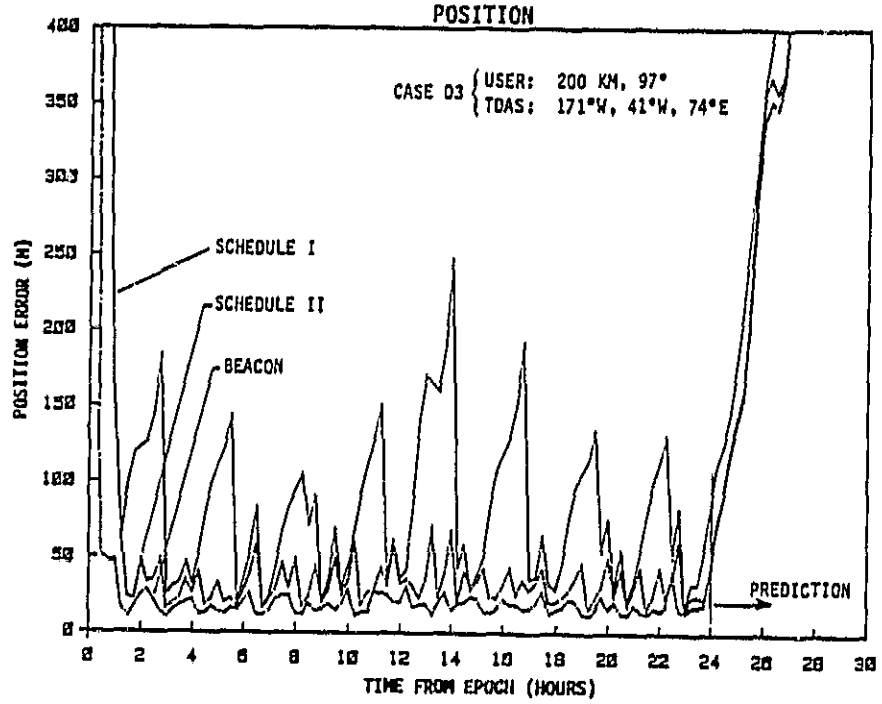

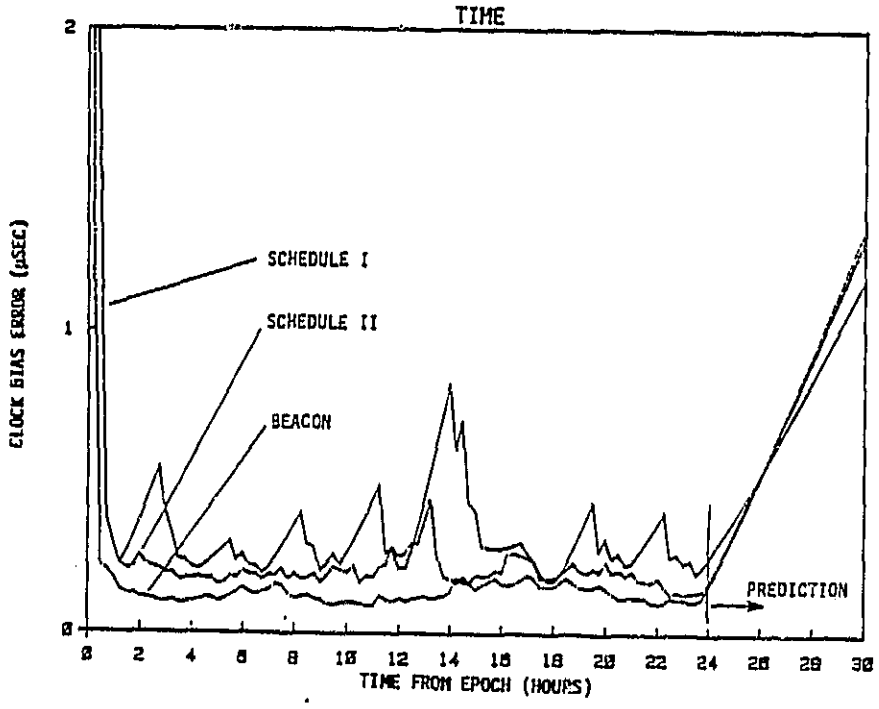

STANFORD TELECOMMUNICATIONS INC.

FIGURE D-13
CASE E1 TRACKING SCHEDULES

USER ORBIT (E): 98°, 600 KM
TDAS CONST.(i): 171°W, 41°W

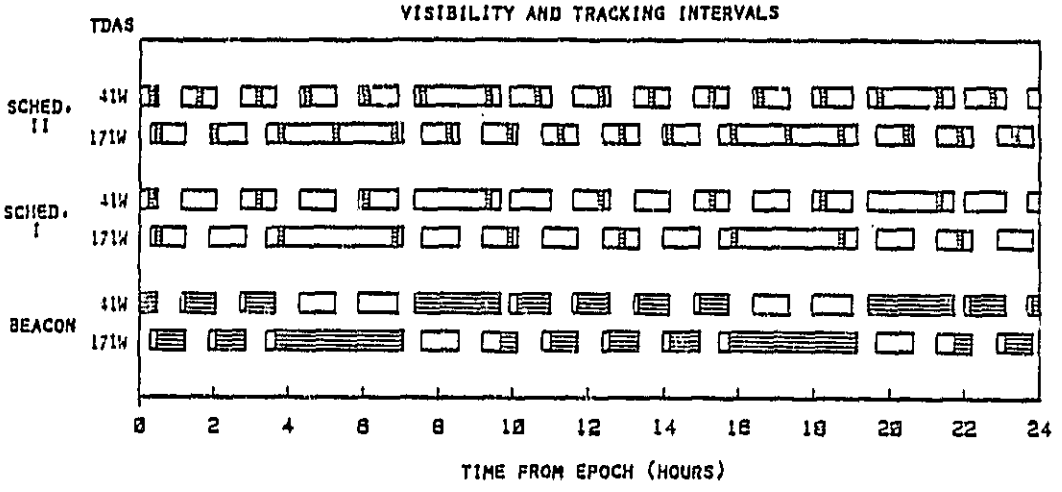

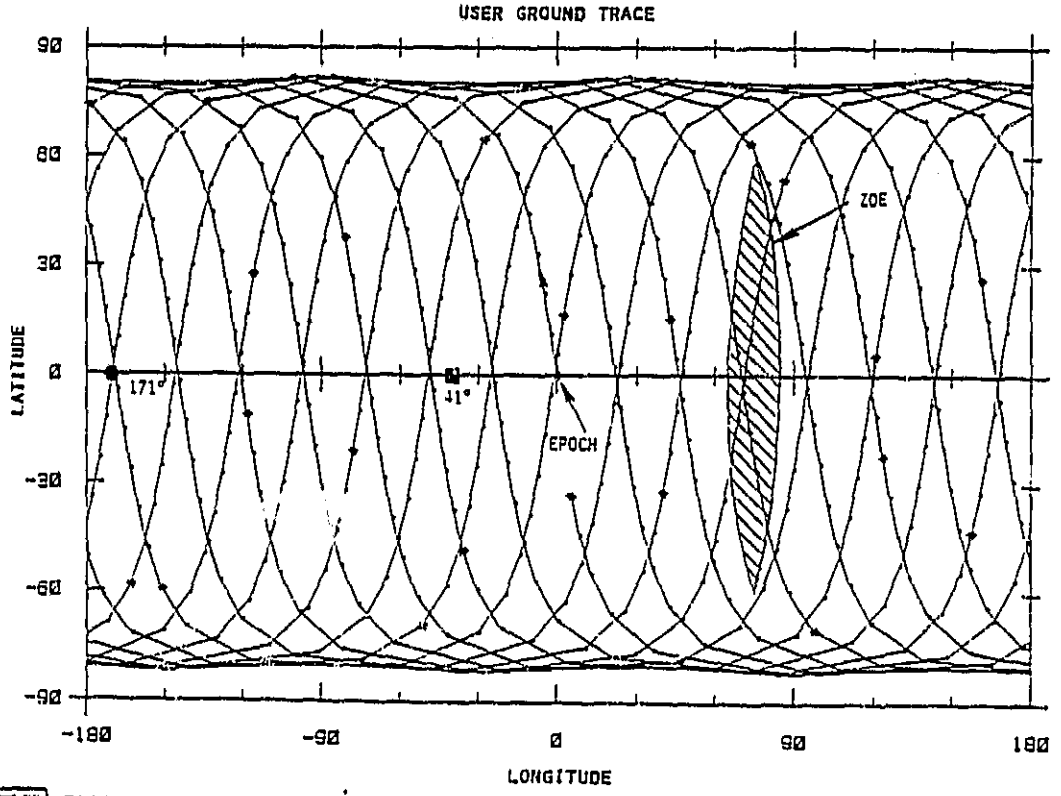

STANFORD TELECOMMUNICATIONS INC.

FIGURE D-14
USER POSITION AND TIME ACCURACY WITH 1-WAY TDAS TRACKING - CASE E1
(SEQUENTIAL DATA PROCESSING)

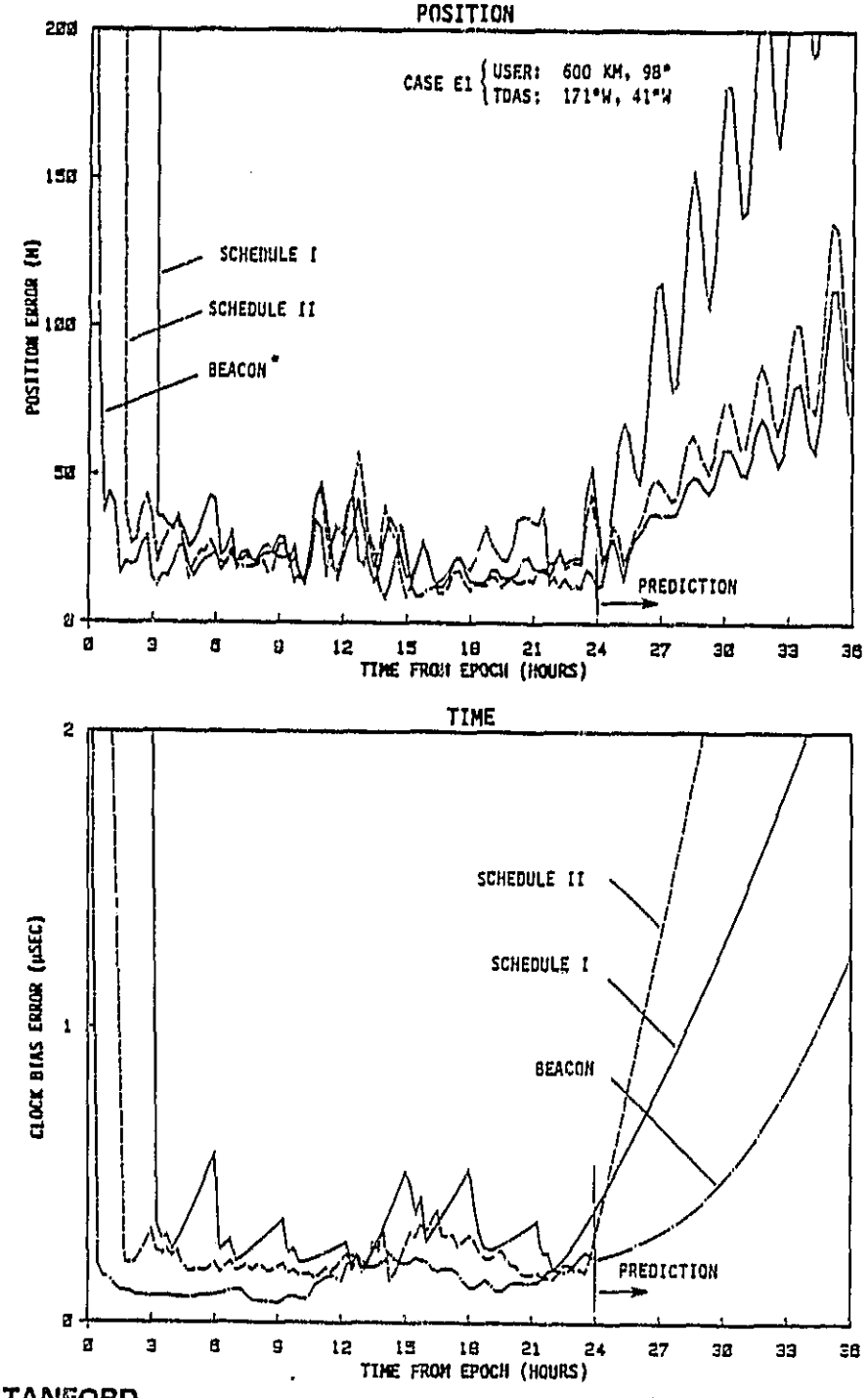

STANFORD TELECOMMUNICATIONS INC.

* MODIFIED FILTER TUNING STATE NOISE:
VELOCITY STATES: 10^{-10} m^2/sec^3

FIGURE D-15
CASE E2 TRACKING SCHEDULES

USER ORBIT (E): 98°, 600 KM
TDAS CONST.(2): 100°W, 98°E

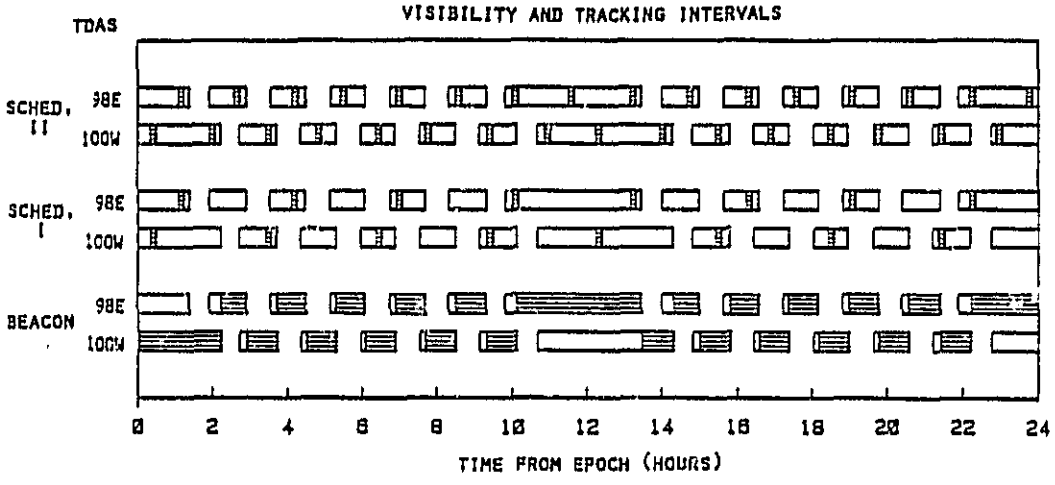

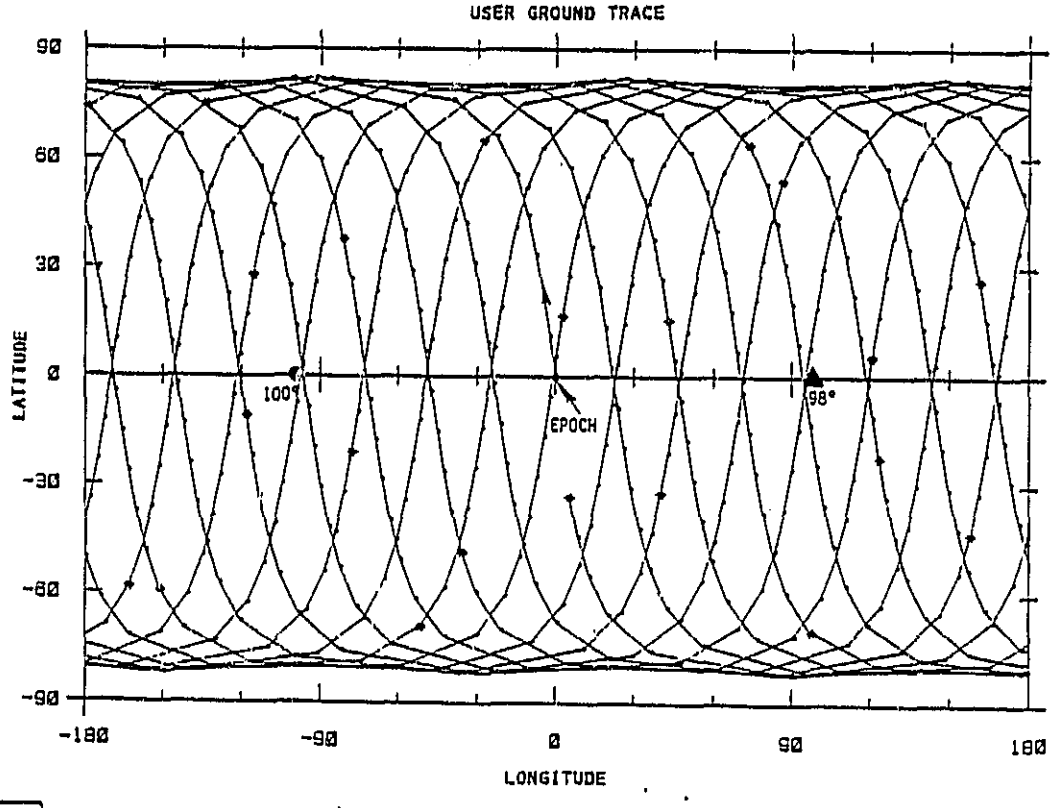

STANFORD TELECOMMUNICATIONS INC.

FIGURE D-16
USER POSITION AND TIME ACCURACY WITH 1-WAY TDAS TRACKING - CASE E2
(SEQUENTIAL DATA PROCESSING)

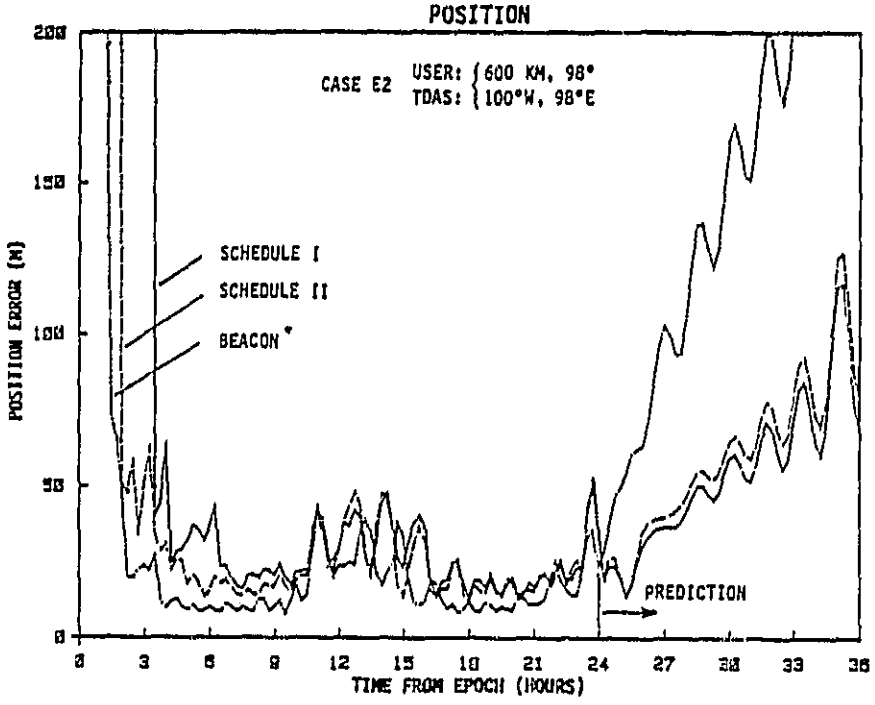

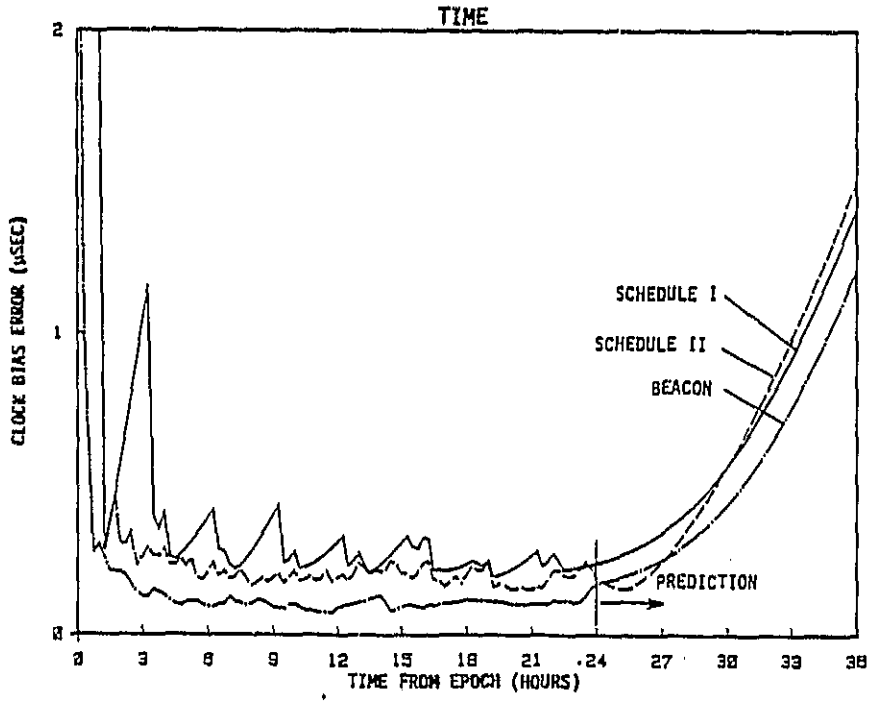

STANFORD TELECOMMUNICATIONS INC.

* MODIFIED FILTER TUNING STATE NOISE:
VELOCITY STATES: 10^{-10} m^2/sec^3

FIGURE D-17
CASE E3 TRACKING SCHEDULES

USER ORBIT (D): 98°, 600 KM
TDAS CONST. (3): 171°W, 41°W, 74°E

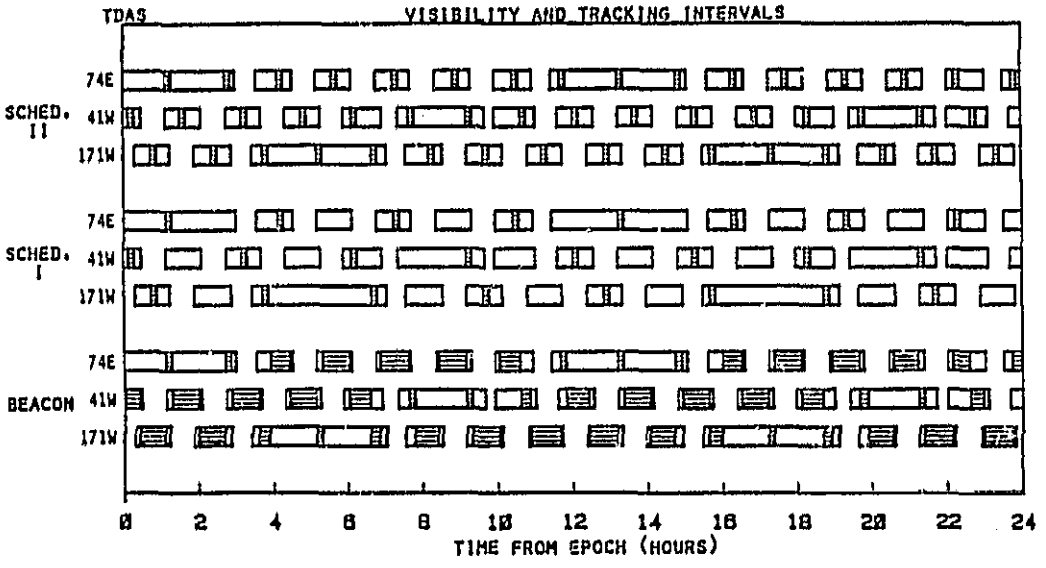

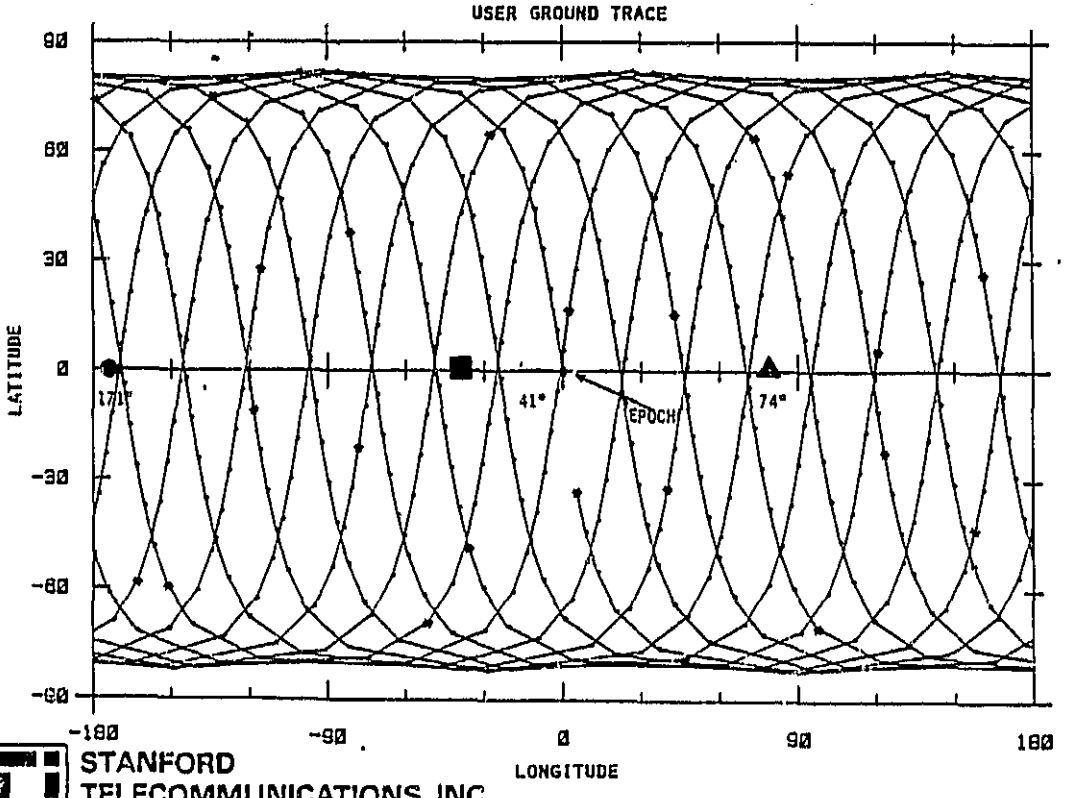

STANFORD TELECOMMUNICATIONS INC.

FIGURE D-18

USER POSITION AND TIME ACCURACY WITH 1-WAY TDAS TRACKING - CASE E3
(SEQUENTIAL DATA PROCESSING)

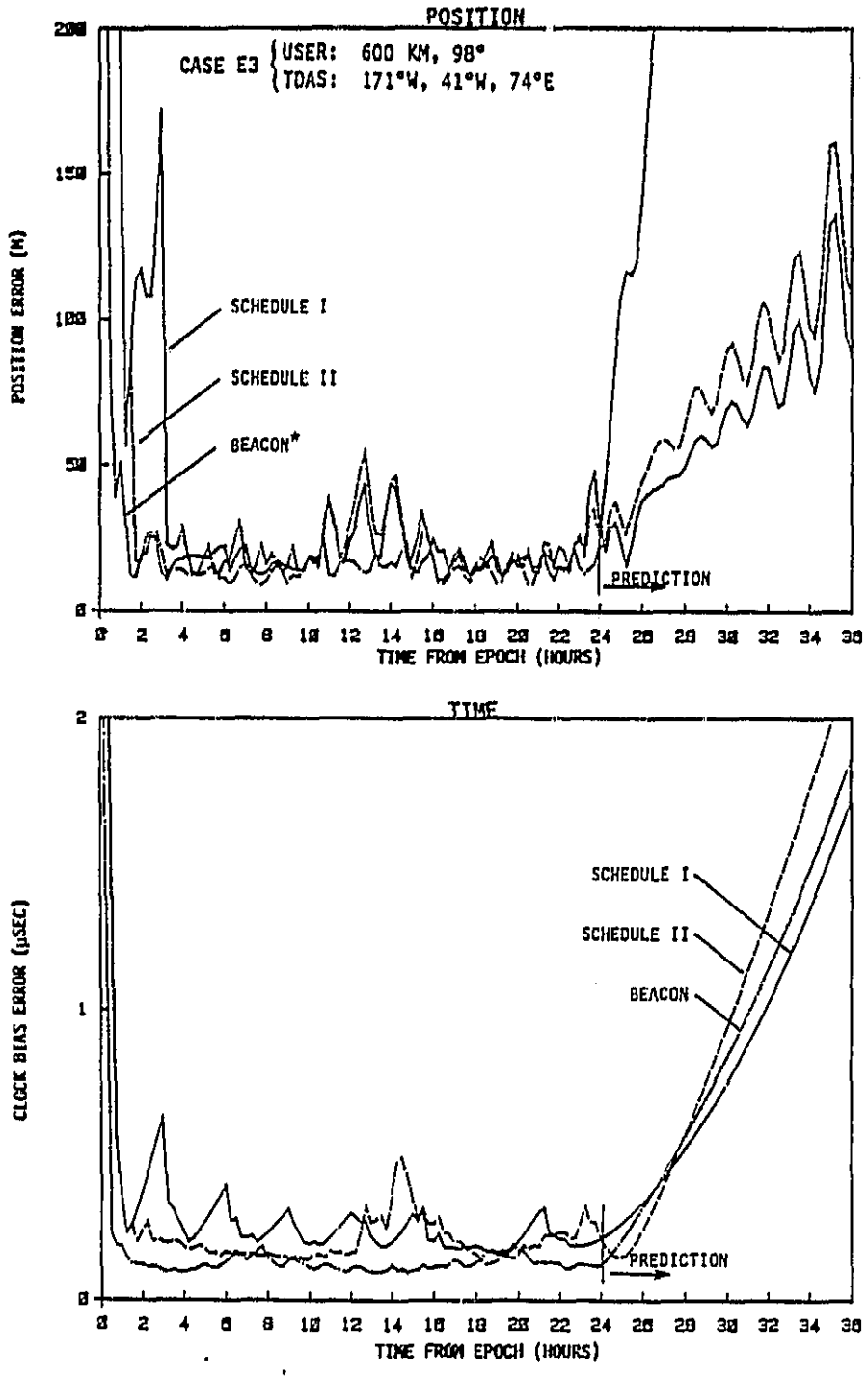

STANFORD TELECOMMUNICATIONS INC.

* MODIFIED FILTER TUNING STATE NOISE:
VELOCITY STATES: 10^{-8} m^2/sec^3

FIGURE D-19

USER POSITION ACCURACY WITH TDAS BEACON TRACKING - CASE E3

(AS A FUNCTION OF SEQUENTIAL PROCESSOR TUNING)

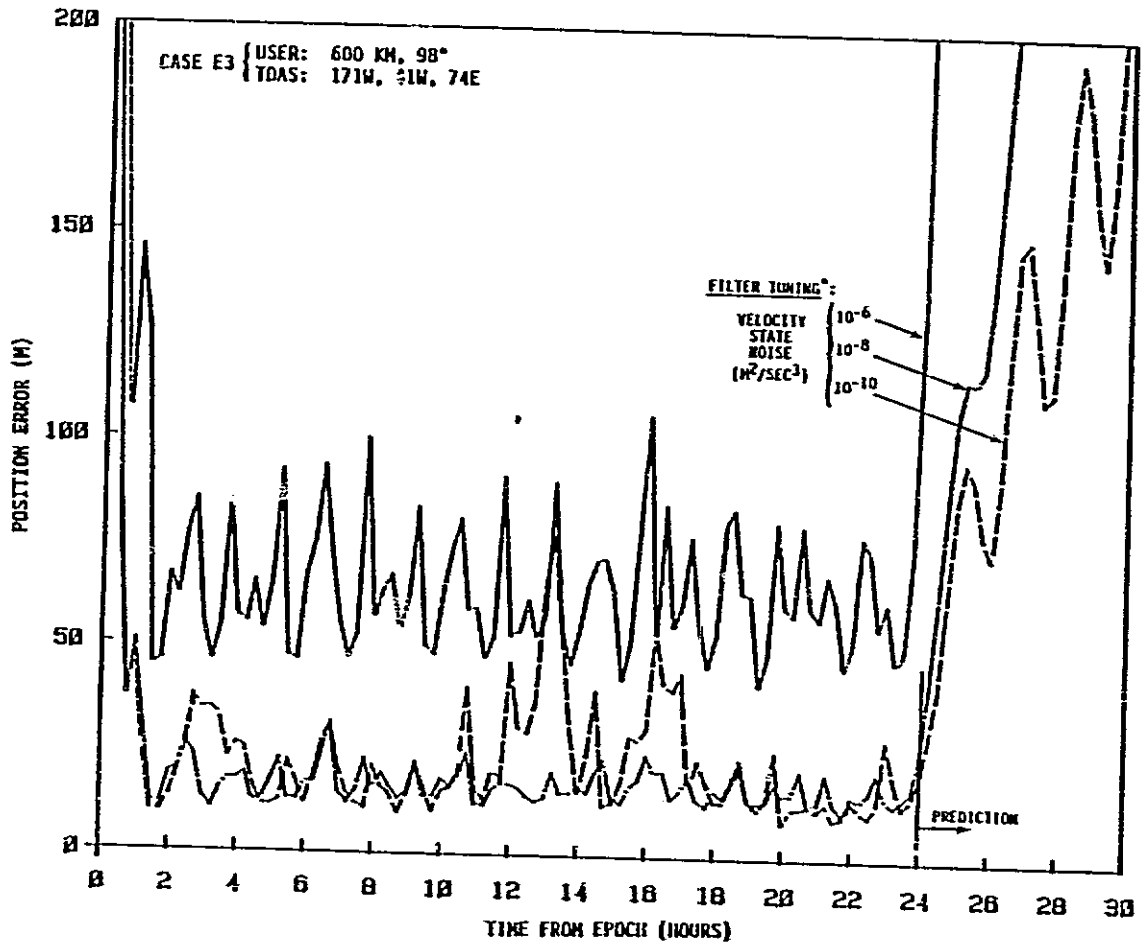

* CLOCK DRIFT STATE NOISE = 10^{-6} NSEC^2/SEC^3

STANFORD TELECOMMUNICATIONS INC.

FIGURE D-20
CASE F1 TRACKING SCHEDULES

USER ORBIT (F): 98°, 1000 KM
TDAS CONST.(1): 171°W, 41°W

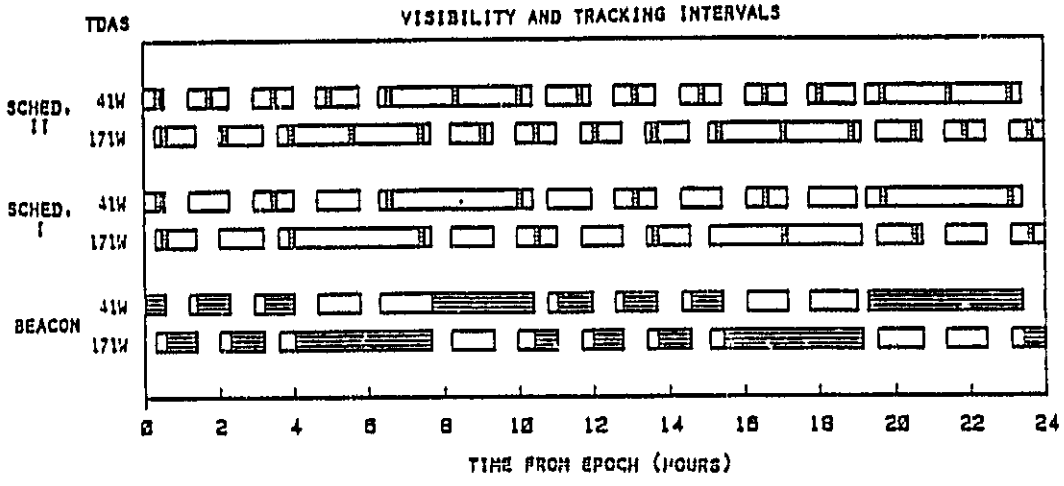

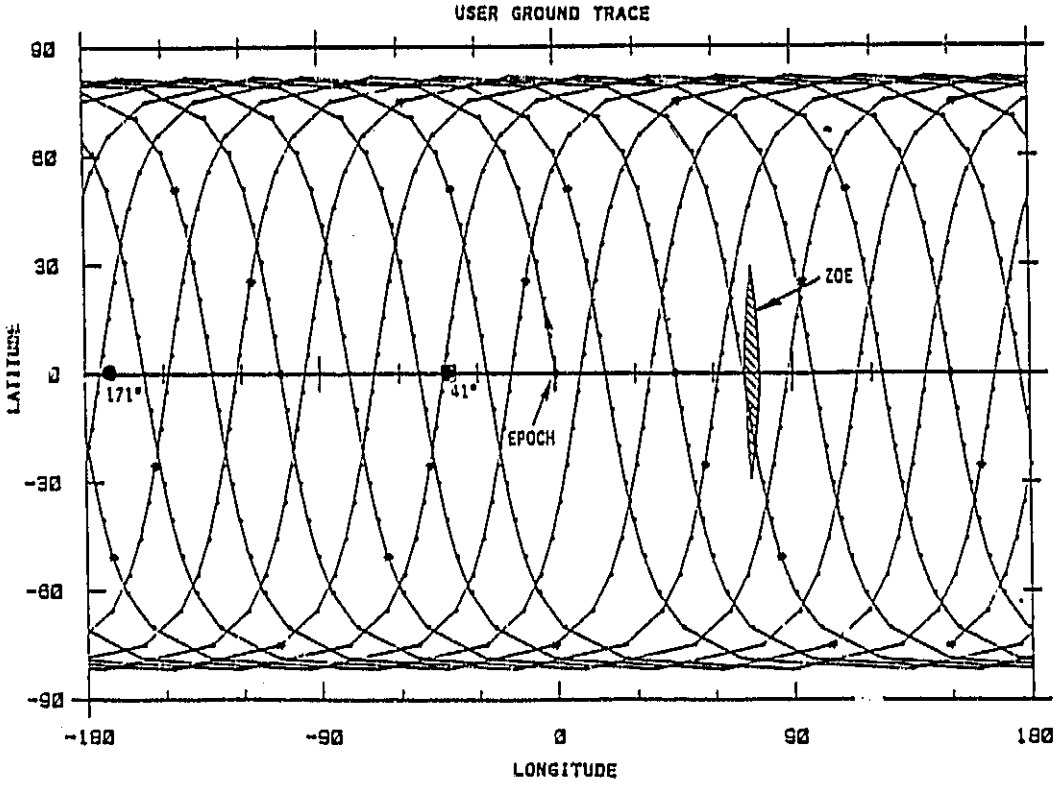

STANFORD TELECOMMUNICATIONS INC.

FIGURE D-21A

USER POSITION AND TIME ACCURACY WITH 1-WAY TDAS TRACKING - CASE F1
(SEQUENTIAL DATA PROCESSING)

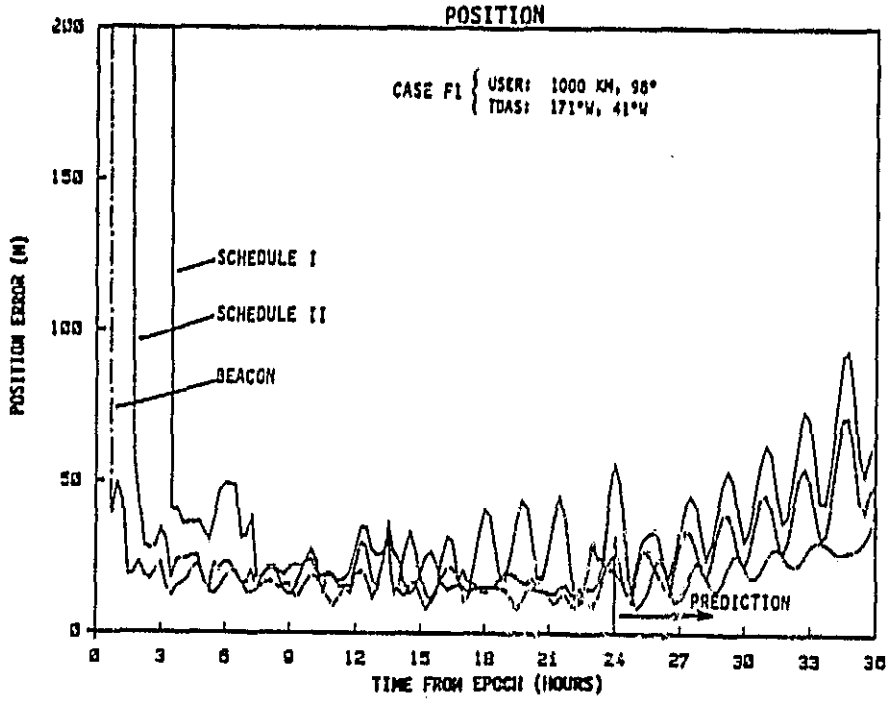

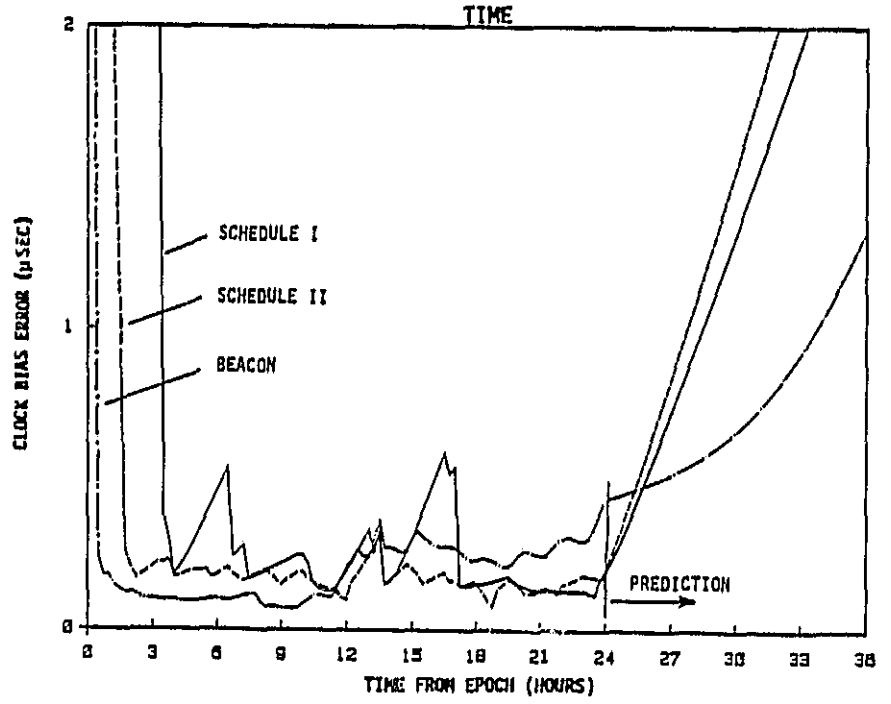

STANFORD
TELECOMMUNICATIONS INC.

FIGURE D-21
USER POSITION AND TIME ACCURACY WITH 1-WAY TDAS TRACKING - CASE F1
(SEQUENTIAL DATA PROCESSING)

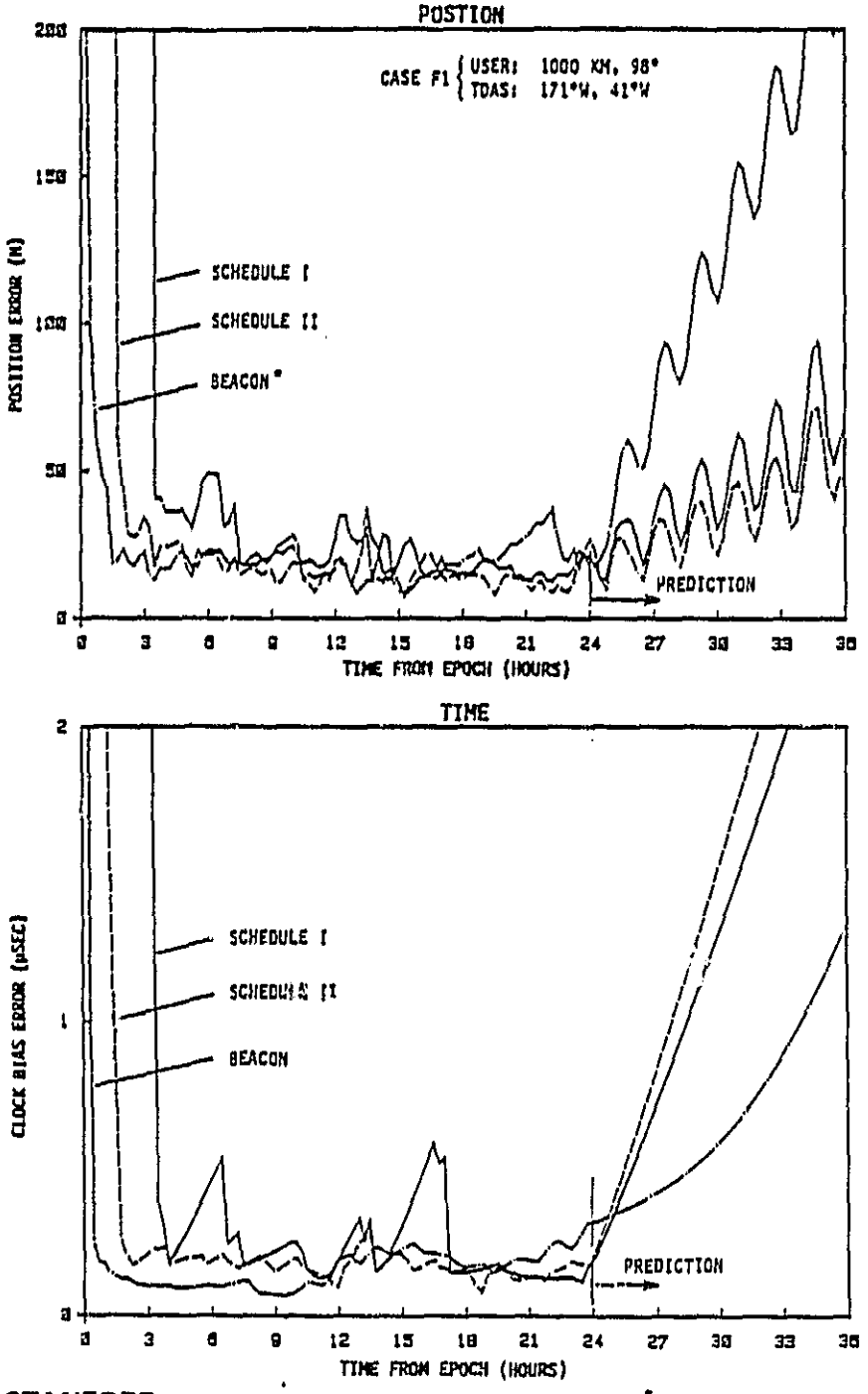

STANFORD TELECOMMUNICATIONS INC.

* MODIFIED FILTER TUNING STATE NOISE:
VELOCITY STATES: 10^{-10} m^2/sec^3

FIGURE D-22
CASE F2 TRACKING SCHEDULES

USER ORBIT (F): 98°, 1000 KM
TDAS CONST.(2): 100°W, 98°E

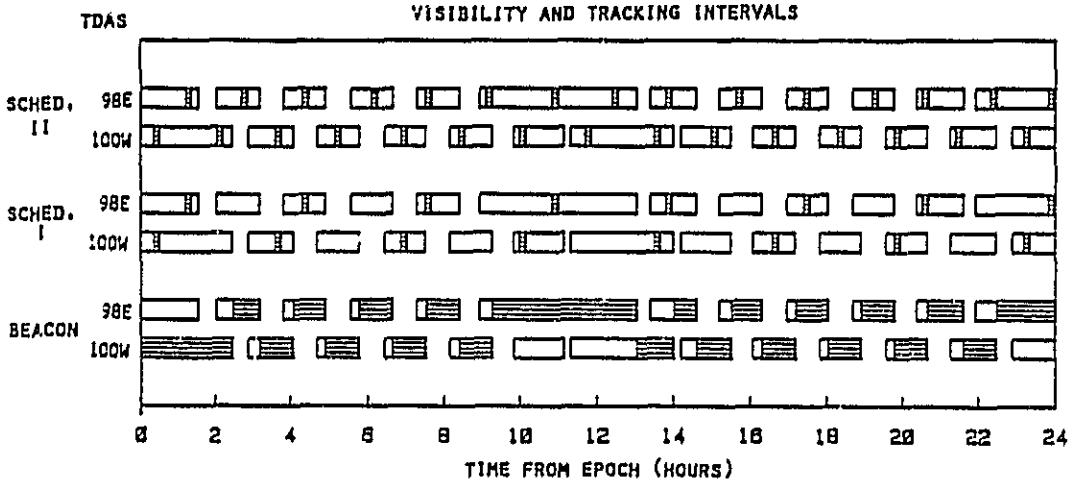

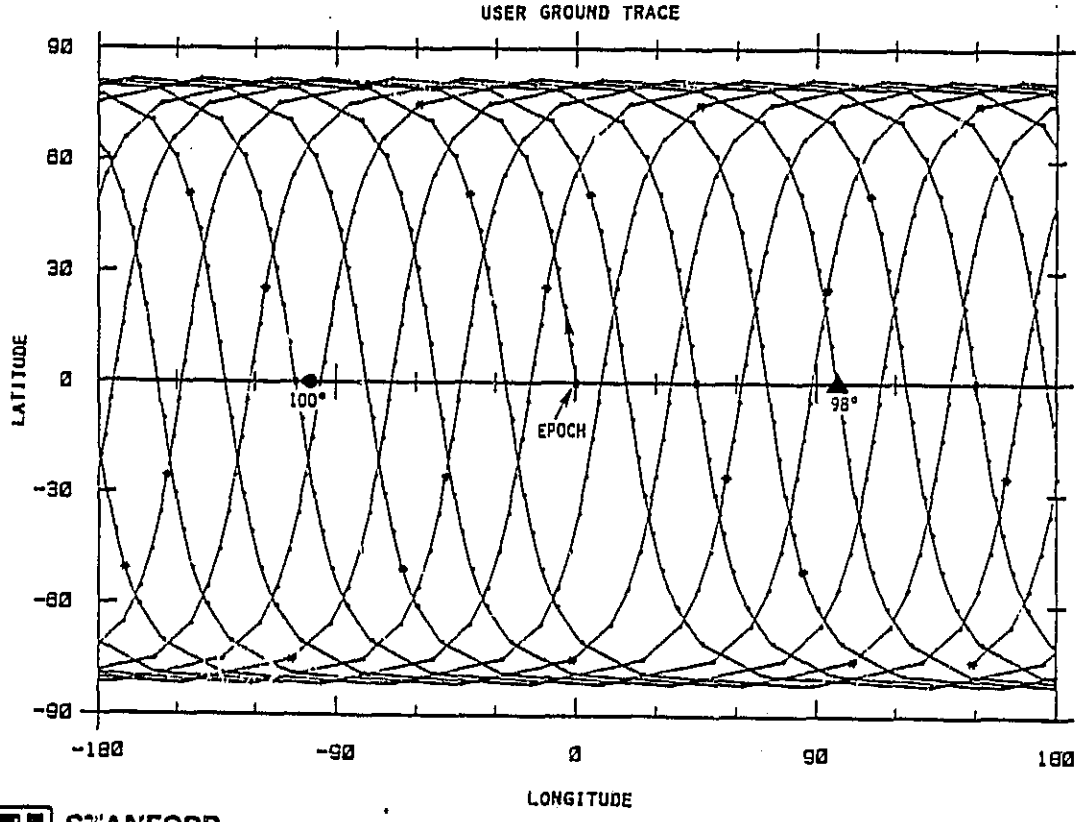

STANFORD TELECOMMUNICATIONS INC.

FIGURE D-23
USER POSITION AND TIME ACCURACY WITH 1-WAY TDAS TRACKING - CASE F2
(SEQUENTIAL DATA PROCESSING)

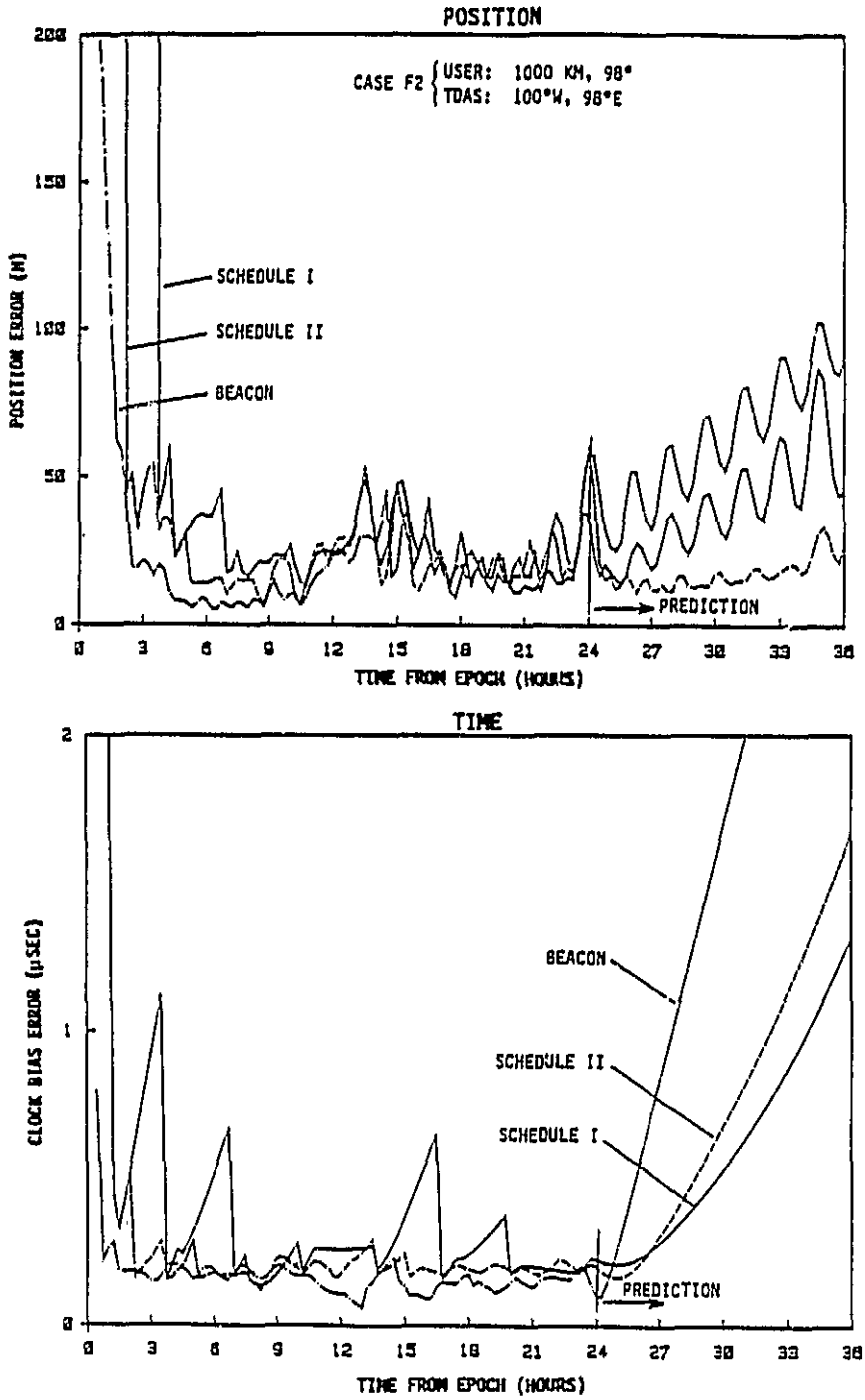

FIGURE D-24
CASE F3 TRACKING SCHEDULES

USER ORBIT (D): 98°, 1000 KM
TDAS CONST. (3): 171°W, 41°W, 74°E

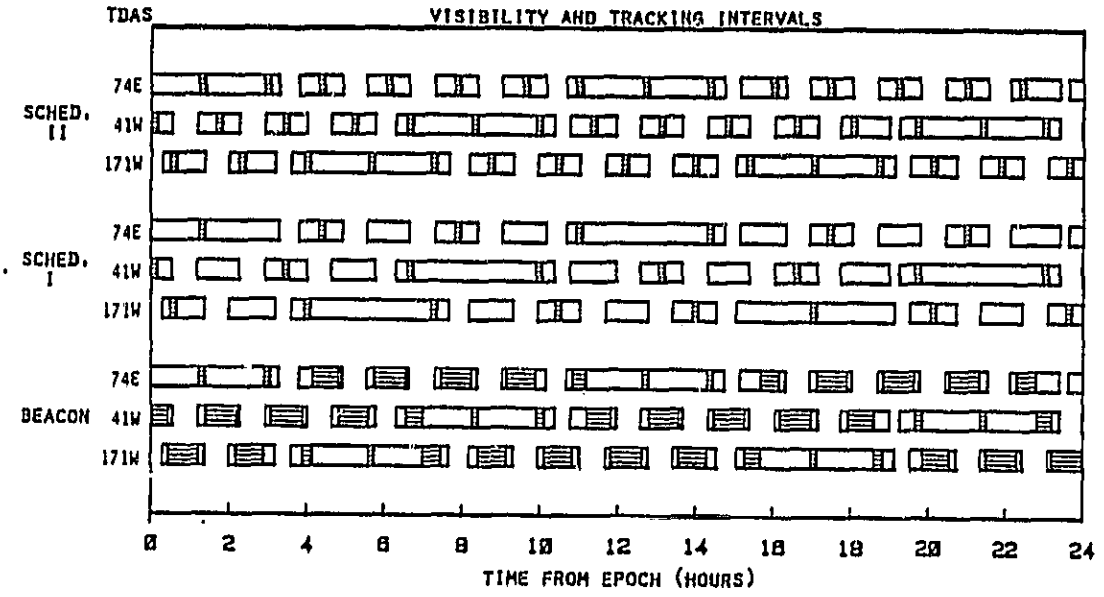

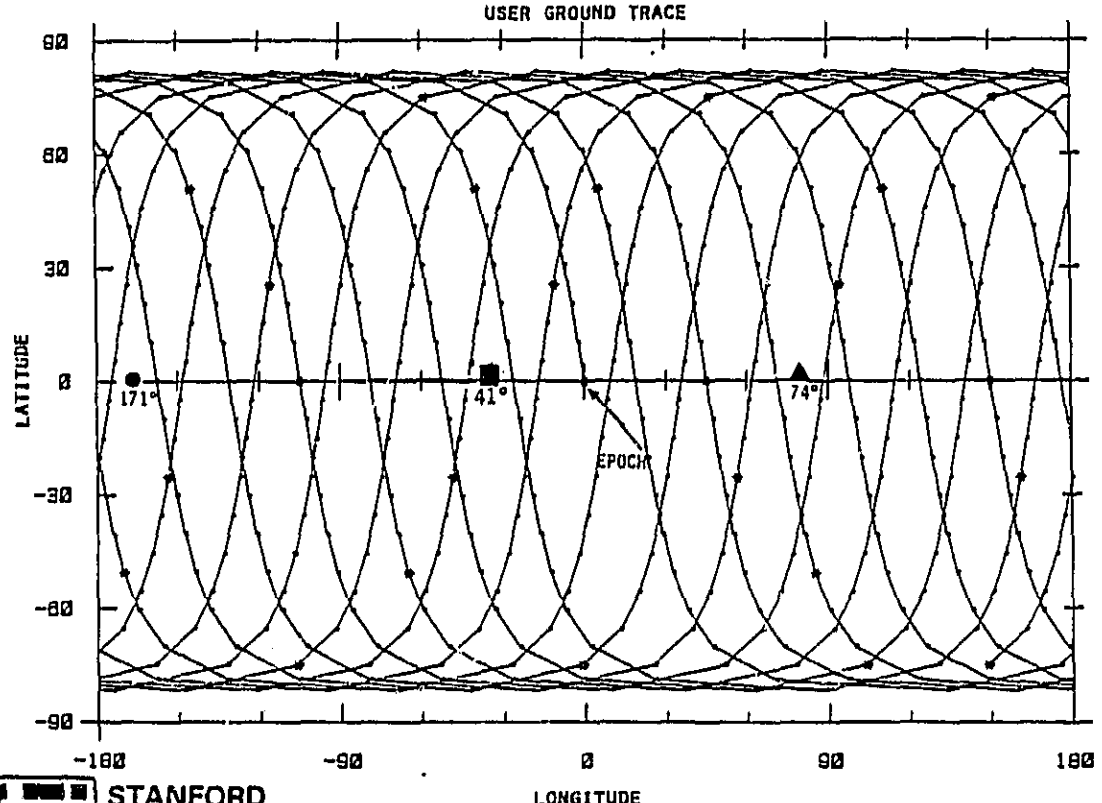

STANFORD TELECOMMUNICATIONS INC.

FIGURE D-25

USER POSITION AND TIME ACCURACY WITH 1-WAY TDAS TRACKING - CASE F3 (SEQUENTIAL DATA PROCESSING)

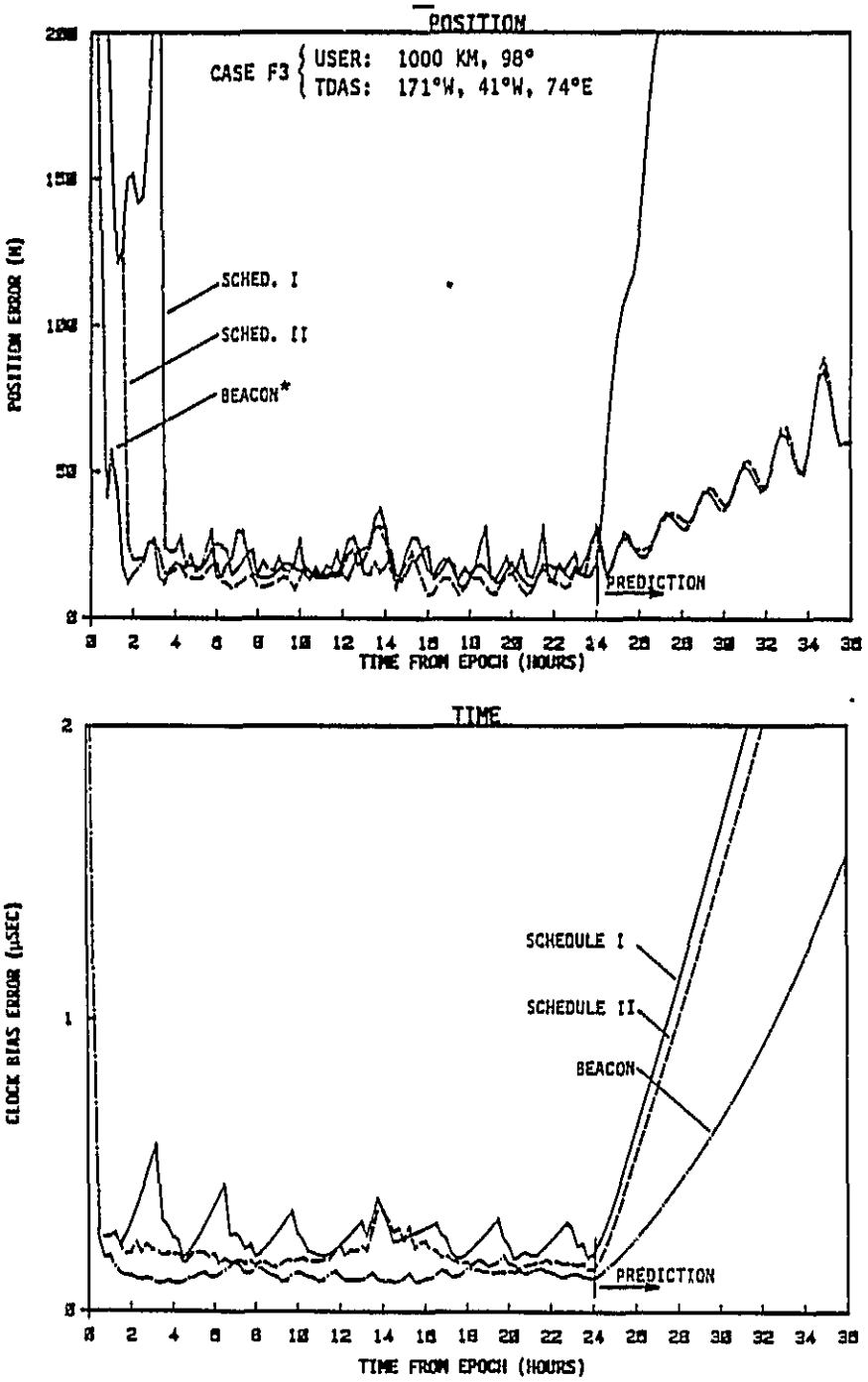

STANFORD TELECOMMUNICATIONS INC.

* MODIFIED FILTER TUNING STATE NOISE:
VELOCITY STATES: 10^{-8} m^2/sec^3

TABLE D-1
USER NAVIGATION PERFORMANCE SUMMARY - MAX POSITION ERROR (M)
(SEQUENTIAL DATA PROCESSING)

TRACKING CONFIGURATION			FLBT	FLST		RLST							
			BEACON	SCHEDULE		SCHEDULE II				SCHEDULE I			
						NAV UPLOAD RATE (HOURS)				NAV UPLOAD RATE (HOURS)			
USER ORBIT	TDAS CONST	CASE		II	I	1.5	3	6	12	1.5	3	6	12
28° 200 KM	171/41	A1	38	102	240	242	566	>1000	>1000	394	778	>1000	>1000
	100/98	A2	29	82	278	153	430	>1000	>1000	334	692	>1000	>1000
	171/41/74E	A3	20	44	177	150	419	>1000	>1000	232	547	>1000	>1000
97° 200 KM	171/41	D1	64	117	290	207	449	>1000	>1000	327	607	>1000	>1000
	100/98	D2	116	128	396	260	475	>1000	>1000	408	735	>1000	>1000
	171/41/74E	D3	31	71	248	209	427	>1000	>1000	265	532	>1000	>1000
98° 600 KM	171/41	E1	42	44	47	44	47	75	135	53	53	59	113
	100/98	E2	41	48	47	47	50	65	126	53	53	59	117
	171/41/74E	E3	31	55	44	38	59	90	161	48	48	69	136
98° 1000 KM	171/41	F1	38	31	37	27	29	39	71	33	34	54	92
	100/98	F2	45	54	49	61	61	61	61	37	38	39	87
	171/41/74E	F3	31	32	38	27	32	44	89	29	34	44	85

TABLE D-2: DOMINANT ERROR CONTRIBUTORS* TO USER POSITION ERROR (SEQUENTIAL DATA PROCESSING)

TRACKING CONFIGURATION			HIBT	FLST		RLST							
			BEACON	SCHEDULE		SCHEDULE II				SCHEDULE I			
						NAV UPLOAD RATE (HOURS)				NAV UPLOAD RATE (HOURS)			
USER ORBIT	TDAS CONST	CASE		II	I	1.5	3	6	12	1.5	3	6	12
28° 200 KM	171/41	A1	N,D	D,N	N,D	D,N	D	D	D	D,N	D	D	D
	100/98	A2	N,D,H	"	"	"	"	"	"	"	"	"	"
	171/41/74E	A3	N	"	"	"	"	"	"	"	"	"	"
97° 200 KM	171/41	D1	H,N,D,E	N,D,E,H	N,D,H	D,N,H	D,N,H	D	D	D,N,H	D,N,H	D	D
	100/98	D2	H,N,E,D	N,D	"	H,D,N	D,H,N	"	"	D,N	D,H	"	"
	171/41/74E	D3	H,N,E	N,D	D,N	"	"	"	"	"	"	"	"
98° 600 KM	171/41	E1	H	H	H	H	H	H	H	H	H	H	H
	100/98	E2	"	"	"	"	"	"	"	"	"	"	"
	171/41/74E	E3	N,H,E+	"	"	"	"	"	"	"	"	"	"
98° 1000 KM	171/41	F1	H,N	H	H	H	H,E	H	H	H,N	H,E	H	H
	100/98	F2	E,H	"	"	"	H	"	"	"	"	H,N	"
	171/41/74E	F3	N,H,E+	"	"	"	"	"	"	H	H	H	H

* ERROR CONTRIBUTORS ARE ARRANGED IN DECREASING ORDER UNTIL REMAINING CONTRIBUTORS ARE <50% OF LAST ENTRY: N = NOISE, D = DRAG, H = GRAV. HARMONICS, E = TDAS EPHEMERIS.

+ FILTER TUNING STATE NOISE MODIFIED (FROM VALUES IN TABLE 5-2): VELOCITY STATES: 10^{-8} m^2/sec^3.

TABLE D-3
USER NAVIGATION PERFORMANCE SUMMARY - MAX CLOCK ERROR (NSEC)
(SEQUENTIAL DATA PROCESSING)

TRACKING CONFIGURATION			FLBT	FLST		RLST							
			BEACON	SCHEDULE		SCHEDULE II				SCHEDULE I			
						NAV UPLOAD RATE (HOURS)				NAV UPLOAD RATE (HOURS)			
USER ORBIT	TDAS CONST	CASE		II	I	1.5	3	6	12	1.5	3	6	12
28° 200 KM	171/41	A1	125	360	690	555	865	1520	3020	870	1270	2100	3910
	100/98	A2	95	260	565	440	750	1405	2890	620	960	1685	3290
	171/41/74E	A3	140	265	565	455	760	1405	2870	525	825	1465	2935
97° 200 KM	171/41	D1	160	290	500	820	1320	2350	4525	520	755	1280	2540
	100/98	D2	90	250	410	325	525	975	2100	455	700	1240	2535
	171/41/74E	D3	120	445	825	435	730	1345	2760	455	685	1180	2375
98° 600 KM	171/41	E1	230	165	230	750	1300	2340	4150	580	810	1280	2285
	100/98	E2	115	210	250	230	245	560	1315	235	340	560	1275
	171/41/74E	E3	155	330	275	215	400	935	2035	300	425	750	1580
98° 1000 KM	171/41	F1	260	325	460	505	835	1300	2655	440	720	1165	2275
	100/98	F2	230	295	270	200	300	670	1675	230	280	530	1120
	171/41/74E	F3	170	345	390	415	760	1300	2725	495	865	1445	2955

TABLE D-4: DOMINANT ERROR CONTRIBUTORS* TO USER CLOCK ERROR
(SEQUENTIAL DATA PROCESSING)

TRACKING CONFIGURATION			FLBT	FLST		RLST							
			BEACON	SCHEDULE		SCHEDULE II				SCHEDULE I			
						NAV UPLOAD RATE (HOURS)				NAV UPLOAD RATE (HOURS)			
USER ORBIT	TDAS CONST	CASE		II	I	1	3	6	12	1	3	6	12
28° 200 KM	171/41	A1	N,E	N	N	N	N	N	N,O	N,D	N,D	N,D	N,D,O
	100/98	A2	N	E,N	"	"	"	"	"	N,E	N	N	N,O
	171/41/74E	A3	E,N	N	"	"	"	"	"	N	"	"	N,O,D,H
97° 200 KM	171/41	D1	N,E	N	N,H	N,H	N,H	N,H,D	N,H,D,O	N	N	N	N,O
	100/98	D2	N	N,H,E,D	N	N,E	N,E	N,E	N,O,E	"	"	"	N,O,H,E
	171/41/74E	D3	N,E,H	N	H,N	N,H	N,H	N,H,O	N,H,O	"	"	"	H,O
98° 600 KM	171/41	E1	E,H	N	N	N,E	H,N	H	H	N,E	H,N	H,N,O,E	H,O,N,E
	100/98	E2	E,N,H	N,H	N,H	N,H,E	N,H	H,N,O,E	H,O,N,E	N,H,E	N,O,E	N,O	O,N
	171/41/74E	E3	"	H,N,E	N,E	N	H,N	H	H,O	N	N	N,H,O	O,H,N
98° 1000 KM	171/41	F1	E	H,E	N,H,E	E,H	H	H	H	H,E,N	H,N,E	H,N,E	E,N,O,E
	100/98	F2	"	H,E	E,N,H	E	"	"	H,O,E	N	H	H	H,O
	171/41/74E	F3	E,N	H,E,N	H,N,E	H,N	H,N	"	H	H,N	H,N	"	H

* ERROR CONTRIBUTORS ARE ARRANGED IN DECREASING ORDER UNTIL REMAINING CONTRIBUTORS ARE <50% OF PRECEDING ENTRY: N = NOISE, D = DRAG, H = GRAV. HARMONICS, E = TDAS EPHEMERIS, O = USER OSCILLATOR DRIFT.

STANFORD TELECOMMUNICATIONS INC.

APPENDIX E

USER NAVIGATION PERFORMANCE RESULTS - SLIDING BATCH DATA PROCESSING

TDAS user navigation performance was evaluated for two of the one-way tracking alternatives (FLST and RLST) assuming sliding batch processing of tracking data. The error modeling approach and major findings were discussed in Section 5; this section presents further details of the results obtained.

Cases for evaluation were selected from among the TDAS constellation options and user orbit types defined in Figures 5-1 and 5-2. The results that follow cover half of the cases presented in Appendix D for sequential processing — the same user orbits types (A,D,E,F) and two of the TDAS satellite constellation options (1,2).

For each case considered, two types of user position and time accuracy profiles were generated:

- Single Batch Profiles - These were computed to assess the sensitivity of user OD/TD accuracy in the prediction mode to tracking interval selection. Durations of 6, 12, 18, and 24 hours were evaluated for each tracking schedule (I and II).* Figures E-1 and E-2 are examples. The tracking interval yielding the lowest peak error in the first 6 hours from end-of-tracking was selected for generating sliding batch profiles in each case.

* Schedules I and II for a 24 hour tracking interval are identical to those given in Appendix D for corresponding cases. Scheduled contacts for shorter tracking intervals were simply deleted.

- Sliding Batch Profiles - These are comprised of prediction interval segments corresponding to a sequence of single batch solutions, as defined earlier in Figure 5-4. Twenty-four hour profiles were constructed based on a batch interval (P) of 3 hours and a computation/data handling interval (C) of 1.5 hours. Figure E-3 for Case A1 is an example.*

Summary tables (E-1 thru E-4) included at the end of Appendix E record the peak errors and identify the major error contributors for each tracking alternative.

* The time-from-epoch scale on all plots has the same interpretation as in Appendix D, i.e., the time elapsed since the user's initial location, (0°N, 0°E). Individual batch epochs were adjusted backward or forward depending on tracking interval in order to fit a given prediction segment slot.

FIGURE E-1
USER POSITION AND TIME ACCURACY WITH 1-WAY TRACKING - CASE A2
(BATCH PROCESSING - TRACKING SCHEDULE I)

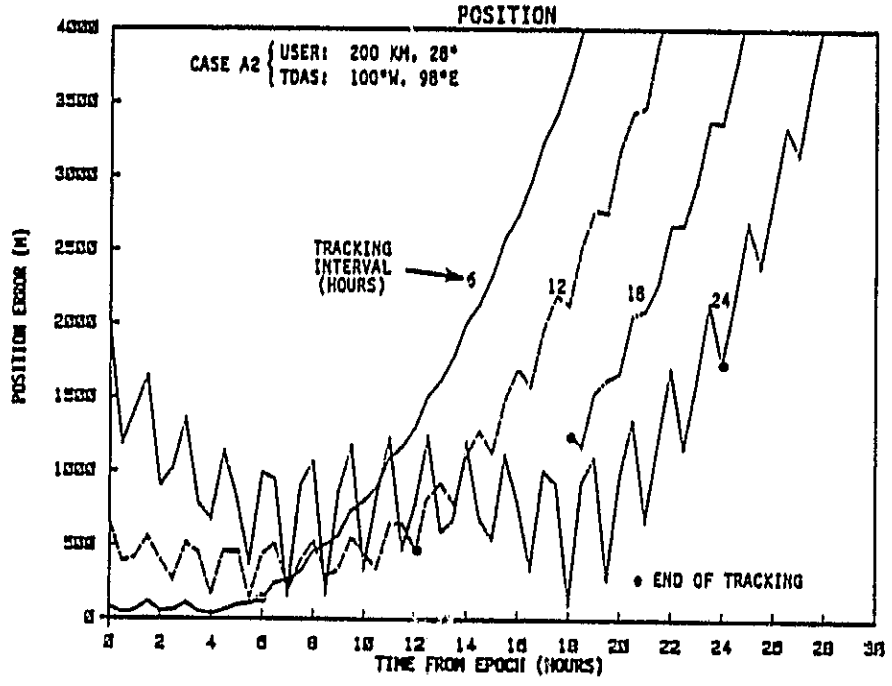

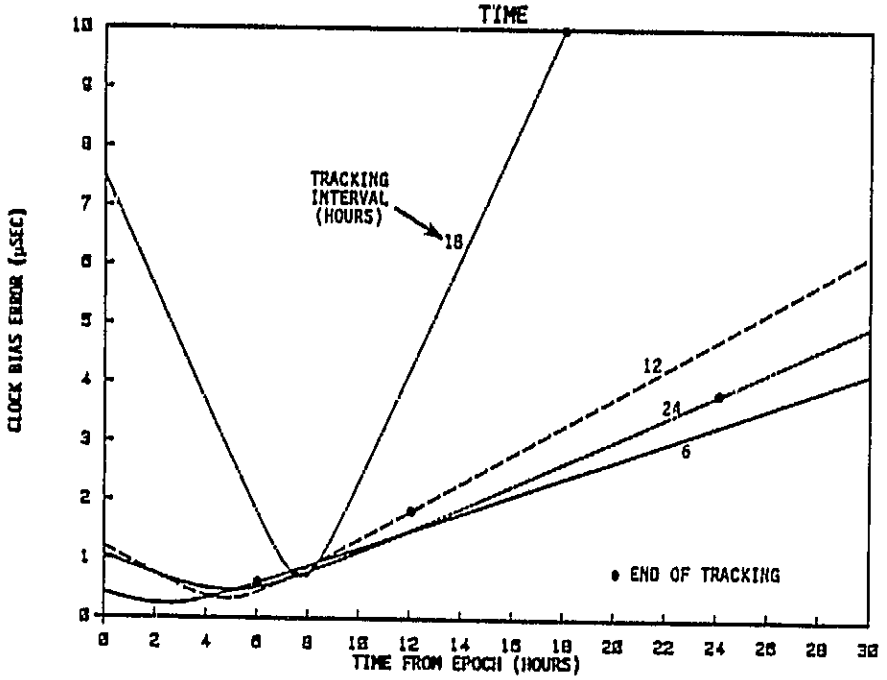

STANFORD TELECOMMUNICATIONS INC.

FIGURE E-2

USER POSITION AND TIME ACCURACY WITH 1-WAY TRACKING - CASE A2
(BATCH PROCESSING - TRACKING SCHEDULE II)

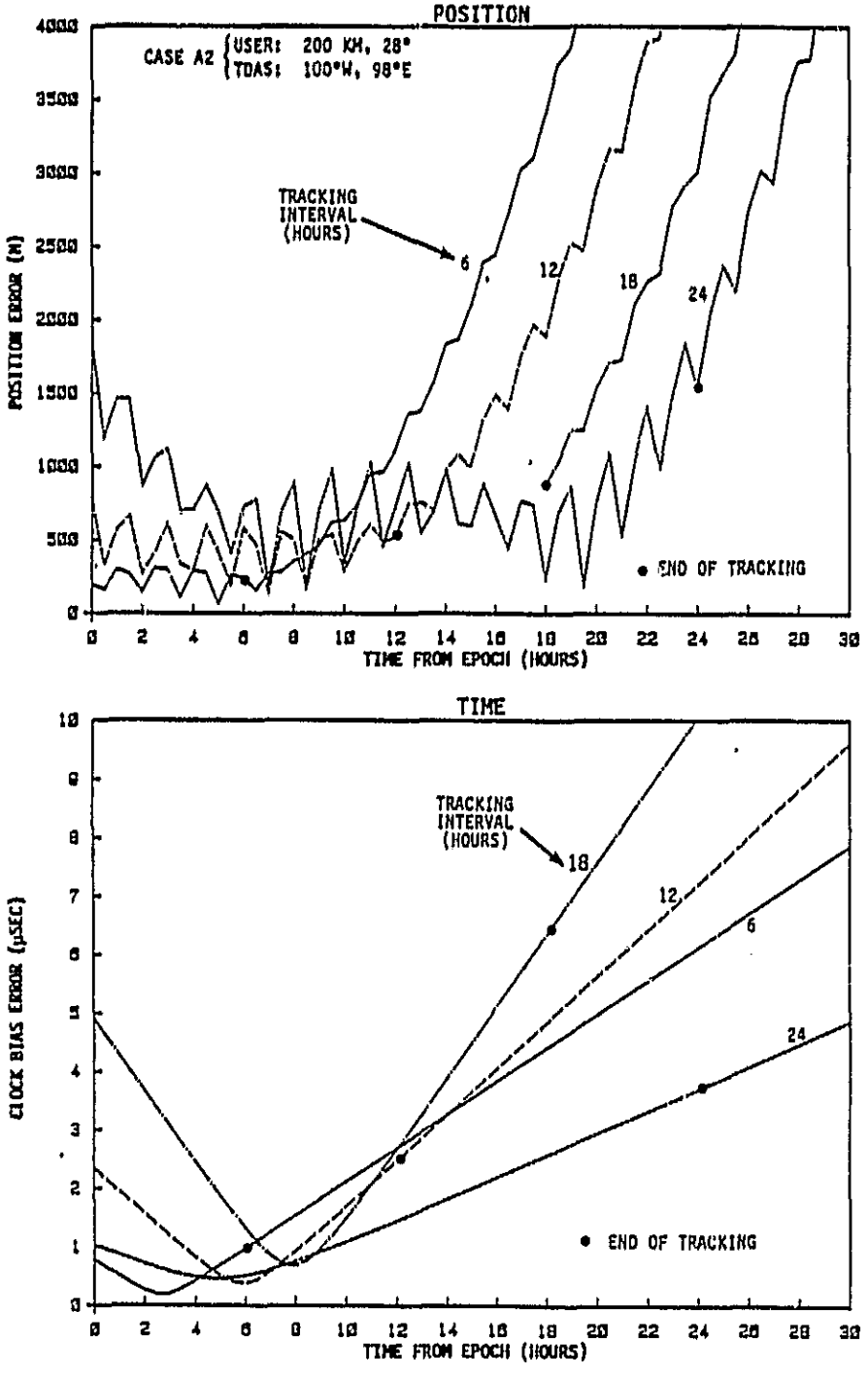

STANFORD TELECOMMUNICATIONS INC.

FIGURE E-3

USER POSITION AND TIME ACCURACY WITH 1-WAY TDAS TRACKING - CASE A2
(SLIDING BATCH DATA PROCESSING - 6 HR TRACKING INTERVAL)

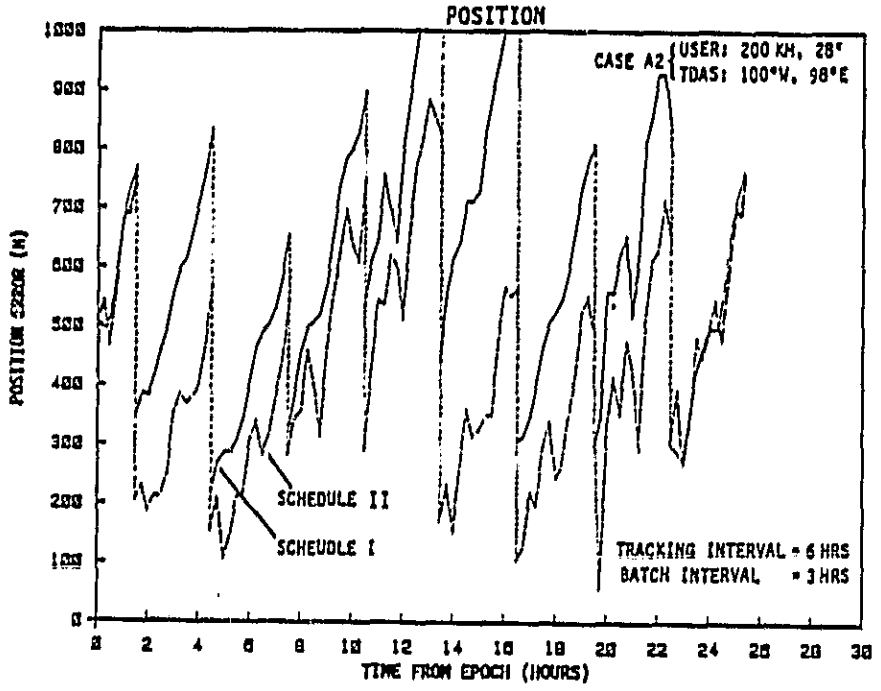

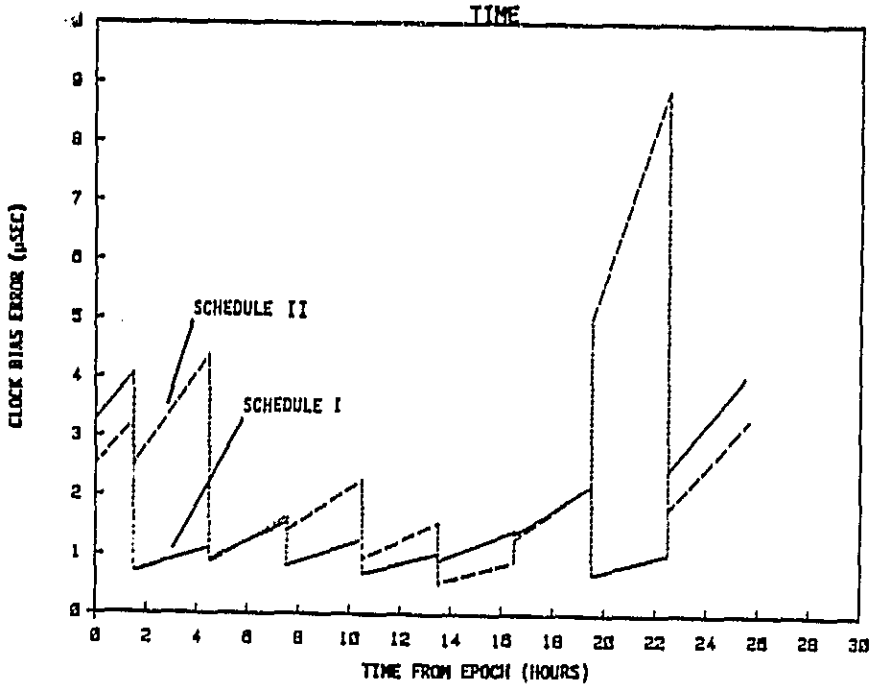

STANFORD
TELECOMMUNICATIONS INC.

FIGURE E-4

USER POSITION AND TIME ACCURACY WITH 1-WAY TDAS TRACKING - CASE D1
(BATCH PROCESSING - TRACKING SCHEDULE I)

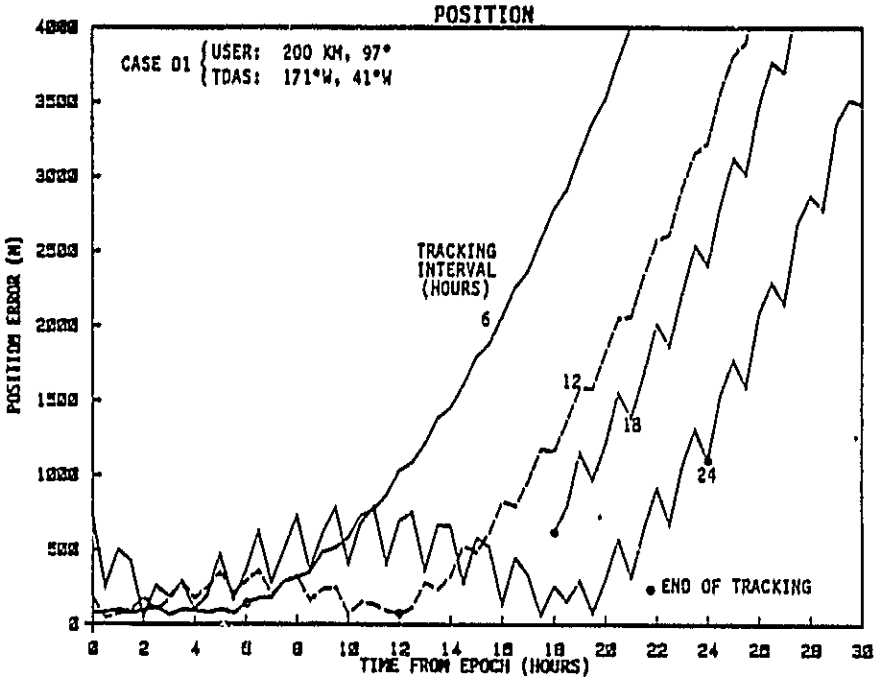

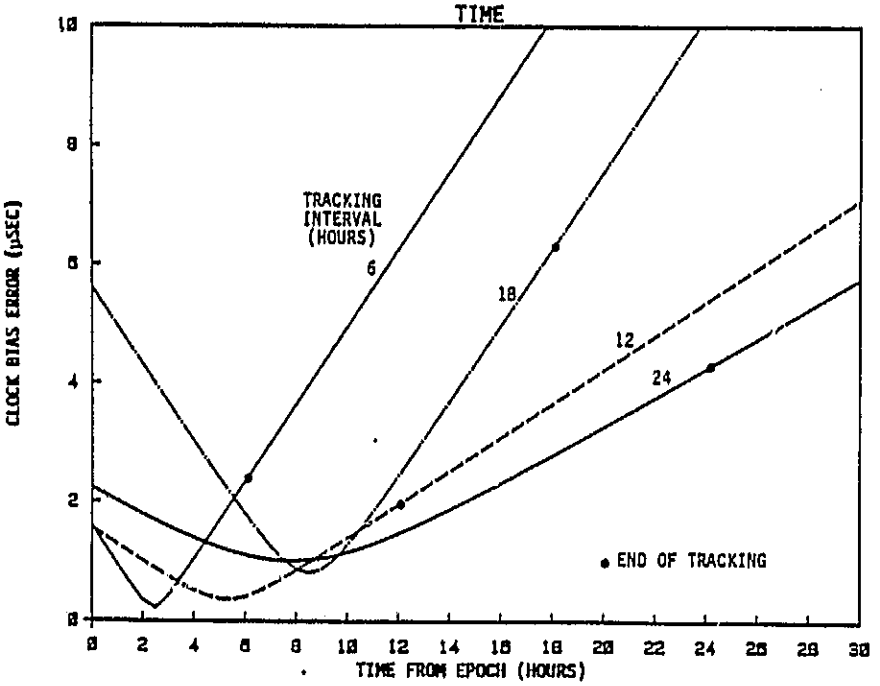

FIGURE E-5

USER POSITION AND TIME ACCURACY WITH 1-WAY TDAS TRACKING - CASE D1
(BATCH PROCESSING - TRACKING SCHEDULE I)

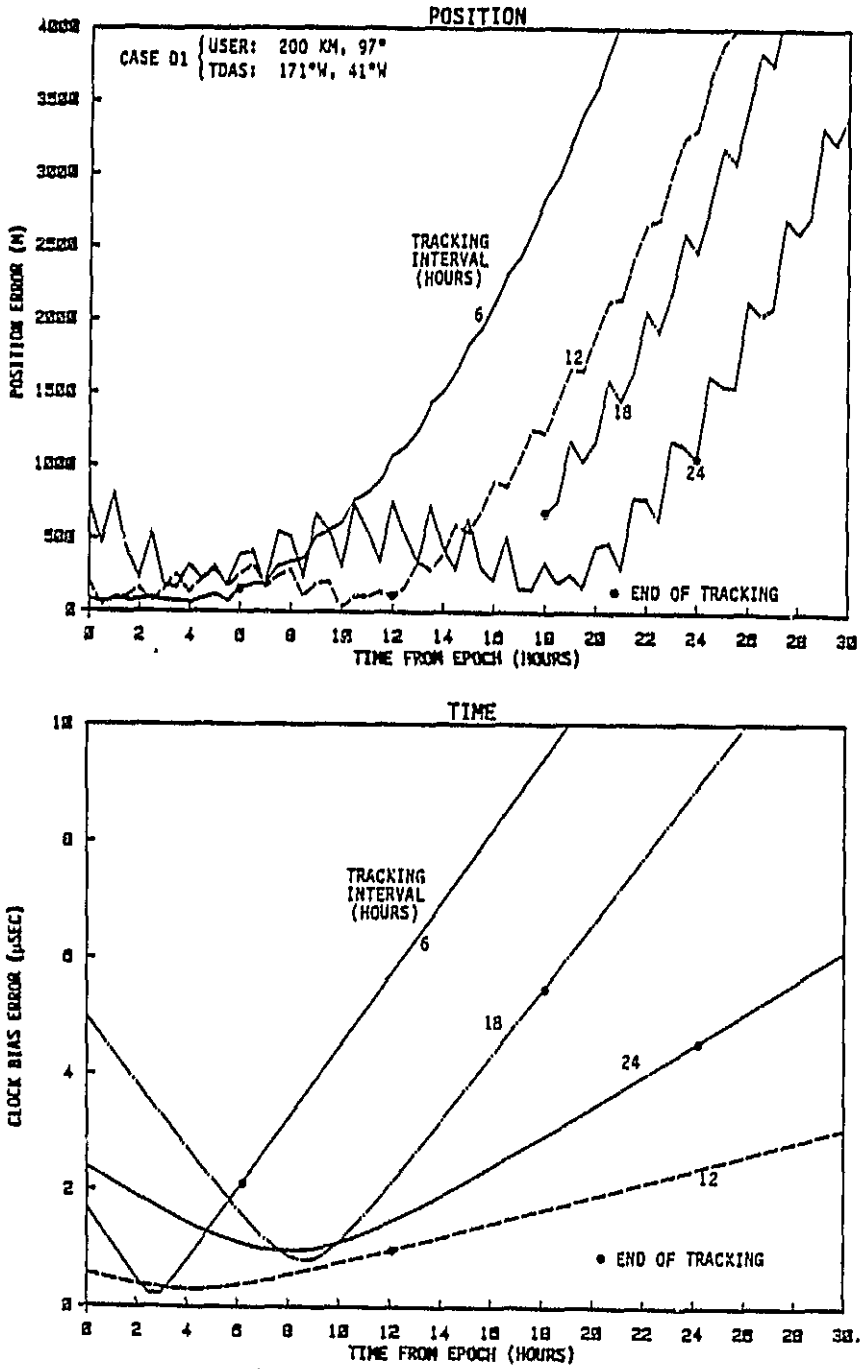

FIGURE E-6

USER POSITION AND TIME ACCURACY WITH 1-WAY TDAS TRACKING - CASE D1
(SLIDING BATCH PROCESSING - 6 HR TRACKING INTERVAL)

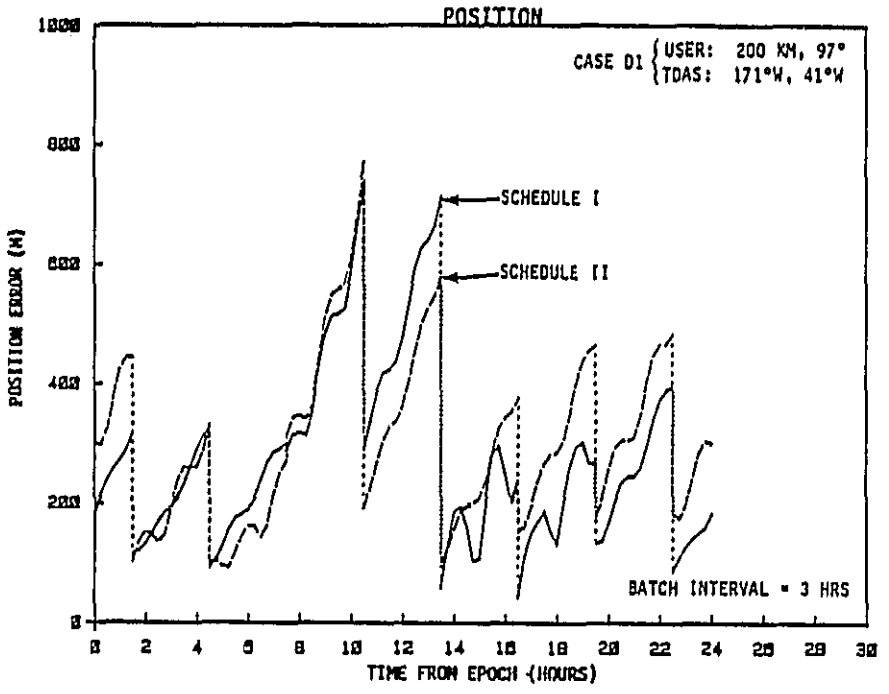

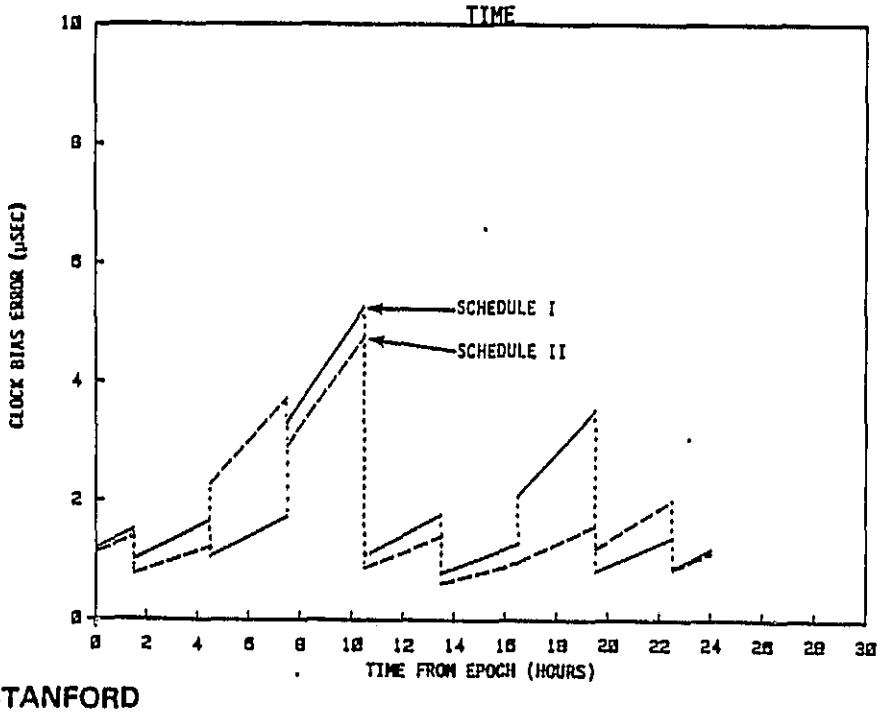

FIGURE E-7

USER POSITION AND TIME ACCURACY WITH 1-WAY TDAS TRACKING - CASE D2
(BATCH PROCESSING - TRACKING SCHEDULE I)

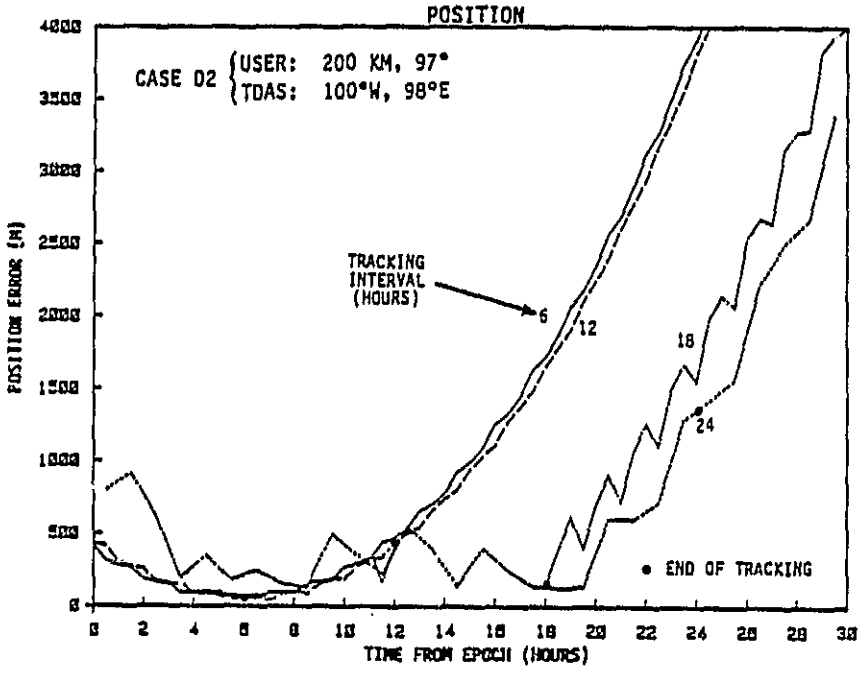

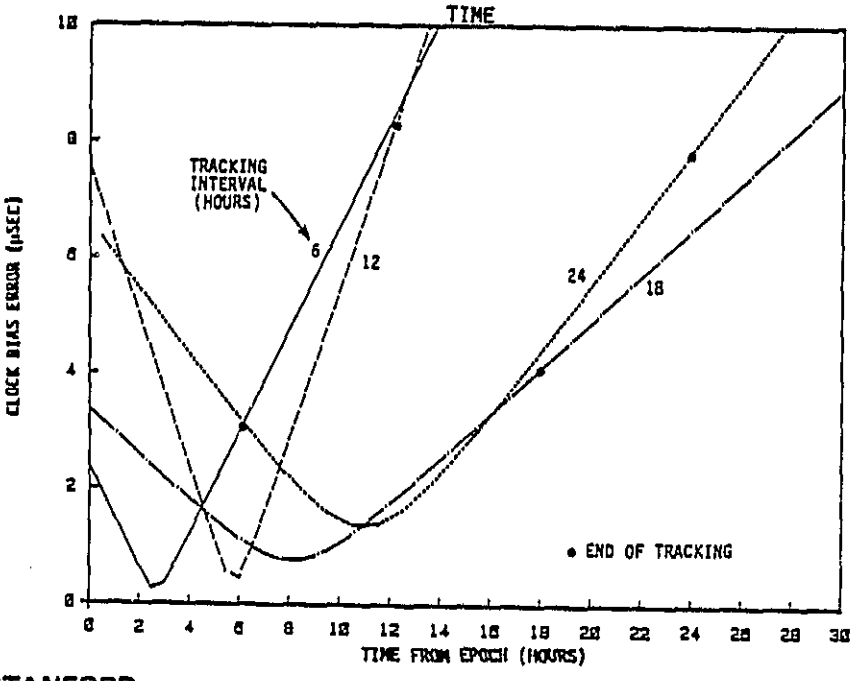

STANFORD TELECOMMUNICATIONS INC.

FIGURE E-8

USER POSITION AND TIME ACCURACY WITH 1-WAY TDAS TRACKING - CASE D2
(BATCH PROCESSING - TRACKING SCHEDULE II)

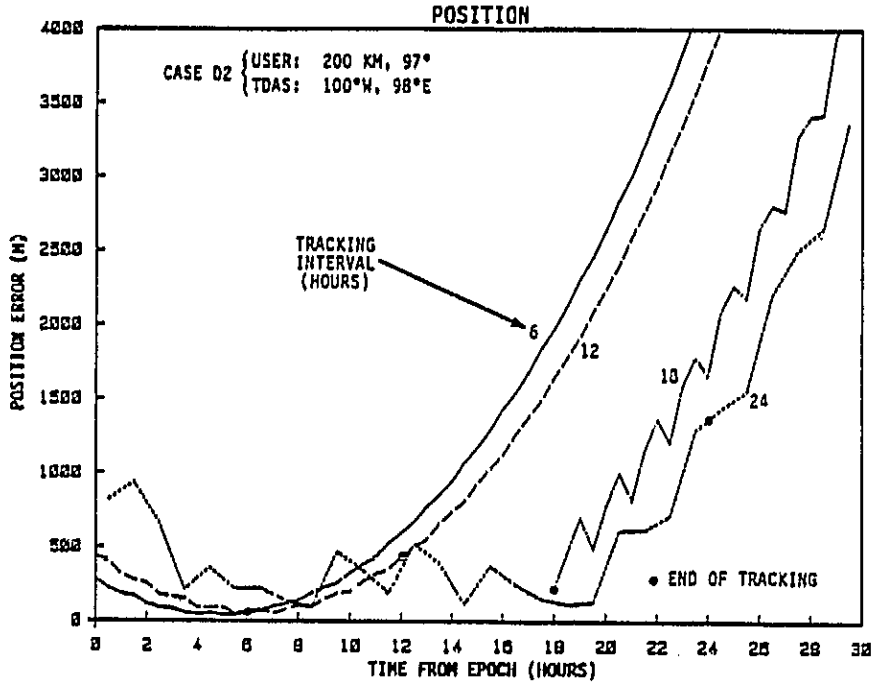

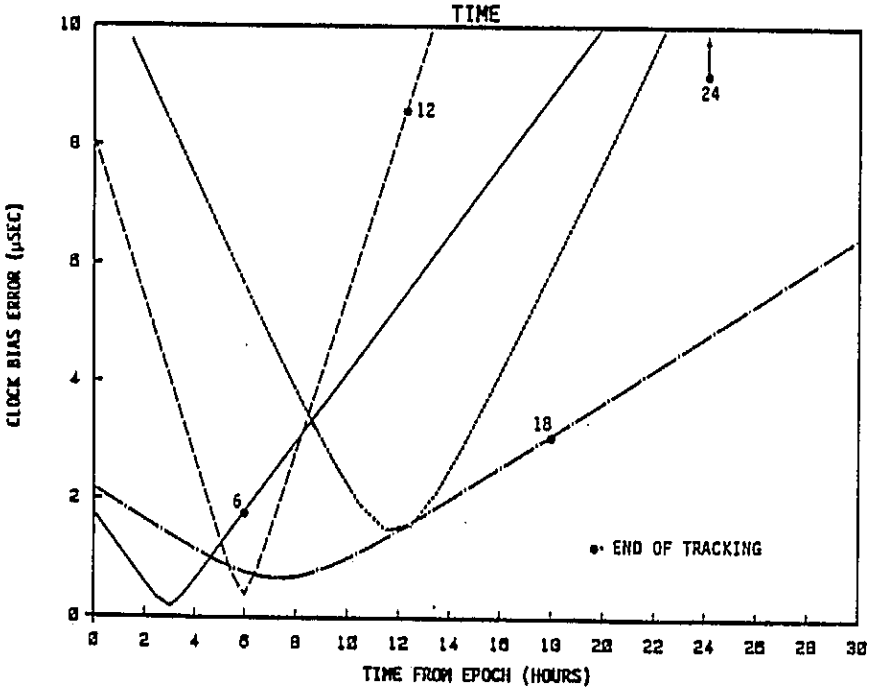

STANFORD TELECOMMUNICATIONS INC.

FIGURE E-9

USER POSITION AND TIME ACCURACY WITH 1-WAY TDAS TRACKING - CASE D2
(SLIDING BATCH DATA PROCESSING - 6 HR TRACKING INTERVAL)

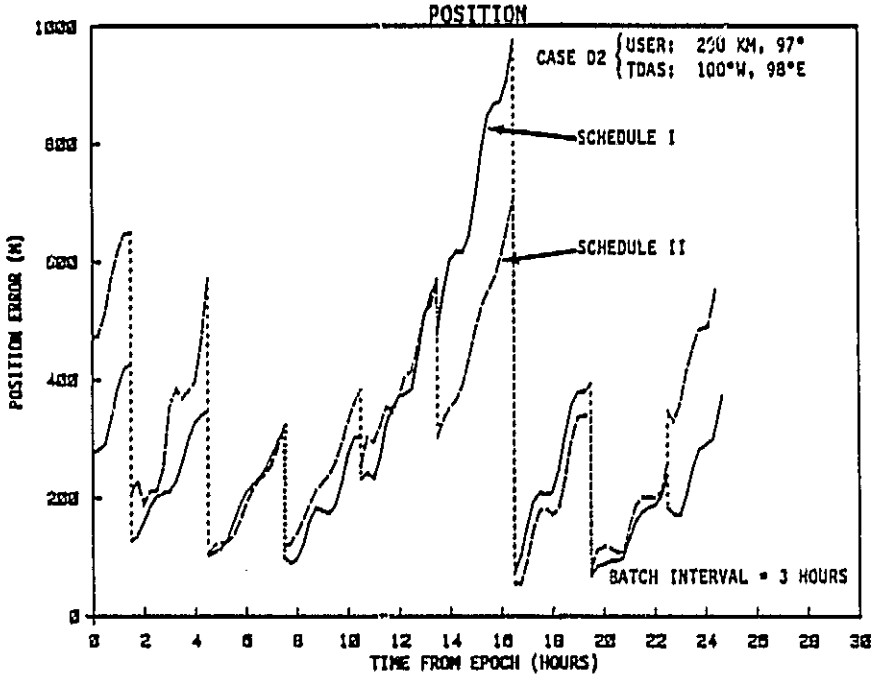

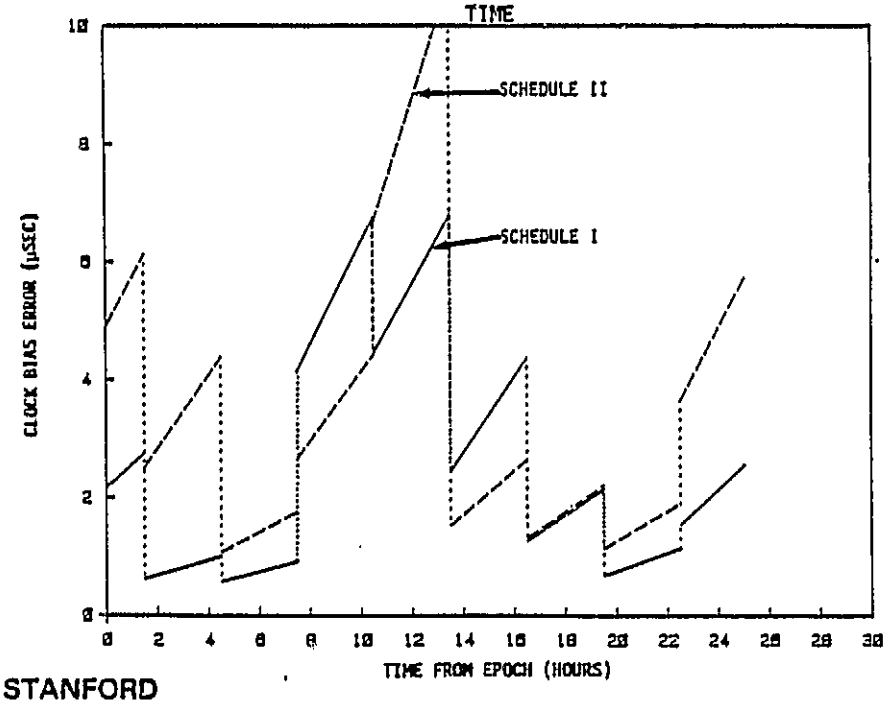

STANFORD
TELECOMMUNICATIONS INC.

FIGURE E-10

USER POSITION AND TIME ACCURACY WITH 1-WAY TRACKING - CASE E1
(BATCH PROCESSING - TRACKING SCHEDULE I)

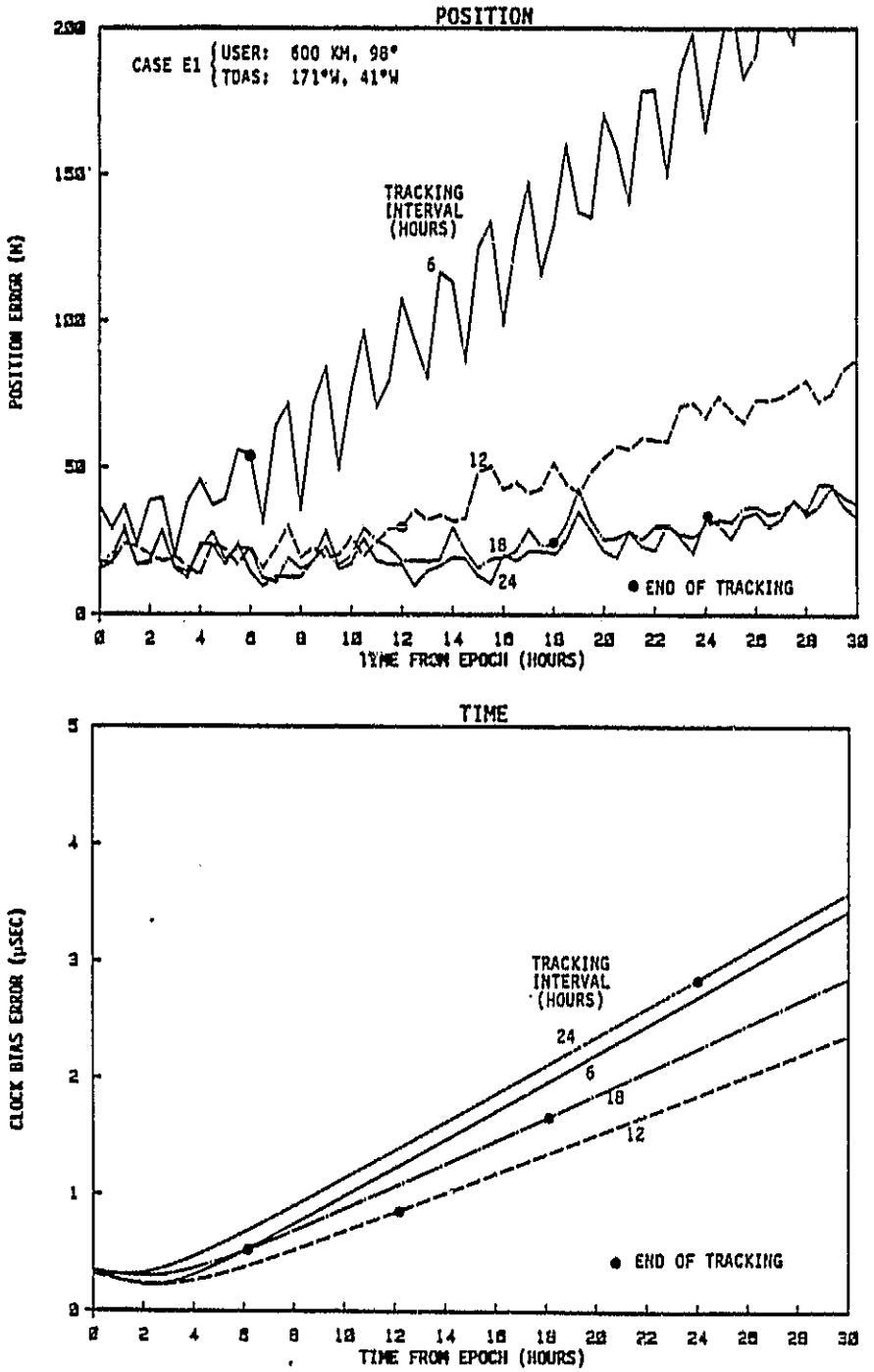

STANFORD TELECOMMUNICATIONS INC.

FIGURE E-11

USER POSITION AND TIME ACCURACY WITH 1-WAY TDAS TRACKING - CASE E1
(BATCH PROCESSING - TRACKING SCHEDULE II)

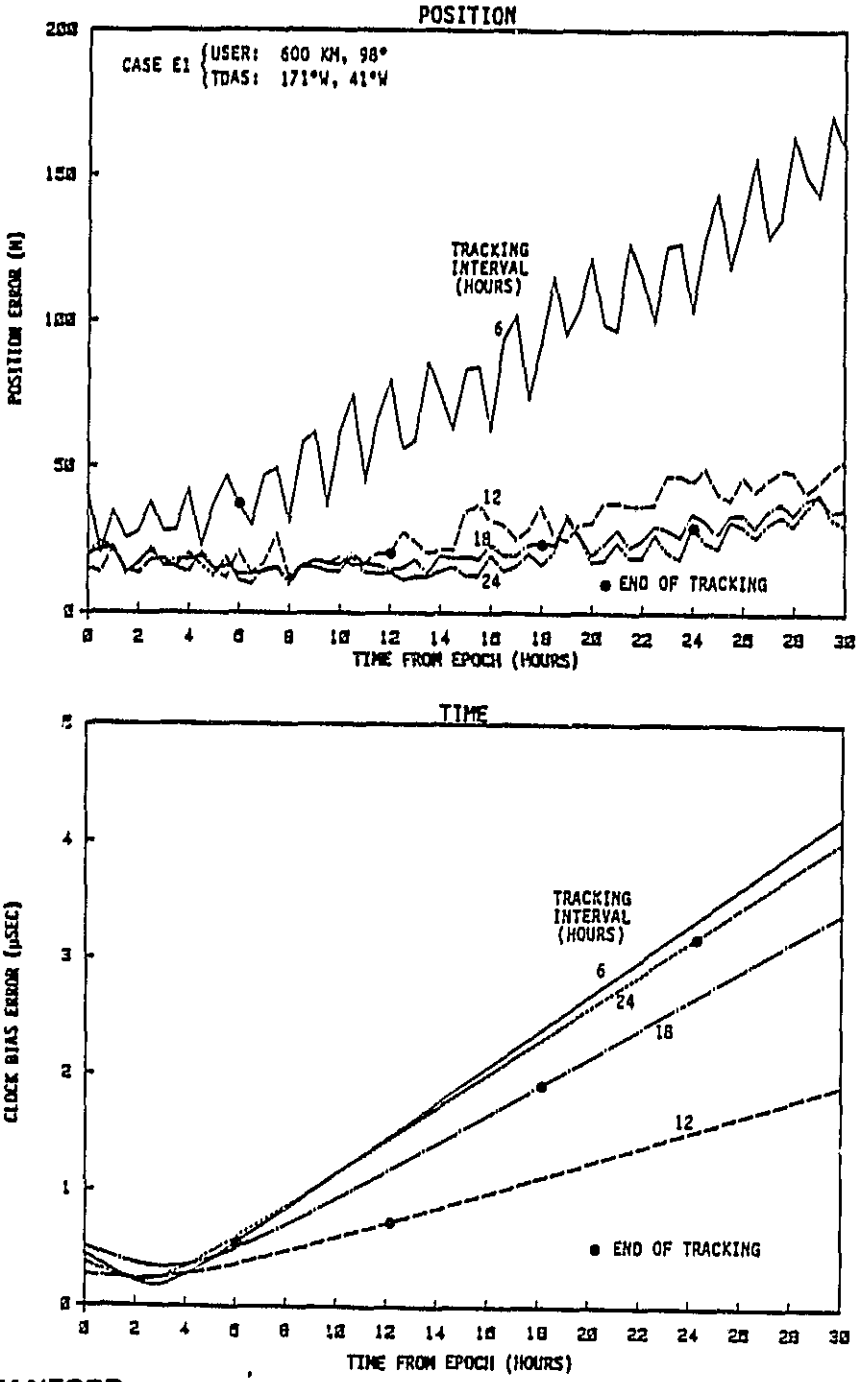

STANFORD TELECOMMUNICATIONS INC.

FIGURE E-12

USER POSITION AND TIME ACCURACY WITH 1-WAY TDAS TRACKING - CASE E1
(SLIDING BATCH PROCESSING - 18 HR TRACKING INTERVAL)

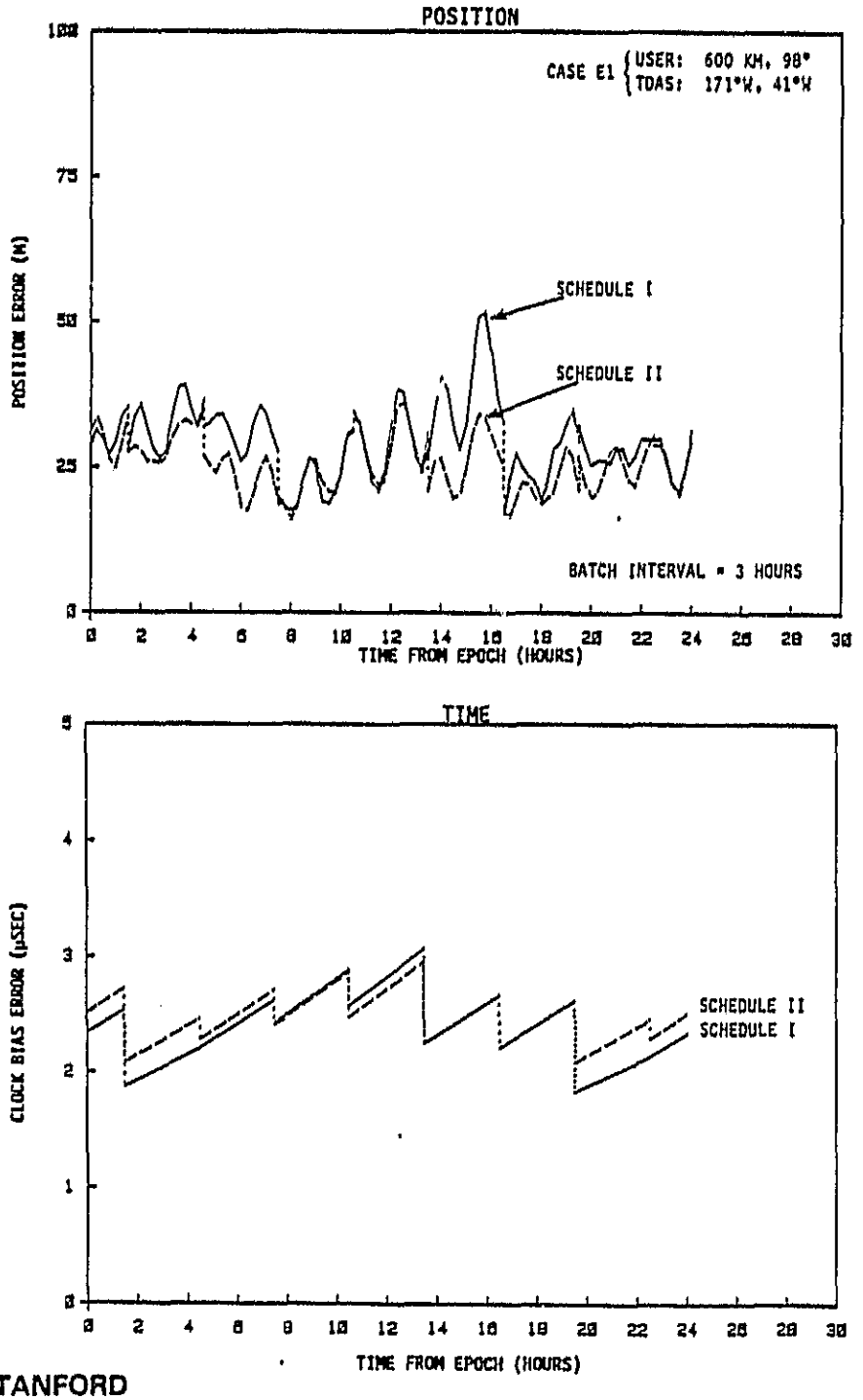

STANFORD TELECOMMUNICATIONS INC.

FIGURE E-13

USER POSITION AND TIME ACCURACY WITH 1-WAY TDAS TRACKING - CASE E2
(BATCH PROCESSING - TRACKING SCHEDULE I)

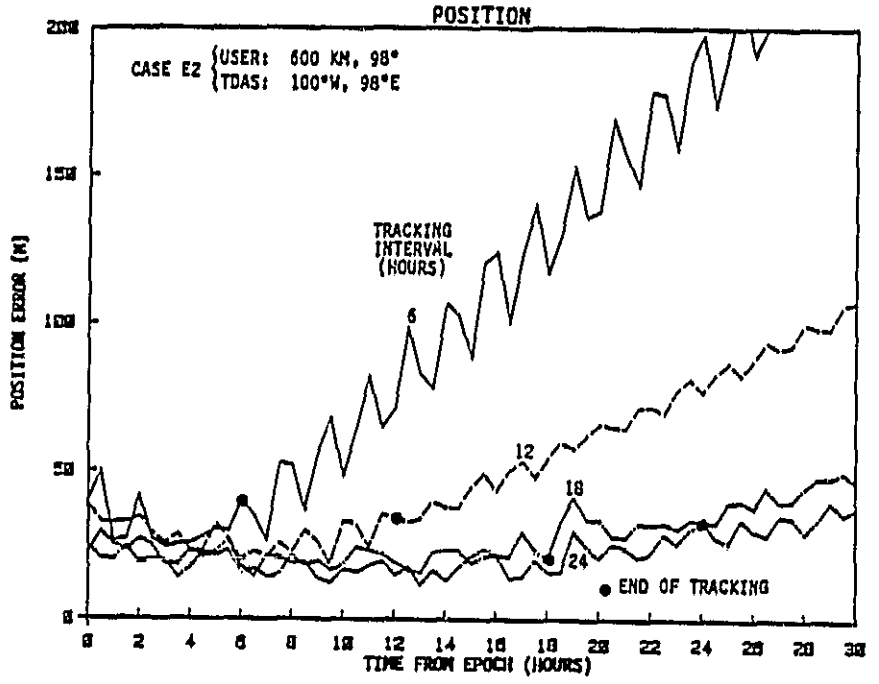

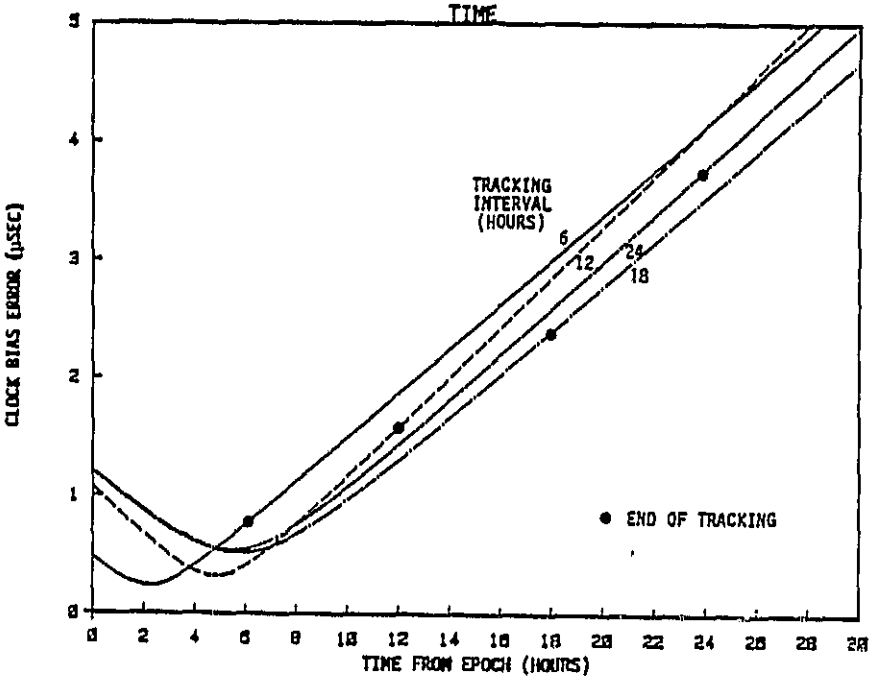

STANFORD TELECOMMUNICATIONS INC.

FIGURE E-14

USER POSITION AND TIME ACCURACY WITH 1-WAY TDAS TRACKING - CASE E2
(BATCH PROCESSING - TRACKING SCHEDULE II)

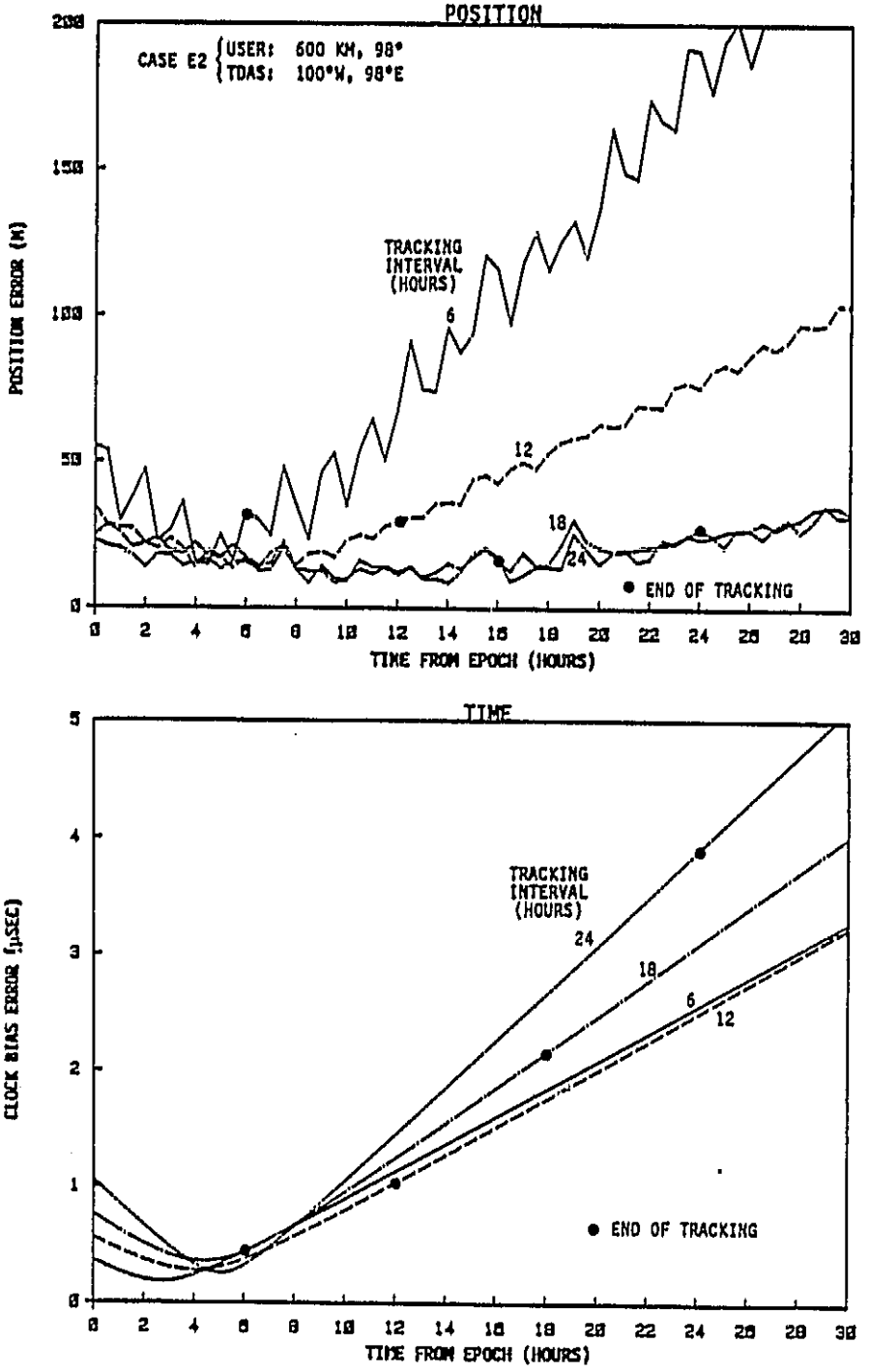

STANFORD
TELECOMMUNICATIONS INC.

FIGURE E-15
USER POSITION AND TIME ACCURACY WITH 1-WAY TDAS TRACKING - CASE E2
(SLIDING BATCH PROCESSING - 6 HR TRACKING INTERVAL)

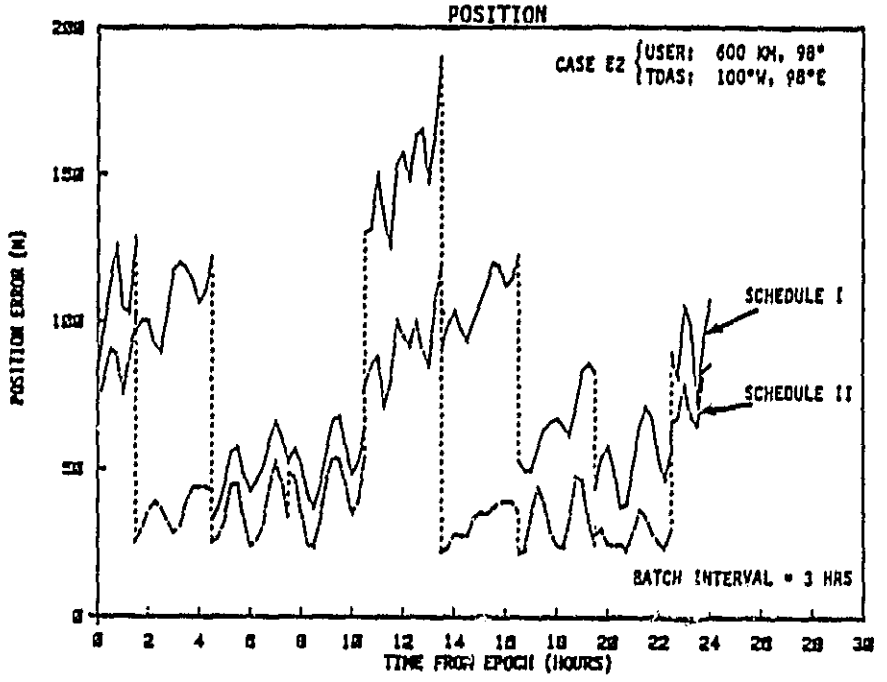

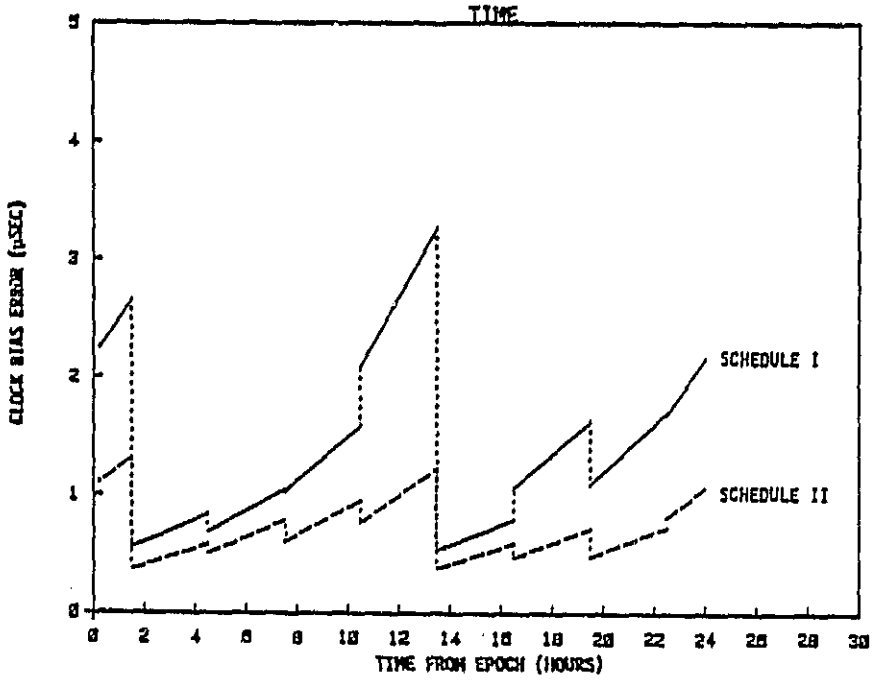

STANFORD TELECOMMUNICATIONS INC.

FIGURE E-16

USER POSITION AND TIME ACCURACY WITH 1-WAY TDAS TRACKING - CASE E2
(SLIDING BATCH PROCESSING - 18 HR TRACKING INTERVAL)

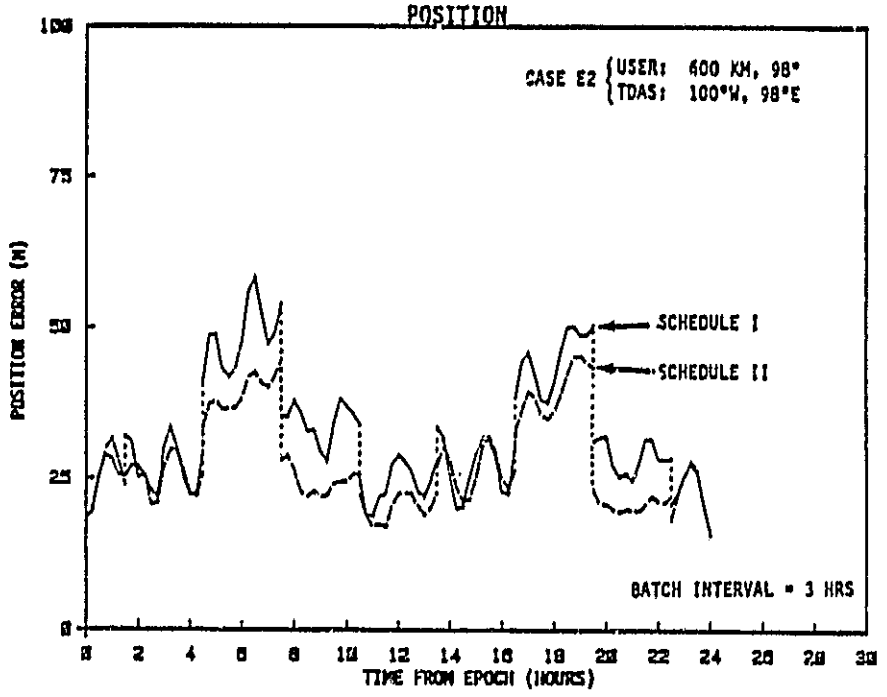

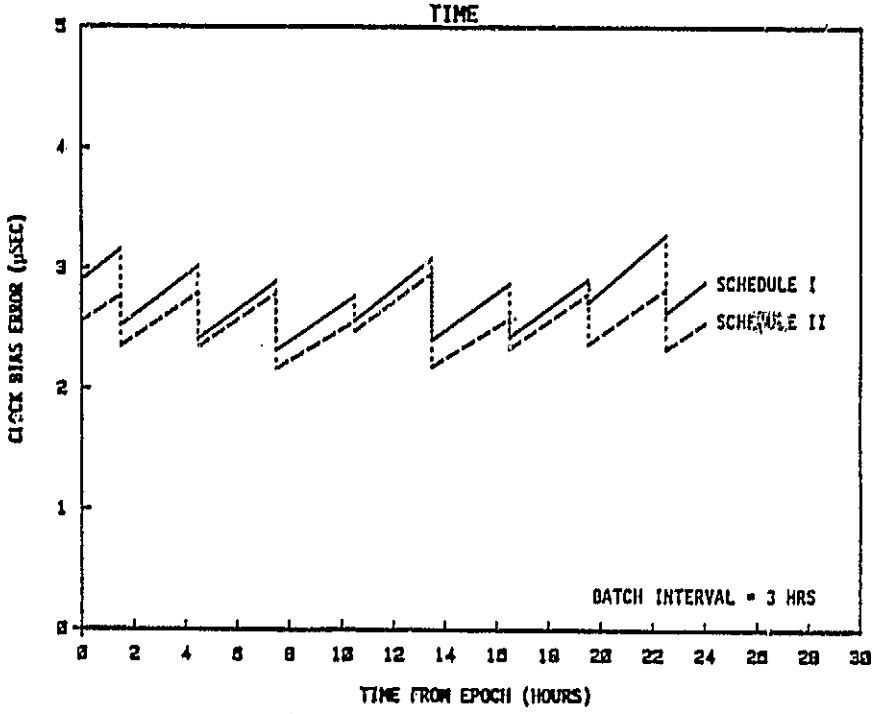

STANFORD TELECOMMUNICATIONS INC.

FIGURE E-17

USER POSITION AND TIME ACCURACY WITH 1-WAY TDAS TRACKING - CASE F2
(BATCH PROCESSING - TRACKING SCHEDULE I)

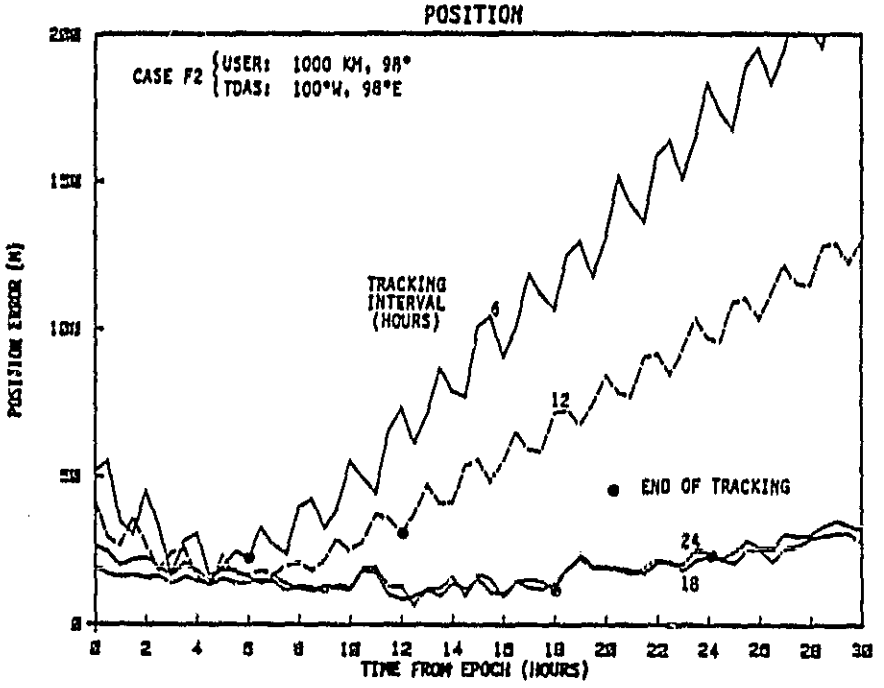

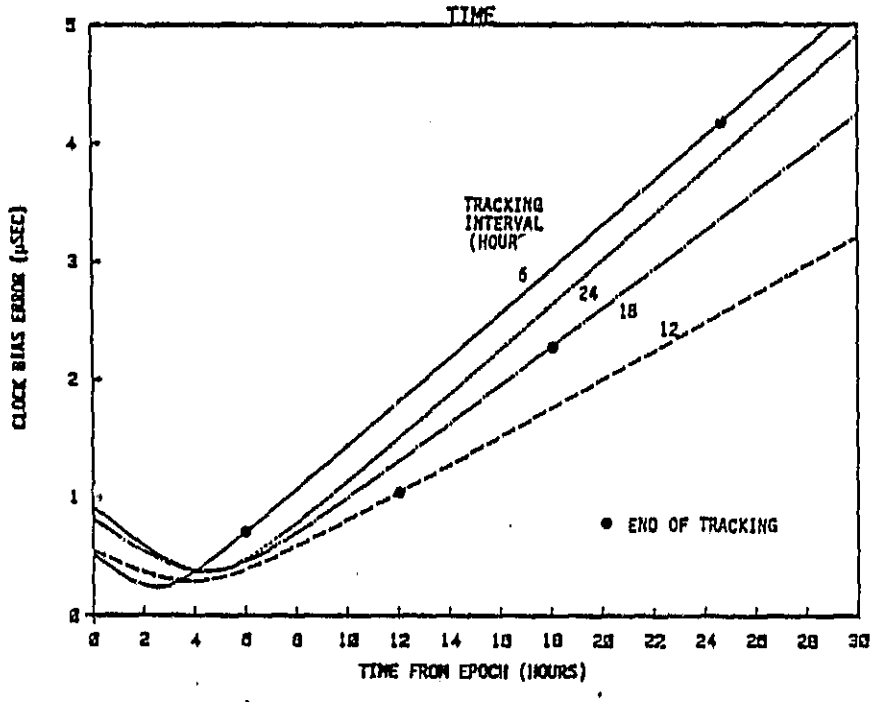

STANFORD TELECOMMUNICATIONS INC.

FIGURE E-18

USER POSITION AND TIME ACCURACY WITH 1-WAY TDAS TRACKING - CASE F2
(BATCH PROCESSING - TRACKING SCHEDULE II)

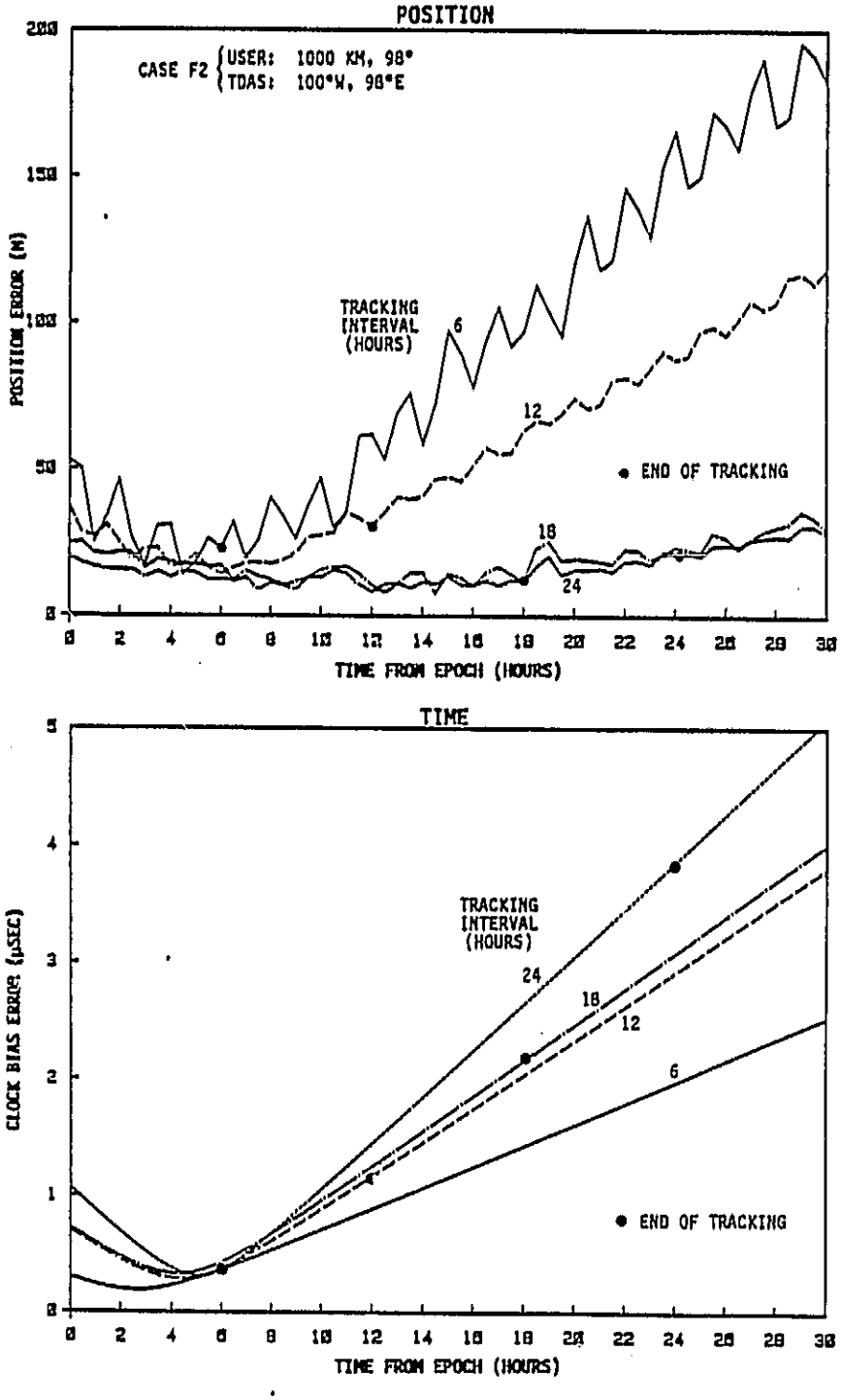

STANFORD TELECOMMUNICATIONS INC.

FIGURE E-19
USER POSITION AND TIME ACCURACY WITH 1-WAY TDAS TRACKING - CASE F2
(SLIDING BATCH PROCESSING - 18 HR TRACKING INTERVAL)

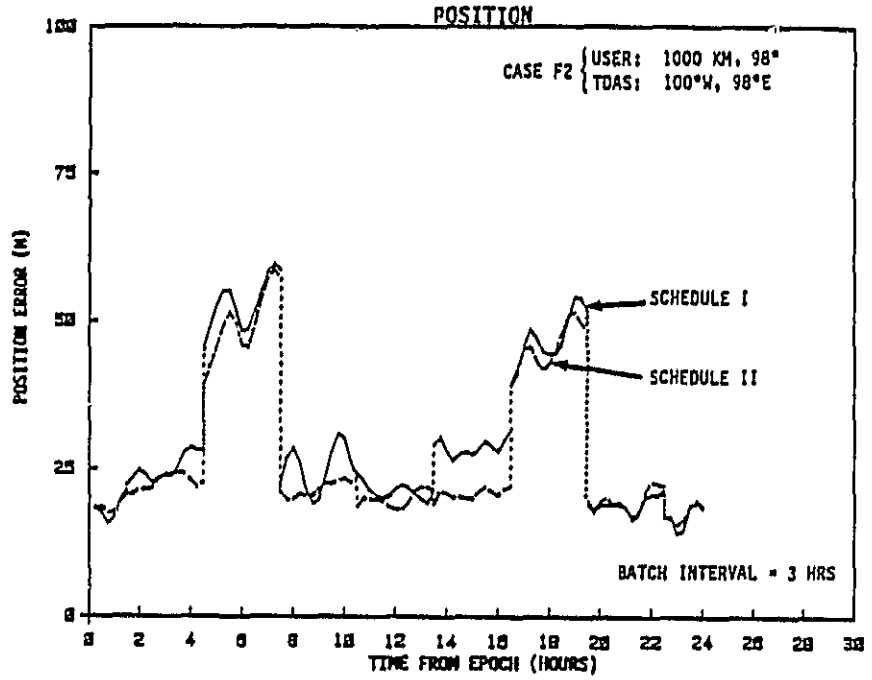

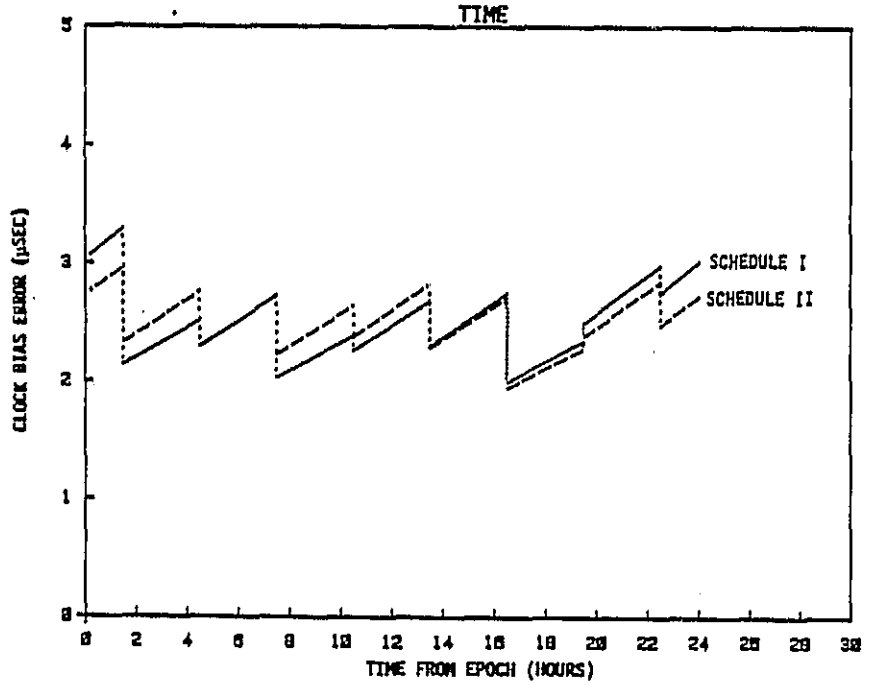

TABLE E-1
USER NAVIGATION PERFORMANCE SUMMARY - MAX POSITION ERROR (M)
(SLIDING BATCH DATA PROCESSING)

TRACKING CONFIGURATION			FLST				RLST					
			SCHEDULE II		SCHEDULE I		SCHEDULE II			SCHEDULE I		
USER ORBIT	TDAS CONST.	CASE	BATCH INTERVAL (HOURS)		BATCH INTERVAL (HOURS)		NAV UPLOAD RATE (HOURS)			NAV UPLOAD RATE (HOURS)		
			1.5	3	1.5	3	1.5	3	4.5	1.5	3	4.5
28° 200 KM	100°/98°E	A2	618	884	797	1151	289	618	884	538	797	1151
97° 200 KM	171°/41°	D1	515	771	485	732	314	515	771	290	405	732
	100°/98°E	D2	486	708	708	974	303	486	708	478	708	974
98° 600 KM	171°/41°	E1	33	36	40	52	33	33	36	35	40	52
	100°/98°E	E2	40	45	49	58	33	40	45	41	49	58
98° 1000 KM	100°/98°E	F2	52	59	55	60	40	52	59	45	55	60

TABLE E-2
DOMINANT ERROR CONTRIBUTORS* TO USER POSITION ERROR
(SLIDING BATCH DATA PROCESSING)

TRACKING CONFIGURATION			FLST				RLST					
			SCHEDULE II		SCHEDULE I		SCHEDULE II			SCHEDULE I		
			BATCH INTERVAL (HOURS)		BATCH INTERVAL (HOURS)		NAV UPLOAD RATE (HOURS)			NAV UPLOAD RATE (HOURS)		
USER ORBIT	TDAS CONST.	CASE	1.5	3	1.5	3	1.5	3	4.5	1.5	3	4.5
28° 200 KM	100°/98°E	A2	D	D	D,H	D	D,H	D	D	D,H	D,H	D
97° 200 KM	171°/41°	D1	"	"	D	D	D	"	"	D	D	"
	100°/98°E	D2	"	"	"	"	"	"	"	"	"	"
98° 600 KM	171°/41°	E1	O	O,H	O	O,H	O,E	O	O,H	O,E	O	O,H
	100°/98°E	E2	"	"	"	"	O	"	"	O	"	"
98° 1000 KM	100°/98°E	F2	O	O	O	O	O	O	O	O,H	O	O

* ERROR CONTRIBUTORS ARE ARRANGED IN DECREASING ORDER UNTIL CONTRIBUTORS ARE 50% OF LAST ENTRY:
D = DRAG, H = GRAV. HARMONICS, E = TDAS EPHEMERIS, O = USER OSCILLATOR DRIFT.

TABLE E-3

USER NAVIGATION PERFORMANCE SUMMARY - MAX CLOCK ERROR (μSEC)
(SLIDING BATCH DATA PROCESSING)

TRACKING CONFIGURATION			FLST				RLST					
			SCHEDULE II		SCHEDULE I		SCHEDULE II			SCHEDULE I		
USER ORBIT	TDAS CONST.	CASE	BATCH INTERVAL (HOURS)		BATCH INTERVAL (HOURS)		NAV UPLOAD RATE (HOURS)			NAV UPLOAD RATE (HOURS)		
			1.5	3	1.5	3	1.5	3	4.5	1.5	3	4.5
28° 200 KM	100°/98°E	A2	6.9	8.9	3.3	4.0	5.0	6.9	8.9	2.2	3.3	4.0
97° 200 KM	171°/41°	D1	3.9	4.8	4.3	5.3	2.9	3.9	4.8	3.3	4.3	5.3
	100°/98°E	D2	8.7	10.7	5.6	6.8	6.6	8.7	10.7	4.5	5.6	6.8
98° 600 KM	171°/41°	E1	2.7	2.9	2.8	3.0	2.4	2.7	2.9	2.5	2.8	3.0
	100°/98°E	E2	2.6	2.9	3.0	3.2	2.4	2.6	2.8	2.9	3.0	3.2
98° 1000 KM	100°/98°E	F2	2.7	2.9	3.0	3.3	2.3	2.7	2.9	2.7	3.0	3.3

TABLE E-4

DOMINANT ERROR CONTRIBUTORS* TO USER CLOCK ERROR (SLIDING BATCH DATA PROCESSING)

TRACKING CONFIGURATION			FLST				RLST					
			SCHEDULE II		SCHEDULE I		SCHEDULE II			SCHEDULE I		
USER ORBIT	TDAS CONST.	CASE	BATCH INTERVAL (HOURS)		BATCH INTERVAL (HOURS)		NAV UPLOAD RATE (HOURS)			NAV UPLOAD RATE (HOURS)		
			1.5	3	1.5	3	1.5	3	4.5	1.5	3	4.5
28° 200 KM	100°/98°E	A2	D	D	D	D	D	D	D	D,O,E	D	D
97° 200 KM	171°/41°	D1	"	"	"	"	"	"	"	D	"	"
	100°/98°E	D2	"	"	"	"	"	"	"	"	"	"
98° 600 KM	171°/41°	E1	O	O	O	O	O	O	O	O	O	O
	100°/98°E	E2	O,E,H	O,E,H	O,E	O,E	O,H,E	O,E,H	O,E,H	O,E	O,E	O,E
98° 1000 KM	100°/98°E	F2	O	O	O	O	O	O	O	O	O	O

* ERROR CONTRIBUTORS ARE ARRANGED IN DECREASING ORDER UNTIL CONTRIBUTORS ARE 50% OF LAST ENTRY:
D = DRAG, H = GRAV. HARMONICS, E = TDAS EPHEMERIS, O = USER OSCILLATOR DRIFT.

APPENDIX F

GLOSSARY OF ACRONYMS

BRTS	Bilateration Ranging Transponder System
CONUS	Contiguous United States
DSN	Deep Space Network
EOT	End of Tracking
FLBT	Forward Link Beacon Tracking
FLST	Forward Link Scheduled Tracking
GPS	(NAVSTAR) Global Positioning System
KSA	K_u-Band Single Access
LSA	Laser Single Access
MA	Multiple Access
MCC	Mission Control Center
NASCOM	NASA Communication Network
NCC	Network Control Center
OD	Orbit Determination
OD/TD	Orbit and Time Determination
OSCF	Orbit Support Computing Facility (GSFC)
POCC	Project Operations Control Center
RLST	Return Link Scheduled Tracking
SA	Single Access
SMA	S-Band Multiple Access
TD	Time Determination
VLBI	Very Long Baseline Interferometry
WSA	W-Band Single Access
WSN	White Sands (NM)
ΔVLBI	Differential VLBI (using two signal sources)

APPENDIX G

REFERENCES

1. "Tracking Data Acquisition System Study", Stanford Telecommunications, Inc., Draft Final Report to GSFC under Contract NAS5-26546, STI/E-TR-25066, 31 May 1983.

   a. Executive Summary, Volume I

   b. TDAS User Community Characteristics, Volume II

   c. TDAs Communications Mission Model, Volume III

   d. TDAS Space Segment Architecture, Volume IV

   e. TDAS Ground Segment Architecture and Network Operations, Volume V

   f. TDAS Navigation System Architecture, Volume VI

   g. TDAS Space Technology Assessment, Volume VII

   h. TDAS Frequency Planning, Volume VIII

2. "Tracking and Data Relay Satellite System Users' Guide", Rev. 4, STDN 101.2, NASA/GSFC, January 1980.

3. A.R. Chi, "Satellite Time Transfer Via TDRSS and Applications," TM 80605, NASA/GSFC, December 1979.

4. J. Teles, Orbit Support Computing Division, NASA/GSFC, personal communication.

5. "Automated Orbit Determination System (AODS) - Requirements Definition and Analysis", Fairchild Space & Electronics Co. Report to GSFC under Contract NAS5-24300, September 1980.

6. "A Study of Requirements for Implementing an On-Board Orbit Determination System with The NASA Standard TDRSS User Transponder", Motorola Report to GSFC under Contract NAS5-26193, March 1981.

7. "On-Board Orbit Determination Experiment Study", Fairchild Space & Electronics Co. Report to GSFC under Contract NAS5-25576, April 1981.

8. "Functional and Performance Requirements for the Bilateration Ranging Transponder System", STDN 203.6/BRTS, NASA/GSFC, February 1983.

9. "Very Long Baseline Interferometry (VLBI) Tracking of TDRSS",

   a. Proposed RTOP - GSFC Memorandum (P. Liebrecht to W. Redisch), 14 June 1982.

b. GSFC Technical Direction (#1016) to Bendix Field Engineering Corp., 23 February 1983.

10. A. J. Van Dierendonck, et. al., "The GPS Navigation Message", ION Journal, Vol. 25, No.2, Summer, 1978.

11. D. L. Hall and A. C. Long. "Spacecraft Ephemeris Representation for On-Board Computation", AIAA/AAS Astrodynamics Conference Proceedings, Palo Alto, CA, August 1978.

12. J. J. Spilker, "GPS Signal Structure and Performance Characteristics", ION Journal, Vol. 25, No. 2, Summer, 1978.

13. B.D. Elrod and F. D. Natali, "Investigation of a Preliminary GPS Receiver Design for General Aviation", STI/E-TR-8022, SAMSO TR-79-34 (ADA 069059), 14 July 1978.

14. "2nd Generation TDRSS User Transponder Development Program - System Concept and Requirements Review", Motorola Briefing to GSFC under Contract NAS5-26818, 17 June 1982.

15. J. Ransom - Westinghouse/GSFC Code 405 (TDRSS Project-Systems Engineering), personal communication, December 1982.

16. "ORAN: Multi-Satellite Error Analysis Program", Version 8001.2 at NASA/GSFC, 6 May 1980.

17. J. J. McCarthy, "Operations Manual for ORAN", Wolf R&D Group - EG&G/ WASC, Inc., Riverdale, MD, January.

18. I. Greenfeld, "TDRS Position and Velocity Uncertainties As A Function Of Tracking Data Arc Length and Epoch Times", Bendix Field Engineering. Corp. Report for GSFC/OSCD, TDG-82-183, June 1982.

19. J. Ellis, "Tracking and Data Relay Satellite System (TDRSS) Navigation with DSN Radio Metric Data", Jet Propulsion Laboratory, TDA Progress Report 42-64, May/June 1981.

20. D. B. Shaffer-Interferometrics, Inc. (supporting GSFC Code 974 - User Terminal and Locations Systems Branch), personal communication, March, 1983.

21. W. B. Senus and R. W. Hill, "GPS Applications to Mapping, Charting and Geodesy", ION Journal, Vol. 28, No. 2, Summer, 1981.

22. J. R. Kuhn, "Sequential Orbit Determination Error Analysis Program (SEA) - Programmer's Reference and Users' Guide", Vols. I and II, Computer Sciences Corp. Report. CSC/SD-81/6037 (GSFC Contract NAS5-24300), May 1981.

23. Y. Nakai and D. Smart, "Research and Development Goddard Trajectory Determination System (RDGTDS) - User's Guide", CSC Report, CSC/TM-82/6005UD1 (GSFC Contract NAS5-24300), May 1982; Update 1, September 1982.

24. B. T. Fang, "Error Analyses for Landsat-D Type Orbits Computed Sequentially from TDRSS Data", CSC Report, CSC/TM-81-6125, June 1981.

25. H. D. Hartman, "Analysis of a Dithering Loop for PN Code Tracking", IEEE Trans. Aerospace & Electronic Systems, Vol. AES-10, January 1974, pp. 2-9.

26. M. K. Simon, "Noncoherent Pseudo-Noise Code Tracking Performance of Spread Spectrum Receivers", IEEE Trans. Comm., Vol. COM-25, No. 3, March 1977, pp. 327-345.

27. J. J. Spilker, Jr., Digital Communications by Satellite, Prentice-Hall, Inc., Englewood Cliffs, NJ, 1977.

28. W. C. Lindsey and M. K. Simon, Telecommunication Systems Engineering, Prentice-Hall, Inc., Englewood Cliffs, NJ, 1973.

29. A. Weinberg, "Wide-Dynamics Demodulator (WDD) Analysis Update", STI briefing to GSFC, 16 December 1982; "WDD Modelling Analysis & Evaluation - Phase 2 Study", STI/E Report (expected) August 1983.

30. W. C. Lindsey and K. Tu, "Phase Noise Effects on Space Shuttle Communications Link Performance", IEEE Trans. Comm., Vol. COM-26, No. 11, November 1978, pp. 1532-1541.

31. "Cesium Beam Frequency Standard 5061A", Hewlett-Packard Technical Data, August 1979.

32. "Self Contained Quartz Frequency Standards: FTS 1050 and 1150," Frequency and Time Systems, Inc., D1051, January 1981.

33. B. T. Fang and B. P. Gibbs, "TDRSS Era Orbit Determination System Review Study", Wolf R&D Group, EG&G/WASC, Inc., MT010-75, December 1975.

34. R. Burns, et al, "On-Board Orbit Determination Using TDRSS Data", ORI Report to GSFC under Contract NAS5-25414, July 1979.

35. F. Lerch, et al, "Gravity Model Improvements Using GEOS 3 (GEM9 and 10)", Journal of Geophysical Research, Vol. 84, No. B8, July 1979.

36. "NASA Geodynamics Program Office - Annual Report", NASA Hdqs., TM84010, May 1981.

37. A. Gelb, et al, Applied Optimal Estimation, MIT Press, 1974.

FIGURE C-6
TDAS MAXIMUM POSITION ERROR CONTRIBUTIONS VS VLBI TRACKING INTERVAL (WITHOUT VLBI BIAS ESTIMATION)

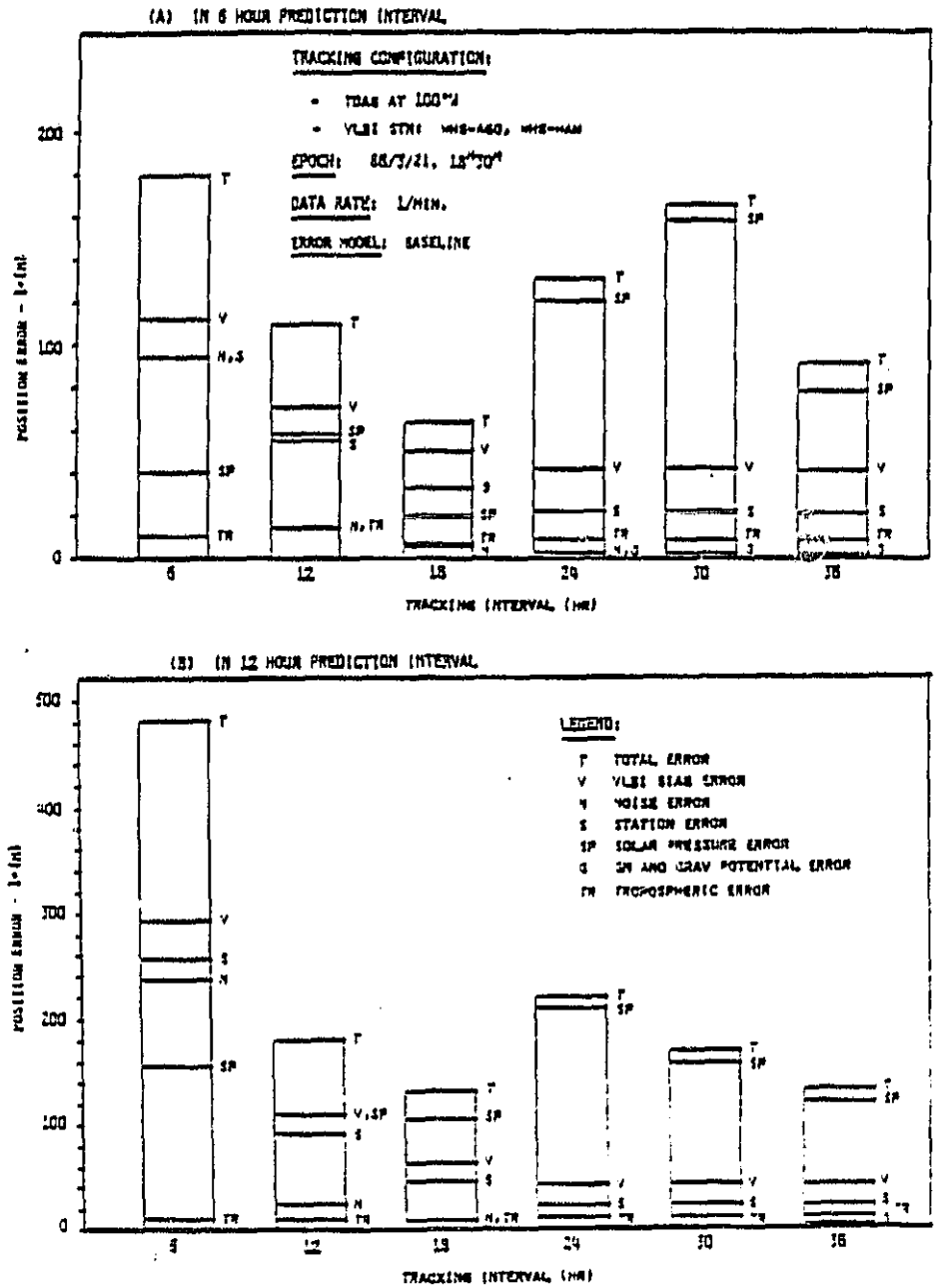

STANFORD TELECOMMUNICATIONS INC.